PREPARATION AND ANALYSIS OF CROSSLINKED LIGNOCELLULOSIC FIBERS AND CELLULOSE NANOWHISKERS WITH POLY(METHYL-VINYL ETHER CO MALEIC ACID) – POLYETHYLENE GLYCOL TO CREATE NOVEL WATER ABSORBING MATERIALS

A Dissertation
Presented to
The Academic Faculty

by

Lee Ann Goetz

In Partial Fulfillment
of the Requirements for the Degree
Doctorate of Philosophy in the
School of Chemistry and Biochemistry

Georgia Institute of Technology
December 2012

PREPARATION AND ANALYSIS OF CROSSLINKED LIGNOCELLULOSIC FIBERS AND CELLULOSE NANOWHISKERS WITH POLY(METHYL-VINYL ETHER CO MALEIC ACID) – POLYETHYLENE GLYCOL TO CREATE NOVEL WATER ABSORBING MATERIALS

Approved by:

Dr. Arthur Ragauskas, Advisor
School of Chemistry and Biochemistry
Georgia Institute of Technology

Dr. Lawrence A. Bottomley
School of Chemistry and Biochemistry
Georgia Institute of Technology

Dr. Facundo Fernandez
School of Chemistry and Biochemistry
Georgia Institute of Technology

Dr. Yulin Deng
College of Engineering, Chemical and Biomolecular Engineering
Georgia Institute of Technology

Dr. Preet Singh
College of Engineering, Materials Science and Engineering
Georgia Institute of Technology

Date Approved: December 2012

This is dedicated to my family and friends for their constant love, support, and encouragement of me throughout this journey. I couldn't have done it without you.

ACKNOWLEDGEMENTS

I wish to thank everyone who has helped me through the process of completing my doctoral studies. I would also like to thank my advisor, Arthur Ragauskas, the IPST@GT Foundation for my IPST GRA, and my committee members. Thank you to Kristiina Oksman and Aji Mathew for sponsoring me at Lulea University, Skelleftea, Sweden and Kristina Knutson for initially writing and receiving the NSF grant that allowed me to travel and study with them. I am grateful to the Georgia Tech Undergraduate Research Opportunities Program GRA sponsorship and the Georgia Tech School of Chemistry and Biochemistry Graduate Teaching Assistantship program.

TABLE OF CONTENTS

LIST OF TABLES

Page

LIST OF FIGURES

Page

LIST OF SYMBOLS AND ABBREVIATIONS

HCl ..... Hydrochloric acid

M ..... Molar

N ..... Normal

NaOH ..... Sodium hydroxide

Conc. ..... Concentrated

H_2SO_4 ..... Sulfuric acid

PMVEMA ..... Poly(methyl vinyl ether – co – maleic acid)

PEG ..... Poly(ethylene glycol)

NaCl ..... Sodium chloride

FQA ..... Fiber Quality Analyzer™

ml ..... milli-liter

L ..... liter

mm ..... milli-meter

sec ..... second

min ..... minute

C ..... Celsius

TEM .....

SEM ..... Scanning electron microscope

AFM ..... Atomic force microscopy

FT-IR ..... Fourier Transform – Infrared

CP/MAS NMR ..... Cross polarization/magic angle spinning nuclear magnetic resonance

MCC ..... Microcrystalline cellulose

CNW ..... Cellulose nanowhiskers

D_2O ..... deuterium

MHz ..... Mega Hertz

kHz ..... kilo Hertz

µs ..... micro-second

DMSO-d_6 ..... Dimethylsulfoxide.

N/m ..... Newtons per meter (AFM – spring constant)

N ..... Newton

h ..... Hour

g ..... Gram

keV ..... Kilo electrovolt

TGA ..... Thermogravimetric analysis

mg ..... Milligram

E_a ..... Activation energy

R ..... Gas constant

T ..... Temperature

T_{50} ..... Temperature at which 50% of the initial weight remained

KBr ..... Potassium bromide

ECF ..... Elemental chlorine free

SW ..... Softwood pulp

HW ..... Hardwood pulp

NaCl ..... Sodium chloride

g/g ..... Grams liquid absorbed per gram dry material

WAV ..... Water absorption value

WRV ..... Water retention value

DI ..... Deionized water

Wt-% ..... Weight percent

SUMMARY

The search for cellulosic based products as a viable alternative for petroleum-based products was the impetus for covalently crosslinking lignocellulosic fibers and nanocellulose whiskers with poly(methyl vinyl ether) co maleic acid (PMVEMA)–polyethylene glycol (PEG). The lignocellulosics used were ECF bleached softwood (pine) and ECF bleached birch kraft pulp. The crosslinking of the PMVEMA to hardwood and softwood kraft ECF bleached pulp fibers resulted in enhanced water absorbing pulp fibers where the PMVEMA is grafted onto the surface of the fibers. The main goal was to determine how to improve water absorption and retention of these fibers. The crosslinking was initiated both thermally and via microwave irradiation and the water absorption and water retention was measured as the percent of grafted PMVEMA. This was the first application of microwave crosslinking of pulp fibers with the goal of creating water absorbing pulp fibers. Ultimately, the water absorption values ranged from 28.70 g water per g dry crosslinked pulp fiber (g/g) to 230.10 g/g and the water retention values ranged from 26% to 71% of the water retained that was absorbed by the crosslinked pulp fibers. The microwave initiated crosslinked fibers had comparable results to the thermally crosslinked fibers with a decreased reaction time, from 6.50 min (thermal) to 1 min 45 sec (microwave).

Cellulose nanowhiskers, crystalline rods of cellulose, have been investigated due to their unique properties. These range from physical properties including nanoscale dimensions, low density, high surface area, mechanical strength, and surface morphology to their surface chemistry and numerous reaction possibilities, to the practical in that they can be made from a variety of local renewable biodegradable cellulose sources – both

woody and non-woody resources. The incorporation of cellulose whiskers into a matrix has been conducted by different mixing methods, primarily via solution casting and extrusion. Prior to this study, the crosslinking of cellulose whiskers incorporated with the matrix via solution casting of liquid suspensions of whiskers and matrix had not been explored. The hypothesis to be investigated was that incorporating cellulosic whiskers with the PMVEMA-PEG matrix and crosslinking the whiskers with the matrix would yield films that demonstrate unique properties when compared to prior work of crosslinking of PMVEMA-PEG to macroscopic ECF bleached kraft pulp fibers.

Solution cast composites of cellulose nanowhiskers-PMVEMA-PEG were crosslinked at 135 °C for 6.5 min and analyzed for crosslinking, thermal stability, strength and mechanical properties, whisker dispersion, and water absorption and uptake rates. The whisker-composites demonstrated unique properties upon crosslinking the whiskers with PMVEMA-PEG, especially the elongation at break and tensile strength upon conditioning of the final materials at various relative humidities. In addition, the whiskers improved the thermal stability of the PMVEMA-PEG matrix. This is significant as methods of improving processing thermal stability are key to developing new materials that utilize cellulose whiskers, PMVEMA, and PEG. This thesis addresses the hypothesis that cellulose nanowhiskers that are crosslinked with a matrix can create new whisker-matrix composites that behave differently after crosslinking. Prior to this thesis project, no-one had addressed the covalent crosslinking of the whiskers with the matrix. This thesis also tests the hypothesis that water absorption and retention can be improved by grafting PMVEMA-PEG to the surface of ECF bleached kraft pulp hardwood and softwood fibers via microwave initiated crosslinking.

CHAPTER 1

INTRODUCTION

Demand for products that utilize biorenewable materials is increasing from consumers, industry, government, and the military [1-4]. This is driven by the goal for less reliance on petroleum market fluctuations and the realization that petroleum is a finite resource. However, these new products must also compete favorably on performance and price when compared to the existing product lines. Cellulose is one biorenewable material that has shown great potential in meeting these demands. Cellulose is the most abundant biopolymer, with estimates of production ranging from 7.5×10^{10} to 10^{11} tons annually [5, 6].

Cellulose sources range from woody plants (lignocellulose) to grassy plants to bacterial, algal and animal sources. However, lignocellulose sources have emerged as a promising feedstock due to the lesser impact on other traditional uses for other sources, most importantly cellulose sources commonly used for human or animal food supplies such as corn. Cellulose has been used by human society for thousands of years, as wood, cotton, hemp, linen, as building supplies, as rope, as material for cloth, and for paper products. Despite this, new research on cellulose materials chemistry is required in order to fundamentally understand how this biopolymer can be manipulated to meet this growing demand. Cellulose nanowhiskers especially show great promise due to their mechanical properties, especially with high aspect ratio, low density (1.6 g/cm^3), surface functionalization potential, and a greater axial elastic modulus than Kevlar -49 [7-10].

With this in mind, this thesis explores utilizing lignocellulose-sourced cellulosic materials, primarily as kraft pulp fully bleached sourced fibers and as cellulose nanowhiskers, in creating novel water absorbing crosslinked materials. One method to improve water absorbency is explored in this thesis. This thesis describes the potential enhancement of water absorbency properties and compares the chemistry of thermal- and microwave-assisted reactions of poly(methyl vinyl ether co – maleic acid) (PMVEMA), polyethylene glycol, and birch pulp fibers and softwood pulp fibers. In addition, cellulose whiskers were crosslinked with the PMVEMA and polyethylene glycol to form a new film-based biomaterial. These films were characterized physically, chemically, and with regard to water absorption kinetics. The behavior of the prepared lignocellulosics-based materials demonstrates how the size of the starting lignocellulosics fibers can affect the properties of the new material.

This dissertation is organized in the following manner. Chapter 2 presents an overview of the literature related to cellulosic modification, both in the creation of cellulose nanowhiskers as well as subsequent chemical modifications. Chapter 3 defines the methods and materials used in the experimental exploration of this topic. Chapter 4 and Chapter 5 compare the grafting of PMVEMA and PEG to wood pulps via microwave and thermal techniques. The results indicate that microwave initiated crosslinking of PMVEMA-PEG to fully bleached kraft pulp fibers results in a shorter reaction time with similar to improved properties when compared to the thermal initiated crosslinked fibers. Chapter 6 introduces the in situ grafting of cellulose whiskers with PMVEMA and PEG through the formation of solution-cast films and is the first published work to have done so. Chapter 7 describes the grafting chemistry using NMR techniques as well as

comparing the mechanical properties of the cellulose whisker-PMVEMA-PEG films conditioned at three different relative humidities. Chapter 8 and Chapter 9 further characterize the fundamental material properties of the crosslinked cellulose whiskers via thermogravitmetric analysis and traditional water absorption kinetics. Finally, the overall results from this dissertation are summarized and future areas of research in this field are proposed.

The major objectives of this research are summarized as follows:

1) Evaluate the efficacy of microwave crosslinking with fully bleached kraft pulp fibers when compared to thermal crosslinking using FT-IR spectroscopy and gravimetric water absorption techniques
2) Develop a procedure for in situ crosslinking of cellulose whiskers with a polymeric matrix
3) Characterize the fundamental chemistry of the crosslinking reaction between the cellulose, PMVEMA, and PEG with NMR spectroscopy
4) Characterize the mechanical properties and water sorption properties of the cellulose whisker-PMVEMA-PEG films

CHAPTER TWO

LITERATURE REVIEW

2.1 Problem Statement.

This body of work focuses primarily on modifying various lignocellulosics to increase water absorbency. A necessary general introduction of the source of these lignocellulosic starting materials is presented first. Next, the research that has been successful in crosslinking the surface of the lignocellulosic fibers to enhance the water absorption of the fiber-polymer is presented. The use of microwave technology as a source of energy to induce chemical and physical changes in lignocellulosic fibers will be presented as an alternative to thermal heating. This will show that there was an opening in the research to compare the results of thermal and microwave crosslinking of pulp fibers with a large chain polymer to enhance the water absorption of the pulp fibers. Microwave-induced reactions with cellulose will be discussed. Finally, the preparation, properties, and uses of cellulose whiskers will be presented to show the depth of work prior to this thesis study that explored the crosslinking of cellulose whiskers with a polymer and the characterization thereof.

2.2 Chemical composition of cell wall.

The primary fiber source in paper-making and in this thesis is lignocellulosic fiber from woody biomass. Native lignocellulosic fibers are composed of three main constituents: cellulose, hemicellulose, and lignin. In addition, a variety of extractable materials are also present in the wood, including terpenes, fatty acids, and alcohols. In softwood trees, lignocellulosic fibers come primarily from the walls of the longitudinal

tracheid cells, while in hardwoods, the fibers come from the tracheid, vessels, and parenchyma cells. The tracheid cell wall is composed of several layers: the middle lamella, primary wall, secondary wall, and lumen. This is described pictorially in Figure 1.

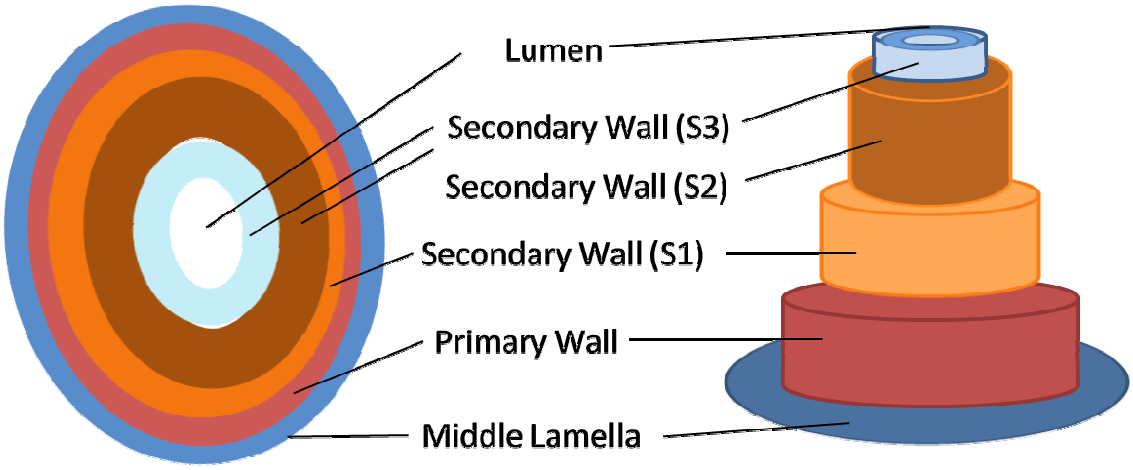

Figure 1. Schematic and Cross Section of Lignocellulosic Fiber Cell Wall (recreated from Hon [5]).

The tracheid cell wall is composed of several layers: the middle lamella, primary wall, secondary wall, and lumen. The middle lamella (ML) is composed primarily of lignin and forms the bond between the fibers, thereby creating the macrostructure of the wood. The primary wall (P) is the outer cell wall. The lumen (L) is the central canal in the fiber that allows for the transport of nutrients and liquids through the fiber. The secondary wall (S) is the largest portion of the cell wall and has three distinct layers, the S1, S2, and S3, which differ from each other according to their cellulose fibril alignment angles. The middle S2 layer is the thickest layer (2 – 10 um). The S1 layer is the outer layer of the secondary wall, while the S3 layer is the inner layer. The amounts of lignin,

cellulose and hemicelluloses vary by species. Table 1 lists typical amounts of cellulose, lignin, and hemicellulose in several softwood and hardwood species [11-16].

Table 1. The percent of lignin, cellulose and hemicelluloses vary by species and within the softwood and hardwood tree types. [11-16]

Wood Species	Cellulose (%)	Lignin (%)	Hemicelluloses (%)
Softwood			
Picea glauca	41	27	31
Abies balsamea	42	29	27
Pinus strobes	41	29	27
Tsuga Canadensis	41	33	23
Norway spruce	46	28	25
Loblolly pine	39	31	25
Thuja occidentalis	41	31	26
Hardwood			
Eucalyptus globules	45	19	35
Acer rubrum	45	24	29
Ulmus Americana	51	24	23
Populus tremuloides	48	21	27
Betula papyrifera	42	19	38
Fagus grandifolia	45	22	29

While these constituents—cellulose, hemicellulose, and lignin—are frequently discussed as separate, independently-occurring polymers, in reality they are all interconnected and intertwined with one another in the cell wall. Cellulose provides the strength of the cell wall and the plant stalk. Lignin provides the stability of the material and engulfs the cellulose fibrils, while the hemicelluloses act as connectors between the cellulose and the lignin. This study utilized lignin-free kraft ECF bleached fibers.

2.2.1 Cellulose.

Cellulose is located in the plant cell wall and typically comprises 40 – 50% of this structure. It is partially due to this percentage that cellulose is the most abundant natural polymer, with an estimated annual biosynthesis rate of 100 x 10^9 metric tons [17]. Cellulose is also present structurally in a wide variety of plants and animals, as well as in algae, fungi, bacteria, amoeba protozoans, and invertebrates. Structurally and chemically, it is a linear, fibrous, water-insoluble polysaccharide consisting of β- D-glucopyranose ring monomers in the $^4C_1$ chair conformation. These β- D-glucopyranose ring monomers are connected by β -(1,4) glycosidic bonds as shown in Figure 2, with each D-glucose monomer rotated 180° from its neighboring unit [5]. The repeating unit is called cellobiose and is frequently described as having a reducing end and a non-reducing end in the biopolymer cellulose chain. In addition, the cellulose polymer is stabilized via hydrogen bonding, as all of the –H units are in the axial vertical plane, while the –OH units are all in the equatorial ring plane.

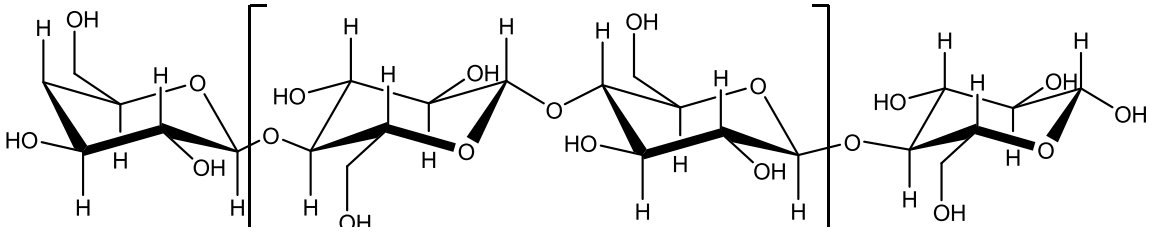

Figure 2. The chemical structure of cellulose is a linear polysaccharide of D-glucose monomers connected by (1,4)-β glycosidic bonds [5].

The degree of polymerization of cellulose varies according to its source and can decrease due to processing conditions. Native cellulose has a chain length of up to 10,000 cellulose units, which can be decreased to less than 2000 units after alkaline pulping [18]. Table 2 lists the degree of polymerization of various cellulose sources and processing types [19-23] .

Table 2. The degree of polymerization of cellulose varies by source and processing conditions [19-23]**.**

Cellulose Source	Degree of Polymerization
Algae	20,000
Cotton (unprocessed)	15,000
Loblolly pine (SW)	12,000
Jack pine (SW)	10,300
Aspen (HW)	7,900
Corn stover	7,000
Eucalyptus (HW)	6,000
Poplar (HW)	5,500
Wheat straw	4,000
Bacterial cellulose	2,000-5,000
Cotton (processed)	2000
Kraft pulp (unbleached)	1600
Kraft pulp (bleached)	1300
Sulfite pulp (bleached)	1255
Raylon	305

During biosynthesis, it is believed that individual cellulose chains are extruded via terminal complexes that are arranged in a rosette form. Ultimately, thirty-six of these cellulose chains aggregate together due to inter- and intra-hydrogen bonding and van der Waals forces. This aggregate of cellulose chains is termed a cellulose microfibril. Under ideal biosynthesis conditions, the cellulose chains are primarily crystalline; amorphous regions do exist, however, where the crystalline microfibrils are distorted by internal strain in the fiber. The microfibril cellulose chain bundles then aggregate further into cellulosic fibers, which are helical around the fiber axis. Native cellulose has both

amorphous and crystalline regions in the polymer chain [18]. Amorphous cellulose is described as the cellulose chains that are present in disordered domains. The degree of crystallinity of cellulose varies according to the source; between ~40 and ~65% of the cellulose of most wood pulps is crystalline. However, other sources such as *Valonia ventricosa* have a 91% crystallinity index [24] , and the bacterial cellulose from *Acetobacter xylinum* has a crystallinity of 76% [24]. Table 3 details the percent crystallinity of specific hardwood and softwood pulps, as well as that of a variety of other cellulose sources [24-27].

Table 3. The degree of crystallinity of cellulose varies by cellulose source [24-27].

Cellulose Source	**Crystallinity, %**	**Method**	**Reference**
HW Kraft pulp (bleached)	43	CP-MAS ^{13}C NMR	[24]
Spruce, Chemithermal Mechanical Pulp	45	CP-MAS ^{13}C NMR	[25]
Aspen Chemithermal Mechanical Pulp	47	CP-MAS ^{13}C NMR	[24]
Spruce, Kraft	49	CP/MAS ^{13}CNMR	[25]
SW Kraft pulp (unbleached)	52	CP-MAS ^{13}C NMR	[24]
SW Kraft pulp (bleached)	52	CP-MAS ^{13}C NMR	[24]
Loblolly Pine	62.5	CP-MAS ^{13}C NMR	[26]
Acetobacter xylinum (bacterial cellulose)	76	CP-MAS ^{13}C NMR	[24]
Cotton (unprocessed)	85.3	X-Ray Diffraction	[27]
Cotton (unprocessed)	85.6	X-Ray Diffraction	[27]
Valonia ventricosa	91	CP-MAS ^{13}C NMR	[24]

Cellulose has six different crystalline forms, known as polymorphs, designated as Cellulose I_α, I_β, II, III, IV_I, and IV_{II}. Cellulose I is the only one found in nature. The other crystalline polymorphs are formed using various chemical reactions, as shown in Figure 3.

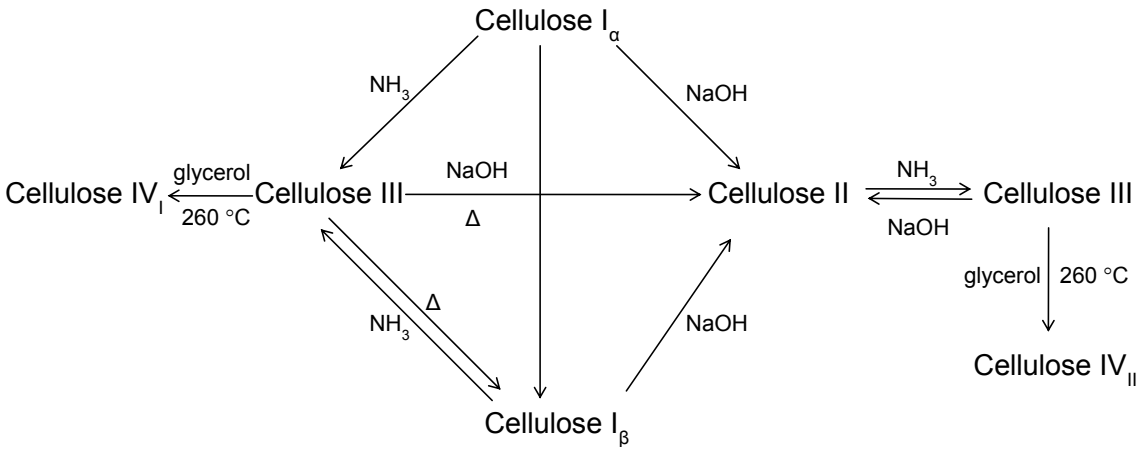

Figure 3. Cellulose has six crystal polymorphs [28].

Cellulose I consists of parallel chains of cellulose and is the native form of cellulose produced by plants and organisms. Atalla and VanderHart demonstrated using CP-MAS ^{13}C NMR that cellulose I exists in two forms, I_α and I_β [29]. Cellulose I_α has one cellulose chain in a triclinic unit cell, while Cellulose I_β has two conformationally-distinct chains in a monoclinic unit cell [30]. In addition, the crystalline cellulose I_α is converted to crystalline cellulose I_β almost completely when heated at higher temperatures. This can be explained by the fact that cellulose I_β is the more thermodynamically stable of the two allomorphs by 8.7 kJ/mol/cellobiose [31]. Both allomorphs are found together in the same cellulose source, though the proportions of each do vary by species. In general, cotton-, ramie-, and wood-sourced cellulose fibers have proportionally more I_β, while bacterial and algal celluloses are richer in I_α [32-34]. Both I_α and I_β form sheets of dense, hydrogen-bonded parallel chains of cellulose that are arranged in stacks. However, I_α and I_β differ in the hydrogen-bonding pattern in the stacking of these sheets, a difference which is displaced in the chain direction.

The crystalline structure of cellulose II consists of anti-parallel chains of cellulose that are hydrogen bonded but are comparatively less dense than those in cellulose I. Cellulose II is formed by the mercerization reaction of the aqueous sodium hydroxide with cellulose I. Cellulose II is thermodynamically the most stable allomorph. While Cellulose III and IV have been characterized, this thesis study focuses on Cellulose I.

FT-IR, ^{13}C NMR, and x-ray crystallography are instrumental tools that are used to characterize the crystalline allomorphs present in a cellulose sample. Electron diffraction studies and FT-IR have been used to confirm that there are two distinct crystalline structures of native cellulose (Cellulose I_α and I_β) [35, 36]. Deconvolution by spectral line fitting of the cellulose C4 region of the ^{13}C NMR spectra has been used to quantify the percent of cellulose I_α, I_β, crystalline cellulose, amorphous cellulose, and, if present, cellulose II [24, 37-40].

2.2.2 Hemicellulose.

Hemicelluloses are non-crystalline amorphous heteropolysaccharides that form various bonds with components of the cell wall: hydrogen bonds with cellulose, predominantly α-benzyl ether covalent bonds with lignin, and ester bonds with acetyl units and hydroxycinnamic acids. Five sugars predominantly combine to form hemicelluloses: D-glucose, D-mannose, D-galactose, D-xylose, and L-arabinose (Figure 4). Other sugars include D-glucuronic acid, 4-O-methyl-D-glucouronic acid, D-galacturonic acid, L-rhamnose, and L-fucose. These combine to form branched polymers with a degree of polymerization (DP) between 50 – 300 DP.

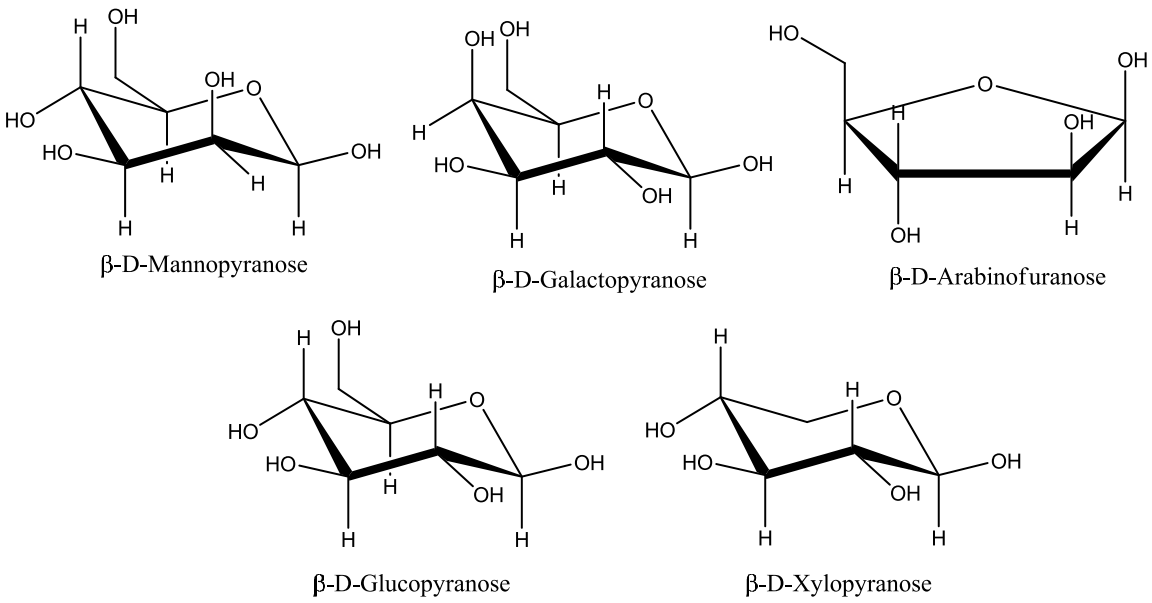

Figure 4. There are five common monomers that combine to comprise the majority of hemicelluloses [41].

Hemicellulose content and proportions vary with wood species. Softwoods generally have a hemicellulose content of 20-30%, the most prevalent hemicelluloses being galactoglucomannan and arabinoglucuronoxylan. Hardwoods have a hemicellulose content of 25-35%, the main hemicellulose being glucuronoxylan [42]. Hemicelluloses will hydrogen bond with the cellulose microfibrils, both intra- and inter-fibrilly, as seen in Figure 5.

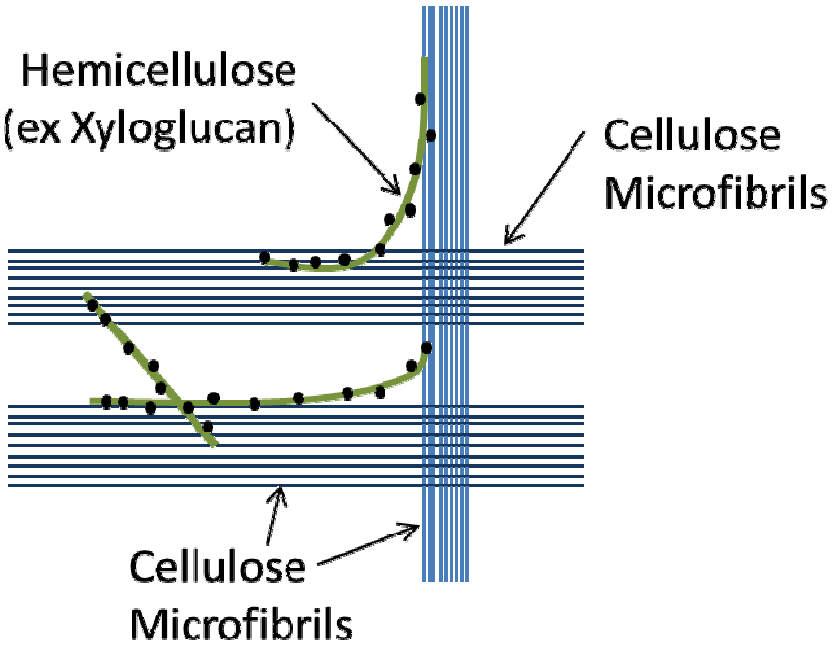

Figure 5. Hemicelluloses form intra- and inter-fiber hydrogen bonds with cellulose microfibrils (Figure adapted from Ishii and Shimizu) [41].

2.2.3 Lignin.

Briefly, lignin is an aromatic amorphous polymer material that acts as a matrix surrounding the cellulose and hemicellulose polymers [43]. The percent lignin in lignocellulosic fibers ranges from 10 to 30% [44]. While the chemical structure of the lignin structure is under debate due to the difficulty of removing the lignin without chemical modification, components of the polymer are known. It is formed through the polymerization of ρ-coumaryl, sinapyl, and coniferyl alcohols (Figure 6), via the formation and coupling of phenoxy radical groups (Figure 7).

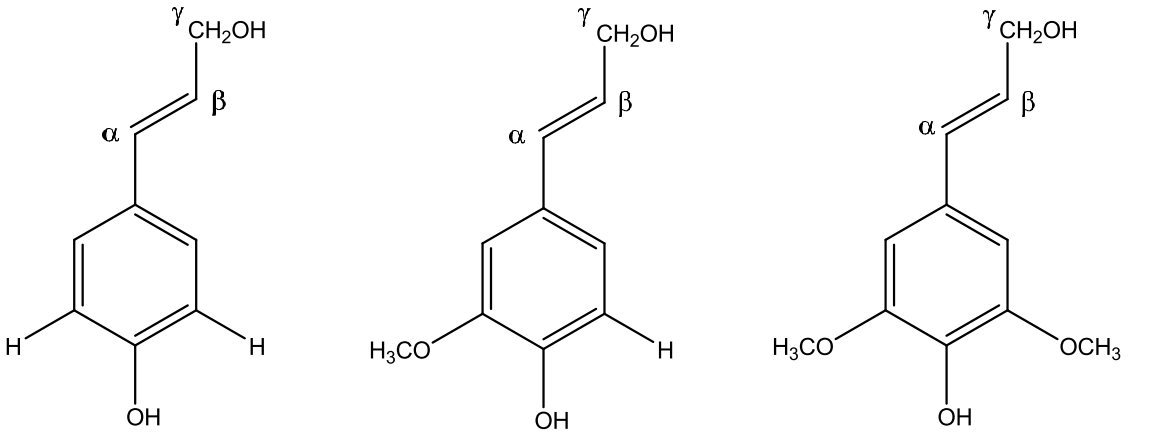

Figure 6. The building blocks of lignin are p-coumaryl alcohol, coniferyl alcohol/guaiacyl, and sinapyl alcohol/syringyl [45]

Due to the reactivity of the five possible resonance structures of the phenoxy radical, a large number of different linkages are possible. This leads to the great complexity of lignin (Figure 7).

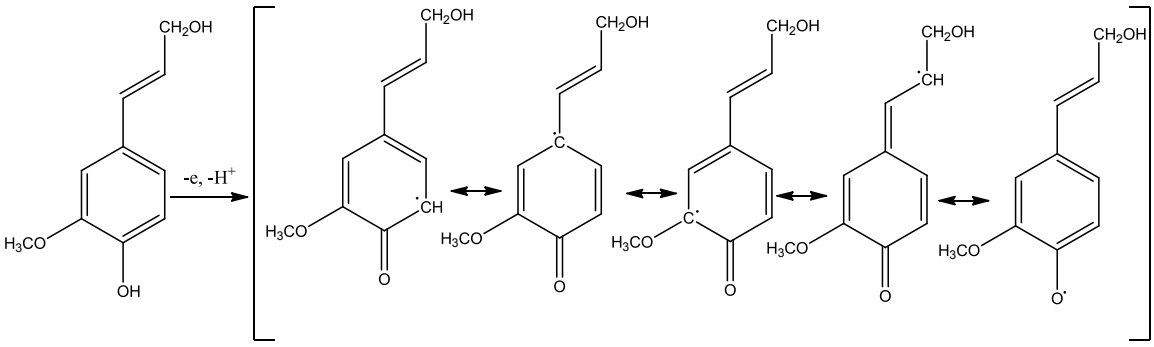

Figure 7. There are five possible resonance structures of the lignin phenoxy radical upon the dehydrogenation of the starting building block, for example coniferyl alcohol [46, 47].

Despite the numerous possibilities, there are eight common linkages in lignin, shown in Figure 8, of which the β – O – 4 ether linkage is the most abundant. Table 4 summarizes the abundance of the most common linkages in hardwood and softwood species and the

differences in the composition of hardwood and softwood lignin [47-51].

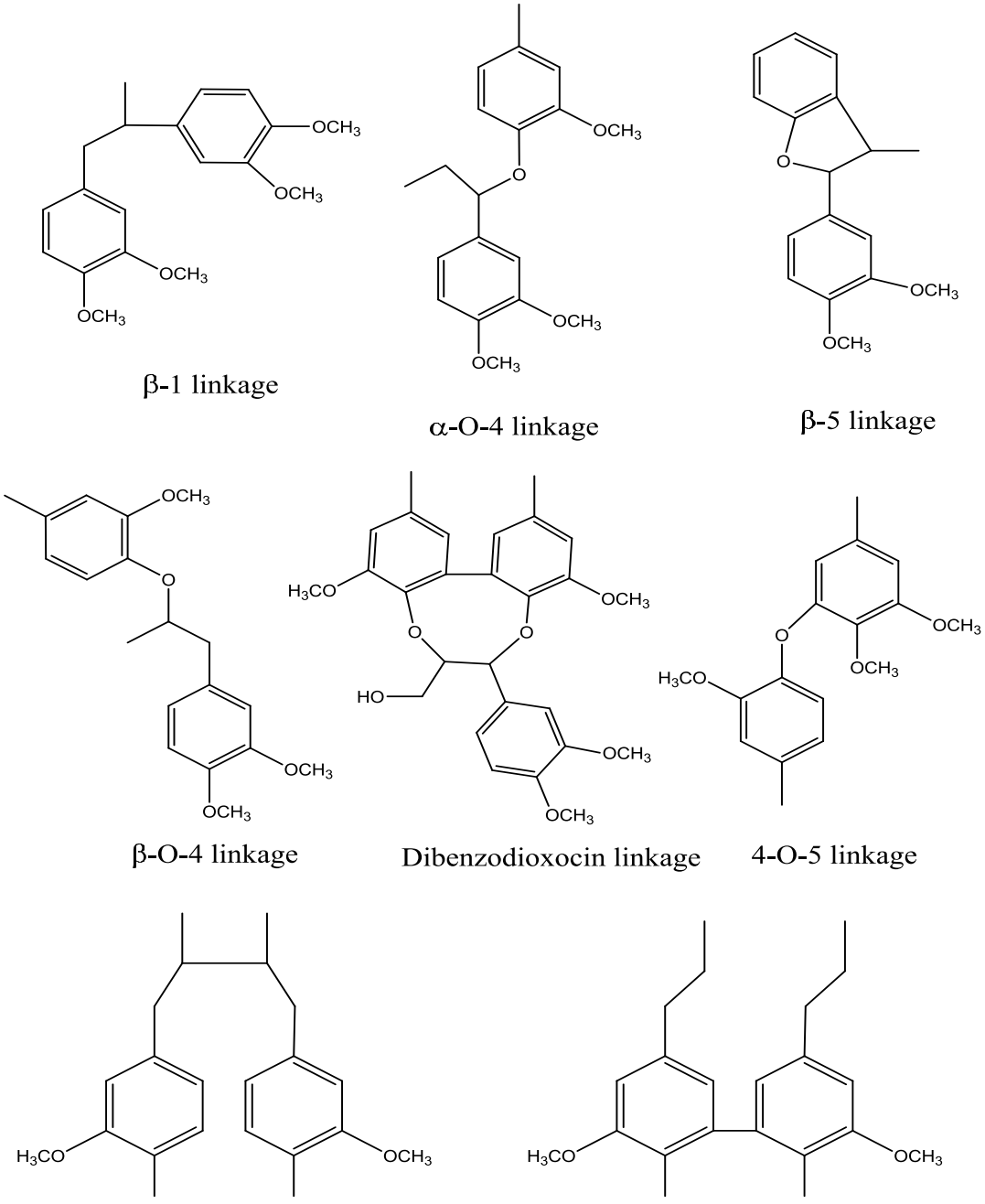

Figure 8. While the lignin structure is complex, there are eight linkages that are most common: β-aryl ether (β -O-4), α-aryl ether (α -O-4), phenylcoumaran (β-5), biphenyl and dibenzodioxocins (5-5'), diphenyl ether (4-O-5), 1,2-diphenylpropane (β-1), and β- β linked structures (β- β) [47-51].

Table 4. Lignin linkage frequency varies between hardwood and softwood [47-51].

Type	Name	Softwood (%)	Hardwood (%)
β -O-4	β -aryl ether	45 – 50	60
α-O-4	α -aryl ether	6 - 8	7
β -5	Phenylcoumaran	9 - 12	6
5-5'	Biphenyl and Dibenzodioxocins	18 - 25	7
4-O-5	Diphenyl ether	4 - 8	5
β -1	1,2 - diphenylpropane	7 - 10	7
β -β	β - β linked structures	3	3

2.3 Cellulose Whiskers.

Cellulose nanowhiskers are conventionally defined as cellulose crystallite rods with at least one size dimension in the nanometer scale [7, 10, 52, 53]. The dimensions of these rods can range from 3 - 70 nm in diameter and from 25 nm to more than 1000 nm in length, depending upon the source of the cellulose and the reaction conditions [7, 10, 52, 53]. Examples of the wide variety of cellulose whisker sources and sizes are shown in Table 5. As cellulose whisker research is a relatively recent field in the chemistry, materials science, and pulp and paper research areas, there are a number of different terms used in the literature to describe cellulose nanowhiskers. Common terms for cellulose whiskers include whiskers, crystalline cellulose whiskers, nanocrystalline rods, cellulose crystallites, cellulose nanocrystals, or cellulose microfibrils or nanofibrils. Unfortunately some of these terms are very nebulous; the terms that will be used throughout this thesis are cellulose nanowhiskers, cellulose whiskers, or whiskers, abbreviated CNW. Interest in utilizing cellulose whiskers is due to their unique properties, which include nano-dimension size, high aspect ratio, low density, high surface area per gram, high strength properties, liquid crystalline behavior and liquid chiral nematic ordering, and optical properties [7, 10, 52, 53]. Interest in cellulose

whiskers is also generated by the opportunities for almost limitless surface functionalization, which is due to the cellulose structure, and the near-worldwide availability of cellulose sources from which the whiskers can be obtained [7, 10, 52, 53].

Table 5. Cellulose nanowhisker (CNW) dimensions span a wide range of lengths, from less than 100 nm to more than 1 μm.

Cellulose Source	**CNW Length, (nm)**	**CNW Cross-sectional Diameter/Width, (nm)**	**CNW Size Measurement Technique**	**Ref.**
Bacterial	100-1000	10-50	TEM	[54]
	100-1000	5-10 x 30-50	TEM	[55, 56]
Cotton	100-150	5-10	TEM	[57]
	70 – 170	~7	TEM	[58]
	200-300	8	TEM	[59]
	255	15	DDL	[60]
	150-210	5-11	AFM	[61]
Cotton linter	100-200	10-20	SEM-FEG	[62]
	25-320	6-70	TEM	[63]
	300-500	15-30	AFM	[64]
Microcrystalline Cellulose	25-265	3-48	TEM	[63]
	250-270	23	TEM	[65]
	~500	10	AFM	[66]
	150-300	3-7	TEM	[67, 68]
Ramie	150-250	6-8	TEM	[69]
	50-150	5-10	TEM	[70]
Sisal	100-500	3-5	TEM	[71]
	150-280	3.5-6.5	TEM	[72]
Tunicate	-	8.8 x 18.2	SANS	[73]
	1160	16	DDL	[60]
	500– 1000	10	TEM	[74]
	1000-3000	15 – 30	TEM	[75]
	100-1000	15	TEM	[59]
	1073	28	TEM	[76]
Valonia	>1000	10-20	TEM	[77]
Softwood pulp	100-200	3-4	TEM	[78, 79]
	100-150	4-5	AFM	[80]
Hardwood pulp	140-150	4-5	AFM	[80]
Sugar beet pulp	210	5		[81]

As mentioned in the discussion of cellulose, cellulose is a long-chain polymer composed of microfibrils. Within these microfibrils are chains of cellulose. Again, depending upon the source of the cellulose, these chains are mixes of crystalline and amorphous regions. Cellulose nanowhiskers are isolated from these crystalline regions through reactions that preferentially attack the amorphous cellulose regions first [7]. Acid hydrolysis of the cellulose sources is the most common method and is presented in this study. While the idea that the crystalline regions of cellulose in the nanometer scale can be isolated from the microfibrils was first investigated in the mid-20th century, it did not become a topic of intensive interest until the late 1990's.

Nickerson and Habrle were among the first to observe that cellulose fibers appeared to reach a finite size and a constant rate of hydrolysis. They noticed after boiling cotton cellulose fibers in either 2.45 N HCl-0.6 M $FeCl_3$ or 2.5 N H_2SO_4 acids for 1 h and 6 h, respectively, that the resulting cellulose exhibited greater crystallinity [82]. Their work was supported by Staudinger and Sorkin, who also investigated the effects of acid hydrolysis via viscometric methods and demonstrated that cellulose chain fragments reach a leveling off of the degree of polymerization, a point which ranges from 150 – 200 glucose units [83]. In the early 1950's, Ränby and Ribi were the first to observe that sulfuric acid hydrolysis of cotton and wood cellulose sources produces colloidal suspensions of cellulose crystals [84, 85]. Transmission electron microscopy was used to determine that the dimensions of these colloidal particles were 50-60 nm length by 5 – 10 nm width [86]. In addition, Mukherjee used electron diffraction to demonstrate that these colloidal crystalline particles had the same crystalline structure as the starting cellulosic materials [86]. The current commonly-used sulfuric acid method of producing crystalline

cellulosic whiskers was first conceived by Mukherjee, Sikorski and Woods [86, 87] and later modified by Marchessault, Morehead and Walter, who were the first to use an ultrasonic treatment to separate aggregated whiskers [88]. Marchessault, Morehead and Walter produced colloidal suspensions displayed birefringent behavior dispersions of crystalline cellulose from a variety of cellulosic sources including native bleached ramie, bleached mercerized ramie, cotton linters, dissolving grade pulps and bacterial cellulose [88, 89]. Concurrently, Battista was developing a hydrochloric acid hydrolysis process that included sonication to produce microcrystalline cellulose (MCC) [90]. Revol, Bradford, Giasson, Marchessault, and Gray revisited this field in 1992 when they confirmed that cellulose whiskers did form a stable chiral nematic liquid crystalline phase when the whiskers were in an aqueous phase [91, 92]. These studies began the current interest in the isolation and usage of cellulose whiskers.

Acid hydrolysis of cellulose sources has become the preferred method of isolating cellulose nanowhiskers [7, 10, 52, 53] . Sulfuric acid, hydrochloric acid, hydrobromic acid [93] and phosphoric acid [94, 95] have all been utilized. The most commonly-used acid is sulfuric acid, and the second most popular is hydrochloric acid [7, 10, 52, 53].

The acid hydrolysis reaction of cellulose to isolate cellulose whiskers is a heterogeneous reaction involving the diffusion of the acid into the cellulose fibers and the subsequent cleavage of the glycosidic bonds of cellulose [96]. The proposed mechanism of the acid hydrolysis of cellulose is presented in Figure 14 below. The cellulose glycosidic bonds in the disordered parts of the cellulose chains are attacked first by the acid groups. The crystalline regions are more resistant to the acid hydrolysis reaction than are the amorphous regions. The cellulose crystal structure is degraded by the peeling off

of angular cellulose sheets. The pathway for this mechanism is presented in Figure 9. The first step is the protonation of the glycosidic oxygen by the acid group [96]. A cleavage of the ether linkage forms a cyclic carbocation through a unimolecular reaction step. Water then reacts with the carbocation, establishing the anomeric center and regenerating the acid.

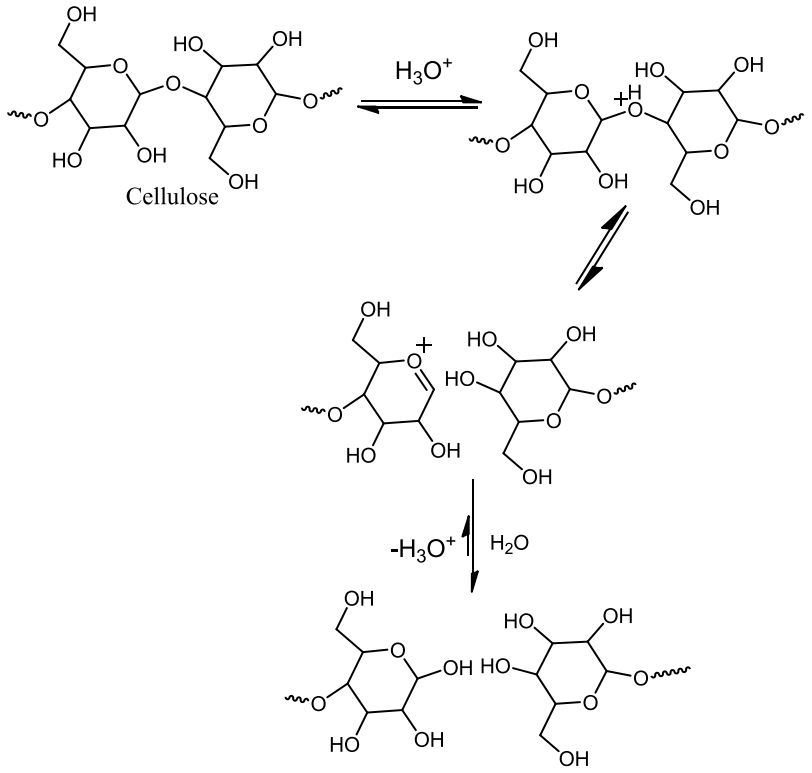

Figure 9. Cellulose whiskers are prepared via an acid hydrolysis reaction [96].

When sulfuric acid is used, sulfate esters are formed with the cellulose hydroxyl groups as shown in

Figure 10 [91]. When hydrochloric acid is used, however, the surface functionalization remains unchanged from that of native cellulose [79]. The sulfate esterification of the cellulose allows for the sulfuric-acid-hydrolyzed whiskers to exhibit

birefringence due to the electrostatic repulsion of the individual whiskers from each other. This esterification also allows for a better individual dispersion of whiskers in an aqueous solution. The sulfuric acid process generates cellulose whiskers that have formed sulfate esters, SO_3^-. This results in the electrostatic repulsion of the sulfuric acid-reacted whiskers from each other, leading to better dispersion throughout the solution, and therefore causing birefringent chiral nematic behavior [91, 92, 97-101].

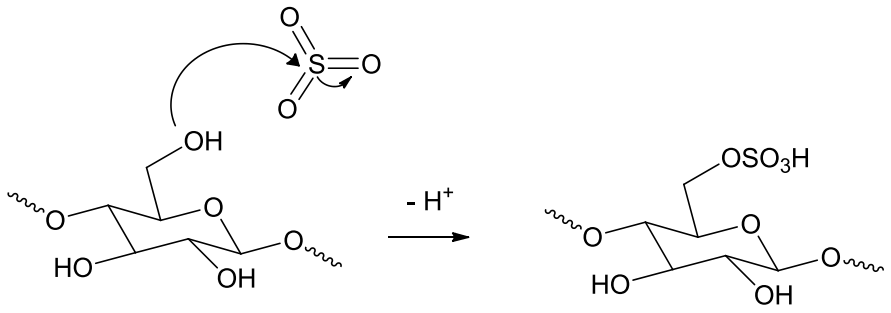

Figure 10. Sulfate ester formation on cellulose whiskers occurs during acid hydrolysis [102].

The whiskers will align themselves to reduce these electrostatic repulsions, forming classic liquid crystalline arrangements. The 'fingerprint type patterns' that are a hallmark of the chiral nematic ordering of liquid crystalline arrangements are observed using polarized optical microscopy while the whisker solution is agitated [88]. This birefringement behavior, and the accompanying fingerprint pattern, can be seen when the whiskers are observed through cross-polarized lenses. This characteristic birefringence shows that the cellulose whiskers are capable of behaving as liquid crystals. The hydrochloric-acid-hydrolyzed cellulose whiskers are not surface charged, and as such do not exhibit birefringence, and tend instead towards agglomeration. The hydrochloric acid hydrolysis does not affect the surface charge, and therefore those whiskers tend to

flocculate together in loose aggregates due to van der Waals forces, and do not display the same birefringent character as the sulfuric-acid-hydrolyzed whiskers [79].

2.3.1 Acid hydrolysis methods to produce cellulose whiskers.

The acid hydrolysis of cellulose sources to create cellulose nanowhiskers is dependent upon six variables: type of acid used, concentration of the acid, ratio of mass of cellulose source to volume acid, cellulose type, time, and temperature of the reacting solution. According to Bondeson, Mathew, and Oksman's optimization study of the sulfuric acid hydrolysis of microcrystalline cellulose, the most important experimental factors affecting acid hydrolysis are time, temperature and acid concentration [67]. Table 6 shows representative reaction conditions from a variety of acids and cellulose sources. The sulfuric acid hydrolysis method is the most common, independent of cellulose source, with the concentration of the sulfuric acid ranging from 63-65 wt-%. This sulfuric acid concentration value was originally proposed and tested experimentally by Mukherjee, Sikorski and Woods [87]. The reaction time and temperature do vary according to the cellulose source, and several studies on optimizing reaction conditions for specific cellulose sources have been performed (Table 6).

Table 6. Selected cellulose nanowhisker preparation techniques.

Cellulose Source	Acid	Acid Concentration, wt %	Time of Hydrolysis Reaction, min	Reaction Temp., °C	CNW Dimensions (length x width), nm	Ref.
Micro-crystalline Cellulose	H_2SO_4	63.5%	130	45	200-400 x <10	[67]
Black Spruce Sulfite Bleached Pulp	H_2SO_4	64%	25	45	141 ± 6 x 5.0 ± 0.3	[103]
Eucalyptus Pulp	H_2SO_4	64%	25	45	147 ±7 x 4.8 ± 0.4	[103]
Black Spruce Sulfite Fully Bleached Pulp	H_2SO_4	64%	45	45	120 ± 5 x 4.9 ± 0.3	[103]
Whatman No. 1 Filter Paper	H_2SO_4	64%	60	45	115 x 7	[58, 92]
Tunicate	H_2SO_4	55%	20	60	2000 x 10-20	[104]
Tunicin, *Halocynthia roretzi*	HCl	2.5 N	45		2000 x 10-20	[105]
Wheat Straw Cellulose	H_2SO_4	65%	60	25	150-300 x 5	[106]
Tunicin, *Halocynthia roretzi*	H_2SO_4	48%	13 h	55	1560 x 34	[76]
Cottonseed Linter Pulp	H_2SO_4	64%	120	60	70-150x10-20	[107]
Bleached Softwood Kraft Pulp	H_2SO_4	65%	10	70	180 ± 75 x 3.5	[79]
Bleached Softwood Kraft Pulp	HCl	4 N	225	80	180 ± 75 x 3.5	[79]

Bondeson, Mathew and Oksman optimized the sulfuric acid hydrolysis of microcrystalline cellulose from Norway spruce bleached pulp to cellulose whiskers using an experimental factorial design matrix [67]. The optimal reaction conditions were determined to be acid hydrolysis of microcrystalline cellulose (10.2 g MCC per 100 ml w/w 63.5% H_2SO_4) for 130 min at 45 °C. This procedure resulted in a 30% yield of cellulose whiskers by starting weight of microcrystalline cellulose. Whisker dimensions ranged from 200 – 400 nm length and < 10 nm diameter [67]. Kvien, Tanem, and Oksman analyzed the dimensions of whiskers produced using the Bondeson method which resulted in cellulose whiskers of 210 ± 75 nm length and 5 ± 2 nm width [68].

Beck-Candanedo, Roman and Gray evaluated the sulfuric acid hydrolysis of black spruce pulp (3-4 mm) and eucalyptus (0.5 – 1.5 mm), a hardwood and a softwood, respectively, in order to determine the effects of acid hydrolysis time and reaction temperature while also comparing two different wood pulp sources [103]. As softwood pulps are longer than hardwood pulps, 3-4 mm and 0.5 – 1.5 mm respectively, it was important to determine whether this translated into differing cellulose whisker lengths. Surprisingly, the two suspensions of eucalyptus pulp and black spruce pulp produced whiskers that were essentially the same length, with a eucalyptus whisker average particle length of 147 ± 7 nm and a black spruce average particle length of 141 ± 6 nm [103]. An increase in hydrolysis time, from 25 min to 45 min, resulted in smaller cellulose whisker lengths (120 ± 5 nm) with a smaller standard deviation in length (45 nm). When the acid to pulp ratio was increased from 8.75 ml/g to 17.5 ml/g, the whisker length decreased 12.5% from 120 ±5 nm to 105 ± 4 nm [103]. As both of the acid to pulp ratios resulted in reaction conditions where the acid was in excess relative to the pulp, it

was concluded that the acid to pulp ratio does not play a significant role in cellulose whisker length.

Dong, Revol, and Gray evaluated the effect of hydrolysis time at 45 °C on the total sulfur content and surface charge as (OSO_3^-) when cotton cellulose was acid hydrolyzed with 64% w/v in a 1:8.75 g/ml paper to acid ratio at varying reaction times [108]. As hydrolysis time increased, the total sulfur content also increased, as shown in Table 7. The total sulfur content was measured using elemental analysis, while the surface charge was measured using conductometric titration.

Table 7. When Whatman No. 1 filter paper powder undergoes acid hydrolysis, as hydrolysis time increases, correspondingly, total sulfur content and surface charge also increases [108].

Hydrolysis time, (min)	**Total sulfur content, %**	**Surface charge (OSO_3^-) (S%)**
10	0.53	0.30
20	0.50	0.33
30	0.58	0.50
45	0.62	0.64
60	0.69	0.68
120	0.74	0.68
240	0.75	0.62

The second most common acid used in the acid hydrolysis of cellulose sources to produce cellulose whiskers is hydrochloric acid (2.5 – 4 N) [7, 10, 52, 53]. Araki, Wada, Kuga, and Okano were the first to publish a hydrochloric acid method in 1998 [79]. This method was similar to one published by Marchessault in 1959 that used 2.5 N HCl to prepare chitin whiskers from crab shells [88]. Araki, Wada, Kuga and Okano were

interested in preparing cellulose whiskers with a minimal surface charge and believed that a procedure using hydrochloric acid as the acid catalyst would achieve this, as the specific acid used also affects the final product. The surface charges on the cellulose whiskers that are generated using sulfuric acid are not reproduced when hydrochloric acid is used in the reaction process. Examples of surface charges from different hydrolysis methods are shown in Table 8 below.

The hydrochloric-acid-hydrolyzed whiskers were prepared by hydrolyzing bleached softwood kraft pulp (5 g) with 4 N HCl (175 ml) at 80 °C for 225 min [79]. After the hydrolysis reaction, the resulting mixture was centrifuged, and the supernatant was collected and purified using dialysis versus distilled water and sonicated for future use [79]. In addition to this, the flow properties of the cellulose whiskers (described nebulously in the paper as microcrystalline cellulose) prepared via the acid hydrolysis of bleached softwood kraft pulp with either 65% (w/w) H_2SO_4 or 4 N HCl were compared.

It was demonstrated that (1) HCl whiskers aggregated more than whiskers prepared using sulfuric acid, (2) whiskers of similar dimensions (180 ± 75 nm long by ~3.5 nm wide) could be produced using either acid method, and (3) the sulfuric-acid-hydrolyzed whiskers had surface charges attributed to both strong acids (84 mmol kg^{-1}) and weak acids (26 mmol kg^{-1}) while the hydrochloric acid whiskers had no surface charges from strong acids (0 mmol kg^{-1}) and a small contribution from weak acids (<18 mmol kg^{-1}) [79].

Table 8. The surface charges of cellulose whiskers vary according to reaction conditions, especially the acid used.

Cellulose Whiskers Source – Hydrolysis acid,	Surface Charge, e/nm^2	Reaction Conditions	Ref.
Softwood bleached kraft pulp (SWBKP) (3.5 nm wide and 180±75 nm) - H_2SO_4,	0.186	10 g SWBKP:100 ml 65wt% H_2SO_4, 70 °C for 10 min	[79]
Softwood bleached kraft pulp (SWBKP) (3.5 nm wide and 180±75 nm) – HCl	0.0286	5 g SWBKP:175 ml 4 N HCl, 80° C for 225 min	[79]
Bacterial cellulose (Primacel) – not hydrolyzed	0.0095	Not hydrolyzed	[56]
Bacterial cellulose (Primacel) – H_2SO_4	0.233	0.066 mol H_2SO_4:1 g cellulose, 65% H_2SO_4	[56]
Tunicin (1-2 um x 8-15 nm) - H_2SO4	0.31	65% (wt/wt) H_2SO4 solution at room temperature	[109]
Ramie (150-250 nm x 6- 8 nm) - H_2SO4	0.63	65% (wt/wt) H_2SO4 solution at room temperature	[109]
Cotton (115 ± 10 nm x 7 nm) - H_2SO_4	0.155	Whatman No. 1 filter paper, 20 mesh 20 g: 175 ml 64% sulfuric acid at 45 °C for 1 h	[58]

Roman and Winter also studied the effect that reaction time, sulfuric acid concentration, and ratio of mmol acid per g cellulose had on surface charge [56], with results summarized in Table 9 below. When reaction time was increased from 1 h to 3 h and the sulfuric acid concentration and mmol acid to gram cellulose ratio were kept constant, the surface charge density increased from 0.021 e/nm^2 to 0.033 e/nm^2 in Samples C and F, respectively. Also, as the mmol acid to gram cellulose ratio increased while reaction time (1 h) and temperature (40 °C) were kept constant in Samples C, D, and E, the surface charge density increased from 0.021 e/nm^2 to 0.027 e/nm^2 to 0.031 e/nm^2, respectively. When the ratio of sulfuric acid (mmol) to cellulose (g) increased as the amount of acid relative to the amount of cellulose increased, the surface charge density also increased.

Table 9. Roman and Winter investigated the effect of acid concentration, ratio of acid per gram cellulose, temperature and hydrolysis time on surface charge density [56].

Sample	Sulfuric acid concentration, (%)	mmol acid/g cellulose	Temperature, °C	Hydrolysis Time (h)	Surface charge density
A	0 (unhydrolyzed)	-	-	-	0.000
B	12	188	104	2	0.007
C	65	66	40	1	0.021
D	65	199	40	1	0.027
E	65	663	40	1	0.031
F	65	66	40	3	0.033
G	61	618	40	3	0.162
H	65	66	60	2	0.233

Surface charge of the whiskers also affects the thermal stability properties of the cellulose. The sulfuric-acid-hydrolyzed cellulose whiskers decompose at a lower temperature (~200 °C) than do the hydrochloric-acid-hydrolyzed cellulose whiskers, which is due to the presence of the charged sulfate esters which help to catalyze the degradation reactions. Roman and Winter studied the effect that different charges of sulfuric acid have on the thermal decomposition of cellulose whiskers and found that as sulfonation increases, the onset temperature of thermal degradation decreases [56]. The thermal degradation of hydrochloric-acid-hydrolyzed cellulose whiskers was studied and shown to have an onset of thermal degradation of ~300 °C [79].

2.3.2 Physical properties of cellulose whiskers.

The mechanical properties of cellulose whiskers make them extremely appropriate for use as reinforcing materials. A Raman spectroscopy technique developed by Eichorn was utilized to determine that the axial Young's modulus of cellulose whiskers from cotton and tunicate is 105 and 143 GPa, respectively [110-112]. These

values are comparable to the estimated Young's modulus for native cellulose crystals of 167 GPa [113].

The degree of crystallinity of cellulose whiskers relates directly back to the starting cellulose material. Habibi, Hoeger, Kelley, and Rojas determined the crystallinity index of cellulose whiskers produced from sisal, ramie, and cotton using wide-angle X-ray diffraction to be 81%, 88%, and 88%, respectively [114]. Martins, Teixeira, Correa, Ferreira, and Mattoso the crystallinity of cellulose whiskers prepared from a commercial cotton source using X-ray diffraction [115]. The crystallinity of cellulose whiskers was determined to 90-91% crystalline. This was an increase from the commercial cotton starting material which was 71% crystalline.

One of the highly-cited positive attributes of cellulose whiskers is the large available surface area due to the aspect ratio and density of the whiskers. The aspect ratio, defined as length divided by width, of the cellulose whiskers can vary greatly depending upon the cellulose source and reaction conditions; a commonly used range is 5 – 100 (Table 5). As such, the potential available surface area per gram of these nanocellulose whiskers can be substantial, especially considering the low density (1.6 g/cm^3) of crystalline cellulose [116, 117]. For example, Angles and Dufresne calculated that tunicate whiskers with an aspect ratio of ~67 to have a surface area per gram of ~170 m^2/g [118]; correspondingly, in a 25 wt% tunicin whisker composite, the specific area available on the whiskers was calculated to be ~ 425,000 cm^2/cm^3 [119]. Due to these physical properties and the wide variety of chemistry functionality inherent to cellulose, it is not surprising that the first applications of cellulose whiskers were to evaluate whether the whiskers might act as nano-reinforcements in a variety of polymer matrices.

2.3.3 Incorporation of cellulose whiskers in composite-type materials.

There are two primary methods of whisker incorporation: solution casting/evaporation techniques and sol-gel processing methods [8, 120]. In addition to these, other groups have explored using extrusion [70, 121-132], electrospinning [133-139], and layer by layer deposition [140, 141]. This thesis research describes using in-situ crosslinking via solution casting. These techniques attempt to achieve uniform dispersion of the whiskers with minimal flocculation and aggregation within the matrix. This is the major problem that needs to be addressed in whisker composite-type research when investigating the possibility of using whiskers in new materials.

The casting/evaporation technique is one by which the whiskers are typically mixed with a matrix and cast into molds, after which the solvent evaporates, leaving the whiskers imbedded into the matrix. An even dispersion of whiskers in the matrix is the goal of this technique. The cellulose whiskers can be in an aqueous solution, an organic solution, or freeze dried. This is a common lab-bench technique that allows for a good replication of materials produced, as well as reproducible density values. However, this technique is typically not used for commercial production.

One of the first applications explored utilizing cellulose whiskers was incorporation of cellulose whiskers with various polymer matrices, after which the effect of the whiskers on the physical properties of the matrices was evaluated, especially their effect on mechanical strength and thermal degradation. Favier, Chanzy, Canova, Dufresne, Cavaille, and Gauthier incorporated an aqueous suspension of cellulose whiskers (0 – 14 wt-%) in a styrene butyl acrylate latex matrix by solution casting [104, 142]. The films were characterized using DMTA; the shear modulus value (G) showed a

significant improvement above T_g when cellulose whiskers were incorporated into the latex [104, 142]. The styrene butyl acrylate latex matrix was extensively evaluated as different sources of cellulose whiskers were utilized (tunicate and wheat straw). Wheat straw cellulose whiskers were incorporated into the latex at 0 - 30 wt%, solution cast, freeze dried, and hot pressed. The 30 wt% latex film improved the relaxed modulus of the neat latex by more than one thousandfold [143, 144]. Favier also evaluated the percolation effect of incorporating cellulose whiskers into latex polymers, and ultimately determined that the cellulose whiskers form an interconnected structure (a skeleton) in the matrix. These whiskers are connected by hydrogen bonds that are characterized as having 'tight interactions' [145, 146]. Chazeau produced similar findings concerning the improvement of the physical properties of various polymer matrices when increasing amounts of cellulose whiskers were incorporated with poly(vinyl chloride) plasticized with diethylhexyl phthalate as well as investigating the percolating cellulose whisker network theory using modeling techniques, ultimately concluding that a percolating network forms due to chains adsorbed to the whisker surface[147-150].

Extrusion methods have also been investigated as a method for preparing cellulose whisker nanocomposites, with varying degrees of success [122, 126-129, 131, 132, 151]. Hajji, Cavaille, Favier, Gauthier, and Vigier compared the effect that three different processing methods had on the mechanical/tensile properties of cellulose whisker-poly(styrene-co-butyl acrylate) composites [129]. Solution casting and evaporation; freeze drying and hot pressing; and freeze drying, extrusion and hot pressing were the three methods chosen. The extrusion method had the lowest modulus and tensile strength of the three methods, while the solution casting and evaporation method

had the greatest, attributed to the degradation of the whiskers due to the more extreme processing conditions.

After investigating simple mixtures of whiskers and matrices, the effects of plasticizing additions to these mixtures began to be evaluated as a way to ensure non-flocculation of the whiskers within a matrix [147]. In one study, Samir Azizi, Mateos, Alloin, Sanchez, and Dufresne prepared a nanocomposite with cellulose whiskers, poly(oxyethylene), and tetra(ethylene) glycol dimethyl ether, which was used as a plasticizing agent [152]. The use of the plasticizer resulted in heterogeneous composites, with plasticizer-rich and plasticizer-poor regions. Glycerol was also used as a plasticizer by Angles and Dufresne when they prepared a starch/cellulose whisker nanocomposite [119, 153, 154]. Transcrystallization zones formed around the cellulose whiskers in the glycerol plasticized starch/cellulose whisker composites and are attributed to the decrease in the composite mechanical properties. Mathew, Thielemans and Dufresne used sorbitol as a plasticizer in starch/cellulose whisker nanocomposites and concluded that sorbitol had a single glass transition temperature [155, 156]. The incorporation of 30 wt% cellulose whiskers with soy protein isolate thermoplastics and glycerol resulted in a greater Young's modulus (from 44.7 to 133.2 MPa) and tensile strength (5.8 to 8.1 MPa) than those measured in neat soy protein isolate thermoplastic [157].

2.3.4 Surface and chemical modification of cellulose whiskers.

There has been interest in surface modification of cellulose whiskers as well as interest in the further grafting of various polymers to cellulose whiskers to enhance the compatibility of the whiskers in a variety of solvents and matrices. The initial studies

undertaken for the surface modification of cellulose whiskers focused on modifying the surface chemistries of cellulose whiskers so that the whiskers would be easily dispersible (non-flocculating) in non-polar solvents. Surface acetylation of cellulose whiskers was first reported by Sassi and Chanzy [158]. They were successful in producing cellulose whiskers that demonstrated non-flocculating behavior in solvents such as acetone or acetic acid. Gousse, Chanzy, Excoffier, Soubeyrand, and Fleury partially silylated cellulose whiskers with isopropyldimethylchlorosilane (IPDM-SiCl), *n*-butylmethylchlorosilane (BDMSiCl), *n*-octyldimethylchlorosilane (ODMSiCl) and *n*-dodecyldimethylchlorosilane (DDMSiCl) and observed the behavior of those whiskers in various organic solvents [159]. As the silylation of the cellulose whiskers, measured by degree of substitution (DS), increased from DS 0.4 – 1.0, the cellulose whiskers had the same crystallization as non-substituted whiskers. However, as DS increased above 1, a decrystallization of the whiskers was observed. The silylated cellulose whiskers (DS <1) were dispersible in tetrahydrofuran (THF), displaying non-flocculating and birefringent behaviors [159].

Heux, Chauve, and Bonini explored coating the cellulose whiskers with surfactants to improve the dispersion of the whiskers in cyclohexane and toluene [160, 161]. A commercially available surfactant, Beycostat NA, a phosphoric ester of polyoxyethylene nonylphenyl ether, was mixed with cellulose whisker suspensions in a 4:1 (w/w) ratio of surfactant to cellulose whiskers. The suspensions were adjusted to pH 9 and then freeze dried. The surfactant-coated whiskers were dispersed successfully in cyclohexane and toluene, demonstrating stable non-flocculating dispersion of whiskers [160].

Montanari, Roumani, Heux, and Vignon first carboxylated surface hydroxyl groups to carboxylic acids using TEMPO-mediated oxidation procedure to improve the dispersion of hydrochloric-acid-hydrolyzed cellulose whiskers [162]. Habibi, Chanzy, and Vignon also utilized a TEMPO-mediated oxidation process to oxidize cellulose whiskers that had been produced using hydrochloric acid hydrolysis and confirmed the previous results of Montanari et al. [163]. The resulting oxidized cellulose whiskers did not flocculate in suspension and did display birefringence, the opposite behavior of non-TEMPO-oxidized hydrochloric-acid-hydrolyzed whiskers [163].

Oxidation of cellulose whiskers was also undertaken by Zhang, Jian, Dang, Elder and Ragauskas via periodate oxidation followed by treatment with sodium bisulfite, resulting in sulfonation of the cellulose whiskers at the C2 and C3 carbons of the cellulose. The water retention of the cellulosic whiskers was measured and found to increase post-oxidation-sulfonation [164].

Ljungberg, Bonini, Borolussi, Boisson, Heux, and Cavaille evaluated the effects that the surface modification of cellulose whiskers has on the overall nanocomposite properties by incorporating cellulose whiskers that had no surface modifications, cellulose whiskers surface-grafted with maleated polypropylene, or surfactant-coated (phosphoric ester of polyoxyethylene(9) nonylphenyl ether) cellulose whiskers [165]. Solution-cast films of atactic polypropylene with each type of whiskers were prepared at 6 wt% of cellulose whiskers [165]. After evaporation of the solvent, the films were pressed at 150 °C for 20 min at 7 MPa pressure. The surfactant-coated cellulose whisker film had the greatest density of all of the composite films, as well as the largest Young's modulus, 1.4 GPa. The Young's modulus of the non-modified cellulose whisker-

polypropylene nanocomposite was 1.3 GPa, while the Young's modulus of the grafted cellulose whisker-polypropylene nanocomposite was only 0.5 GPa. Unfortunately, these values were all less than that of the neat polypropylene film (5 GPa). The incorporation of cellulose whiskers with polypropylene did result in 15.25- to 46.25-fold improvements in the tensile modulus when compared to that of the neat polypropylene film (0.4 MPa), and 12.3- to 22.31-fold improvements in the tensile strength when compared to that of the polypropylene film (0.026 MPa). Ljungberg believed that the surfactant-coated cellulose whiskers were acting as plasticizers and could be a way to avoid the brittleness that normally results when non-surface-modified cellulose whiskers are incorporated with polymer matrices.

Yuan, Nishiyama, Wada, and Kuga utilized surface acylation of cellulose whiskers with alkyenyl succinic anhydride to improve the hydrophobicity of the whiskers [166]. Both *iso*-octadecenyl succinic anhydride and *n*-tetradecenyl succinic anhydride emulsions were mixed with a cellulose whisker suspension. The whiskers were collected via filtration, freeze-dried, and then heated at 105 °C for 5 – 240 min. The unreacted succinic anhydride was removed by rinsing the whiskers with acetone. Acylation was confirmed using FT-IR. Dispersion of the whiskers in a variety of solvents was evaluated, with good dispersion of the acylated whiskers occurring in ethanol, acetone, and methanol, where non-modified cellulose whiskers had previous shown poor to no dispersion. Wang, Ding, and Cheng explored the possibility of grafting the whiskers via acetylation, hydroxyethylation, and hydroxypropylation techniques [167].

Braun and Dorgan developed a method to both isolate and functionalize cellulose whiskers in a single-step reaction method using cotton linters as the cellulose source

[168]. This is a demonstrated improvement from the previous surface-modification procedures in which the cellulose whiskers were chemically altered after acid hydrolysis isolation. In the new process, the esterified cellulose whiskers were produced via a Fischer esterification single-reaction technique using a combination of HCl and an organic acid, such as acetic acid or butyric acid, for the acid catalyzation step [168]. Cotton linters were immersed overnight in either acetic or butyric acid. They were then heated to 105 °C and dilute hydrochloric acid was added. The final concentrations of the acids in this mixture were 17.5 M acetic acid/0.027 M HCl and 10.9 M butyric acid/0.027 M HCl. The organic acid concentration of the mixture was 90 wt%, and the cotton linter to total liquid ratio was 0.04 g cotton linter/1 ml acid solution. Reaction times varied from 4 – 120 min after the solution was heated to 105 °C and dilute hydrochloric acid was added. This produced cellulose whiskers similar in dimension to those produced in hydrochloric acid, which were presented as a control [168]. Whisker length varied from 170 nm to 280 nm while whisker diameter had less variation, ranging from 25 – 50 nm. The resulting esterified whiskers also had similar thermal stability to that of the HCl-produced whiskers, with an onset of degradation around 300 °C [168]. Esterification was confirmed using FT-IR and the esterified whiskers were found to be dispersible in toluene and ethyl acetate.

The surface esterification of cellulose whiskers with gas phase palmitoyl chloride was performed by Berlioz, Molina-Boisseau, Nishiyama, and Heux, resulting in highly-substituted palmitic-acid-esterified cellulose whiskers [169]. The overall goal in developing this method—to minimize the number of procedure steps—was successful, despite reaction times ranging from 2 h to 13 h.

Samir, Alloin, Sanchez, Kissi, and Dufresne were the first to explore crosslinking a matrix around cellulose whiskers [170]. Cellulose whiskers, dispersed in DMF, were mixed with an unsaturated polyether and a photoinitiator, 4-(2-hydroxyethoxy)-phenyl-(2-hydroxy-2-propyl)ketone. This mixture was then solution-cast into aluminum plates and cured using UV radiation in an argon atmosphere at room temperature [170]. The crosslinked matrix around the whisker films demonstrated increasing tensile modulus and stress at break as the whisker content increased, from 0.81 MPa and 0.4 MPa without whiskers, respectively, to 22.3 MPa and 10.6 MPa at 6 wt% cellulose whisker content [170]. Prior to this, cellulose whiskers had been incorporated into matrices by physical methods.

Pranger and Tannenbaum performed a study that was similar to the previous work, in-situ polymerizing furfuryl alcohol monomers to form poly(furfuryl alcohol) polymers around cellulose whiskers [66]. Pranger and Tannenbaum found that the incorporation of cellulose whiskers with the matrix resulted in an improvement of the thermal stability of the nanocomposite, with an increase of 77 °C in the onset point of thermal degradation, from 246 to 323 °C [66]. The effects of the crosslinking of a polymer matrix to cellulose whiskers have not been presented until this thesis research.

2.4 Grafting lignocellulosic fibers with carboxylic acids to improve water absorption.

While various methods have been employed to improve the water absorption of pulp fibers, this literature review will focus on the covalent bonding of polymers to cellulosic fibers, predominantly lignocellulosic fibers. This review will also cover the results of the work that has previously been performed, including the reaction conditions,

reactants, and the water absorption characteristics of the final products in each prior study.

Wood pulp fibers (lignocellulosic fibers) are used in a wide variety of ways to absorb liquids, including urine and water. One of the most commonly-known uses of pulp fiber is as 'fluff pulp' in diapers. Fluff pulp quickly wicks liquids from the surface of the diaper to the center of the diaper, where there is a superabsorbent material, which allows the diaper-wearer to remain comfortable after an accident.

There has been interest in modifying these cellulosic fibers to improve their water absorbency. Cellulose fibers exhibit excellent capillary action, but do not retain significant quantities of liquids (Table 11) while water-absorbing polymers are capable of absorbing and retaining liquids, such as water, via osmotic pressure and flow, but have inferior wicking abilities to those of cellulose fibers [171]. The grafting of water-absorbing polymers to the surface of the cellulose fiber is one way to combine the benefits of both materials.

Table 10. The water retention values of several different lignocellulosic pulps have been experimentally determined.

Cellulose source	**Water retention value, g/g**	**Reference**
Unbleached softwood sulphate pulp	1.77	[172]
Bleached softwood sulphate pulp	1.23	[172]
Bleached Scandinavian softwood kraft pulp	1.05	[6]
Bleached southern pine softwood kraft pulp	0.75	[6]
Bleached spruce CTMP	1.18	[6]
Bleached spruce HTCTMP	1.18	[6]
Unbleached northern softwood kraft pulp	3.00	[173]
Bleached mixed pine and sawmill waste fluff bisulfite pulp (BioFluff-TD)	5.11	[174]

Surface grafting of water-absorbing polymers or those polymers that encourage hydrogen bonding and form networks that entrap water has been studied [171]. The polymerization methods of the grafting of polymers onto cellulose fibers can be catalogued into two primary categories, "grafting to" and "grafting from." The 'grafting to' approach describes a method by which a fully prepared polymer is grafted directly onto the cellulose surface via the polymer end group functional units, which react with the cellulose functional groups (Figure 11).

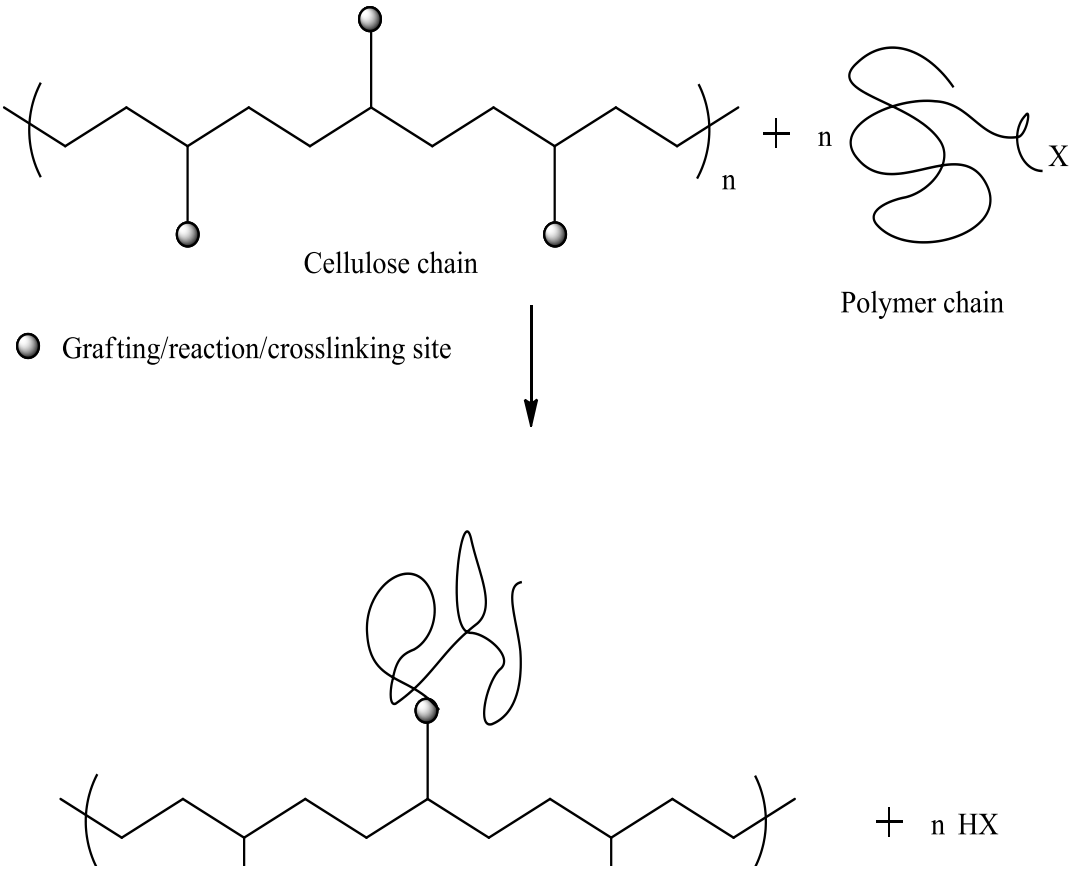

Figure 11. The 'grafting to' polymerization scheme is pictorially depicted [171].

In contrast, the ‘grafting from’ approach describes the concurrent grafting of the monomer to the cellulose chain and subsequent polymerization of the monomer units. This is shown in Figure 12.

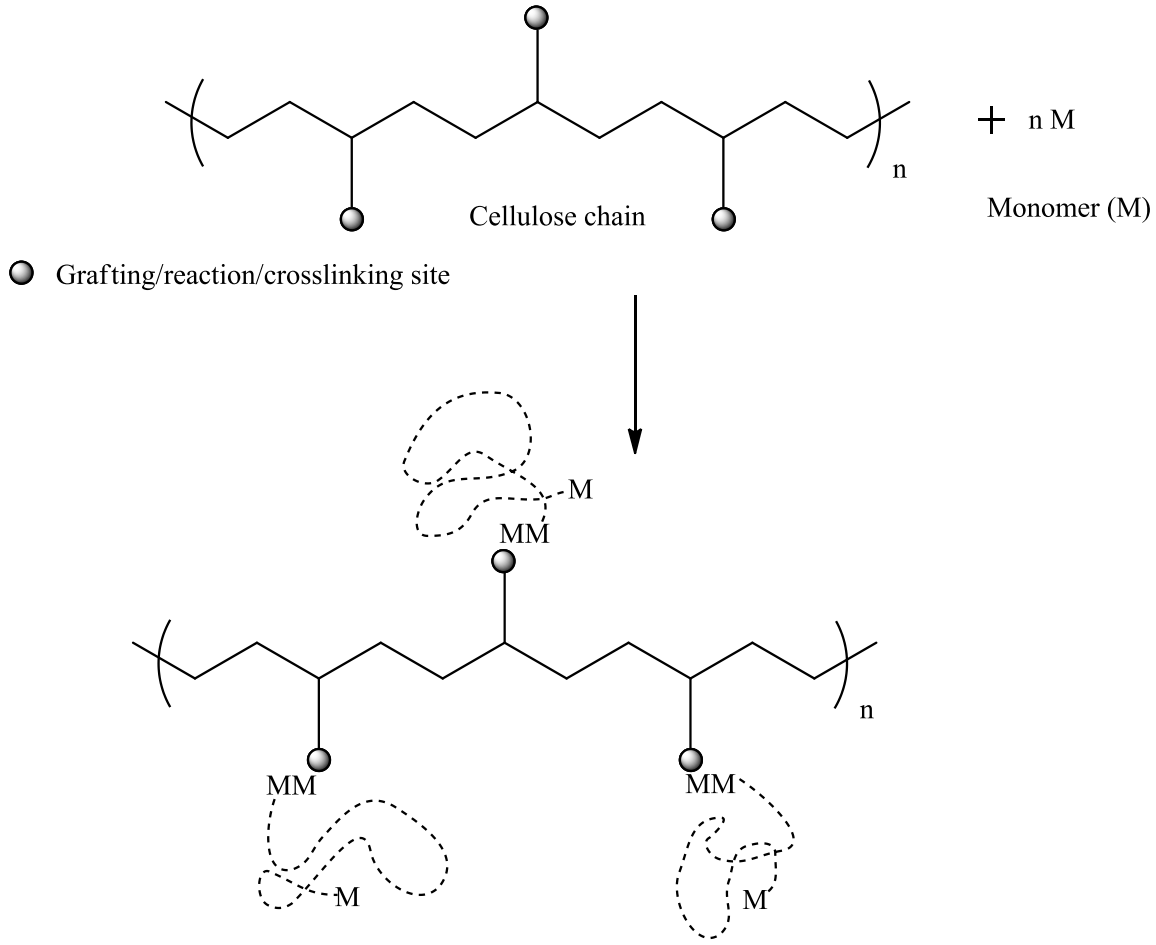

Figure 12. The 'grafting from' polymerization scheme [171].

The ‘grafting from’ approach allows for a higher grafting density than does the ‘grafting to’ approach. This is due to the steric hindrance that the larger polymers have in finding grafting sites along the cellulose chain during the ‘grafting to’ reaction method. With the ‘grafting to’ approach, the polymers can be fully characterized prior to the

grafting reaction process. The opposite is true with the 'grafting from' approach, resulting in a grafted polymer which is not fully characterized. However, the 'grafting to' approach allows the polymer to be fully characterized prior to grafting, which the 'grafting from' method does not accommodate. The 'grafting from' approach is more commonly used in cellulose grafting.

A review article by Chang and Zhang thoroughly describes cellulose-based hydrogels [175]. However, this review does not review cellulose-based hydrogels that were prepared from cellulose fibers such as cotton, wood-based pulp fibers, cellulose whiskers, or fibrillated cellulose, but instead reviews celluloses that were solubilized using a variety of methods, including NaOH/urea, ionic liquids, DMAP, LiCl, NMMP [175]. There has been relatively less material published on cellulose fibers that are grafted specifically to be evaluated for potential use as hydrogels. Reaction methods for grafting polymers onto such cellulose fibers include free radical polymerization, atom transfer radical polymerization, ozonation, and dry curing. The grafting reaction methods utilized are predominantly of the 'grafting from' approach, such as free radical polymerization, in which ceric ammonium nitrate is the initiator.

The cerium ion grafting approach is a 'grafting from' method and is one of the most common methods in the literature for preparing cellulose polymer grafted materials, especially hydrogels, using the grafting of vinylic monomers via the redox reaction with Ce^{4+} [171]. A reaction scheme of the Ce^{4+} free radical polymerization is shown in Figure 13 below. Briefly, the cellulose is pretreated with cerium ammonium nitrate, forming a Ce^{4+} complex with cellulose. When this complex is exposed to acid, such as HNO_3, free radicals are formed via a single electron transfer process. Vinyl monomer polymerization

with the cellulose fiber occurs. Ceric ion initiation is a preferred reaction method as it has a higher grafting efficiency than do other re-dox systems such as Fe(II)-H_2O_2), and has a correspondingly high rate of polymerization, even at low reaction temperatures.

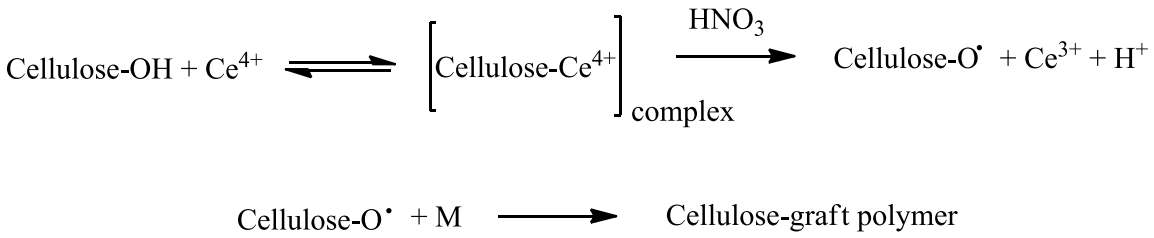

Figure 13. Simplified mechanistic scheme of Ce(IV) ion initiated cellulose graft copolymerization [171].

The predominant monomers associated with grafting using cerium ammonium nitrate are acrylics, such as acrylamide, acrylic acid, ethyl acrylate, acrylonitrile, and methyl acrylate. The patent literature has also explored crosslinking cellulose fibers with acrylic-containing polymers/monomers to improve water absorption [176-185]. Lepoutre is frequently cited as one of the first to explore grafting using cerium-ion-initiated free radical polymerization [186]. Rezai and Warner performed a large study evaluating the grafting of various acrylic monomers onto unbleached northern softwood kraft pulp fibers, unbleached southern softwood kraft pulp fibers, unbleached aspen pulp fibers, unbleached eucalyptus pulp fibers and cotton linters with several types of pulp fibers [173, 187, 188]. The ceric (IV) ammonium nitrate grafting procedure developed by Lepoutre and Hui [189, 190] was utilized and the grafted pulp fibers were evaluated for water retained after centrifugation, the effect of monomer to pulp fibers ratio variations on water retention, and the effects of the incorporation of grafted fibers on handsheet properties [173].

Rezai and Warner evaluated six different monomers (2-acrylamido-2-methylpropanesulfonic acid, dimethyl itaconate, acrylic acid, ethyl acrylate, acrylonitrile, and methyl acrylate) for maximum tea bag gel volume upon grafting onto unbleached northern softwood kraft pulp fibers using a ratio of monomer to pulp of 3:1 [173]. The results are summarized in Table 11 below. Of the six evaluated, the grafted methyl acrylate – unbleached northern softwood kraft pulp fibers and the acrylonitrile grafted unbleached northern softwood kraft pulp fibers retained the greatest mass of water, 41 g/g and 34 g/g, respectively (Table 11). The authors suggest that homopolymerization of the other monomers occurred in preference to grafting to the pulp fibers. This is reflected in the lower yields achieved (Table 11). Tea bag gel volume is the mass of the water retained by the pulp fibers after achieving maximum water absorption and subsequent centrifugation of pulp fibers at 125*g* for 30 min.

Table 11. Evaluation of various monomers' water capacity after centrifugation via tea bag gel volume, TBGV, (g/g) and grafting yield after grafting to unbleached Northern softwood kraft pulp fibers[173].

Monomer	TBGV* (g/g)	Yield, %
None (ungrafted)	3	-
2-acrylamido-2-methylpropanesulfonic acid	3	Very low
Dimethyl itaconate	6	30
Acrylic acid	10	20-25
Ethyl acrylate	10	50
Acrylonitrile	34	80-90
Methyl acrylate	41	70-80

*TBGV is tea bag gel volume and is a measure of the water retained by the grafted pulp fibers after centrifugation at 125 g for 30 min.

Rezai and Warner observed that as the ratio of monomer to pulp fiber increased from 0.5:1 to 4:1, the tea bag gel volume (TBGV - water retention after centrifugation of

pulp fibers at 125*g* for 30 min) increased and reached a maximum TBGV (g/g) at the 3:1 monomer to pulp weight ratio. This was true for both the methacrylate grafted unbleached southern softwood pulp fibers and the methyacrylate grafted unbleached northern softwood pulp fibers, which were measured at 39.1 g/g and 36.1 g/g, respectively [173]. In addition, they observed the swelling behavior of the grafted pulp fibers using light microscopy. In doing so, it was observed that unrestrained swelling of the fiber occurred at the higher monomer to fiber ratios, but ballooning of fiber sections occurred at lower monomer to fiber ratios. This ballooning was attributed to localized grafting of the monomer to the fiber, whereas the unrestrained swelling was attributed to the near complete surface grafting of the monomer to the fiber.

Jain, Xiao and Ni grafted poly(methyl acrylate) onto bleached sulfite pulp fibers via a free radical polymerization reaction using ceric ammonium nitrate as the initiator to produce water-absorbing cellulose pulp fibers [191]. Reaction conditions, including the effect of fiber concentration during grafting, effect of fiber length, effect of initial monomer concentration, and effect of reaction time ceric ion charge, were evaluated. Using a typical ceric-ion-initiated free radical grafting and polymerization procedure, a conversion of the monomer of up to 95% (poly(methyl acrylate) (PMA) was achieved. Only water retention values (no water absorption values) were reported. Water retention value was measured by centrifuging grafted and ungrafted samples at 900g for 30 min [192]. Water retention values of the PMA grafted sulfite pulp fibers showed an improvement of 908% to 1360% above the ungrafted control sulfite pulp fibers [191]. The maximum water retained, 91.2 g/g, was obtained using reaction conditions of 10% fiber concentration and a ratio of monomer to pulp of 4:1, with a 3.5 wt% ceric

ammonium nitrate charge relative to pulp providing the highest grafting yield [191]. Jain et al. also investigated the effect of fiber size on grafting efficiency, ultimately concluding that grafting efficiency remained approximately the same as pulp fiber size decreased (reaction conditions of 2:1 monomer to pup ratio, CAN charge of 3.5 wt % of pulp, and reaction time of 4.0 h) [191].

Kim and Mun prepared cellulose superabsorbents using graft copolymerization of acrylamide with N,N'-methylenebisacrylamide (MBAM) as a crosslinking agent [193]. With the MBAM as a crosslinking agent, the grafted pulp fibers demonstrated significant improvement in water absorption and water retention when compared with pulp fibers from other studies. The grafted pulp fibers' water absorption was predicated upon the grafting yield, reaching a maximum water absorption value of 2700 g/g at 220% grafting efficiency, and then decreasing dramatically to 500 g/g as grafting yield continued to increase [193]. Saline absorbency was ~60 g saline/g dry grafted fiber; saline absorbency followed the same trend, reaching a maximum absorbency of saline and then decreasing as grafting yield continued to increase. Grafting yield generally increased as reaction time increased, with the best grafting yield occurring at a reaction time of 180 min [193].

Several other research groups have investigated similar reaction conditions, such as the grafting of acrylate monomers via a ceric ion redox reaction, which have resulted in similar findings; the grafting of the monomers onto the cellulose fiber did result in greater water retention values when compared to those of the ungrafted pulp fibers. For example, Ali, Saikia, and Sen grafted acrylonitrile to α-cellulose from *Hibiscus sabdariffa*, which resulted in grafted fibers that demonstrated a TBGV value of 5.35 – 5.60 g/g, an improvement from the 1.27 – 1.32 g/g water retention values obtained by the

ungrafted cellulose [194]. Up to 60 g/g and 36 g/g maximum water and saline absorption values, respectively, were achieved by Deo and Gotmare upon the grafting of acrylonitrile to gray cotton using a $KMnO_4 – HNO_3$ redox reaction system [195].

There has been considerable interest in developing cellulose-based water absorbent materials in the last few years, coinciding with this thesis work [191, 196-203]. For example, Dahou, Ghemati, Oudia, and Aliouche grafted acrylic acid and acrylonitrile, separately, onto cellulose fluff pulp to measure the water absorption and retention of the grafted fibers in water, saline and synthetic urine, and to determine the antimicrobial capability of said grafted fibers [174]. The water absorption value of the cellulose-poly acrylic-acid-grafted fibers was 21.84 g/g and the water retention value was 13.83 g/g; the water absorption value of the acrylonitrile-grafted cellulose fluff pulp was 22.25 g/g with a water retention value of 14.57 g/g [174]. By comparison, the ungrafted cellulose water absorption and water retention values were 10.75 g/g and 5.11 g/g, respectively [174]. However, when the acrylic acid was co-polymerized with EDMA, the resulting grafted pulp fibers demonstrated considerable improvement in water absorption and retention values, which were recorded as 32.68 g/g and 20.04 g/g, respectively [174].

Atom-transfer radical polymerization (ATRP) has also been utilized as a grafting method to create water-absorbing cellulose-based materials [204]. Coskun and Temüz individually grafted styrene, methyl methacrylate, methylacrylamide, and acrylomorpholine to chloroacetate cellulose powder, with CuBr and 1,2-dipiperidinoethane as the transition metal compound and ligand, respectively [204]. After reacting for 20 hr at 130 °C, the grafted cellulose was analyzed for water and dye uptake. While all grafted celluloses demonstrated improved water absorption compared

to that of the starting cellulose powder, a maximum water uptake of 895% was obtained using the cellulose-grafted methacrylamide [204]. Comparatively, the chloroacetate cellulose (non-grafted) had a maximum water uptake of 423%, the cellulose-grafted methylmethacrylate water uptake was 467%, and the cellulose-graft – acrylomorpholine water uptake was 770% [204].

Temuz, Coskun, and Oelcuecue also explored grafting cellulose methacrylate powders with a variety of amides and determining the water uptake, as well as the dye and metal absorption [205]. Various amide monomers, including N-phenylmethacrylamide (PPMA), 4-acryloylmorpholine (PAcM), and 2-methacrylamidopyridine (PMAP), were grafted onto the cellulose methacrylate powder via free radical polymerization with α,α'-azobisisobutyronitrile (AIBN) as the initiator. The amide-grafted methacrylate celluloses had water uptake percentages of 532.4%, 736.8%, and 954.5%, which were greater than those of cellulose (376.6%) and cellulose methacrylate (503.1%) [205].

An ozone-induced graft polymerization method was utilized by Karlsson and Gatenholm to create cellulose-based hydrogels [206]. The cellulose fibers from cotton filter paper linters were conditioned in 100% relative humidity were exposed to ozone gas to induce the formation of hydroperoxides. Immediately after this, the ozone-treated fibers were crosslinked with the monomers (acrylic acid and ethyleneglycol dimethacrylate) via a redox reaction with iron(II) ammonium sulfate hexahydrate acting as the redox initiator [206]. Unlike most other similar procedures, Karlsson and Gatenholm did not further saponify the grafted fibers to improve their water absorption and retention capabilities. The water absorption behavior of these grafted cellulose fibers

in various pH solutions was the focus of the swelling studies reported. A maximum water absorption of approximately 14 g solution/g grafted fiber was achieved at pH 8 and pH 11, with a minimum value of approximately 3 g/g and 4 g/g at pH 2 and 3, respectively [206].

Östenson and Gatenholm improved the wettability of pulp fibers via gas phase ozonation [207]. This was demonstrated using a contact angle analysis of a droplet of water on the fiber whereby the contact angle decreased as ozonation exposure increased. After 60 min ozonation time, the contact angle was zero, a dramatic decrease from an initial contact angle of 62° for the untreated fibers [207]. In addition, the time of initial absorption of a droplet of water was measured. Initial absorption of the untreated fibers was approx. 415 ms, while initial absorption of the 1 min treated fibers showed a 75% reduction in absorption time, with the absorption occurring in only 140 ms [207]. The time of initial absorption continued to decrease as time of ozonation increased, with a low of approx. 50 ms at 60 min [207].

There has been some research analyzing the potential of grafting polycarboxylic-acid-containing monomers/polymers to cellulosics with the intention to create a hydrogel. Of these studies, the vast majority of the published research has focused on the potential of polycarboxylic acid polymers as a viable substitute for formaldehyde in creating wrinkle-free cloth [208-215]. Polycarboxylic acids are now also being investigated for their ability to act as flame retardants [216, 217]. The crosslinking of cellulosics with polycarboxylic acids has also been investigated as a method to improve the wet strength of paper [218-221]. In addition, industry has demonstrated interest in the field in the

form of patent literature concerning crosslinking with polycarboxylic acids to improve the water absorption and retention of cellulose pulp fibers [176, 183, 184, 222-227]}.

Yang characterized the reaction mechanism between carboxylic acids and cellulose using FT-IR techniques. In doing so, it was demonstrated that the esterification of cellulose by a polycarboxylic acid occurs in a two-step process, as shown in Figure 14. First, a dehydration step, in which the water is removed and the two carboxylic acid groups form a cyclic anhydride intermediate. Next, the cyclic anhydride intermediate reacts with the primary alcohol of the cellulose to form an ester linkage via an esterification reaction. Pantze, Karlsson, and Westermark demonstrated that a pH less than 2 is ideal for the esterification of cellulose with carboxylic acids and that at a pH greater than pH 5-6 ester bonding is greatly diminished [228].

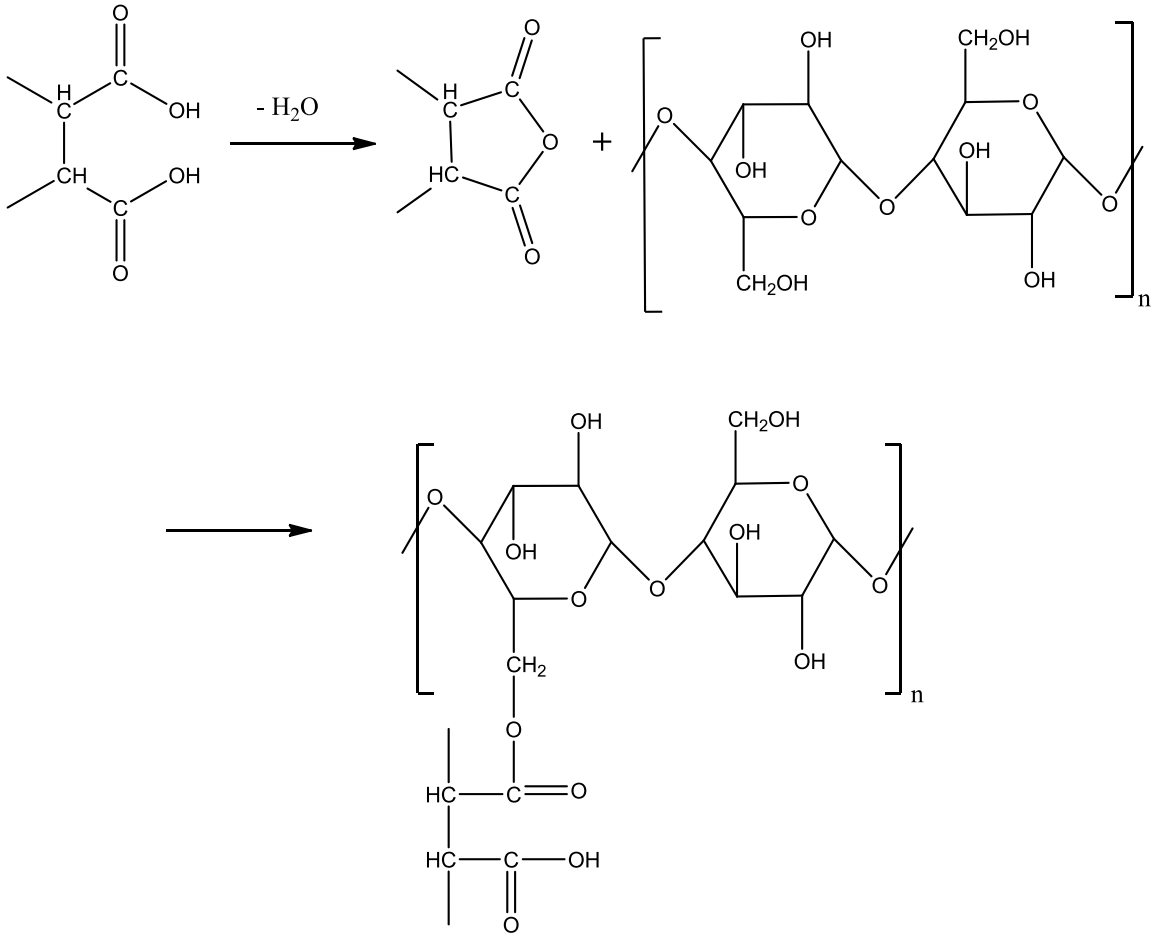

Figure 14. Scheme of the two-step reaction mechanism of the esterification of cellulose by a polycarboxylic acid.

Xu and Yang also compared the effects of crosslinking unbleached kraft pulp with small and large polycarboxylic acids, specifically poly(maleic acid) and poly(methyl vinyl ether co maleic acid), M_n of 800 and 1,130,000, respectively, on both the dry and wet performance of paper sheets [218, 219]. The polymers were crosslinked with the kraft paper sheets via a thermal esterification reaction with sodium hypophosphite as a catalyst. It was determined that the larger polycarboxylic acid polymer, PMVEMA (M_n 1,130,000) predominantly bonded with the paper fibers via interfiber crosslinking. The smaller polymer with the M_n of 800, poly(maleic acid) (PMA), was able to penetrate the

pores of the wood cellulose fibers and form intrafiber crosslinking between cellulose fibers. Due to the differences in inter- and intra-fiber bonding, the swelling capabilities and the dry and wet performance of the crosslinked paper sheets can be explained. However, the intra-fiber bonding of the larger PMVEMA explains why the PMVEMA-crosslinked paper sheets showed a ~20% improvement in dry strength, while the inter-fiber bonding of the PMA improved the wet strength.

The grafting of celluloses with carboxylic-acid-containing polymers has been presented in the patent literature. For example, Westland, Jewell, and Neogi crosslinked poly(maleic acid) and poly(acrylic acid) with wood pulp fibers, including softwood sourced pulp fibers [183, 184, 227]. Ultimately, the water absorbent volume of the crosslinked cellulose fibers ranged from 10 – 30 g/g. Barcus and Bjorkquist crosslinked a poly(maleic acid)-containing co-polymer with polyethylene glycol and pulp fibers with a goal of finding a method of chemically combining the cellulose fibers with the superabsorbent materials used in diapers [229]. At the time, diapers were made of separate layers of cellulose and superabsorbent material, which at the time had a tendency to leak out of the diaper. They evaluated PMVEMA polymers of varying size (M_n from 20,000 to 80,000), crosslinking PMVEMA variations and poly(ethylene glycol) to the cellulose fibers from a variety of pulp fibers (sulfite pulp, softwood kraft, hardwood kraft) [229]. While the initial data in the patent was promising, with water absorption values ranging from 15 – 100 g/g, they did not explore the specific chemistry of the reactions [229].

2.5 Microwave-assisted synthesis and crosslinking.

2.5.1 Introduction to microwaves.

Microwaves are part of the electromagnetic spectrum, falling between infrared and radio waves (Figure 15). While microwaves have a frequency range of 300 MHz to 300 GHz, and wavelength range of 1 m to 1 cm, it has been mandated that for commercial use microwaves be limited to three ISM bands of 2.45 GHz, 915 MHz, and 27.12MHz (wavelengths of 12.24 cm, 37.24 cm, and 11.05 m, respectively).

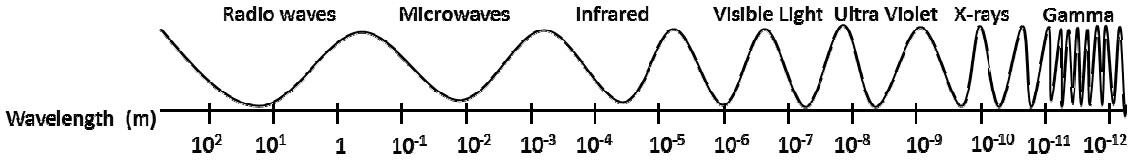

Figure 15. The electromagnetic wave spectrum ranges in wavelength from 10^2 m to 10^{-12} m [230].

Microwave oven reactors use a cavity magnetron to generate microwaves by converting electric current to microwaves [2, 172]. Briefly, electrons move from the cathode to an anode as an electric field is applied. In addition, a magnetic field is applied orthogonally to the electric field and parallel to the cathode. As the electrons move from the cathode to the anode, the magnetic field forces the electrons to move in a rotating pattern. The electrons impinge upon the cavity sides, causing the cavities to oscillate due to a transfer of energy from the impinging electrons. These oscillations are then captured by and transmitted (through an antenna, for example) as microwaves, in this case into a

microwave reactor. These microwaves can then interact with matter in three different ways: absorption, reflection, and transmission [172, 231].

Absorption of microwaves occurs in materials or molecules that have either a permanent or an induced dipole moment [231]. The mechanism of this absorption is called dielectric heating. The electric and magnetic force parts of the microwave rapidly change direction at a rate of 2.4×10^9 per sec. When microwaves are absorbed by such materials, the microwaves induce atomic motion (rotation). The molecules try to move with the oscillations, albeit with a slight lag. With each movement of the molecule, the molecule can freely rotate or can collide to interact with a neighboring molecule. It is this collision and subsequent rotation which converts the electromagnetic energy into kinetic energy, manifested as thermal heat. During this 'dielectric coupling' energy can be lost; this is described as dielectric loss. This occurs throughout the entire substance as long as certain penetrating depths of microwaves into the medium are maintained. This method differs from traditional conduction heating methods where the heat travels as a gradient through the material being heated.

Materials are compared according to their ability to absorb microwaves and efficiently transfer electromagnetic energy. This ability is expressed using the individual loss tangent (tan δ) [231]. A high loss tangent value indicates that the material is able to absorb microwaves and generate heat efficiently. This value is calculated using the following equation [231],

$$\tan \delta = \varepsilon' / \varepsilon''$$

where ε', relative permittivity, is the ability of a molecule to be polarized by an electric field and ε'', the dielectric loss value, describes the ability of the material to convert dielectric energy into heat. As such, tan δ is used to define the ability of a material to convert electromagnetic energy into heat energy at a specified temperature, frequency of the electromagnetic waves, physical state of the material, and composition of the material. A final consideration for using microwaves in reactions is that consideration must be given to the penetrating depth of the microwaves as well as to the volume and heat capacity of the reaction mixture.

The most often ascribed benefits of microwave-assisted reactions are reduced reaction times, improvement of yields and selectivity of products, and the ability to have solvent-less reactions or solid phase reactions [230]. These benefits are seen repeatedly in the literature and will be highlighted throughout this review.

Microwave-assisted reactions and synthesis have been applied to virtually every field of science and chemistry. The initial step when using microwaves in reaction synthesis is to determine if microwaves can be an effective method to generate product. Once this is determined and the process is optimized, the reaction process is simply treated as another option in the chemist's arsenal of reaction techniques.

While microwave and microwave oven technologies have developed since their first introduction in the 1940's, the first published works on the utilization of microwaves and the effect microwaves can have on matter did not appear until the late 1960s. The first uses of microwave-irradiation crosslinking focused primarily on microwave curing of polyurethane foams, resin coatings, or rubber in industrial uses, as this method appeared to result in uniform crosslinking. It was not until 1986, when two papers were

published in Tetrahedron Letters on using microwaves in chemical synthesis, that the use of microwaves began to expand [232, 233]. Both the Giguere paper and the Gedye paper were important in demonstrating that microwave irradiation was a viable chemical synthesis technique that could increase reaction rate and yield. Gedye showed that the microwave-assisted reactions had increased rates, ranging from 6 to 240 times the convention reaction times. In addition, percent yields of the microwave-assisted reactions were comparable to those of the conventional systems. The most dramatic of these was the S_N2 reaction of 4-cyanophenoxide ion with benzyl chloride, in which the classical synthesis reaction time was 16 hr with an 89% yield, while the microwave synthesis reaction time was just 4 min to achieve a 93% yield, an overall rate increase of 240 times. Table 12 summarizes the reactions and the results.

Table 12. The results of the Gedye experiments show decreases in reaction time when microwave reaction times are compared to the classical reaction method reaction rates [232].

Reaction	Micro-wave Reaction Time and Yield, %	Classical Reaction Time and Yield (%)
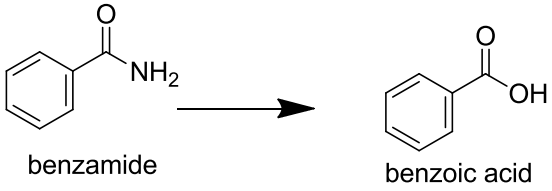	10 min, 99%	1 hr, 90%
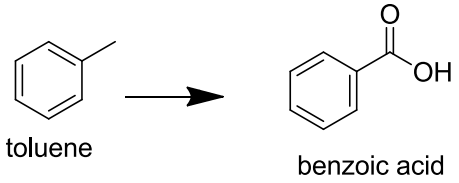	5 min, 40%	25 min, 40%
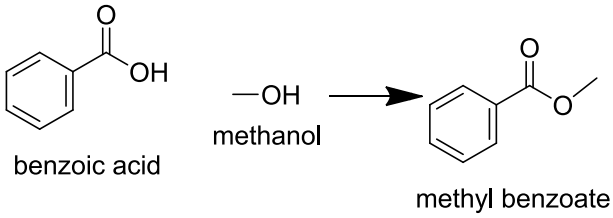	5 min, 76%	8 hr, 74%
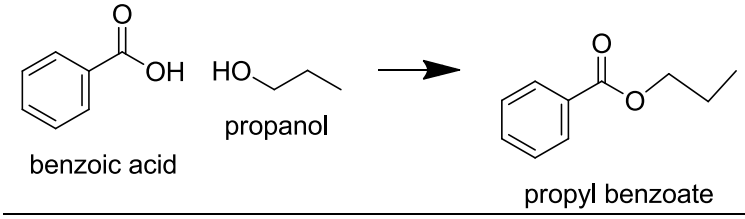	18 min, 86%	7.5 hr, 89%
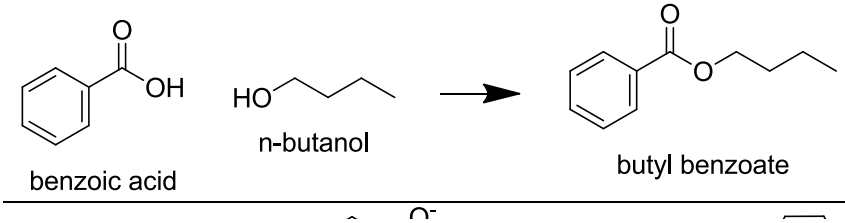	7.5 min, 79%	1 hr, 82%
	3 min, 74%; 4 min, 93%	12 hr, 72%; 16 hr, 89%

2.5.2 Microwave assisted reactions of cellulosic materials.

As a result of research such as the Gedye study, microwave irradiation became a research topic that was explored by a variety of industries, including the wood, pulp and paper, and, more recently, the biofuel industries. An early example of a microwave-assisted reaction involving non-solubilized cellulose was conducted by several groups who were interested in utilizing microwave irradiation to graft polymers to wood specimens to protect wood color [234, 235] and to impart anti-swelling properties [236] as well as to enhance the diffusion of chemicals from the wood surface [237]. Timar, Maher, Irle, and Mihai performed a two-step esterification on sawdust from Aspen wood Populus tremula where maleic anhydride was first esterified with sawdust using thermal treatment (120 °C). The sawdust was subsequently oligoesterified with glycidyl methacrylate and maleic anhydride in order to compare conventional heating and microwave irradiation [238]. Similar results, including degree of modification and physical properties, were obtained for both conventional heating and microwave irradiation; the microwave irradiation reaction time was approximately half that of the conventional heating, 3-4 h versus 7 h, respectively.

Microwave irradiation of bio-based materials, such as lignocellulosics, for the improved extraction of sugars, lignins, and other compounds contained within these biomaterials has been of most recent interest. A variety of cellulose sources has explored, including sugar beet pulp, kenaf pulp, sugarcane bagasse, corn stover, and wheat straw [239-244]. This has come under further scrutiny as methods to decrease the recalcitrance of separation of the lignin from cellulose and hemicellulose are becoming

especially important in finding ways to utilize woody materials for petroleum-substitute products.

There has also been interest in using microwave irradiation in the processing of pulps. For example, microwave irradiation of wood pulps has been explored as a method of bleaching. Wan approached bleaching thermomechanical pulp (TMP) using non-alkaline bleaching methods (hydrogen peroxide and magnesium carbonate) by irradiating 93% consistency TMP pulp samples using a 2.4 GHz microwave at 300 W for 90 sec [245]. This method was successful in increasing the brightness of the TMP by 20 – 25 points, a significant improvement. Wu, Zhao, Li, and Chen were successful in utilizing microwave irradiation in the hydrogen peroxide bleaching of soda-anthroquinone wheat straw pulp. While demonstrated improvements in pulp brightness were observed when were compared to traditional methods, the microwave bleached-pulp had lower fiber lengths [246].

Chadlia and Farouk formed ester linkages via microwave irradiation between cyclic anhydrides (such as maleic, succinic, and pthalic anhydrides) and cellulose extracted from *Posidonia* [247]. Esterification of the solubilized cellulose, using the LiCl/DMAc system, was optimized at 160 W for 10 min using an organic catalyst, an inorganic catalyst, and no catalyst, with the goal of reducing reaction time and increasing reaction efficiency. Ultimately, DMAP (the organic catalyst) resulted in the highest percent grafting of the anhyrides to the cellulose, while $CaCO_3$ (the inorganic catalyst) performed slightly less efficiently, and no catalyst was the least effective. The microwave-assisted esterification was achieved in 10 min at 160 W, a significantly lower

reaction time than the traditional conventional heating process, which took 12 h at 130 °C.

Satge used microwave irradiation to esterify solubilized cellulose with long-chain acyl chlorides using N,N-dimethylaminopyridine (II) as a catalyst (Figure 16) in a typical acylation reaction via an electrophilic substitution mechanism [248]. The reactants were microwave-irradiated for 1 min at 300 W. As the same reaction procedure under conventional heating procedures can take anywhere from 30 min to 2 days, this was a successful application of microwave irradiation in chemical synthesis in terms of reaction efficiency improvement.

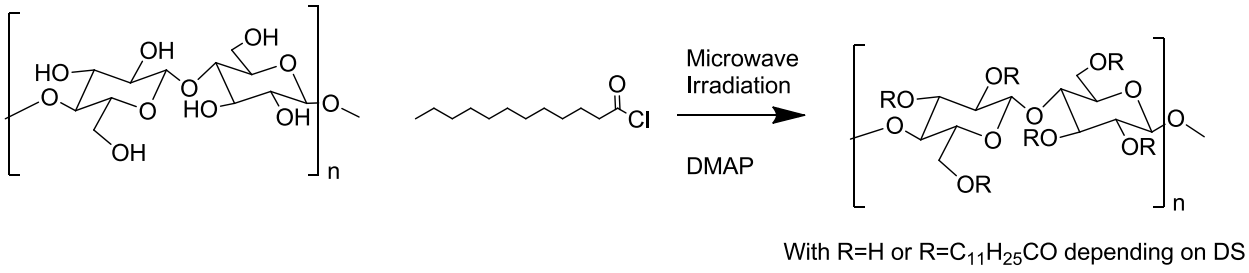

Figure 16. Microwave irradiation at 300 W and 1 min resulted in esterified cellulose with long-chain acyl chlorides [248].

Successful microwave irradiation of cellulose sources solubilized in Li/DMAC has included Takano, Ishikawa, Kamitakahara, and Nakatsubo's study, in which they used solubilized microcrystalline cellulose as a reactant to produce 6-amino-6-deoxycellulose [249].

Another method of microwave-initiated homogeneous cellulosic reactions is the use of microwave irradiation to assist in dissolving cellulose in ionic liquids [250]. Common ionic liquids used as cellulose solvents include 1-butyl-3-methylinidazolium chloride and 1-allyl-3-ethylimidazolium chloride (Figure 17).

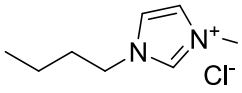

1-N-butyl-3-methylimidazolium chloride

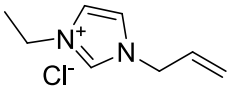

1-allyl-3-ethylimidazolium chloride

Figure 17. Commonly used ionic liquids to solubilize cellulose with microwave irradiation [250].

Lin, Zhan, Liu, Fu, and Huang were successful in grafting acrylic acid onto cellulose that was solubilized using the ionic liquid 1-butyl-3-methylinidazolium chloride for the purpose of creating an adsorbent to remove Cu^{2+} ions from wastewater [251]. Lin et al. used microwave irradiation both to solubilize the cellulose in the ionic liquid and for the reaction of the grafting of the acrylic acid to the cellulose with ammonium persulfate as the initiator and N,N'-methylenebisacrylamide as the crosslinker. The reaction time of the acrylic acid grafting was reduced from 2 h to 3 min. Figure 18 shows the reactants used in this reaction.

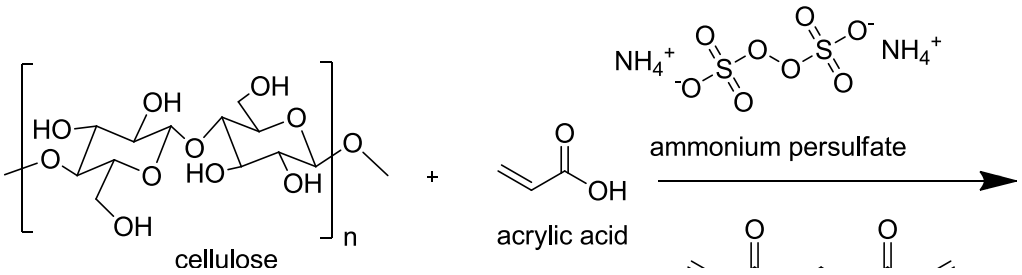

Figure 18. Reactants used by Lin, Zhan, Liu, Fu, and Huang to graft acrylic acid to cellulose using microwave irradiation [251].

Other groups have explored similar microwave reactions with ionic liquids, cellulose and grafting agents with similar results of decreased reaction times. Reduced reaction times and enhanced selectivity for microwave irradiation of cellulosics are reported benefits of this technology. For example, Satge, Granet, Verneuil, Branland, and Krausz have successfully esterified soluble microcrystalline cellulose with 4-dimethylaminopyridine and lauroyl chloride using microwave irradiation to reduce to 1 min reaction times that ranged initially from 0.5 h – 48 h [248].

One of the benefits of microwave irradiation is that it allows for research into fields such as grafting onto cellulosic fibers. There has been some research work in this field utilizing microwave irradiation; however, this research has been not nearly as extensive as the studies of homogeneous reactions of solubilized cellulose described in the section above. This thesis work will utilize this capability of heterogeneous non-solvent microwave reactions.

Li, Zhang, Peng, Bian, Yuan, Xu and Sun optimized the microwave-assisted solvent-free acetylation of cellulose with acetic anhydride and using iodine as a Lewis acid catalyst (Figure 19) [252]. This reaction was optimized for microwave irradiation power (300 – 800 W), reaction time (5 min – 40 min), reaction temperature (80 – 130 C), and catalyst concentration (1 – 15 mol%). Reaction conditions were optimized to 30 min at 400 W, with the values of the reactants being 0.4075 g cellulose, 10 ml acetic anhydride, and 5 mol% iodine as catalyst. It was determined in the optimization process for this reaction that reaction time and temperature had a greater influence on the degree of substitution (DS) than the microwave power did. These conditions resulted in a yield

of 35%, determined as increase in grams of the acylated cellulose per gram of starting cellulose.

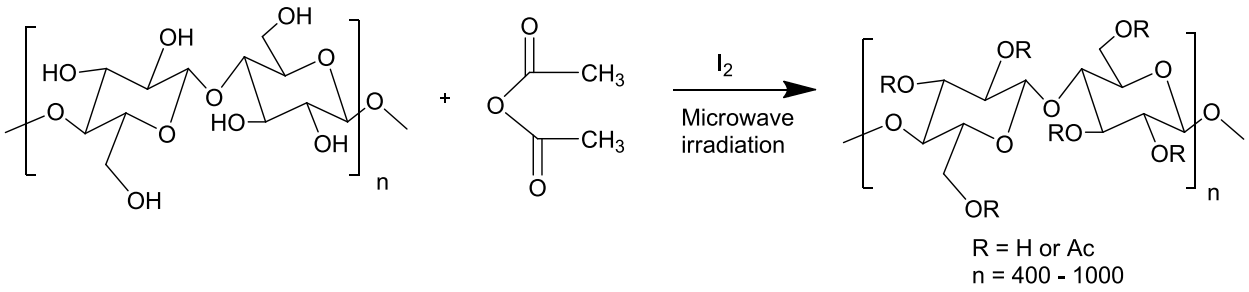

Figure 19. Li et al. successfully acylated cellulose with acetic anhydride using microwave irradiation [252].

Lin, Chen, Huang, Dufresne and Chang grafted polycaprolactone to cellulose whiskers using a ring-opening polymerization procedure and microwave irradiation with an ultimate goal of improving the mechanical properties of polylactic acid by incorporating these grafted whiskers with the PLA matrix [253]. Improvement of the mechanical properties was demonstrated, with an optimal incorporation by weight of 8%, an improvement of 1.9 times strength and 10.7 times elongation over neat PLA.

Feng, Li, and Wang grafted polymerized acrylic acid to flax shive cellulose with microwave irradiation using KPS and N,N'-methylenebisacrylamide as a crosslinking agent [254]. The crosslinked fibers demonstrated good effectiveness as superabsorbents for water as well as NaCl, KCl, $FeCl_3$, and urine solutions with absorbency values of 1000 g/g, 56.47 g/g, 54.71 g/g, 9.89 g/g and 797.21 g/g, respectively.

Yang, Mao, Lu, Ran, Gu, and Liu esterified Luffa cellulose with acetic anhydride and compared the esterification degree of microwave and thermal mechanisms [255].

The microwave reaction time of 20 min was dramatically lower than the hot oil heating esterification method reaction time of 90 min. In addition, the microwave reaction method was determined via FT-IR analysis to be a more effective esterification reaction method than the conventional oil bath.

Wan described the microwave irradiation grafting of methylmethacrylate onto bamboo-sourced cellulose using ceric ammonium nitrate as the initiator [256]. Antova, Vasvasova, and Zlatanov synthesized cellulose stearate via a transesterification reaction of low molecular weight microcrystalline cellulose and methyl stearate [257]. Zhao investigated grafting of acrylamide and acrylic acid to cellulose via microwave irradiation in preparing a material to adsorb copper (II) from wastewater [258]. Similarly, Matahwa et al. utilized microwave irradiation to graft polymerize N-isopropyl acrylamide and methyl acrylate to alpha-cellulose with cerium (IV) ammonium nitrate and potassium persulfate (KPS) as the initiating system [259]. Guo et al. synthesized cellulose carbamate utilizing microwave irradiation at 255 W for 2-5 min [260]. Kaith et al. grafted methyl methacrylate onto Saccharum spontaneum (wild sugarcane grass native to southeast Asia) L. fibers [261]. The grafting efficiency was maximized to 62.3% with reaction parameters of time, initiator molar ratio, monomer concentration, microwave power, pH, and solvent optimized. The resulting fibers were moisture-resistant and further characterized using FT-IR, SEM, XRD, TGA, DTA, and DTG.

There have been microwave-assisted reactions in a variety of fields and methods, with excellent examples of the broadness of scope of microwave-assisted reactions. However, the use of microwave-assisted irradiation reactions to create hydrogels or

superabsorbent polymers using wood pulp fibers has been investigated by few research groups, a gap in the body of research which this thesis work addresses.

CHAPTER THREE

EXPERIMENTAL MATERIALS AND METHODS

3.1 Materials.

3.1.1 Chemicals.

Poly(methyl vinyl ether-co-maleic acid) (PMVEMA) (MW1.98 x 10^6) was donated by ISP Corp. New Jersey, under the trade name Gantrez S-97, in dry powder form. Polyethylene glycol (PEG) (MW 3350) was purchased from VWR, USA. Both were used without further purification. Microcrystalline cellulose (VIVAPUR® 105) was acquired from JRS Pharma (Germany) and used without further modification to produce cellulose nanowhiskers. All other chemicals, including NaOH pellets and 1 M NaOH, concentrated H_2SO_4, 1 M HCl were purchased from Aldrich or VWR and used as received. Water used in all experiments was distilled or deionized water and is noted as such in the experimental procedures.

3.1.2 Pulp.

Paper mill produced fully bleached ECF (elemental chlorine free) kraft never dried birch pulp, donated by Metso Inc, Botnia, Finland was used as the source birch pulp. The birch pulp fiber was in never-dry sheet form stored in a sealed plastic bag in the pulp refrigerator (40 °C) and used as-is for the pulp fiber hydrogel materials. Commercial ECF (elemental chlorine free) bleached southern softwood kraft pulp was used as a source of softwood cellulosic fibers. The softwood pulp fiber was originally in air dry sheet form. To prepare it for use, it was wetted in excess water, mechanically agitated by stirring with magnetic stir bar, air dried and stored in plastic sealed bags. The

birch pulp and the air dry softwood pulps were mechanically milled using the Wiley Mill Grinder, USA. Pieces of pulp were added to the grinder, milled, collected, and analyzed using the Fiber Quality Analyzer (FQA) as shown in Figure 20. After milling, milled pulps were stored until further use. Figure 21 visually compares the starting softwood pulp with the milled softwood pulp.

Figure 20. Birch and mixed softwood pulp fibers were added to the Wiley mill, milled to a consistent size, and collected in a plastic bag for future storage.

Figure 21. The size contrast between the starting softwood pulp fibers and the milled softwood pulp fibers is visually obvious and were confirmed using the Fiber Quality Analyzer.

3.1.2.1 Fiber analysis using the Fiber Quality Analyzer.

Pulp fibers, milled pulp fibers, and crosslinked pulp fibers were all analyzed using the Fiber Quality Analyzer (FQA), (Optest Equipment, Hawkesbury, Canada) following procedures described in the operating manual, Fiber Quality Analyzer, Code LDA96, (Figure 22). Representative samples were mixed with D.I. water (~0.0008% consistency) and injected into the FQA. Results were analyzed based on tests of 5000 counted fibers and included average length, kink, and percent fines. Average fiber length was determined using an internal proprietary image analysis program and the fiber length (mm) as calculated via length weighted averaging is presented in Table 13.

Table 13. Fiber size, length weighed, for the fibers and the Wiley-milled fibers.

Fiber description	**Fiber length (mm) (length weighted)**
Bleached mixed softwood pine fibers	2.499
Wiley milled bleached mixed softwood pine fibers	0.450
Bleached birch fibers	0.962
Wiley milled bleached birch fibers	0.500

Figure 22. The Fiber Quality Analyzer was used to determine size of starting pulp fibers and milled pulp fibers.

3.2 Experimental procedures for the preparation of the pulp fiber hydrogels materials.

3.2.1 Preparation of water absorbing pulp fibers.

PMVEMA (3.350 g) and PEG (0.5000 g) was added to D.I. water (40.00 mL) preheated to 68 °C and acidified to pH 2 with 1.00 N HCl. ECF bleached softwood was then added and mixed at room temperature until a viscous slurry resulted, approximately 3-5 min. Three compositions were prepared and classified based on the percent PMVEMA used by mass and described based on the percentage of PMVEMA (i.e., 32%, 49%, and 66%). Table 14 further describes how the mass of pulp to PMVEMA and PEG were varied. This procedure was repeated to prepare crosslinked hydrogel materials with the birch kraft pulp and both the milled ECF bleached SW kraft pulp and the milled birch kraft pulp. Further variations in component mixtures were also prepared to remove the PEG influence for comparison as described in Table 14.

Table 14. Name and composition of pulp hydrogels based on masses of pulp fibers, PMVEMA, and PEG.

Pulp (g)	PMVEMA (g)	PEG (g)
3.000	3.350	0.5000
3.000	1.675	0.5000
3.000	6.700	0.5000
3.000	3.350	0.0000
3.000	1.675	0.0000
3.000	6.700	0.0000

The slurry was spread (~ 3 mm) on to an aluminum foil sheet or aluminum tray, air dried, removed from the aluminum foil and then cured in either a microwave (Hobart, 1600 W) or thermal convection oven. Example photos of the dried and crosslinked milled birch pulp at this experimental step is shown in Figure 23.

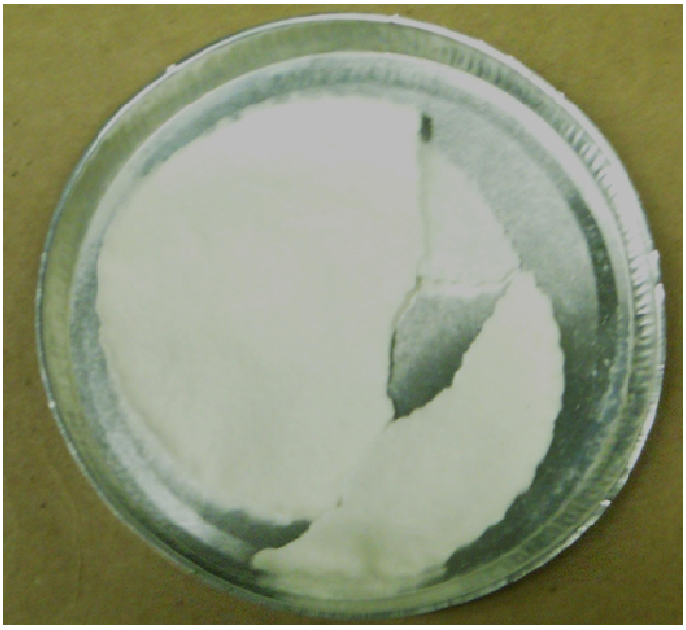

Figure 23. Example of crosslinked milled birch - PMVEMA-PEG dry slurry.

The curing condition for the convection oven was 6.5 min at 130 °C. The microwave curing conditions were optimized to an irradiation time of 105 sec at 1600 W by

repeating the preparation of the 49PMVEMA-pine pulp and repeating the experimental conditions by varying microwave irradiation time and microwave power. The samples were then wetted in deionized water (500.0 ml) and the pH of the solution was adjusted to pH 2.00, dispersed using a blender for 60 sec, and rinsed with water (1 l), and collected via suction filtration. The collected fibers were dispersed in water (500.0 ml) and the solution pH of this mixture was raised drop-wise to pH 8.50 (1.00 M NaOH, VWR), collected and freeze dried for further characterization. This is outlined in the following flow diagram (Figure 24).

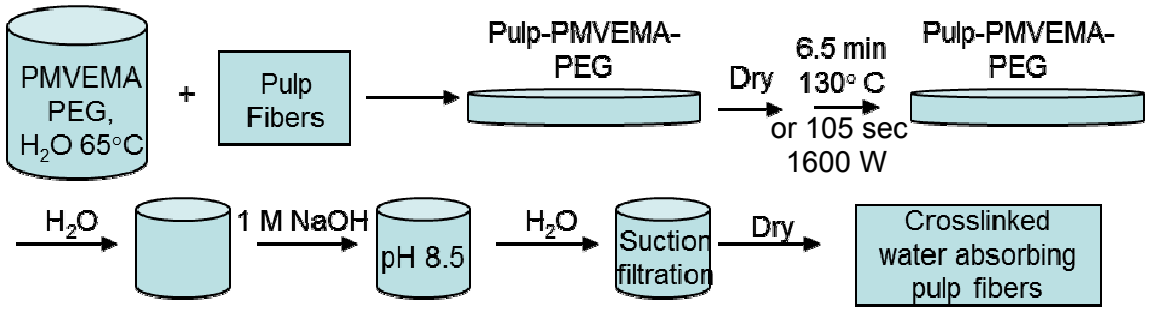

Figure 24. General flow diagram detailing the experimental steps in the preparation of crosslinked ECF bleached kraft pulp fiber hydrogels**.**

To freeze dry the samples, the collected water absorbent fibers were placed in HDPE (plastic) containers, allowed to freeze completely in a lab refrigerator for at least 24 h at °C, and then placed in the freeze dryer until completely dry, generally requiring 3-5 days. An example of the final freeze dried product is shown in Figure 25.

Figure 25. An example of the freeze dried crosslinked pulp fibers is shown.

3.2.2 Water and 0.1 M NaCl absorption and retention – Tea Bag method.

Water and 0.10 M NaCl sorption measurements of the crosslinked pulps and milled pulp were conducted using the traditional tea bag test method [262]. Briefly, 0.1000 g (oven dry g) sample (W_1) was added to a tea bag, heat sealed, weighed (W_2), and immersed in deionized water or a 0.10 M NaCl aqueous solution for 8 h (Figure 26).

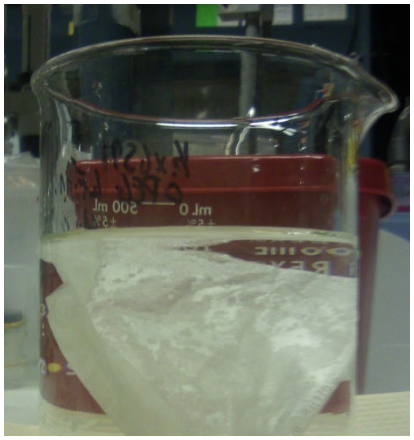

Figure 26. A sealed teabag with crosslinked pulp - PMVEMA-PEG is immersed in deionized water in a glass beaker.

The tea bag was subsequently allowed to drip dry for 10 min and weighed (W_3). A Beckman centrifuge was then used to centrifuge the tea bags at 770 rpm for 10 min and re-weighed (W_4) to calculate the retention value. The tea bag was dried in an 105 °C oven and was re-weighed for a final mass (W_5). The total water absorbed was calculated based on the following equation and is reported as g absorbed per g dry hydrogel (g/g).

Absorption Value

$$\frac{W_3-(W_1+W_2)}{W_5-W_2}$$

The retention value was calculated similarly and reported as g retained per g dry hydrogel (g/g). Replicates were measured and the average is reported with the error stated as the calculated standard deviation of all replicates.

Retention Value

$$\frac{W_4-(W_1+W_2)}{W_5-W_2}$$

The percent retained is the average retention value divided by the average absorption value and multiplied by 100%. Student's t-test calculations were also conducted to assure statistical relevance.

3.2.3 Scanning electron microscopy.

Representative samples of starting pulp fibers and freeze dried crosslinked hydrogels were mounted on stubs and gold sputter coated prior to imaging. The fiber surfaces were imaged with a LEO 1530 thermally-assisted field emission (TFE) SEM with a 10 keV acceleration voltage and a Hitachi S800 field emission gun SEM with a 15 and 20 keV acceleration voltage.

3.2.4 Inverted light microscopy.

A Leica DM-IRM Inverted Light microscope (Leica Microsystems GmbH, Germany) was used to compare the starting and crosslinked fibers in both the dry and swollen state. Dry fibers were placed onto standard glass microscope slides and a glass coverslip placed onto the fibers. Pictures were taken using a Hamamatsu ORCA-ER digital camera that was connected directly to the computer. A 50 W metal halide lamp was used as necessary. Magnification was 10x or 40x with a correction collar for the glass slide. Fibers were wetted and then placed onto the slides and imaged and dry fibers were placed on the slides, imaged, and drops of water were added to the slides to observe swelling of the fibers from dry to wet state.

3.2.5 FT-IR analysis of pulp fibers and crosslinked fibers.

A Nicolet Magna-IR^{TM} 550 Spectrometer FT-IR in transmission mode was used to collect the infrared spectroscopy data. Resolution for the infrared spectra was 4 cm^{-1} with 128 scans for each spectrum taken from 400 cm^{-1} to 4000 cm^{-1}.The fibers and crosslinked fibers was soaked in 0.10 M NaOH solution for 5 min, air dried and mixed using a mortar and pestle with 0.5 g KBr powder to obtain an IR spectra [263]. A second set were mixed using a mortar and pestle with KBr powder to obtain a comparison spectra. KBr pellets were prepared by mixing pre-packaged and measured 0.5 g KBr, mixed with a mortar and pestle for at least 1 min, and then the resulting mixture placed into a pellet press. Pellets were uniformly pressed to 20,000 psi for 2 min.

3.2.6 Soxhlet extraction to determine grafting ratio.

The grafting ratio and efficiency were evaluated using a Soxhlet extraction procedure in which 0.25 g of the crosslinked pulps were placed into a Whatman 603 cellulose thimble, washed with deionized water for 15 h, dried in a 105 °C oven for at least 8 h, and weighed. The percentage of the starting material that remained after the Soxhlet extraction was determined using the following equation:

$$\frac{SW_1 - SW_2}{SW_1} \times 100\%,$$

where SW_1 is the initial sample mass, and SW_2, is the sample mass after Soxhlet extraction.

The estimated grafting ratio was determined using the following formula:

$$\frac{SW_2 - P\%*SW_1}{PMP\%*SW_1} \times 100\%,$$

where P% is the theoretical percentage of pulp in the crosslinked pulp, and PMP% is the theoretical percentage of PMA/PEG in the crosslinked pulp.

3.3 Preparation of cellulose whisker crosslinked hydrogels.

3.3.1 Preparation of cellulose whiskers with microcrystalline cellulose.

Cellulose nanowhiskers were isolated from microcrystalline cellulose ((VIVAPUR® 105, JRS Pharma) by acid hydrolysis with 63% H_2SO_4 resulting in a 40% yield based on the procedure reported by Bondeson, Mathew and Oksman [67]. Microcrystalline cellulose (MCC) (120.00 g) was added to 598 ml deionized water. This was placed in an ice bath and a mechanical stirrer was used to mix the slurry.

Concentrated sulfuric acid (602.0 ml) was added dropwise to ensure that the mixture did not become overheated. This final mixture was then heated on a hot plate to a temperature of 45 °C for 130 min. To stop the reaction, excess deionized water (~10-fold the volume of the reaction solution) was added to the mixture, allowing the hydrolyzed cellulose to settle to the bottom of the container. The excess supernatant was carefully removed to ensure limited transfer of the hydrolyzed cellulose.

The remaining hydrolyzed cellulose in solution was centrifuged for 10 min at 14,000 rpm. The supernatant was removed and replaced with fresh deionized water. The sediment and the fresh deionized water were then thoroughly mixed so that the sediment was dispersed throughout the solution. This was then re-centrifuged for 5 min at 10,000 rpm and the process repeated where the removal of the supernatant, addition of fresh deionized water, and centrifugation was repeated three times to remove the excess acid. The collected sediment was placed into dialysis membrane tubing (SpectraPor, molecular weight cutoff of 25,000) to dialyze against deionized water to further remove excess acid and to raise the pH. The deionized water was replaced as needed via monitoring the pH of the bath water. The dialysis was further enhanced by placing a stir bar in the room temperature water bath to circulate the water.

After dialyzing for 24 h, the contents were added to a beaker and magnetically mixed with Amberlite MB150, Mixed Bed Resin ion exchange beads (Rohm and Haas, Philadelphia, PA USA) with a stir bar to raise the pH to pH 6. After the Amberlite settled to the bottom of the beaker and the magnetic stir bar was removed, the whisker solution was decanted into a second beaker, which was placed into an ice bath and probe sonicated for 20 min.

The sonicated whisker mixture was centrifuged for 5 min at 14,000 rpm and the cloudy supernatant collected and saved. The remaining sediment was mixed with distilled water, sonicated, and centrifuged again for 5 min at 14,000. This process was repeated until no cloudy supernatant is formed.

The collected cloudy supernatant (the whiskers) are concentrated by dialyzing the suspension in dialysis tubing (SpectraPor, MWCO 25,000) against a polyethylene glycol (MW35000) solution with the amount of polyethylene glycol added as needed until the desired concentration of whiskers is reached [143]. The final concentrated whiskers are removed from the dialysis tubes and stored in the refrigerator for future use. A flow diagram of this process is shown in Figure 27.

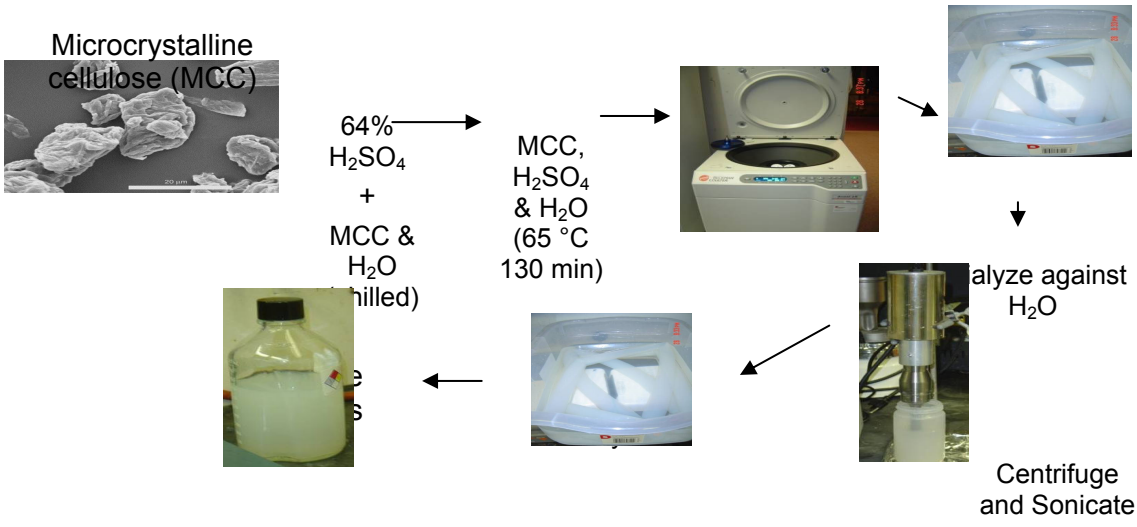

Figure 27. Flow chart of the method for preparing cellulose whiskers.

3.3.2 Characterization of cellulose whiskers.

3.3.2.1 Flow birefringence of cellulose whisker solutions.

A solution of whiskers was viewed through cross-polarized light filters cut from a lab stock polarized film sheet to observe the presence of birefringence using a setup similar to that in the figure below [264] (Figure 28). Briefly, a dilute whisker solution was placed on a magnetic stir plate between two polarized light films (8 cm x 8 cm) that were cross-polarized arranged (VWR, USA). While the solution was stirring, a tungsten filament generating unpolarized light was shined through one filter, through the stirring solution, and through the other filter. Birefringence was observed and photographed using a digital camera.

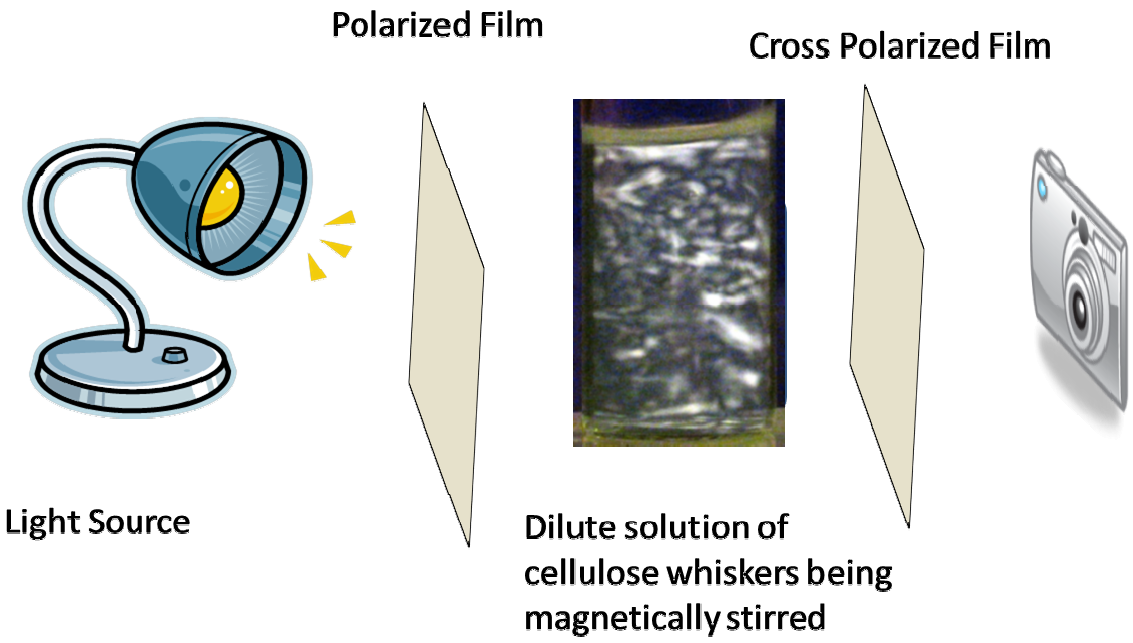

Figure 28. The birefringent properties of cellulose nanowhiskers were observed by viewing the whisker solution through cross polarized films.

3.3.3 Preparation of crosslinked cellulose whisker film hydrogels.

The procedure for preparing the PMVEMA-PEG/CNW nanocomposite hydrogels is described as follows. A 6.700:1.000 mass ratio of PMVEMA:PEG (3.850 g) was added to deionized water (40.00 mL) preheated to 68 °C and acidified to pH 2.00 with 1.00 N HCl. The reaction mixture was then thoroughly mixed with different concentrations of cellulose whiskers (CNW). Five compositions were prepared and classified based on the percent cellulose whisker mass content in the resulting films including 0.000%, 25.00%, 50.00% 75.00%, and 100.0% cellulose whisker by mass. These films are described as 0CNW, 25 CNW, 50CNW, 75CNW, and 100CNW, respectively for simplification. Table 15 further details the compositions. Each

PMVEMA-PEG/CNW mixture was degassed, solution cast onto Teflon petri dishes, air dried overnight and then cured at 135.0°C for 6.50 min. After curing, the films were allowed to cool to room temperature and stored in a desiccator at varying relative humidity for future experimental testing. The relative humidity values were 2%, 54%, and 92% and were maintained using saturated salts. An unreacted control film of 50 wt-% whiskers-50 wt-% matrix was also prepared using the same method as the crosslinked nanocomposite hydrogels with the exception of not being cured.

Table 15. Composition of the PMVEMA-PEG/CNW nanocomposite hydrogels were classified by the percent of cellulose whiskers, by mass.

Sample Code	CNW, wt %	PMVEMA-PEG, wt %
0CNW	0.000	100.0
25CNW	25.00	75.00
50CNW	50.00	50.00
75CNW	75.00	25.00
100CNW	100.0	0.000

3.4 Characterization of crosslinked cellulose whisker hydrogels.

3.4.1 Fourier transform infrared spectroscopy.

A Nicolet Magna-IR^{TM} 550 Spectrometer FT-IR in transmission mode was used to collect the infrared spectroscopy data. Resolution for the infrared spectra was 4 cm^{-1} with 128 scans for each spectrum taken from 400 cm^{-1} to 4000 cm^{-1}.

One set of CNW films was soaked in 0.10 M NaOH solution for 5 min, air dried, ball milled for 1 min and mixed using a mortar and pestle with 0.5 g KBr powder to obtain an IR spectra [263]. A second set were ball milled for 1 min and mixed using a

mortar and pestle with KBr powder to obtain a comparison spectra. KBr pellets were prepared by mixing pre-packaged and measured 0.5 g KBr, mixed with a mortar and pestle for at least 1 min, and then the resulting mixture placed into a pellet press. Pellets were uniformly pressed to 20,000 psi for 2 min.

3.4.2 Nuclear magnetic resonance (NMR) analysis.

3.4.2.1 NMR analysis of starting materials.

PMVEMA, PEG, and PMVEMA-PEG were dissolved in DMSO-d_6 and analyzed as liquids ^{13}C and ^{1}H NMR in NMR tubes on the Bruker Avance-400 spectrometer operating at frequency of 100.59 MHz, with a 44.8 us dwell time, 1.468 sec acquisition time, and acquiring 10240 scans per sample.

3.4.2.2 NMR analysis of cellulose whisker films.

In preparation for NMR analysis, the nanocomposite hydrogels were Soxhlet extracted with water for 24 h to ensure removal of unreacted material. These were then oven dried and ball milled. The NMR samples were prepared by using samples conditioned at ambient air relative humidity/temperature or swelling the ball milled nanocomposites in 100% D_2O for 4 h and loading them into 4-mm cylindrical ceramic MAS rotors. Repetitive steps of packing the sample into the rotor were done to fully compress and load the maximum amount of sample.

^{13}C CP/MAS solid-state NMR measurements were carried out on samples conditioned at ambient air relative humidity/temperature on a Bruker DSX-400 spectrometer operating at frequencies of 100.55 MHz for ^{13}C in a Bruker double-

resonance MAS probe head at spinning speeds of 10 kHz. CP/MAS experiments utilized a 5 μs (90°) proton pulse, 1.5 ms contact pulse, 4 s recycle delay and 8000 scans.

^{1}H spin-spin (T_2) NMR experiments on samples swollen in 100% D_2O were performed on a Bruker DSX-400 spectrometer, operating at frequencies of 399.875 MHz for ^{1}H in a Bruker double-resonance MAS probe head at 2 kHz. A standard Carr-Purcell-Meiboom-Gill (CPMG) sequence with a τ = 50 us, utilized a 5 μs (90°) proton pulse, 2 s recycle delay and 128 scans. The resulting T_2 decay profiles were analyzed using a single-component exponential or two-component Gaussian-exponential model.

3.4.3 Atomic force microscopy. Cellulose whiskers and films.

The cellulose whiskers, as well as the nanocomposites, were characterized using a Veeco MultiMode scanning probe microscope with a Nanoscope V controller. For the analysis of CNWs, a droplet of the aqueous whisker suspension (0.5% by weight) was dried on a mica surface prior to AFM examination. Images (1μ x 1μ) of the whisker films were directly imaged using a tapping mode etched silicon tip, with a nominal spring constant of 5.0 N/m and a nominal frequency of 80 kHz. The nanocomposite hydrogels were embedded in epoxy and ultramicrotomed before using the AFM to map the morphology. The images from the cross-section of the nanocomposite samples were collected using a tapping mode etched silicon tip, with a nominal spring constant of 5 N/m and a nominal frequency of 270 kHz.

3.4.4 Tensile measurements of cellulose whisker films.

The tensile measurements were performed on an Instron 4411 (USA) with a 500 N load cell. Rectangular shaped strips (0.300 mm – 0.400 mm thickness) were cut from the nanocomposites. The gauge length was 25.0 mm and a stain rate of 5.0 mm/min was applied. The maximum strength and modulus were calculated. The values given are based on 5 tests per composition. The error in the measurements was reported as the standard deviation. An example of the test equipment and this test being performed is shown in Figure 29.

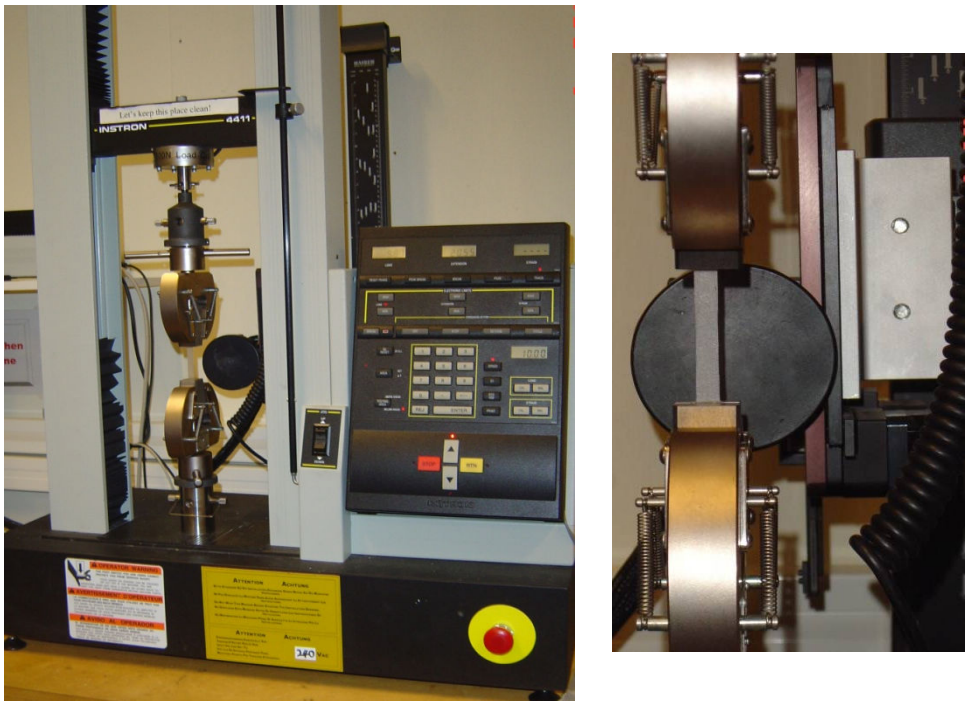

Figure 29. An Instron 4411 was used to determine physical properties of the crosslinked whisker films conditioned at three different relative humidities.

3.4.5 Water sorption studies. Whisker films.

The film samples used for water sorption studies were circular discs 20 mm in diameter, cut from films conditioned at 54% relative humidity [265]. The cut samples initial weight and dimensions were measured and recorded. After this, the discs were placed in excess (approximately 150 ml) deionized water at room temperature. The samples were removed at time intervals appropriate for each composition, gently blotted with KimWipe® paper to remove excess water on the surface of the films and weighed; the error due to evaporation was found to be insignificant. Three replicates were performed for each composition. This process was continued until equilibrium swelling was reached which is indicated by constant weight. The water uptake was then calculated using the following equation.

$$\text{Water Uptake} = \frac{M_r - M_i}{M_i} \times 100\%$$

M_r is the relative mass of the crosslinked composite and M_i is the initial mass of the 54% relative humidity conditioned sample. The maximum water uptake quantities were statistically analyzed using Student's t-test using the following parameters and equation.

$$t = \frac{\bar{x}_1 - \bar{x}_2}{s}$$, where

, where

n=number in each group,

s_1 = standard deviation of group one

s_2 = standard deviation of group two

$\bar{x}_1$ = mean of group one

$\bar{x}_2$ = mean of group two

3.4.6 Gel content of whisker films.

Gel content of the prepared films was measured using an adapted ASTM Standard 2765 [266]. One sample from each composition was cycled with water for three days, after which, the samples were removed, air dried, and weighed. Gel content was calculated with the following equation.

$$= [(W_3 - W_4)/((W_2 - W_1) - F(W_2 - W_1))] \times 100$$

$$= [(W_3 - W_4)/((1-F)(W_2 - W_1))] \times 100$$

where:

W_1 = weight of the mesh pouch, open

W_2 = weight of specimen and pouch open

W_3 = weight of specimen and pouch closed

W_4 = weight of specimen and pouch after extraction and drying

F = fraction of whiskers in film

Gel content = 100 – percent extract

3.4.7 Percent extractable content. Cellulose whisker films Soxhlet extraction.

Soxhlet extractions were carried out on the 0CNW, 25CNW, 50CNW, and 75CNW crosslinked films as well as an unreacted mixture of the 50CNW. The films (0.50 g) were Soxhlet extracted with deionized water for 24 h. The Soxhlet extraction was performed by placing a pre-weighed film sample with an average weight of 0.50 g into a 25 mm x 80 mm Soxhlet thimble. The thimble was then placed into an 85 ml capacity Soxhlet extraction apparatus, and the test was carried out for 24 h with deionized water at 100 °C. Upon completion, the disk sample was removed and placed in an 105 °C oven to dry. The samples were then re-weighed to calculate the percent extractable content.

3.4.8 Scanning electron microscopy. Solution cast cellulose whisker films.

Representative samples of the air dry solution cast crosslinked films (0CNW – 100CNW) were mounted on double-sided SEM tabs and stubs and gold sputter coated and imaged using a JEOL JSM-5200 SEM at 15 keV.

3.4.9 Scanning electron microscopy. Water swollen cellulose whisker films.

The 25CNW, 50CNW, and 75CNW films were placed in ~150 ml deionized water and freeze dried. The freeze dried films were then mounted on double-sided SEM

tabs and gold sputter coated. The water swollen films were imaged using a Hitachi S800 field emission gun SEM at 15 keV.

3.4.10 Thermogravimetric analysis.

Thermal properties analyses of the starting materials and the prepared films were performed on a TGA TA Instruments Q 500 (USA). Samples of 6–10 mg samples were heated from room temperature to a maximum temperature of 600 °C at a rate of 10 °C/min. The TGA tests are based on three measurements.

CHAPTER FOUR

COMPARISON OF THERMALLY-ASSISTED AND MICROWAVE-ASSISTED CROSSLINKING TECHNIQUES IN PREPARATION OF ENHANCED WATER ABSORBING POLYMER-GRAFTED ECF BLEACHED KRAFT SOFTWOOD PULP FIBERS[1]

4.1 Introduction.

There is great interest in developing new products from natural resources as sustainable alternatives to petroleum-derived products [17, 267-277]. Cellulose is one of the key natural resource building blocks being investigated as a potential source of sustainable biomaterials with the intention to reduce the global carbon footprint and serve as a key resource for biofuel production, as it is the most abundant naturally-occurring polymer [17, 272, 278-280].

The grafting of chemical reagents onto lignocellulosics has been examined to determine the effect of this process on the fibers. For example, the esterification of carboxylic acid with wood pulps and cotton has demonstrated that this is a promising approach to enhancing water absorption, increasing wet strength, and imparting anti-wrinkle properties [281-285]. Common reaction methods of preparing esterified cellulose fiber-based hydrogels have included free radical methods requiring catalysts such as ceric ion catalysts [286, 287], sodium hypophosphite methods [288, 289], and

---

[1] This work was published in the Journal of Applied Polymer Science as "Preparation of microwave-assisted polymer-grafted softwood kraft pulp fibers. Enhanced water absorbency." Journal of Applied Polymer Science (2011), 119 (1), 387-395. Other authors were Jessica R. Sladky and Arthur J. Ragauskas from the Institute of Paper Science and Technology and School of Chemistry and Biochemistry at Georgia Institute of Technology.

ATRP methods [290]. However, the esterification of cellulose with carboxylic acids using thermal curing methods has been successful without catalysts [228, 284, 291].

While poly (methyl vinyl ether co maleic acid) (PMVEMA) has been extensively used in oral care products under the trade name Gantrez S-97 [292-301], there has been interest in expanding its use to include other avenues, such as drug delivery [302-304] and cellulosic material applications [291]. Barcus and Bjorkquist initially developed a procedure for reacting PMVEMA and PEG with a variety of pulps using a thermally-initiated esterification reaction as an alternative method for grafting cellulose without the need for a metal catalyst [291]. The treated pulps were shown to absorb water with a range of absorption from 25 g/g to 90 g/g [291].

The use of microwave irradiation to induce multi-component polymerization reactions is a research topic of increasing interest [305]. It is already well-appreciated that microwave irradiation has a shorter reaction time than does traditional thermal treatment [232, 233]. For example, Satge, Granet, Verneuil, Branland and Krausz successfully esterified soluble microcrystalline cellulose with DMAP and lauroyl chloride using microwave irradiation time of 1 min, a significant reduction of the previous reaction time of up to 2 days [248]. The microwave irradiation of cellulose has been used to produce 6-amino-6-deoxycellulose [249], as well as to enable the esterification of cotton waste to produce cellulose laurate films [306], the transesterification of methyl esters of rapeseed oil with carboxymethylcellulose [307], and the graft polymerization of N-isopropyl acrylamide and methyl acrylate onto α-cellulose [308].

Microwave irradiation has been utilized in the processing of wood pulps. For example, the microwave irradiation of thermomechanical pulp was successful in increasing the brightness of the pulp by 20 – 25 points through bleaching with hydrogen peroxide and magnesium carbonate or calcium carbonate [309].

The use of microwave irradiation to facilitate the reaction of an ECF bleached kraft soft wood pulp and carboxylic acid containing a polymer such as PMVEMA has not been investigated. The aim of this study was to investigate whether microwave irradiation could be used to produce hydrophilic grafted softwood pulps, with water absorption properties comparable to those produced using thermal curing techniques, in a reduced reaction time.

4.2 Materials and methods.

Poly (methyl vinyl ether-co-maleic acid) (PMVEMA), poly (ethylene glycol) (PEG), and all other reagents used were described in Chapter 3 (Section 3.1.1 Chemicals) and used as received. Commercial ECF bleached southern softwood kraft pulp (0.863 mm arithmetic average fiber length) was used as a source of cellulosic fibers and is described in Chapter 3 (Section 3.1.2 Pulp). A sample of this pulp was mechanically milled using a Wiley mill to an average fiber length of 0.276 mm as described in Chapter 3 (Section 3.1.2 Pulp). Average fiber lengths were measured using a Fiber Quality Analyzer^{TM}, OpTest Equipment Inc., Canada as described in Chapter 3 (Section 3.1.2.1 Fiber Quality Analyzer).

4.2.1 Preparation of absorbent hydrogels.

The crosslinking procedure described in Chapter 3 (Section 3.2.1 Preparation of water absorbing fibers) was followed to prepare crosslinked hydrogel materials with ECF bleached SW kraft pulp and Wiley milled ECF bleached SW kraft pulp. Table 14 in Chapter 3 Section 3.2.1 describes how the mass of the pulp to PMVEMA and PEG was varied and classified the three compositions based on the percentage PMVEMA used by mass (i.e., 32% as 32PMVEMA, 49% as 49PMVEMA, and 66% as 66PMVEMA).

4.2.2 Characterization.

4.2.2.1 FT-IR.

The FT-IR spectra of the pulp, PMVEMA, PEG, and reaction products were obtained using the procedures in Chapter 3 (Section 3.2.5 FT-IR analysis of pulp fibers and crosslinked fibers) [263].

4.2.2.2 Grafting ratio.

The grafting ratio and efficiency were evaluated using a Soxhlet extraction procedure described in Chapter 3 (Section 3.2.6. Soxhlet extraction procedure to determine grafting ratio).

4.2.2.3 Water absorbency.

The water and 0.10 M NaCl sorption measurements of the crosslinked and milled pulps were conducted using the tea bag test method described in Chapter 3 (Section 3.2.2. Water and 0.1 M NaCl absorption and retention – tea bag method).

4.2.2.4 Scanning electron microscopy.

Freeze-dried pulp fibers and crosslinked hydrogels were imaged using SEM as described in Chapter 3 (Section 3.2.3. Scanning electron microscropy).

4.3 Results and discussion.

4.3.1 Preparation of the superabsorbent hydrogels – determination of microwave settings and reaction time.

The proposed final structure and the crosslinking reactions between the components and the final structure are shown in Figure 30 and Figure 31. The PMVEMA and pine pulps were expected to undergo an esterification reaction between the primary hydroxyl group of the cellulose and the acid group of the PMVEMA. The PEG was also expected to react with the PMVEMA in a second esterification reaction.

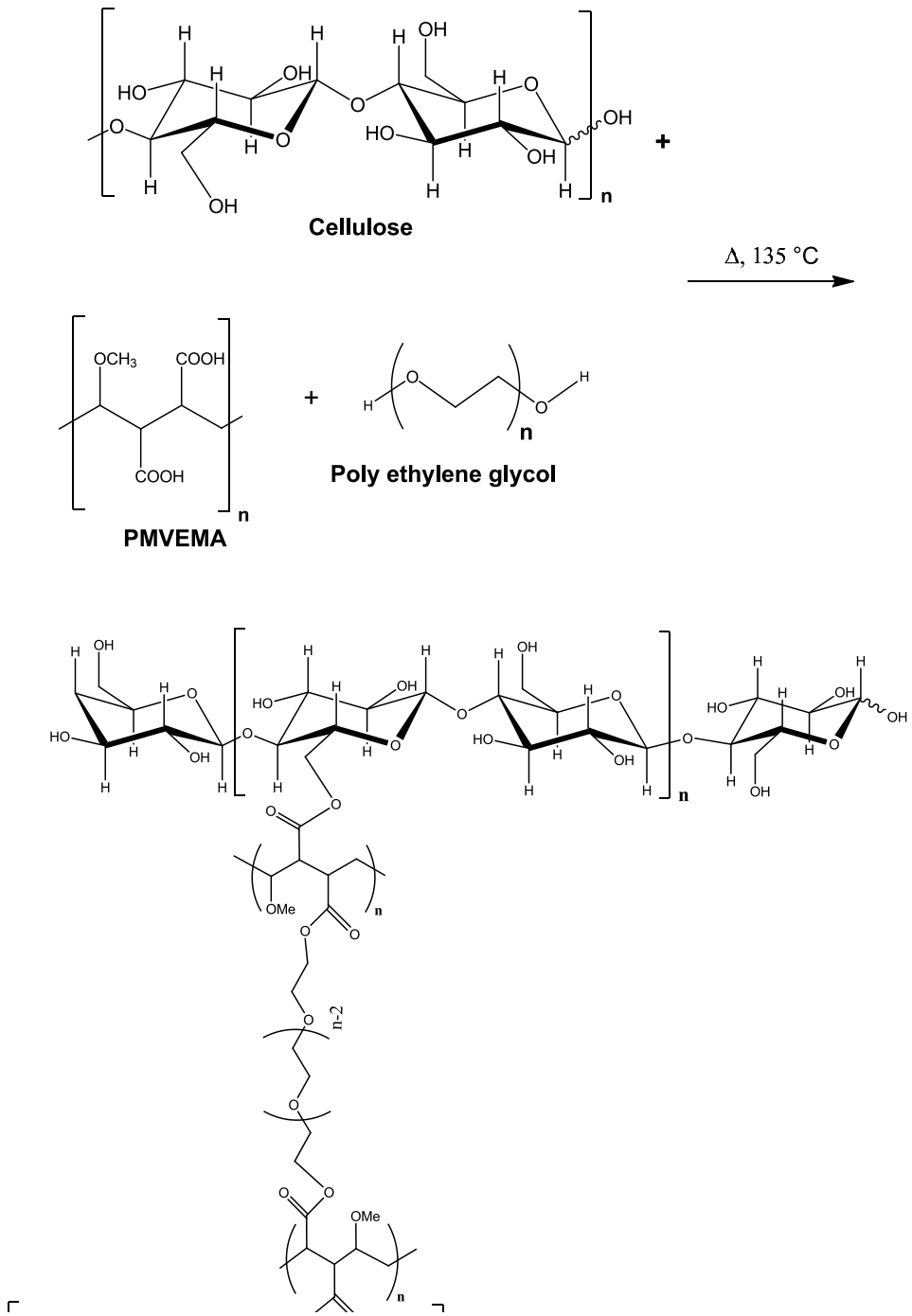

Figure 30. The proposed chemical structure of cellulose, PMVEMA, and PEG and the expected crosslinked cellulose fibers.

The expected reactions between the PMVEMA and the cellulose and between the PMVEMA and the PEG are Fischer-Speier esterification reactions, via a nucleophilic acyl substitution reaction mechanism, as shown in Figure 31, below. Hydrochloric acid protonates the carbonyl group oxygen rendering it more electrophilic and more reactive to nucleophilic attack by the nucleophilic oxygen of either PEG or cellulose (PEG shown in Figure 31). Upon nucleophilic attack, the tetrahedral intermediate is formed and a rapid proton rearrangement occurs upon the transfer of a proton from oxygen to a second oxygen creating a second tetrahedral intermediate. This converts the hydroxyl group into a good leaving group resulting in the removal of a proton and water, regenerating the acid catalyst and forming the esterification product between PMVEMA and PEG (shown) and PMVEMA and cellulose. The water is driven away as this reaction is occurring which drives the reaction to form the ester linkages.

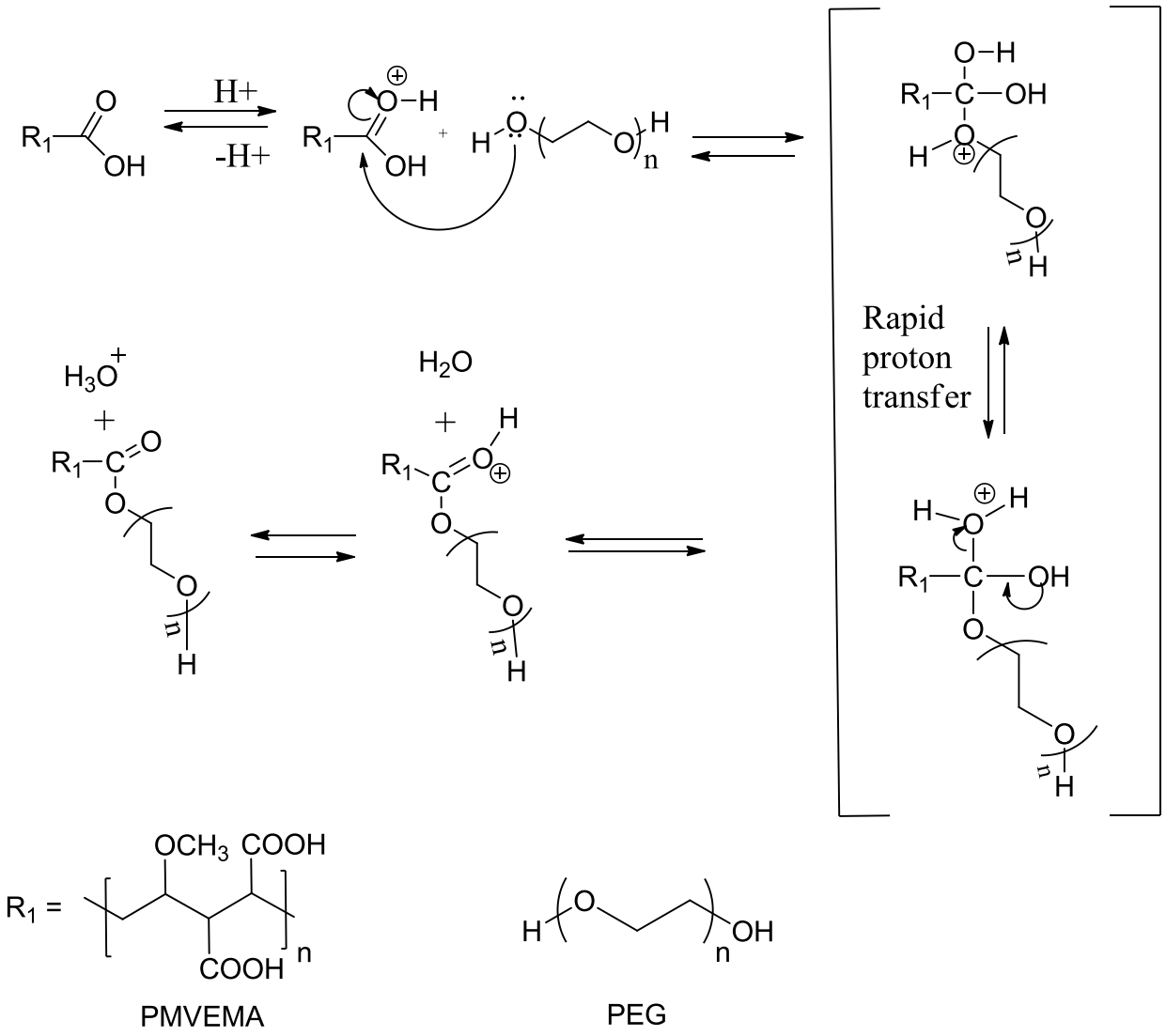

Figure 31 Proposed esterification mechanism in the crosslinking of PMVEMA, PEG, and cellulose [310].

These crosslinked fibers were predicted to be water absorbing primarily due to the hydrophilic properties of the PMVEMA bonded to the cellulose fibers with the PEG acting as spacing units with the PMVEMA. The crosslinking of the PMVEMA to the cellulose fibers allows these materials to be described as hydrogels; hydrogels are

typically defined as a three dimensional structure that is capable of absorbing water without dissolving into the water. Hydration occurs via hydrogen bonding of water molecules with the hydrophilic groups along the polymer chains, such as carboxylic acid groups. The hydrogen atoms of a water molecule are attracted to the lone pairs of electrons of the oxygen atoms. As oxygen atoms have two lone pairs of electrons, two water molecules are capable of hydrogen bonding with each oxygen atom. The ability of a hydrogel to absorb a liquid is a result of the polymer affinity for the solvent, the polymer complexity in not dissolving into the solvent, and also then of the ability of the polymer chains to move to allow the solvent molecules to interact with the polymer.

The thermodynamic model of water absorption described by Flory-Huggins, which attributes swelling to the change in Gibbs free energy of a polymer mixing with a solvent, is applicable in describing the crosslinked fibers prepared in this study. The Flory-Huggins theory describes gel swelling based on the sum of the effects of osmotic pressure (Π_{osm}), polymer elasticity (Π_{elas}), and the Donnan equilibrium (Π_{ion}) [311-313]. Osmotic pressure describes the initial rush of solvent into the dry gel that occurs when the gel is immersed in solvent. As there is more solvent outside of the polymer than there is inside, a pressure variant is created that leads to the solvent molecules being drawn into the gel network. The elasticity term refers to the ability of the polymer chains to move apart from one another as the solvent penetrates, with limitations due to crosslinking of the polymer chains. In this system, the covalent crosslinking between PMVEMA and PEG and between PMVEMA and cellulose is the predicted crosslinking. The Donnan equilibrium term describes how both disassociated ions of the hydrogel polymer system and ions in the solution can affect maximum swelling by acting as counter-ions and

shielding ions with the polymer through the formation of a double layer of fixed charges on the hydrogel pendant groups and ions inside of the gel [311].

Due to the interest in utilizing microwave technology to induce crosslinking to create water absorbing fibers, the microwave power settings and irradiation times were optimized for maximum water absorption capability. The optimal microwave power settings and microwave irradiation times were determined by varying the power (1600 W, 800 W, and 320W) and length of microwave irradiation. 49PMVEMA-bleached kraft fibers were prepared and microwave irradiated for 45-105 s at 1600 W (high), 60-180 s at 800 W (medium), and 120 -1200 s at 320 W (low) power. The final products were then evaluated based on the total water absorbed using the traditional tea bag test.

Water absorption and water retention are two separate methods of evaluating hydrogel behavior. Water interacting with hydrogels can be classified into three categories, free water, interstitial water, and bound water. Free water is water that is very lightly interacting with the hydrogel system; bound water is water that is hydrogen bounded to the polymer chains while interstitial water is trapped between the hydrated polymer chains [314],[315]. Water absorption describes the maximum swelling that a hydrogel is capable of achieving at the given conditions due to free, interstitial, and bound water. The water retention values describe how much water the hydrogel is capable of retaining after a force is applied to it. The free water is removed by this process, with the bound water and some interstitial water remaining.

Figure 32 shows the water absorption values for the pulps microwave irradiated at 800 W and 1600 W at various time intervals. After 105 s at 1600 W, the dried slurry started to char, and longer reaction times exacerbated this charring and decreased the

yield significantly. Similarly, the 320 W setting was not further evaluated when it was determined that after 600 sec and 1200 sec the water absorption of the crosslinking pulp fibers was only 38.9 g/g and 45.3 g/g, respectively, whereas the starting pulp had a value of 30 g/g. These water absorption values were significantly less than the maximums achieved with the 1600 W setting, and the irradiation time was greater than the thermal curing reaction time, making 320 W a dismissible setting.

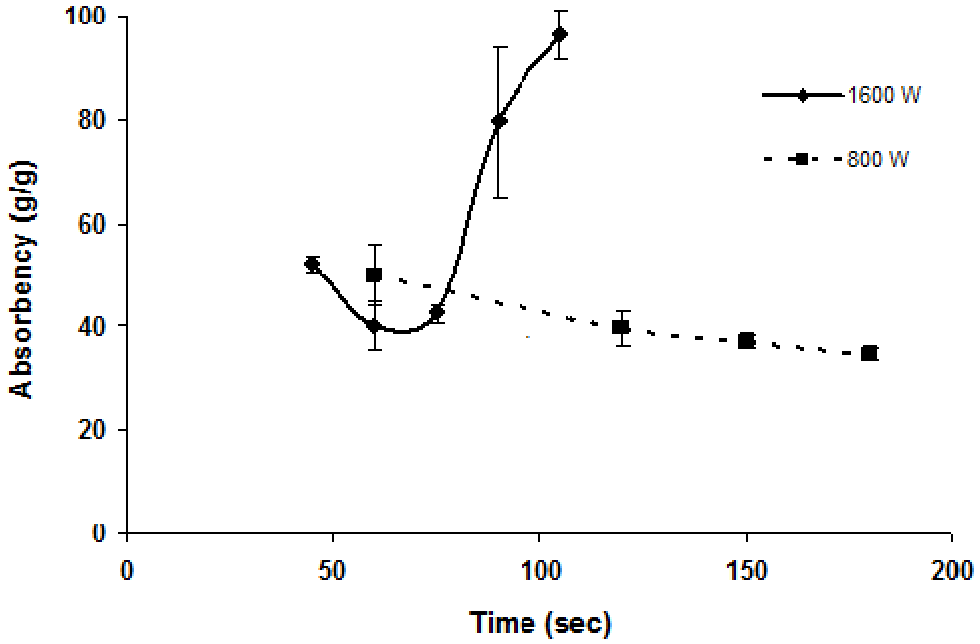

Figure 32. Effect of reaction time and power setting on the water absorption of 49PMVEMA-softwood kraft pulp hydrogels.

Figure 33 shows the water retention capabilities of the 49PMVEMA-kraft pulp-based hydrogels as microwave time and irradiation power level are varied. The water retention values of the pulps treated at 1600 W changed significantly based on the microwave reaction time, while the hydrogels treated at 800 W consistently decreased in terms of g/g water retained after centrifugation. Based on the water absorption and water

retention results, the optimal curing conditions were 105 s microwave irradiation at 1600 W.

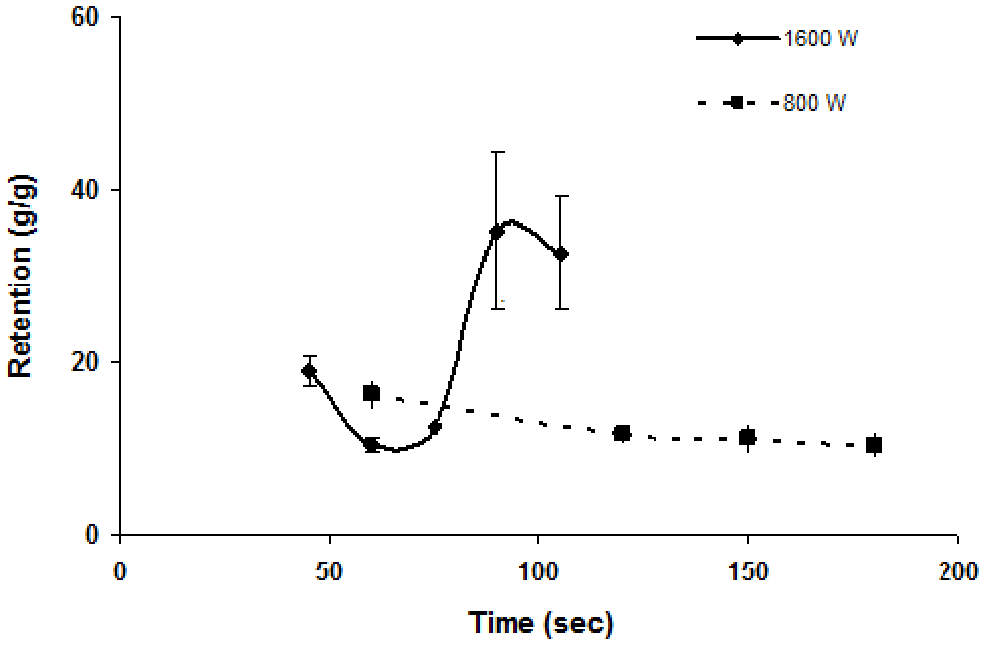

Figure 33. Effect of microwave irradiation time and power level on the water retention of 49PMVEMA-sotwood kraft pulp hydrogels.

The percent water retention describes the amount of water retained after centrifugation relative to the water absorption value. When evaluated as the percentage of water retained based on the amount of water that was initially absorbed, the 800 W irradiated pulps retained between 29 – 32% of their water (Figure 34). The 1600 W irradiated hydrogels varied considerably more as irradiation time increased. The pulp hydrogel that was irradiated for 90 s retained the maximum percentage of water (44%). These initial results show the influence that microwave irradiation time and power have on the reaction and formation of the PMVEMA-PEG-cellulose network and water absorption and retention. The reaction conditions chosen from this study were microwave irradiation at 1600 W for 105 sec.

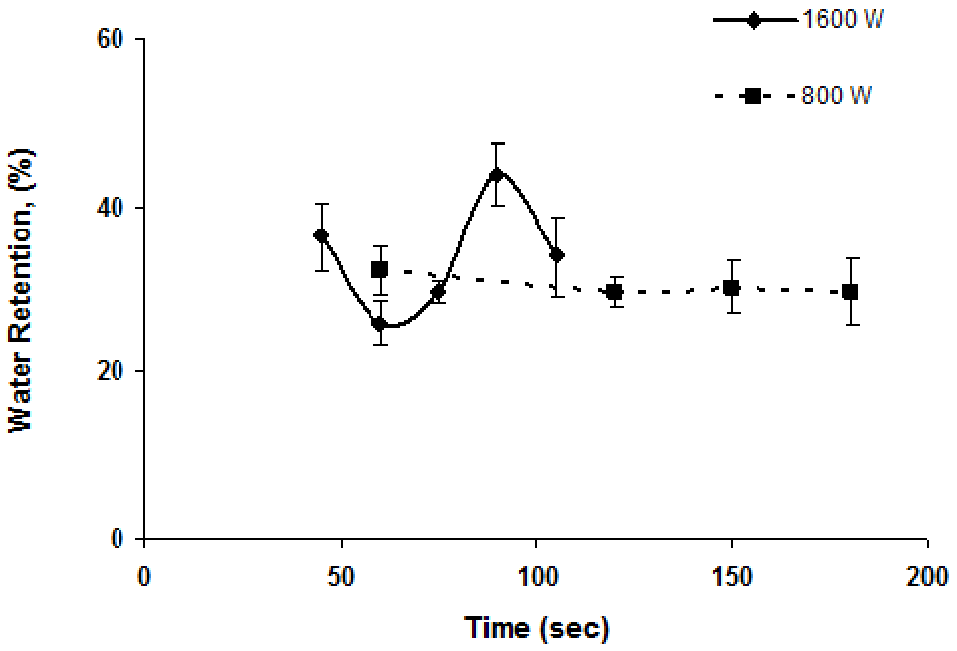

Figure 34. Percentage water retained by the prepared hydrogels as power and irradiation time vary.

4.3.2 Effect of PMVEMA on water absorption and retention.

The influence that the initial amount of PMVEMA in the crosslinking reaction had on the water absorption and retention of the hydrogels was evaluated by measuring the equilibrium swelling and water retained after centrifugation. This was performed because while most typically as the amount of crosslinking polymer increased, the overall water absorption and retention values also increased, some literature results also demonstrated a limiting effect on the maximum values of crosslinking polymers, where the water absorption peaked and then diminished at increasing polymer content [173];[316]. To observe the effect that the PMVEMA has on water absorption and retention, the percent PMVEMA was varied in three different compositions of pine pulp-

based materials, producing samples that contained 32%PMVEMA, 49%PMVEMA, and 66%PMVEMA.

Figure 35 shows that water absorption and retention increased as the PMVEMA concentration increased for both thermal and microwave initiated crosslinking, with maximum water absorption values achieved at the 66PMVEMA. The water absorption of all samples was greater than that of the unreacted pulp. However, there was a significant difference between the water absorption capabilities of the microwave-irradiated pine pulp and the thermally-crosslinked pine pulp; most striking is the near three-fold increase in the water absorption of the 49PMVEMA-Microwave pulp when compared to that of the 49PMVEMA-Thermal pulp. This could be attributable to a lower crosslink density between the PMVEMA-PEG in the microwave fibers which then allows for greater swelling to occur due to the decrease in constraint on the elasticity of the polymer chains. This is supported by the relatively same grafting efficiencies achieved by both 49PMVEMA-Microwave and 49PMVEMA-Thermal (Table 17) and by the higher percent water retained by the 49PMVEMA-Thermal fibers (Figure 35). Similarly, the increase in water absorption as PMVEMA overall increases can be attributed to the increase in the grafting efficiencies' values which are an indication of PMVEMA-cellulose crosslinking, and correspondingly, as the amount of PMVEMA increases, water absorption and swelling should increase as the PMVEMA is the primary hydrophilic polymer in this system.

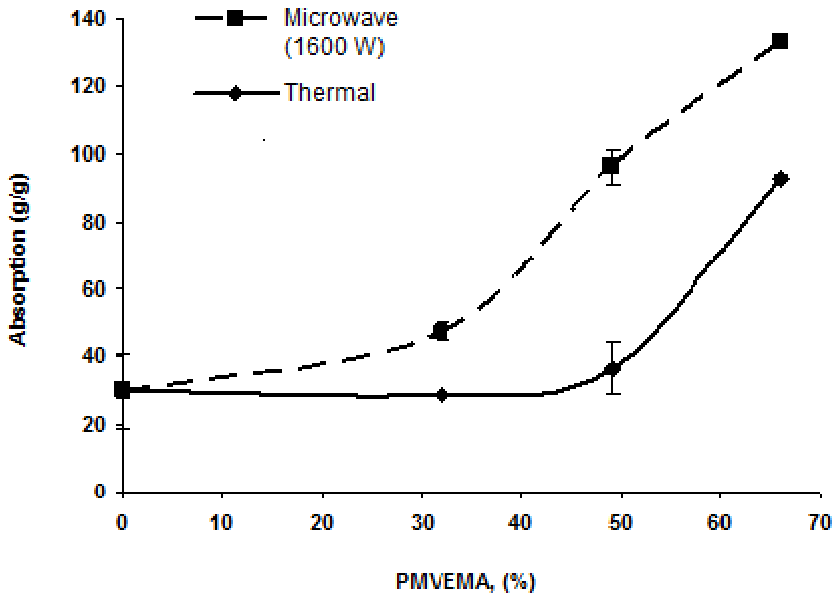

Figure 35. The water absorption increases as percent PMVEMA increases with microwave- and thermal-reacted softwood kraft pulp.

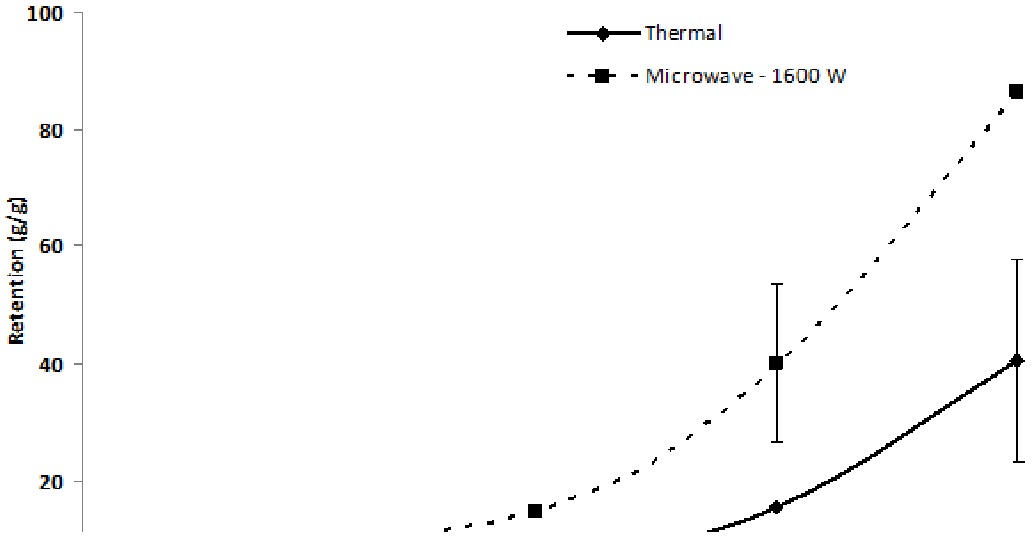

Figure 36. Water retention as PMVEMA is varied with microwave-irradiated and thermal-heated pine pulp.

The water retention abilities of both the microwave- and thermally-treated pulps, evaluated as grams water absorbed per gram pulp (g/g), increased as PMVEMA increased, as shown in Figure 36. However, the water retention of the two samples did not increase at the same rate. When evaluated as a percentage of water retained (Figure 37), the microwave-irradiated 66PMVEMA-kraft hydrogel retained 65% of the water absorbed, while the thermally-treated 66PMVEMA-kraft retained 44% of the water absorbed.

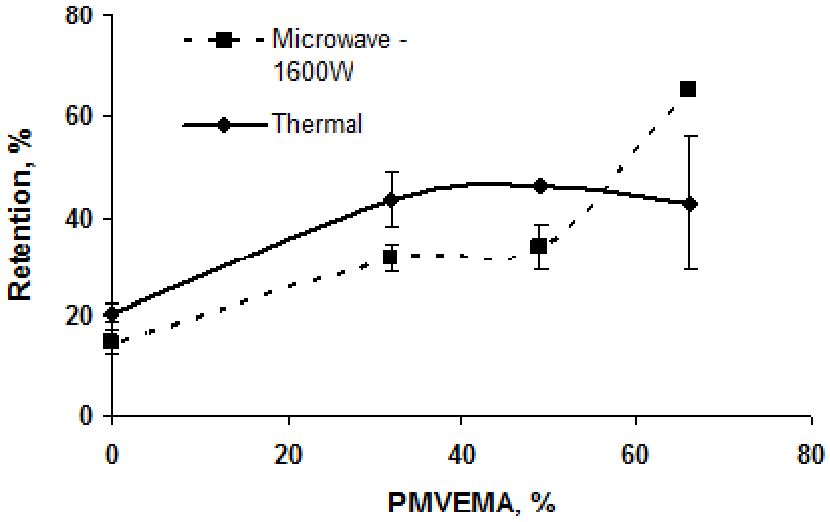

Figure 37. Comparison of percent water retained as PMVEMA is increased between microwave-irradiated and thermally-treated pulp hydrogels.

As controls, PMVEMA-PEG, pulp+PMVEMA, and pulp+PEG were prepared and characterized according to the established methods. Cured PMVEMA-PEG was shown to be soluble in water. The PEG-treated pulps (pulp+PEG) absorbed and retained water values similar to those of the unreacted pulp fibers. While the PMVEMA-treated pulps did absorb more water than did the untreated and PEG-treated pulps, they absorbed 21 –

259% less water than did the PMVEMA-PEG pulps. These results highlight the need for a three-component mixture, and establish PEG's involvement in enhancing water absorption. This involvement is attributed to PEG's involvement in crosslinking chemistry.

4.3.3 Behavior of pulp hydrogels in 0.10 M NaCl.

The absorption and retention of the microwave-irradiated hydrogels in 0.10 M NaCl solution was measured using the tea bag method and the centrifuge technique as were used in the water absorption/retention tests. As expected, the absorption and retention of 0.10 M NaCl was less than the water absorption and retention described in the previous section. The Donnan equilibrium theory and the corresponding counter-ion blocking explains these results.

The thermally-cured pulp hydrogels absorbed and retained more 0.10 M NaCl solution than did the microwave-cured hydrogels. Both thermally-cured and microwave-cured hydrogels absorbed and retained more than the untreated pulp fibers in water (Figure 38). Overall, there was little significant change in the ability of the gels to absorb 0.10 M NaCl solutions as the percent of PMVEMA increased, indicating that pulp with a lower percentage of PMVEMA might be effective enough in certain applications.

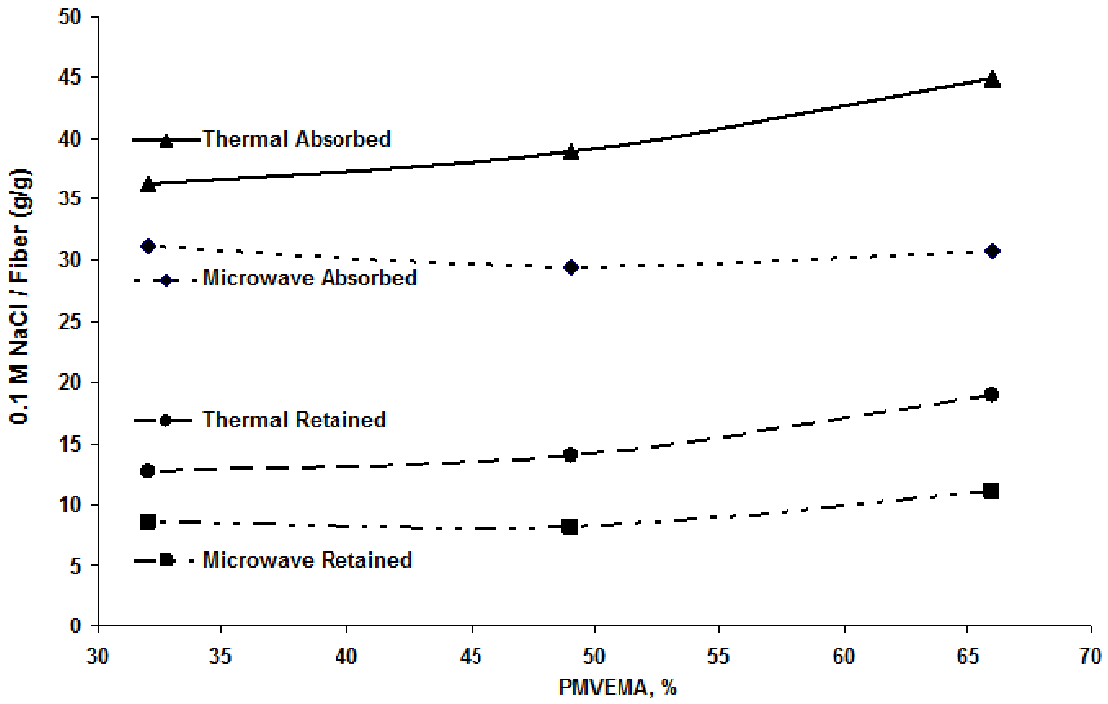

Figure 38. Absorption and retention of 0.1 M NaCl solution by the microwave-irradiated and thermally-treated pulp hydrogels as PMVEMA is increased.

4.3.4 Effect of the size of pulp fibers on water absorption and retention.

The overall effect of pine pulp fiber size on water absorption was evaluated by milling the fully-bleached kraft pulp. The starting pulp had a length weighted average fiber length of 2.503 mm. After milling this was reduced to a length weighted average value of 0.455 mm. The milled fibers were reacted with PMVEMA-PEG and cured under thermal- and microwave-irradiation conditions.

In general, the milled crosslinked pulps absorbed more water than did the unmodified pulp hydrogels. For example, 68PMVEMA milled, thermal-cured pulp

absorbed ~100 g water/g fiber more than 68PMVEMA thermal-cured pulp, while 49PMVEMA milled, the microwave-irradiated pulp absorbed 114 g/g water more than 49PMVEMA microwave-irradiated pulp. Figure 39 shows these trends. However, the 66PMVEMA milled, microwave-irradiated pulp did not follow this trend; this could be attributed to an increase in the crosslinking density of the PMVEMA-PEG during microwave irradiation, which would cause a decrease in the polymer elasticity component of the Flory-Huggins theory, resulting in lower water swelling values.

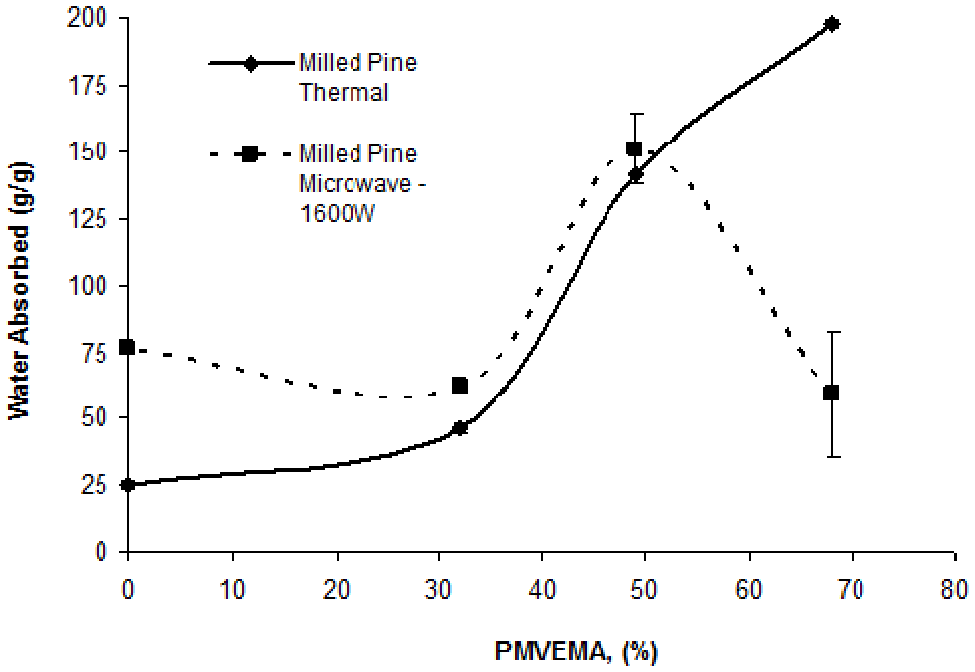

Figure 39. Water absorption of thermally-cured and microwave-irradiated milled pulp hydrogels.

The crosslinked hydrogels were Soxhlet extracted with water to compare the grafting efficiency of the hydrogels prepared with different pulp fiber sizes and crosslinking methods. The milled pulp fibers, both microwave- and thermally-crosslinked, had greater mass retention (Table 16).

Table 16. Percentage mass retained of starting sample after Soxhlet extraction.

	Pulp Fibers		Milled Pulp Fibers	
%PMVEMA	Thermal Crosslinking, %	Microwave Crosslinking, %	Thermal Crosslinking, %	Microwave Crosslinking, %
32	59.36	60.65	67.04	65.72
49	56.28	56.37	76.12	75.55
66	53.88	73.21	79.91	78.16

Grafting efficiency calculations show a similar trend (Table 17). Table 17 shows the grafting efficiencies calculated from the ratio of mass retained and mass of starting pulp fibers.

Table 17. Grafting efficiency of PMVEMA/PEG to the pulp fibers compared via percent PMVEMA, size of pulp fibers, and type of crosslinking.

	Pulp Fibers		Milled Pulp Fibers	
%PMVEMA	Thermal Crosslinking, %	Microwave Crosslinking, %	Thermal Crosslinking, %	Microwave Crosslinking, %
32	3.228	6.317	21.51	18.37
49	29.04	22.09	57.36	56.34
66	35.04	62.27	71.71	69.24

Overall, the milled pulp fibers demonstrated a greater grafting efficiency than did the non-milled pulp fibers, possibly attributable to the increase in the fiber surface area available for PMVEMA-cellulose fiber interactions. This increase can also explain the increased water absorption of the milled pulp fibers compared to the longer initial pulp fibers.

Microwave crosslinking of the milled pulp fibers resulted in grafting efficiencies similar to those produced by thermal crosslinking. The 32PMVEMA milled, thermal-cured fibers had a 566% increase in grafting efficiency when compared to the 32PMVEMA thermal-cured fibers. Similarly, the 66PMVEMA milled, thermal-cured fibers had a 154% increase in grafting efficiency when compared to the corresponding microwave pulp fibers. However, microwave-crosslinked pulp fibers at 32PMVEMA and 66PMVEMA resulted in grating efficiencies that were 1.9 and 1.7 times greater than those of the respective thermally-crosslinked pulp fibers.

4.3.5 FT-IR spectroscopy.

FT-IR spectroscopy was used to evaluate the reactions occurring between the PMVEMA, PEG, and pulp. Rocco, Pereira, and Felisberti have investigated blends of a poly(methyl vinyl ether maleic acid) polymer with varying percentages of polyethylene oxide (PEO) using FT-IR. Their methodology is applicable to this study [317]. Figure 40 illustrates the FT-IR spectra of PMVEMA-PEG, PEG, and PMVEMA. The PEG spectrum (Figure 40b) is a typical PEG FT-IR spectrum with the expected C-O-C bands at 1151, 1109, and 1061 cm^{-1}. The PMVEMA spectrum (Figure 40c) shows the characteristic stretching bands between 1712 and 1728 cm^{-1}. These bands are attributed to the carboxyl carbonyls from the carboxylic acid groups of the maleic acid. In addition, the presence of maleic anhydride groups in the PMVEMA is also demonstrated by the shoulders at 1845 and 1783 cm^{-1}.

In the PMVEMA-PEG spectrum (Figure 40a), both peaks attributed to the carboxyl carbonyl groups shifted to between 1728 and 1737 cm^{-1}, consistent with

crosslinking occurring via esterification between the OH groups of the PEG and the COOH groups of the PMVEMA. The formation of anhydrides is observed in the PMVEMA-PEG spectrum with shoulders at 1784 and 1843 cm^{-1}.

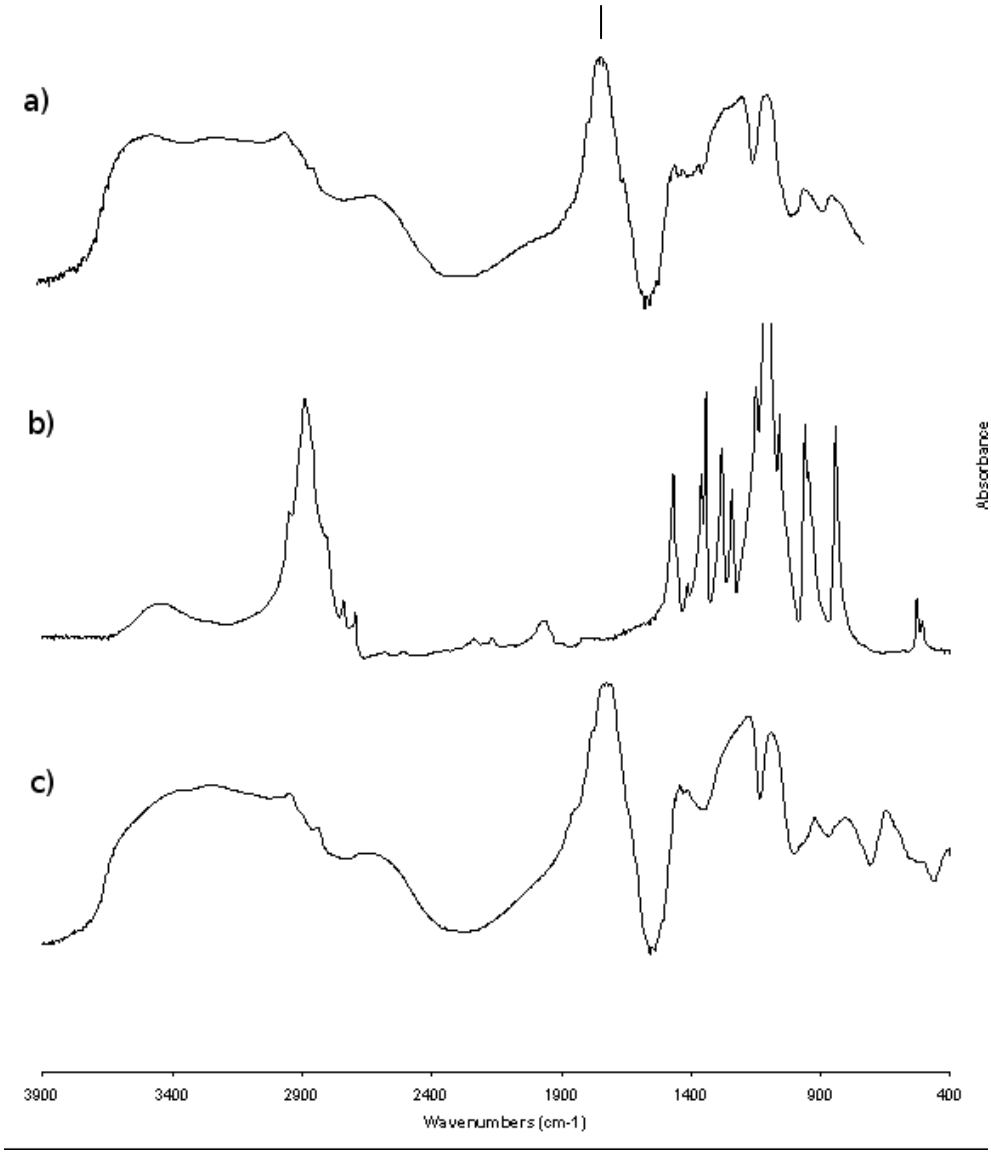

Figure 40. FT-IR spectra of (a) PMVEMA-PEG, (b) PEG, and (c) PMVEMA.

Previous work has demonstrated that the esterification reaction between PMVEMA-PEG and wood pulp can be determined using FT-IR. To separate the contribution of the esterified carboxylic acids from that of the unreacted carboxylic acids,

the samples were briefly immersed in 0.10 M NaOH solution, deprotonating the unreacted acid groups. This allowed the bands present in the carbonyl region to be attributed solely to the esterified carboxyl groups. The carboxylated groups appeared in the FT-IR spectrum at 1588 cm^{-1} after the reaction.

The FT-IR spectrum of the starting cellulose in the milled pine pulp showed the typical spectral bands associated with cellulose (Figure 41b). Specifically, the cellulose showed bands at 1112 cm^{-1} (asymmetric glucose ring stretch), 1163 cm^{-1} (C-O-C asymmetric vibration), 1061 cm^{-1} (C-O stretch), 1033 cm^{-1} (C-O stretch), and at 898 cm^{-1} (glucose ring stretch, C-H deformation). All of the modified pulp samples contained these absorptions. A control sample of PEG, reacted with the milled pulp in the same conditions under which the hydrogels were prepared, resulted in a spectrum that was unchanged from the unreacted milled pulp, most likely because the PEG was washed from the system during the preparation. Figure 41a presents the FT-IR spectrum of a 66PMVEMA-PEG milled, pine, thermal-cured hydrogel treated with 0.10 M NaOH solution. The carboxylated band at 1591 cm^{-1} became evident as a result of the immersion of the sample in the sodium hydroxide solution. The bands at 1734 cm^{-1} are therefore indicative of an esterification reaction between the PMVEMA and the cellulose.

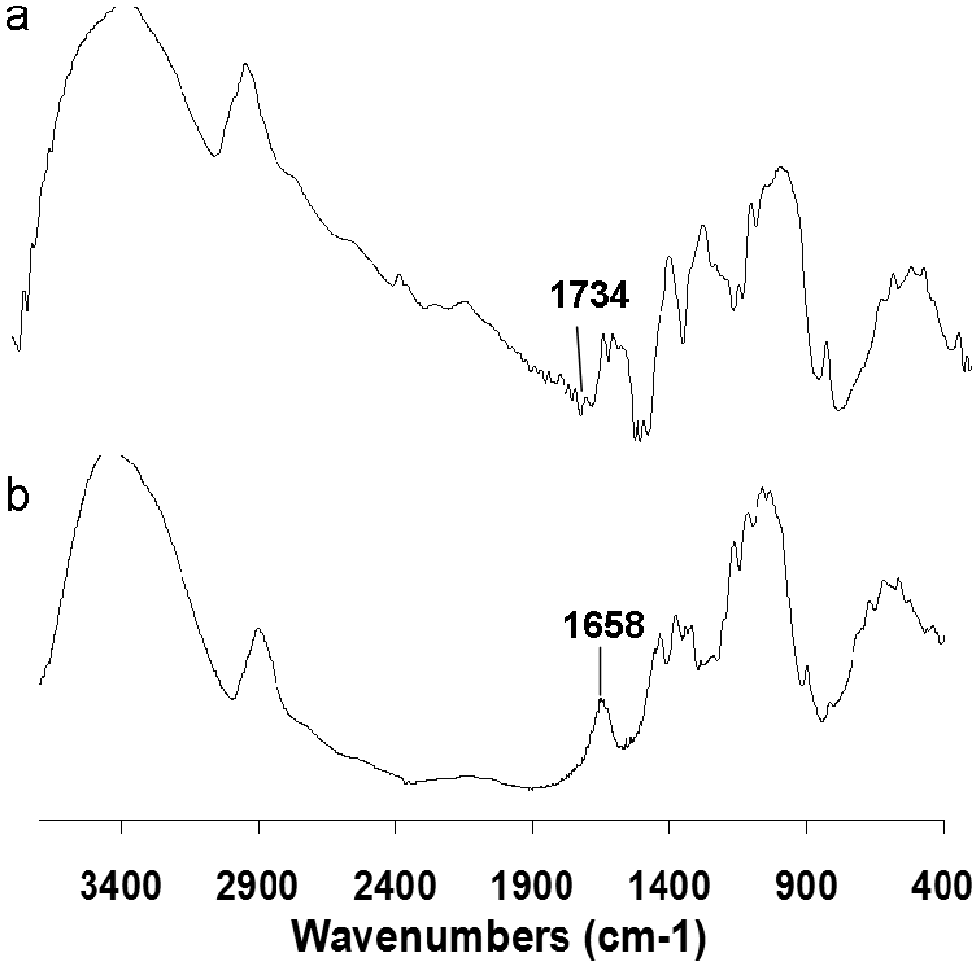

Figure 41. FT-IR Spectra of microwave-treated pine pulps (a) 66PMVEMA-PEG-milled pine pulp and (b) milled pine pulp.

4.3.6 Scanning electron microscopy.

The surface morphology of the fibers was investigated using scanning electron microscopy. As Figure 42 shows, the grafting onto the fibers for both curing techniques retains the fibrous structure of the starting pulp materials**.** The fibrils of the cellulose pulp are observed in Figure 42 (a) and (b). Conversely, in Figure 42 (c) and (d), the

surface of the pulp displays none of these fibrils and instead appears to be relatively smooth. This suggests that the PMVEMA is reacting with hydroxyl groups on the surface of the pulp fibers. Figure 42 (e) and (f) are examples of a microwave-initiated crosslinked pulp hydrogel at 120 sec, 800 W (a sub-optimal condition). These pulp fibrils are observed to be similar to those of the unreacted pulp, potentially indicating a non-complete reaction between the PMVEMA-PEG and the cellulose, in which the non-reacted PMVEMA-PEG was washed away with water in the post-reaction processing steps. This is further supported by the water absorption of these hydrogels when compared to that of the hydrogels imaged in Figure 42 (c) and (d), of 39 g/g and 93 g/g, respectively.

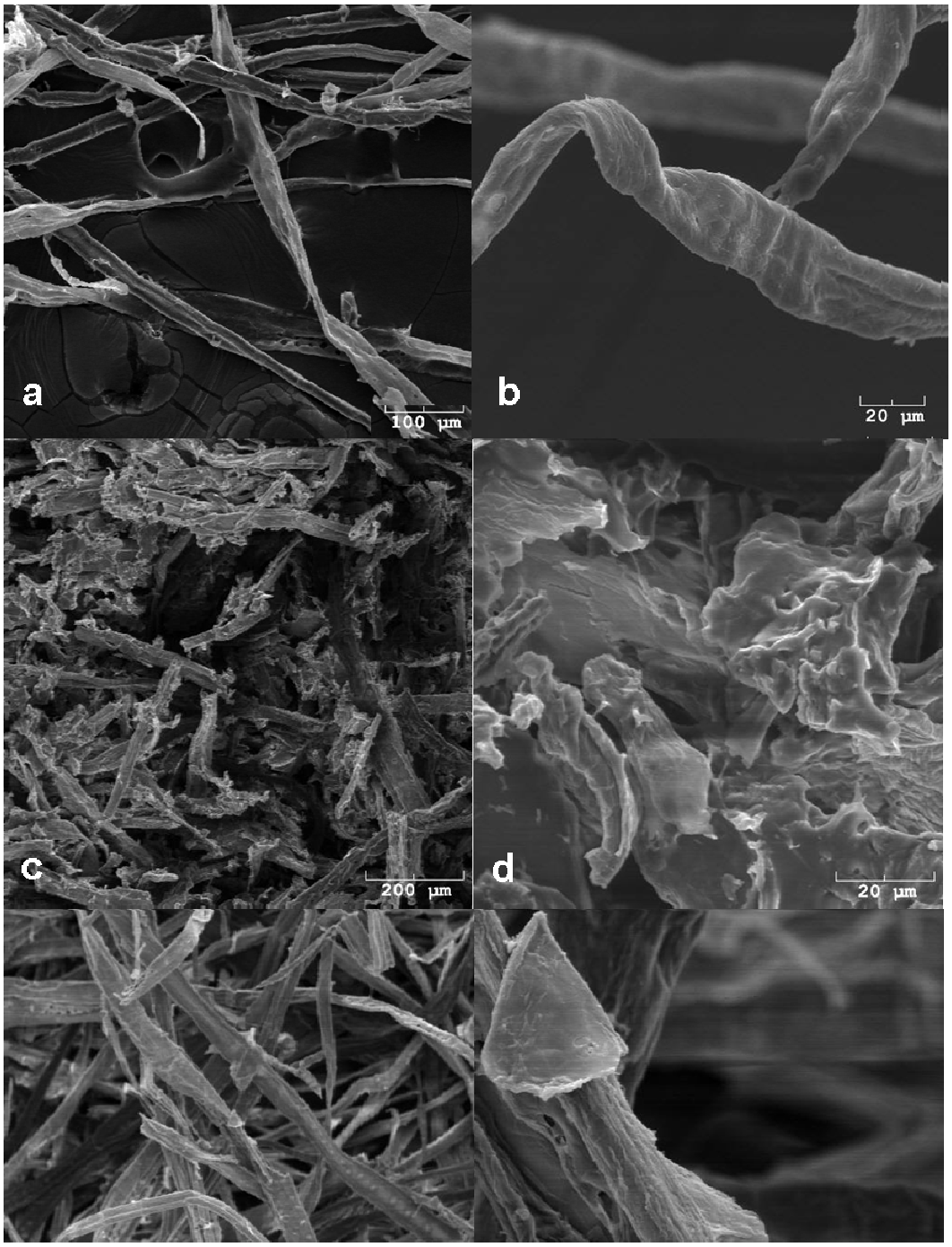

Figure 42. SEM images of (a) and (b) unreacted pine pulp fibers, (c) and (d) 66PMVEMA thermal-cured, (e) and (f) 49PMVEMA microwave-irradiated 120 s 800 W power fibers.

4.4 Conclusion.

Microwave irradiation is an efficient method by which to produce PMVEMA-PEG-crosslinked cellulose-based hydrogels, with a decreased reaction time of 105 sec, significantly less than the reaction time of the thermal procedure, 6.5 min. The thermal-curing method is easily transferred to microwave irradiation, as it does not utilize any metal initiators. The microwave-prepared hydrogels absorbed similar or greater amounts of water than did the thermally prepared hydrogels. In addition, the milled pulp-based hydrogels absorbed 30 – 292% more water than did the non-milled pulp hydrogels. This suggests that the absorption abilities of the hydrogels have a fiber-size dependence. There was one exception, the 66PMVEMA-PEG milled, microwave-irradiated pulp, which absorbed 56% less water than did its un-milled equivalent. However, this deviation is explained by the corresponding increase in the grafting efficiencies of the milled pulps. SEM analysis demonstrated that the PMVEMA-PEG matrix appeared to stay on the fiber surface in both the microwave-initiated and thermal crosslinking procedures, resulting in similar surface morphology. The FT-IR analysis of the pulps confirms that an ester linkage is forming between the PMVEMA and the cellulose and a second ester linkage is forming between the PMVEMA and PEG.

Due to the success of this study and the observation of a fiber size dependence in the water absorption and retention values obtained, a study utilizing commercial ECF bleached kraft birch fibers as the cellulose fiber source to be crosslinked thermally and via microwave irradiation was undertaken. Commercial ECF bleached kraft birch fibers were chosen as a comparison fiber as the birch fibers are a representative hardwood and

as such are smaller in length than the softwood pulp fibers used in this chapter. The results are presented in the next chapter, Chapter 5.

CHAPTER FIVE

INITIAL PREPARATION AND COMPARISON OF MICROWAVE AND THERMAL CROSSLINKING OF BIRCH PULP FIBERS[2]

5.1 Introduction.

Cellulose is a key resource for the future development of biomaterials in the quest to reduce the demand for petroleum-based materials [17, 279, 280, 318, 319]. The crosslinking of wood pulps with polycarboxylic acid groups has been investigated as a promising method by which to chemically modify cellulosics to enhance water absorption, increase wet strength, or impart anti-wrinkle properties [263, 282-284]. Improved water absorbency of the cellulosic components is especially important, as it would curb the excessive use of petroleum-derived superabsorbent polymers. Recent studies have highlighted the potential of microwave irradiation in chemical crosslinking [307-309]. Reduced reaction times and enhanced selectivity are the main advantages of using microwave irradiation [248]. The use of microwave irradiation to facilitate the reaction of fully bleached commercial wood kraft pulp fibers with carboxylic acid containing polymer such as PMVEMA had not been previously investigated.

---

[2] This work was published in Holzforschung as "Analysis of microwave vs. thermally assisted grafting of poly(methyl-vinyl ether co-maleic acid)-polyethylene glycol to birch kraft pulp." Holzforschung (2009), 63(4), 414-417. Other authors were Jessica R. Sladky and Arthur J. Ragauskas from the Institute of Paper Science and Technology and School of Chemistry and Biochemistry at Georgia Institute of Technology. It is available for purchase through www.degruyter.com.

Chapter 4 described cellulose functionalization to improve water absorbency using both a thermal-initiated and microwave initiated reaction method of crosslinking commercial ECF bleached southern softwood kraft pulp, poly(methyl vinyl ether co maleic acid), and polyethylene glycol. Barcus and Bjorkquist [291] initially demonstrated that poly (methyl vinyl ether co-maleic acid) (PMVEMA) and polyethylene glycol (PEG) can crosslink thermally to various lignocellulose fibers. The results from Chapter 4 showed that microwave initiated crosslinking of this system was a viable reaction method with resulting crosslinked pulp fibers that were capable of absorbing water in comparable values to that of thermally crosslinked pulp fibers. In addition, the thermally crosslinked ECF bleached southern softwood kraft pulp fibers demonstrated a size dependence on water absorption where the milled ECF bleached southern softwood kraft pulp crosslinked fibers absorbed 50% to 300% more water.

The intention of the presented research is to demonstrate that the microwave initiated and thermally initiated crosslinking method can be transferred to commercial ECF bleached birch kraft pulp fibers with improved water absorption and retention values. In addition, further evidence of a fiber size dependence on obtaining greater water absorption values is presented upon comparison of results from Chapter 4.

5.2 Experimental section.

5.2.1 Materials.

All materials, including the fully-bleached ECF birch kraft pulp, PMVEMA, and PEG, used are described in Chapter 3 (Section 3.1 Materials).

5.2.2 Crosslinking.

The ECF bleached birch kraft pulp with PMVEMA and PEG were crosslinked in according to the experimental procedure described and outlined in the flow diagram (Figure 24) in Chapter 3 (Section 3.2.1 Preparation of water absorbing fibers) [291]. This procedure was repeated to prepare crosslinked hydrogel materials with the Wiley milled ECF birch kraft pulp. Compositions were prepared and classified based on the percentage PMVEMA used by mass, and described based on this percentage (i.e., 32%, 49%, and 66%) as in Chapter 3 Table 14. Further variations in component mixtures were also prepared to remove the PEG influence for the purposes of comparison.

The microwave curing was performed as described in Chapter 3 (Section 3.2.1 Preparation of water absorbing pulp fibers). Preliminary microwave curing studies (previously described in Chapter 4) indicated that samples irradiated for 60 s yielded a crosslinked pulp with significantly lesser water absorption properties than those of pulps irradiated for 105 s, while samples irradiated for 120 s or longer resulted in charring of the pulp. Hence a microwave irradiation time of 105 s was selected as an optimized time.

The samples were labeled % PMVEMA-Microwave (indicating the percentage of PMVEMA in the reaction). To produce thermally-crosslinked pulps for comparison, the procedure was repeated until the air-drying phase. After this step, the dry slurry of fibers/PMVEMA/PEG was heated at 130°C for 6.5 min in a thermal radiation oven. These later samples were labeled % PMVEMA-Thermal.

5.2.3 Characterization.

The water and 0.1 M NaCl sorption measurements of the final products were conducted using the traditional tea bag method described in Chapter 3 (Section 3.2.2 Water and 0.1 M NaCl absorption and retention – Tea bag method) [262]. The total absorbed value and the retention value were calculated and reported as g absorbed per g dry hydrogel (g/g). Replicates were measured and the average is reported with the calculated standard deviation of all replicates. The retained water is presented as a percentage based on the water absorption. Student t-test calculations were conducted to assure statistical relevance. SEM images were acquired using the procedure described in Chapter 3 (Section 3.2.3 Scanning electron microscopy).

5.3 Results and discussion.

The goal of this study was to utilize both microwave irradiation and thermal heating to induce a crosslinking reaction between the PMVEMA, PEG, and birch pulp fibers to produce a crosslinked hydrogel system. These fibers were then evaluated using classical equilibrium swelling measurements with the traditional tea bag test method to measure the absorption and retention of water and 0.10 M NaCl.

The expected final structure and esterification crosslinking reactions of the PMVEMA, PEG, and ECF bleached kraft birch fibers are described in Chapter 4, Figure 30 and Figure 31, respectively. The concentration of the PMVEMA was varied to determine how PMVEMA concentration affects the absorption and retention of water and 0.10 M NaCl of the crosslinked birch fibers (Figure 43).

Figure 43a compares the trends of water absorption of the samples modified by microwave and thermal radiation as a function of the amount of pulp. Overall, the water absorption increased as the percentage of the PMVEMA used increased. The thermally-treated crosslinked birch pulps absorbed between 210% and 582% more water than did the non-crosslinked birch pulp, which absorbed 29.4 g/g. The microwave-irradiated crosslinked birch pulps absorbed between 45% and 413% more water than did the microwave-irradiated unreacted control birch pulp, which absorbed 37.3 g/g.

As the reacted fibers were thoroughly washed with deionized water, removing extractables, the increases in water absorption can be attributed to the fibers crosslinked with PMVEMA and PEG. The following observation supports this conclusion: samples prepared in an analogous manner with (i) PMVEMA/fiber and (ii) PEG/fiber did not exhibit similar enhanced water absorption and retention. In addition, PMVEMA-PEG

forms a hydrogel that is soluble in water when prepared under the listed reaction conditions.

The water retention capability of these hydrogels after centrifugation is shown in Figure 43b, where the trends for water retained after centrifuging for both the microwave-irradiated and thermally-treated hydrogels as PMVEMA is increased is very similar to that of water absorption. In addition, the 66PMVEMA-Microwave and the 49PMVEMA-Microwave products retained comparable amounts of water when compared to the corresponding 66PMVEMA-Thermal and 49PMVEMA-Thermal hydrogels. The microwave and thermally crosslinking methods produced crosslinked pulp fibers that did not display the disparity in water absorption and retention that was seen in the softwood pulp crosslinked fibers in Chapter 4. The birch fiber crosslinked hydrogels absorbed more water than the mixed softwood fiber crosslinked hydrogels at all PMVEMA concentrations and both the thermally initiated and microwave initiated crosslinking methods. This difference is most dramatic at the 66PMVEMA concentration, where the 66PMVEMA-Birch fiber-Microwave and 66PMVEMA-Birch fiber-Thermal absorbed 191.33 g/g and 200.58 g/g water, respectively, while the 66PMVEMA-Mixed softwood – Microwave and 66PMVEMA-Mixed softwood – Thermal absorbed 132.94 g/g and 93.14 g/g, respectively. This observation of the size dependence of cellulose fibers on maximum water absorption is most likely due to the increased surface area available for crosslinking on the smaller fibers.

The absorption and retention of the 0.10 M NaCl solution by the microwave pulp materials is highlighted in Figure 43c. Overall, the microwave crosslinked pulps absorbed and retained less g g^{-1} liquid when placed in 0.10 M NaCl solution than they did when

placed in water, as expected due to ion interference and displacement. The 66PMVEMA-Microwave pulp hydrogel absorbed and retained the most 0.10 M NaCl, with absorption and retention values decreasing as the percentage of PMVEMA decreased, just as when the pulp hydrogels were immersed in water.

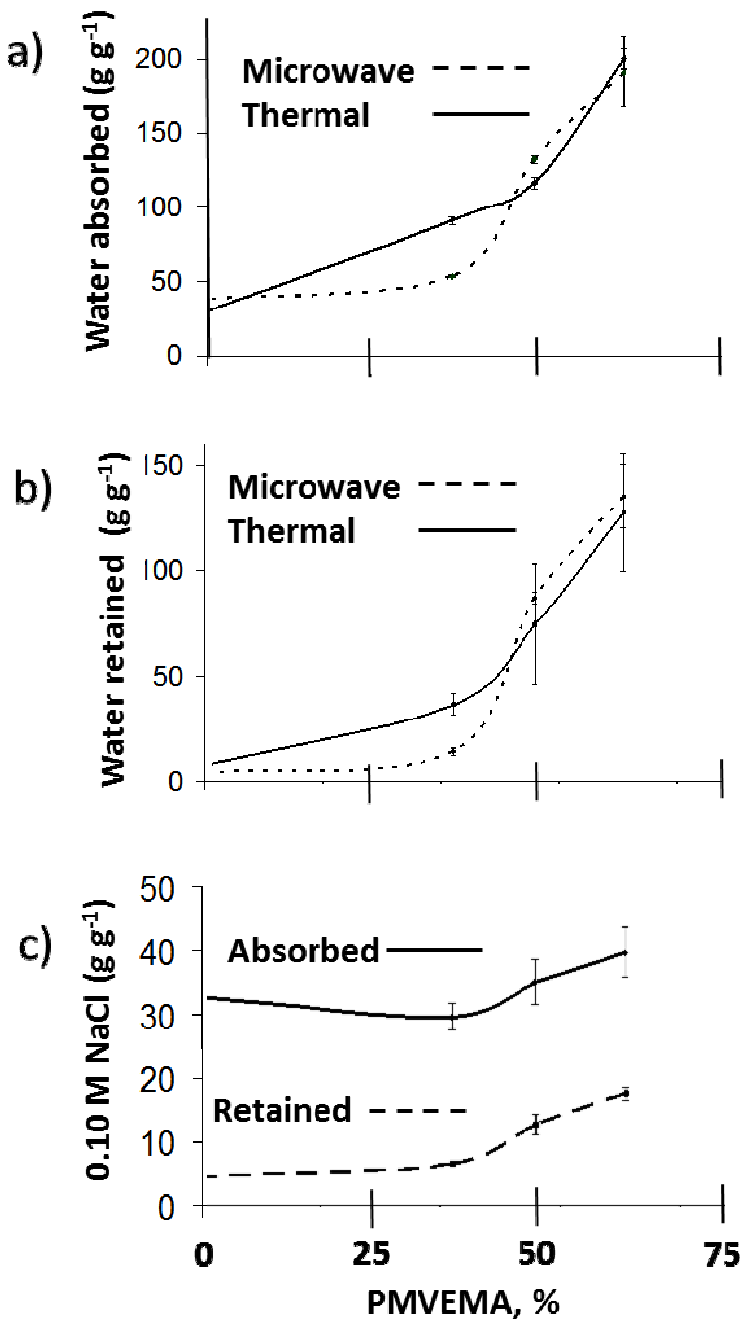

Figure 43. Comparison of (a) water absorption, (b) water retention, and (c) absorption and retention in 0.1 M NaCl for grafted pulps as a function of the birch fiber (BF) participating in the reaction.

The surface morphology of the grafted fibers was studied using scanning electron microscopy (SEM). Representative fibers from both the 44BF-Microwave and 44BF-Thermal samples are shown in

Figure 44. The surface morphology between the microwave and thermal pulps is very similar. This is an indication that the PMVEMA-PEG reacts similarly with the fibers whether it is microwave irradiated or thermally cured. Also, the surface morphology indicates a smoother surface which can be an indication that the PMVEMA is on the surface of the cellulose fibers.

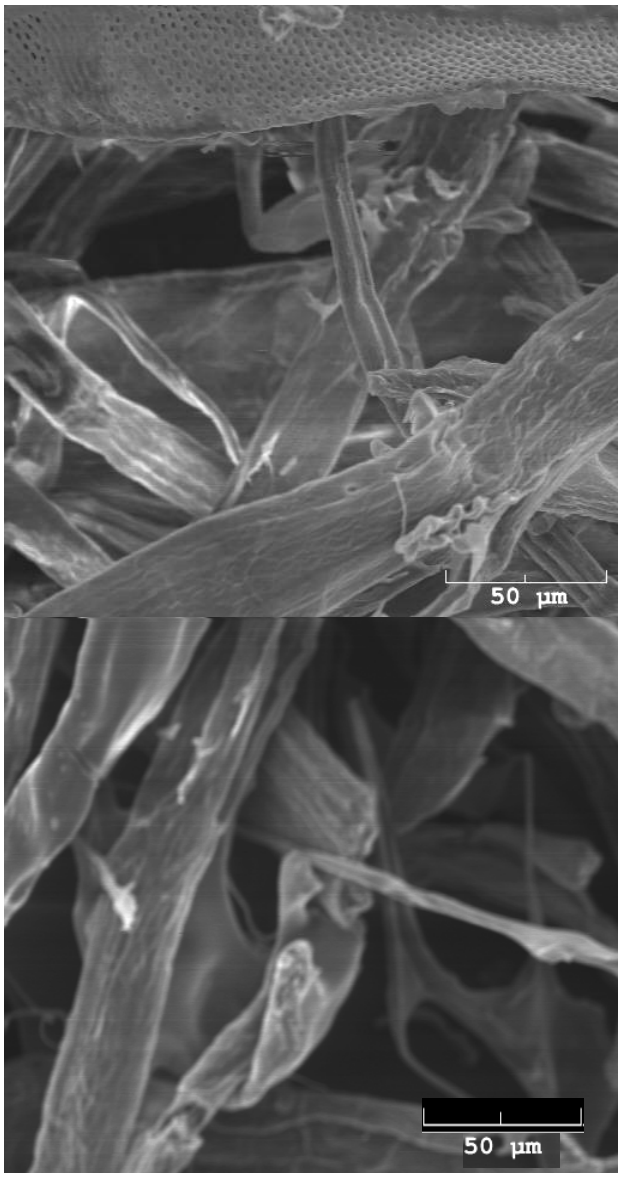

Figure 44. SEM images of grafted birch fibers (BF). (a) 44BF microwave-assisted grafting. (b) 44BF thermal-assisted grafting . © 2009 Holzforschung

5.4 Conclusions.

The water absorbed and retained by unmodified cellulosic fibers is insufficient for many applications. This study demonstrates that crosslinking ECF bleached birch kraft pulp fibers with PEG and PMVEMA can yield 5- to 10-fold increases in water absorption

and retention of the starting ECF bleached birch kraft pulp fibers. Furthermore, these hydrophilic pulps can be rapidly prepared via microwave irradiation, yielding crosslinked pulps with water absorption properties similar to those of oven-cured pulps. The microwave-assisted reactions permit shorter reaction times with high loadings of PMVEMA and PEG. The water absorption values of the crosslinked birch pulp hydrogels were greater than the water absorption values of the crosslinked mixed softwood pulp hydrogels, indicating a size dependence on achieving maximum water absorption values, possibly due to an increase in the surface area per gram pulp fiber available for the PMVEMA to crosslink.

While this study and the results from Chapter 4 successfully demonstrated that cellulose fibers can be successfully crosslinked with PMVEMA-PEG, the experiment utilized fibers on the macro and micro scales. The interesting question then became whether cellulose fibers of nanoscale dimensions could be utilized in this reaction scheme. In order to answer this, cellulose nanowhiskers, rod-like particles of cellulose, were used as the source of nano-dimensional cellulose. The initial results are presented the following chapter, Chapter Six, while further characterization studies of the unique film-like material that resulted are presented in Chapters Seven, Eight, and Nine.

CHAPTER SIX

PREPARATION OF NOVEL CROSSLINKED CELLULOSE WHISKER-PMVEMA-PEG NANOCOMPOSITE FILMS[3]

6.1 Introduction.

Biobased materials are an important global research topic as there is a genuine interest and need to decrease society's dependency on petroleum-based products. Cellulose is the most abundant natural polymer, and considerable interest has been recently focused on finding new material applications for this biopolymer. One of these applications has been the development of cellulose nanocrystals. It is well known that native cellulose, when subjected to strong acid hydrolysis, can be readily hydrolyzed into micro- or nanocrystalline cellulose [7, 10, 27, 52, 53, 67, 103]. The length of the nanocellulose crystals is dependent on the sample origin. Crystals derived from wood sources typically are 100 – 300 nm in length and 3 – 10 nm in width [76, 92, 320, 321]. The crystal modulus of cellulose has been reported as 138 - 167 GPa [113, 322-324].

Cellulose whiskers and their application as a reinforcing material in composites is a relatively new field within nanotechnology and have generated considerable interest in the last decade, especially within the biopolymer community. There are several

---

[3] This work was published in the journal Carbohydrate Polymers as "A novel nanocomposite film prepared from crosslinked cellulosic whiskers." Carbohydrate Polymers (2009), 75 (1), 85-89. Other authors were Arthur J. Ragauskas from the Institute of Paper Science and Technology and School of Chemistry and Biochemistry at Georgia Institute of Technology, Aji Mathew and Kristiina Oksman from the Division of Manufacturing and Design of Wood and Bionanocomposites, Luleå Institute of Technology, Skellefteå, Sweden, and Paul Gatenholm of the Department of Chemical and Biological Engineering Biopolymer Technology, Chalmers University, Göteborg, Sweden.

challenges, however, in using cellulose whiskers with polymers. These include the efficient separation of whiskers from plant resources, the compatibilization of these nano reinforcements with the matrix, and the development of suitable methods for processing these nanocomposites. Aqueous and solvent solution casting is the most common method of preparing cellulose nanocomposites. Oksman, Mathew, Kvien, Bondeson, and Petersson utilized a twin screw melt-extrusion of cellulose nanocomposites with poly (lactic acid) and cellulose acetate butyrate [125, 131, 325]. Samir, Alloin, Sanchez and Dufresne report the development of a cellulose whisker nanocomposite where the matrix phase was crosslinked [170]. However, studies involving the crosslinking of whiskers with a matrix had not been previously reported. In the current study, the preparation and characterization of cellulose whiskers crosslinked with poly (methyl vinyl ether-co-maleic acid) (PMVEMA) and poly (ethylene glycol) (PEG) is reported. This crosslinking methodology has been developed for kraft cellulosic fibers to enhance the water-absorbing properties of treated fibers, as described in Chapters 4 and 5. The current study demonstrates that crosslinked cellulose whiskers are capable of forming novel film-like materials that exhibit unique water-absorbing properties via in situ crosslinking.

6.2 Experimental Materials and Methods.

6.2.1 Experimental materials.

PMVEMA (MW: 1,980,000) was used as supplied by ISP Corp. Poly (ethylene glycol) with a MW of 3,000 was purchased from VWR. Microcrystalline cellulose (VIVAPUR® 105) was acquired from JRS Pharma. All other chemicals were purchased from Aldrich and used as received.

6.2.2 Preparation of cellulose whiskers.

Cellulose nanowhiskers were isolated from microcrystalline cellulose via acid hydrolysis using the procedure reported by Bondeson, Mathew and Oksman and described in detail in Chapter 3 (Section 3.3.1 Preparation of cellulose nanowhiskers from microcrystalline cellulose) [67].

6.2.3 Preparation of crosslinked cellulose whisker film hydrogels.

The crosslinked films were prepared as described in Chapter 3 (Section 3.3.3 Preparation of crosslinked cellulose whisker film hydrogels). Five compositions were prepared and classified based on the percent cellulose whisker mass in the resulting films (0%, 25%, 50% 75%, and 100% whiskers by mass). Each PMVEMA-PEG/CNW mixture was cured at 135 °C for 6.5 min. After curing, the films were stored in a desiccator at 54% relative humidity for one week prior to testing.

6.2.4 Characterization.

The cellulose whiskers, as well as the nanocomposites, were characterized using a Veeco MultiMode scanning probe microscope with a Nanoscope V controller as described in Chapter 3 (Section 3.4.3 Atomic Force Microscopy. Cellulose whiskers and crosslinked cellulose whisker films.).

A Nicolet Magna-IR^{TM} 550 Spectrometer FT-IR in transmission mode was used to collect the infrared spectroscopy data using the procedure described in Chapter 3 (Section 3.4.1 Fourier Transform Infrared Spectroscopy.).

6.2.5 Water absorption studies.

Water absorption study of water absorbed versus time until equilibrium swelling was achieved was conducted as per Chapter 3 (Section 3.4.5 Water Sorption Studies.). The film samples used for the water sorption studies were circular discs 20 mm in diameter, cut from films conditioned at 54% relative humidity. Three replicates were performed for each composition. The maximum water uptake quantities were statistically analyzed using Student's t-test. The gel content of the prepared films was measured using the procedure in Chapter 3 (Section 3.4.6 Gel content of whisker films.)

6.3 Results and discussion.

This study examines the crosslinking of cellulose whiskers with poly (methyl vinyl ether-co-maleic acid) and poly (ethylene glycol) and the resulting film properties. The films were prepared by reacting varying amounts of cellulose whiskers (i.e., 0 – 100%) with the crosslinking agents. The cellulose whiskers for this study were prepared via an acid hydrolysis of microcrystalline cellulose and analyzed by AFM, as summarized in Figure 45a.

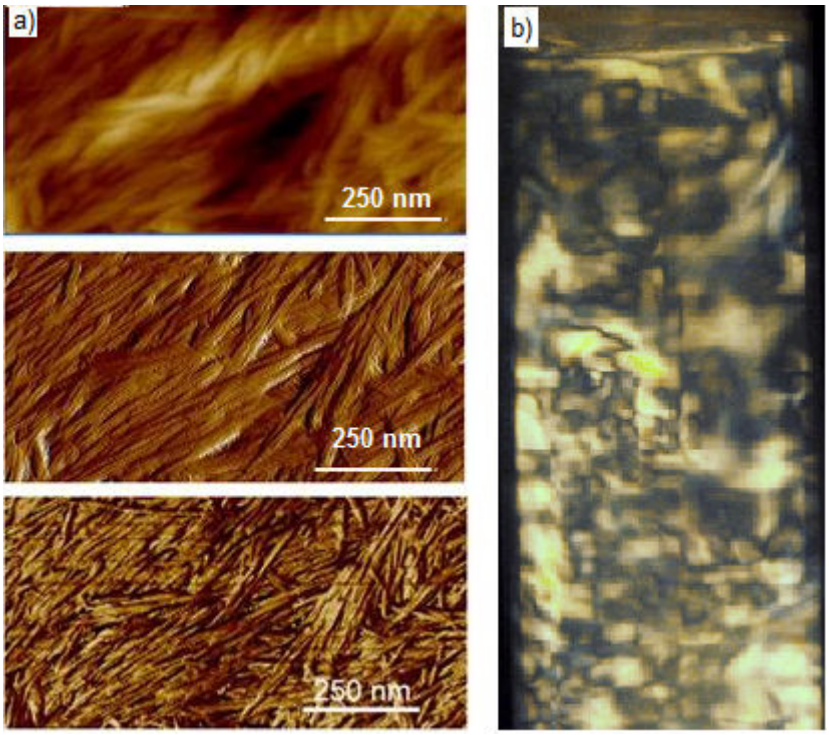

Figure 45. Characterization of cellulose nanowhiskers using a) atomic force microscopy (AFM) (height, amplitude, and phase) and b) birefringence.

The AFM images show the presence of isolated whiskers in the nanometer scale. The dimensions of whiskers prepared using the same isolation process were determined previously using TEM by Kvien, Tanem and Oksman. The whiskers in this earlier study had a diameter of 5 ± 2 nm and a length of 210 ± 75 nm [68]. Figure 45b shows the flow birefringence of aqueous whiskers when viewed under cross-polarized light, which confirms the existence of cellulose whiskers.

The crosslinking of cellulose whiskers with poly(methyl vinyl ether-co-maleic acid) and poly(ethylene glycol) was expected to occur via an esterification reaction between the hydroxyl groups on the cellulose, the terminal hydroxyl groups on the PEG, and the carboxylic acid groups on the poly(methyl vinyl ether-co-maleic acid), as shown

in Chapter 4 Figure 30. The possibilities of intermolecular and interchain reactions exist as well.

The nanoscale morphology of the films was studied using atomic force microscopy. Micrographs of crosslinked nanocomposites with 50% whiskers are provided in Figure 46. The AFM pictures show a multi-phased system, and there is an indication in the phase images that one of the phases is forming a network in the second phase with a relatively homogeneous distribution of the phases.

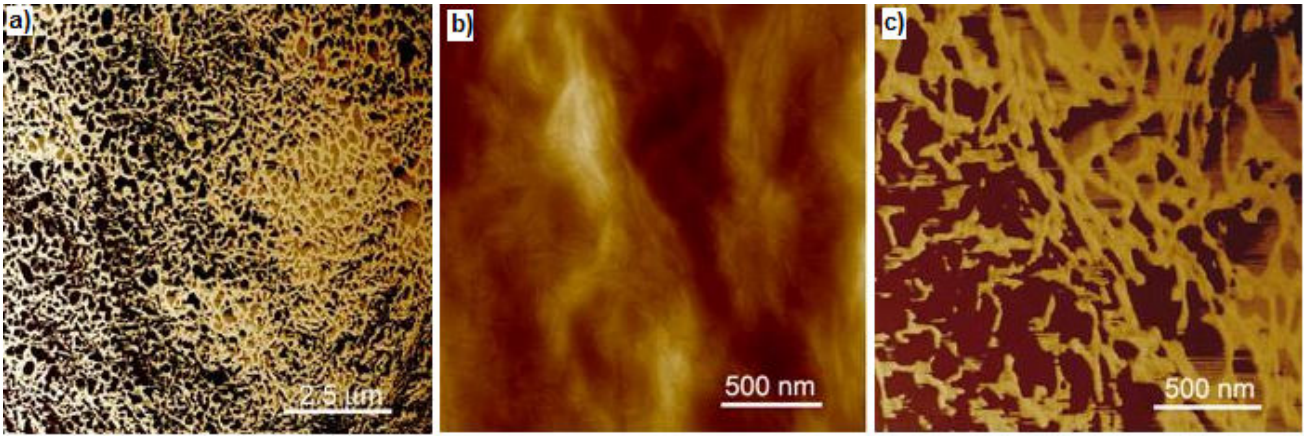

Figure 46. Atomic force microscopy of crosslinked PMVEMA-PEG/CNW50 nanocomposites a) overview (phase) b) detailed view (height) and c) detailed view (phase).

As the behavior of these materials in water and their potential as hydrogels was of interest, the water absorption of the films was investigated. The 100% CNW films, the CNW/PMVEMA-PEG nanocomposites, and 100% PMVEMA-PEG films were compared. The 100% CNW films and 100% PMVEMA-PEG films did not retain structural integrity during the water absorption experiments. However, the nanocomposite films swelled when placed in water and retained their film structure. This

indicates that the crosslinking reaction between the whiskers and the matrix yielded a networked gel.

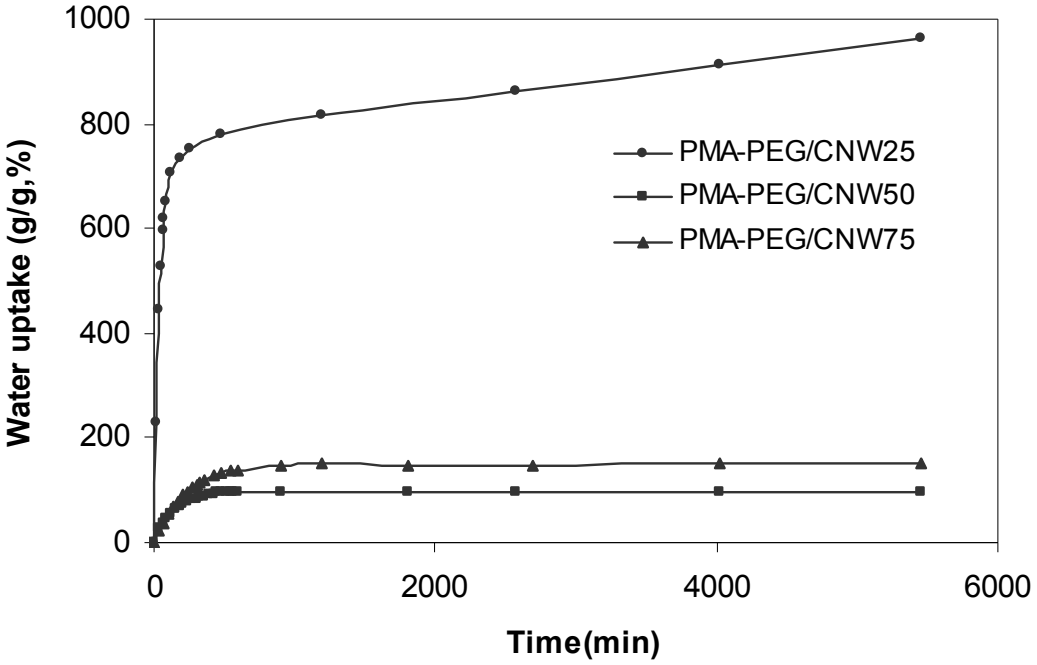

Figure 47. Water absorption curves of crosslinked nanocomposites with varying cellulose nanowhiskers contents (PMVEMA-PEG/CNW25, PMVEMA-PEG/CNW50, and PMVEMA-PEG/CNW75).

The water absorption curves for the nanocomposite films are given in Figure 47. The time it took the 25% CNW film to reach equilibrium mass is significantly longer than the time it took both the 50% and 75% CNW films. In addition, at equilibrium, the 25% CNW film absorbed significantly higher amounts of water (~900%) than did both the 50% CNW film (~100%) and the 75% CNW film (~150%). Upon statistical analysis, presented in Table 18, it was determined that the 50% CNW and 75% CNW composite films were not statistically different and had water uptakes that were in the same range. This could be due to the fact that at 50% is the maximum whisker concentration, after

which an additional amount of whiskers has a negligible effect on the water sorption properties of the prepared films. Further analysis of the swelling of these films using the Flory-Huggins theory, Flory-Rehner theory, and Fickian diffusional characterization is described in Chapter Nine. However, these initial results are similar to those seen in Chapters 4 and 5 where it was determined that, in general, as the amount of PMVEMA increases, so does the equilibrium water absorption. This is most likely attributable to crosslinking density increasing as the percent of cellulose whiskers increases.

Table 18. The maximum water uptake of 25CNW, 50CNW, and 75CNW films at equilibrium was determined using gravimetric dynamic analysis.

	Equilibrium Water Uptake (g/g, %)	**Standard Deviation**	**t-test / 50CNW**	**t-test / 75CNW**
25CNW	963.5	384.5067	3.9178	3.79
50CNW	93.7	1.4996		1.9074
75CNW	120.5	23.95	1.9074	

To further confirm the presence of crosslinking, the gel contents of the prepared composites were determined using the Soxhlet extraction method. These values are summarized in Table 19. The gel content values indicate that the films are lightly crosslinked and that some whiskers were washed out from the matrix upon Soxhlet extraction. The percent gel content is directly proportional to the whiskers content used in the starting mixture, which supports the proposed crosslinking mechanism.

Table 19 The gel content of the crosslinked nanocomposites varied.

Sample	Gel content (%)
PMA-PEG/CNW25	10.4
PMA-PEG/CNW50	32.7
PMA-PEG/CNW75	43.6

Studies by Yang, Xu, and Wang followed the crosslinking of cellulosic fibers with carboxylic and polycarboxylic acids by FT-IR. Especially relevant to this study is their technique to monitor the creation of ester bonds between the carboxylic acids and the cellulose [283, 326] by comparing the FT-IR spectrum of a sample treated with 0.1 M NaOH to that of an untreated sample. Upon comparison, the peak occurring between 1728 - 1735 cm^{-1} in the untreated sample spectrum could be due to both the expected ester linkage between the carboxylic acid groups, and the unreacted carboxylic acid groups [327, 328]. In the 0.10 M NaOH treated sample spectra, a peak between 1580 - 1588 cm^{-1} is attributed by Yang to the carboxylate formed during the interaction of the unreacted carboxylic acid groups and the sodium hydroxide. Yang attributes the peak occurring in the 1721 – 1728 cm^{-1} range solely to the ester crosslinking between the cellulose and carboxylic acid [327, 328].

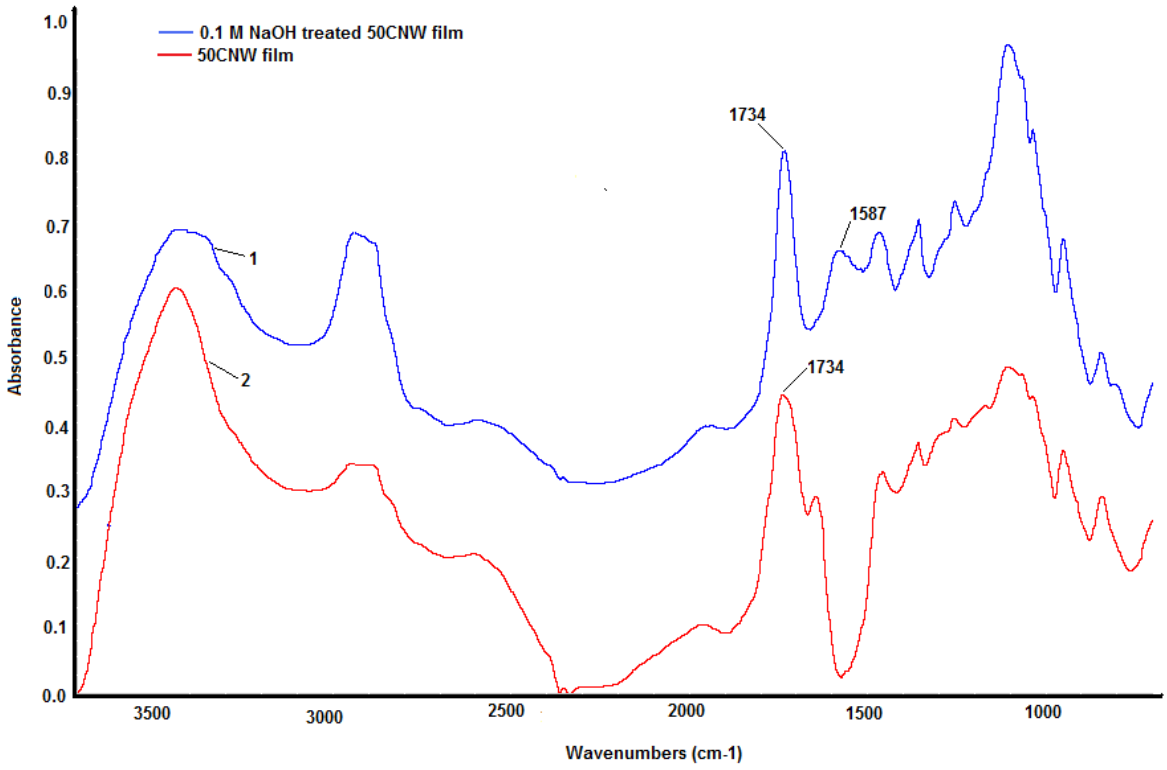

Figure 48. The formation of ester linkages in the PMVEMA-PEG/50CNW films were analyzed using FT-IR.

The crosslinked cellulose whisker films containing 50% CNW were analyzed following this literature methodology, and the representative results are shown in Figure 48. The FT-IR peak at 1743 cm^{-1} in Figure 48 (spectrum 2) is a result of both the ester carbonyl stretch from the crosslinked PMVEMA-cellulose and the unreacted carboxylic acid functional groups from the PMVEMA. The influence of the unreacted PMVEMA carboxylic acid functional groups can be removed by briefly treating the sample with 0.10 M NaOH, as shown in Figure 48 (spectrum 1). Following this methodology, the spectrum 1 FT-IR signal at 1587 cm^{-1} is assigned to the carboxylate carbonyl that results from the treatment of the sample with a base prior to analysis. The resulting ester peak at 1734 cm^{-1} can then be attributed to the formation of an ester linkage between the

PMVEMA carboxylic acid and the cellulose whiskers. The presence of crosslinked cellulose chains is necessitated since the PMVEMA-PEG films did not retain structural integrity upon exposure to water.

6.4 Conclusions.

This study demonstrates that it is possible to develop in-situ crosslinked cellulose whisker nanocomposites using PMVEMA-PEG as a matrix. Water solubilized solutions of PMVEMA and PEG were combined with cellulose whiskers in varying ratios from 0 – 100% CNW, solution cast, and dried to successfully form film-like materials. In-situ crosslinking via thermal treatment of these films was confirmed using FT-IR techniques by the appearance of both the non-carboxylated ester peak at 1734 cm^{-1} and a carboxylated peak at 1587 cm^{-1}. The cellulose nanowhiskers used in this study were confirmed to have birefringent properties and size dimensions of 5 ± 2 nm width and a length of 210 ± 75 nm. As interest in these materials began with the water absorption capabilities of covalently crosslinked PMVEMA-PEG-cellulose fibers (Chapters 4 and 5), initial water absorption studies were undertaken and show that these nanocomposite systems can swell in water and form a stable gel. Maximum water absorption was obtained with the 25CNW film. Water uptake analysis will be discussed in Chapter 9 to further explain these results. Further investigation of these films was necessary in order to quantify the characteristics that were observed in this initial study. Chapter Seven will describe the methods and results of the tensile studies, the atomic force microscopy, and NMR characterization, while Chapter 8 will present the thermogravitmetric analysis of the starting materials and nanocomposites.

CHAPTER SEVEN

CHARACTERIZATION OF IN SITU CROSSLINKED CELLULOSE NANOWHISKER POLY (METHYL VINYL ETHER-CO-MALEIC ACID)-POLYETHYLENE GLYCOL NANOCOMPOSITE[4]

7.1 Introduction.

Though nanocomposites have been reported in the literature as early as the 1950s, polymer-based nanocomposites made a marked impact in industry and academia when Toyota reported layered nanosilicate-based nanocomposites in 1993 [329, 330]. Frequently, the main functions of incorporating nanodimensional-based materials into matrices are to increase mechanical performance, thermal stability and barrier properties [331, 332]. At the nanoscale, the nano-particles have a large surface area and the possibility to interfere with polymer chain mobility, thereby manipulating the matrix properties. However, it is important to understand that these expected improvements are directly dependent on the dispersion and distribution of the nanoparticles in the polymer

---

[4] This work was published in the journal Biomacromolecules as "Poly(methyl vinyl ether-co-maleic acid)-polyethylene glycol nanocomposites cross-linked in situ with cellulose nanowhiskers." Biomacromolecules, (2010), 11(10), 2660-2666. Other authors were Marcus Foston and Arthur J. Ragauskas from the Institute of Paper Science and Technology and School of Chemistry and Biochemistry at Georgia Institute of Technology and Aji Mathew and Kristiina Oksman from the Division of Manufacturing and Design of Wood and Bionanocomposites, Luleå Institute of Technology, Skellefteå, Sweden.

matrix, as well as on the interaction between the matrix and the reinforcing phases. The optimization of the dispersion and interactions of nanoparticles in polymer matrices using mechanical and chemical means is a key factor that enables the development of high-quality nanocomposites.

In recent years, there has been renewed societal interest in the development and utilization of biobased green materials [7, 8, 17, 103, 279, 333]. Cellulose is the most abundant biomaterial, and the discovery of new ways to utilize this biopolymer to create new biobased materials is becoming a priority. Consequently, cellulose nanowhiskers (CNW) have generated much attention recently [8, 9, 53, 334, 335]. Cellulose nanowhiskers are rod-shaped in structure and are formed when native cellulose is subjected to strong acid hydrolysis [103, 333]. The dimensions of the resulting nanowhiskers vary according to the source of the cellulose, but can range from 10-20 nm in diameter and from 100 – 1000 nm in length [113, 333, 336]. The modulus of cellulose nanowhiskers has been experimentally and theoretically calculated to range from 138 GPa (experimentally determined) to 167 GPa (theoretically determined) [113, 322, 324].

Cellulose nanowhiskers (CNW) have been incorporated in a wide variety of matrices, including latex [337, 338], starch [339-341], cellulose acetate butyrate (CAB) [55, 325, 342], polyhydroxyl alkanoates (PHA) [118] and poly(lactic acid) (PLA) [125, 138, 343-346], in order to improve the strength properties of these matrices. The addition of surfactants [347-349] and plasticizers [147, 341, 350-355] has been found to improve the dispersion of nanowhiskers in the matrix and improve physical properties. While an encapsulated matrix around CNW was reported by Samir, Alloin, Sanchez and Dufresne, [170], crosslinking cellulose whiskers with a matrix in-situ to achieve good nanowhisker

dispersion has not been evaluated**.** We have recently reported the co-crosslinking of a poly(methyl vinyl ether co-maleic acid) (PMVEMA) – polyethylene glycol (PEG) matrix with cellulose nanowhiskers [356]. The resulting crosslinked nanocomposite was shown to have unique properties that were distinct from the starting components. Of special interest were the hydrogel properties that facilitated an up to ~900% mass absorption of water [356].

PMVEMA is a polycarboxylic acid-containing polymer that is currently used in health care applications. PMVEMA has recently been investigated for its potential as a bioadhesive polymer for use in drug delivery [357-363]. There has been interest in expanding its use using cellulosic materials. Barcus and Bjorkquist developed a procedure for reacting PMVEMA and PEG with wood fibers using a thermal dehydration reaction as an alternative method for grafting cellulose. This method allows for the creation of a crosslinked material with increased water sorption properties without the use of metal catalysts [291]. Khutoryanskaya, Khutoryanskiy, and Pethrick have investigated blends of hydroxyethylcellulose and PMVEMA [364].

It is expected that the in-situ co-crosslinking of nanowhiskers in a water-soluble biopolymer matrix would lead to the development of a well-dispersed nanocomposite with enhanced mechanical properties and stability in an aqueous medium. Additionally, this crosslinking may allow the dispersed nanowhiskers to be locked within the polymer matrix, and might enable the development of nanocomposite materials with properties that could be tailor-made depending on the degree of crosslinking, the nanowhisker concentration, and the relative humidity conditions.

This chapter investigates the mechanical properties and transverse relaxation of crosslinked PMVEMA-PEG-CNW nanocomposites and the effect of CNW concentration on these physical properties. A promising future use of these materials is in climate-controlled applications and biomedical applications; hence, the behaviour of the prepared hydrogels in different humidity environments was explored.

7.2 Experimental methods and materials.

7.2.1 Materials.

PMVEMA, poly (ethylene glycol) (M_w 3,000), microcrystalline cellulose (VIVAPUR® 105), and all other chemicals were used as received and described in Chapter 3 (Section 3.1 Materials).

7.2.2 Preparation of cellulose nanowhiskers.

Microcrystalline cellulose was hydrolyzed to form cellulose nanowhiskers using the procedure described in Chapter 3 (Section 3.3.1 Preparation of cellulose whiskers from microcrystalline cellulose.) [67].

7.2.3 Synthesis of PMVEMA-PEG/CNW nanocomposite hydrogels.

The procedure for preparing the PMVEMA-PEG/CNW nanocomposite hydrogels is described in Chapter 3 (Section 3.3.3 Preparation of crosslinked cellulose whisker film hydrogels.) [356]. The nanocomposite hydrogels are described according to their initial nanowhisker percentage, as seen in Chapter 3 Table 15, for example 25CNW = 25% cellulose whisker, wt-%. An unreacted control film of 50 wt-% nanowhiskers and 50 wt-% matrix was also prepared using the same method as that which produced the

crosslinked nanocomposite hydrogels, with the exception of the fact that the control film was not heated to 130 °C. The nanocomposite hydrogels were stored in desiccators at varying relative humidities (i.e., 2%, 54%, and 92%) for 1 week prior to physical testing.

7.2.4 Nuclear Magnetic Resonance (NMR) Analysis.

7.2.4.1 Starting materials.

PMVEMA, PEG, and PMVEMA-PEG were dissolved in DMSO-d_6 and analyzed as liquids ^{13}C and ^{1}H NMR on a Bruker Avance-400 spectrometer as described in Chapter 3 (Section 3.4.2.1 NMR analysis of starting materials.).

7.2.4.2 Crosslinked cellulose whisker film hydrogels.

In preparation for NMR analysis, the nanocomposite hydrogels were prepared for NMR analysis as described in Chapter 3 (Section 3.4.2.2 Nuclear Magnetic Resonance (NMR) of cellulose whisker films.)

^{13}C CP/MAS solid-state NMR measurements were carried out as described in Chapter 3 (Section 3.4.2.2 Nuclear magnetic resonance (NMR) of cellulose whisker films.) on a Bruker DSX-400 spectrometer.

^{1}H spin-spin (T_2) NMR experiments were conducted as described in Chapter 3 (Section 3.4.2.2 Nuclear magnetic resonance (NMR) of cellulose whisker films.) on a Bruker DSX-400 spectrometer.

7.2.5 Atomic Force Microscopy (AFM).

The cellulose nanowhiskers, as well as the nanocomposites, were characterized using a Veeco MultiMode scanning probe microscope with a Nanoscope V controller as

described in Chapter 3 (Section 3.4.3 Atomic force microscopy of cellulose whiskers and films).

7.2.6 Stress – strain measurements.

The tensile measurements were performed on an Instron 4411 (USA) with a 500 N load cell as described in Chapter 3 (Section 3.4.4 Tensile measurements of cellulose whisker films.). The values given are based on 5 tests per composition. The error in the measurements was reported as the standard deviation.

7.3 Results and discussion.

The preparation of the nanowhiskers and their chemical characterization are detailed in Chapter 6 [356]. PMVEMA and cellulose nanowhiskers were shown to undergo an esterification reaction primarily between the primary hydroxyl group of the cellulose and the acid group of the PMVEMA (Chapter 4 Figure 30). In addition, PEG was shown to be capable of crosslinks with the PMVEMA in a second esterification reaction. The prior chapters demonstrated that all three components, PEG, PMVEMA, and the cellulose nanowhiskers, were needed to form the reported nanocomposites.

7.3.1 NMR Analysis.

An NMR analysis of the PMVEMA, PEG, PMVEMA-PEG, and crosslinked nanocomposite hydrogels was performed to further analyze the crosslinking. Observed ^{13}C NMR chemical shifts of the starting PEG and PMVEMA agreed with literature values and with the corresponding ^{13}C CP/MAS NMR of the crosslinked nanocomposite hydrogels. The ^{13}C CP/MAS NMR spectra of the cellulose nanowhiskers showed the typical spectra of crystalline cellulose, and based on the integration of the cellulose C_4

peak region (^{13}C δ ~ 80-85 and 85-92 ppm amorphous and crystalline cellulose respectively) the nanowhiskers were shown to have a crystallinity of ~ 61%, which stayed constant upon the incorporation of PMVEMA-PEG components. Moreover, the chemical shifts of the cellulose carbons did not seem to be affected by the incorporation of PMVEMA-PEG components, suggesting that the chemical alteration of cellulose occurs on a small fraction of surface-accessible glycosidic units. As Figure 49 shows, the Soxhlet extracted samples exhibited all three components, as they contained transesterified linkages that clearly displayed carbon resonances overlapping with cellulose at ~ 72 and 50-65 ppm. These resonances were generated by PEG and PMVEMA, respectively. One of the most dramatic observations was of the NMR spectrum of a crosslinked 50CNW nanocomposite when compared to the NMR spectrum of the unreacted control. The carboxylic acid shift from the PMVEMA at ~175 ppm is almost completely removed from the NMR spectrum upon a Soxhlet extraction of the uncured 50 wt.-% CNW mixture. This confirms not only that the Soxhlet extraction procedure removes any noncovalently linked oligomers, but also, and most importantly, that the residual nanocomposite hydrogels are truly crosslinked.

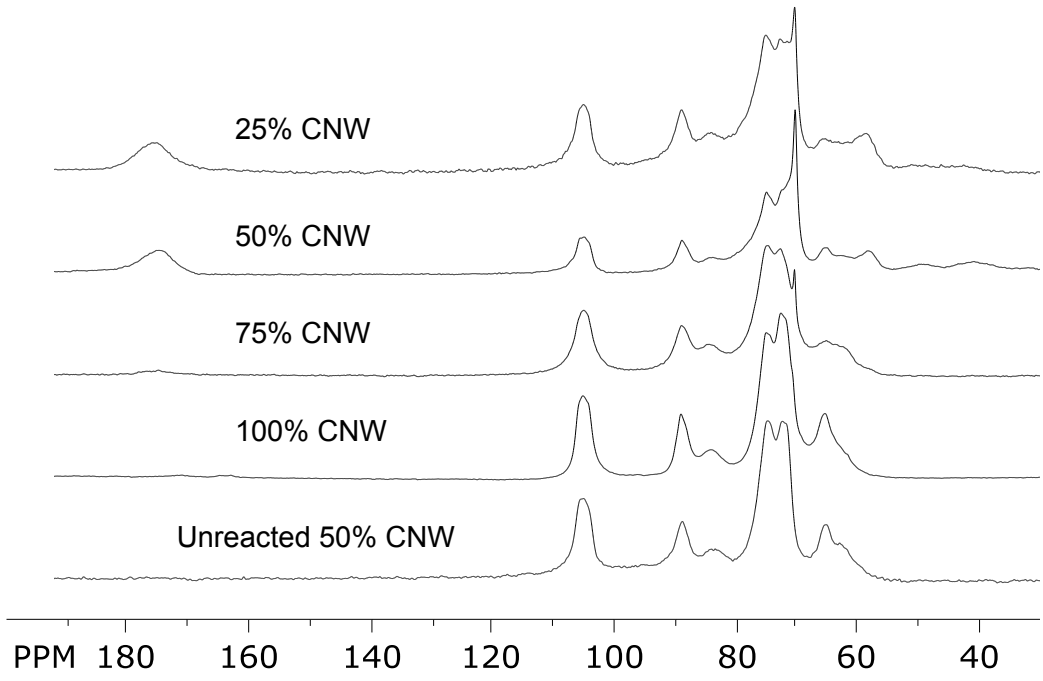

Figure 49. ^{13}C spectra of H_2O extracted CNW nanocomposites.

The ^{1}H MAS NMR spectrum obtained for the 50CNW nanocomposite swollen in D_2O is shown in Figure 50, along with the solid spectrum of pure cellulose nanowhiskers and the solution spectra of the PEG and PMVEMA oligomers, which are stacked beneath. The ^{1}H MAS NMR spectrum shows peaks between ~3.8 - 1.9 ppm that belong to protons on CNW, PEG and PMVEMA. In the solution spectrum of the PEG oligomers and the solid state spectrum of the nanocomposite, there is one chemical shift of note: the chemical shift of the protons on the methylene groups along the backbone of the polymer, which appear at ~3.8 ppm. There are three fairly resolved peaks that appear in both the solution spectrum of the PMVEMA oligomers and the solid state spectrum of the nanocomposite: the chemical shift of the protons on the methine groups attached to pendent carbonyls along the backbone, denoted $C^{e,d}$, at ~3.06 ppm; the methine group attached to a methoxy pendent group along the backbone, denoted C^{c}, at ~3.30 ppm; and

the methoxy pendent group, appearing at ~3.50 ppm and labeled C^b. As evidenced by the spectrum of pure cellulose nanowhiskers, the peak at ~3.50 ppm in the spectrum of the nanocomposite is actually an overlapping resonance of protons from CNW and the C^b on PMVEMA.

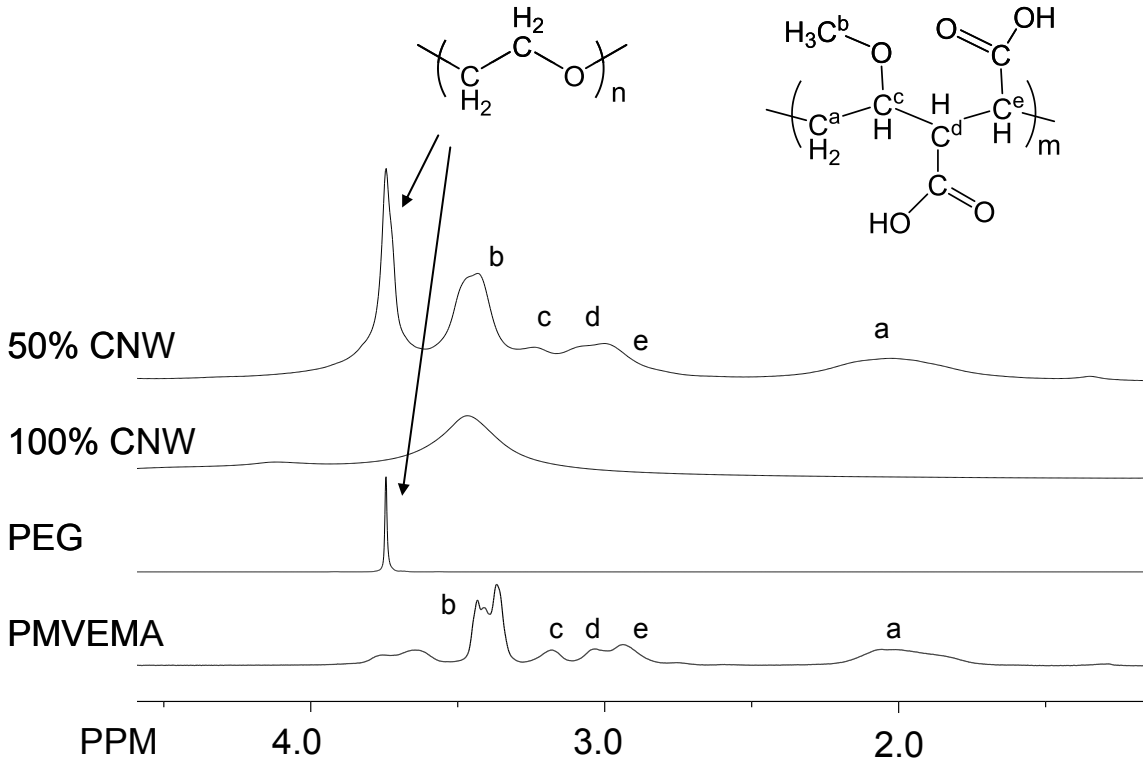

Figure 50. ^{1}H spectra of PEG and PMVEMA dissolved in D_2O and ^{1}H MAS 2 KHz spectrum of H_2O extracted 50CNW nanocomposite swollen in D_2O at 50 °C**.**

The nature of molecular mobility in a polymer system can be probed easily using a T_2 NMR experiment. Spin-spin or T_2 relaxation probes how quickly a nucleus loses transverse magnetization. In T_2 experiments, signal intensity decays as a function of local inhomogeneities in the magnetic field. This is mainly due to perturbation by nuclei through space or to dipolar interactions, and this signal attenuation, or the characteristic relaxation rate for this process, is called the spin-spin relaxation or T_2 time. The T_2 time can be used to describe molecular motion, and is particularly sensitive to chain dynamics

in polymer systems above T_g; the faster the rate of decay, the more rigid and fewer degrees of freedom the chemical group associated with that decay has. ^1H T_2 relaxation can be used in this CNW nanocomposite system to infer information on the length of the chains between junctions of crosslinking points, as well as to explore crosslinking density and the sterical constraints from surrounding chains.

A Carr-Purcell-Meiboom-Gill (CPMG) sequence was used to collect the T_2 data. Figure 51 displays the typical spin-spin decay profiles for PMVEMA protons on carbon positions C^c and $C^{d,e}$ for the D_2O swollen 25CNW and 50CNW nanocomposites at 50 °C. The lines represent a fit based on a two-component, Gaussian-exponential model commonly used in polymer systems. This model contains distinct rigid and mobile components.

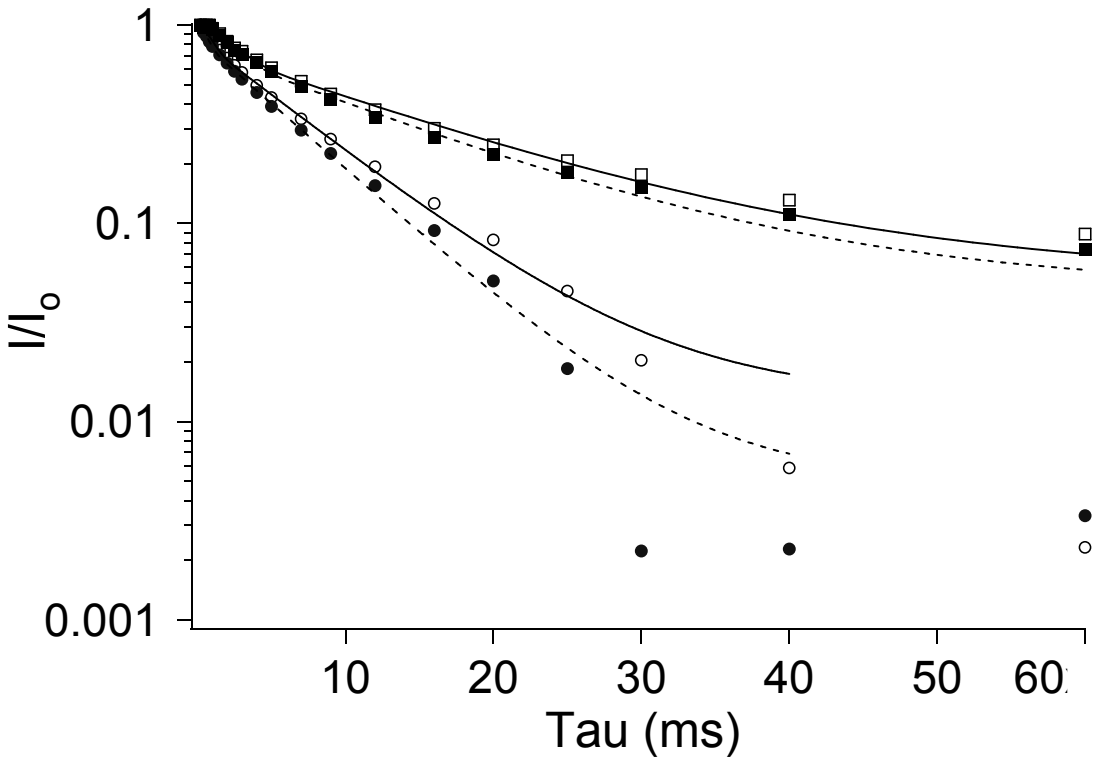

Figure 51. Spin-spin relaxation of the (open) PMVEMA protons on C^c and (closed) PMVEMA protons on $C^{d,e}$ for (○) 50CNW (□) 25CNW nanocomposites at 50 °C.

The CPMG experiments were conducted at an elevated temperature in an effort to impart greater chain dynamics and differences in those dynamics.Figure **51** shows that the relaxation rate of the 50CNW nanocomposite is faster than that of the 25CNW nanocomposite, indicating a much more rigid morphology. This rigidity is mainly interpreted as an increase in crosslinking density. The T2 results for the various other resolvable peaks for the CNW nanocomposite are compiled in Table 20, which lists the relative intensity and T2 time for the rigid repeat units in crosslinking junction points (described by the Gaussian component), as well as more mobile repeat units belonging to chains outside or between junctions of crosslinking points (described by the exponential component).

Table 20. Characteristic 1H spin-spin relaxation (T2) values and relative component intensities based on a Gaussian-exponential model for H_2O extracted 25CNW and 50CNW nanocomposites swollen in D_2O at 50 °C.

		25CNW				50CNW			
Chemical Group	**^{1}H (ppm)**	$\%T_2^{jun}$	$\%T_{2\,in}^{cha}$	T_2^{jun} (ms)	T_2^{chain} (ms)	$\%T_2^{jun}$	$\%T_{2\,in}^{cha}$	T_2^{jun} (ms)	T_2^{chain} (ms)
PEG	**3.81**	*17*	*83*44	44*83*	762	*34*	*66*29	29*66*	525
PMVEMA-C[c]	**3.30**	*26*	*74*28	28*74*	157	*16*	*84*12	12*84*	75
PMVEMA-C[e,d]	**3.06**	*26*	*74*28	28*74*	143	*16*	*84*8	8*84*	65

[jun]: junction point describe repeat units close enough to crosslinking point to have reduced dynamics,
[chain]: chains between junctions describe repeat units between crosslinking points displaying "unrestricted" dynamics.

The methylene protons on PEG were analyzed using the aforementioned two-component model. The results for the faster-relaxing PEG component of the 25CNW nanocomposite show a T_2 of ~44 ms. This component describes a portion of the composite in which PEG chains have low mobility and are attributed to PEG repeat units adjacent to junction points. The slower-relaxing PEG component, on the other hand, had a T_2 of ~762 ms, and since the extractable PEG had been removed in the exhaustive extractions, the order of magnitude difference suggests that this component describes highly mobile PEG chain repeat units. These mobile units most likely link between or outside junction points and/or in areas of appreciably low crosslink density.

The results in Table 20 for protons on PMVEMA show that in the T_2 of the 50CNW nanocomposite was approximately half of that of the 25CNW nanocomposite. This suggests that, on average, the PMVEMA components have half as many degrees of freedom. Essentially, upon the incorporation of additional nanowhiskers, PMVEMA

itself exhibits slower dynamics, most likely due to the formation of additional attachments to the polymer composite system.

The T_2 values for both the junction and chain portions of the PEG in the 50CNW nanocomposite are slightly lower than those of the 25CNW nanocomposite. This again shows that upon the addition of more cellulose, the PEG becomes less mobile. This is due to an increased number of attachment points and an overall increase in sterical constraints. More interesting is the increase in the relative intensity of the junction component and the decrease in the relative intensity of the chain component. The change in the relative intensity of the junction component seems to indicate that twice as many PEG-related junction points exist in the 50CNW nanocomposite than do in the 25CNW nanocomposite. The chemistry involved in this PEG, PMVEMA, and CNW composite preparation suggests that PEG uses PMVEMA to attach to the composite system only at oligomeric PEG end-groups. This is supported by a T_2 relaxation profile that explicitly exhibits two-component mobile/rigid behavior: an order of magnitude difference in relaxation times between those components and changes in component relative intensity scales directly with CNW concentration. Moreover, these results not only suggest that PEG is bonded solely to the PMVEMA chains, they also suggest that the PMVEMA chains within the nanocomposite are in close proximity to the CNW surface for the majority of the nanowhisker length.

The methine and methyl protons on PMVEMA were also analyzed using the two-component Gaussian-exponential model. The characteristic T_2 time results for the faster-relaxing PMVEMA component of the 25CNW nanocomposite show a T_2 of ~28 ms for protons at carbon locations C^c and $C^{d,e}$. The slower-relaxing PMVEMA component had

T_2 times of ~157 and 143 ms for protons at carbon locations C^c and $C^{d,e}$, respectively. It is evident that there must be a lesser difference in chain dynamics between the two components for PMVEMA than for PEG. This is true because PMVEMA's relaxation rates for the junction and chain components are more similar. This most likely is because PMVEMA can bond to the composite system at various points along its backbone. This would limit the mobility of these much shorter chain portions, and provide more junction points than are available to PEG-related bonds. This is reflected in Table 20. The T_2 values for all PMVEMA-related resonances and components are lower for the 50CNW nanocomposite than for the 25CNW nanocomposite. In this case, this is mainly due to an appreciable increase in steric constraints upon the incorporation of additional cellulose.

7.3.2 Microscopy.

The size and size distribution of the nanowhiskers used for this study is shown in Figure 52. The nanowhiskers are needle-shaped crystals with diameters between 15 and 17 nm. The diameter measurements were made using Nanoscope V software and were determined using the height of the nanowhiskers. This methodology is more accurate for the characterization of CNW, since AFM tip scanning has a broadening effect, which is minimized in comparison to width measurements. It is worth mentioning that the efficiency of the measurements is restricted by the aggregation of nanowhiskers during sample preparation, leading to difficulties in obtaining a monolayer of well-dispersed whiskers for measurements. In most cases, a majority of the nanowhiskers will be only partially separated or even bundled together.

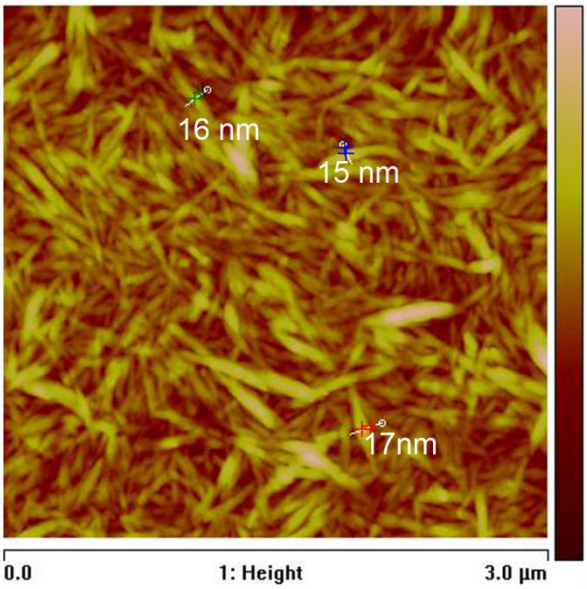

Figure 52. The height image of the nanowhiskers, showing the diameter measurements of the cellulose nanowhiskers.
.

An overview and a detailed view of the 25 and 50 CNW crosslinked nanocomposites are shown in Figure 53. These results demonstrate an equally-distributed second phase in a continuous matrix phase.

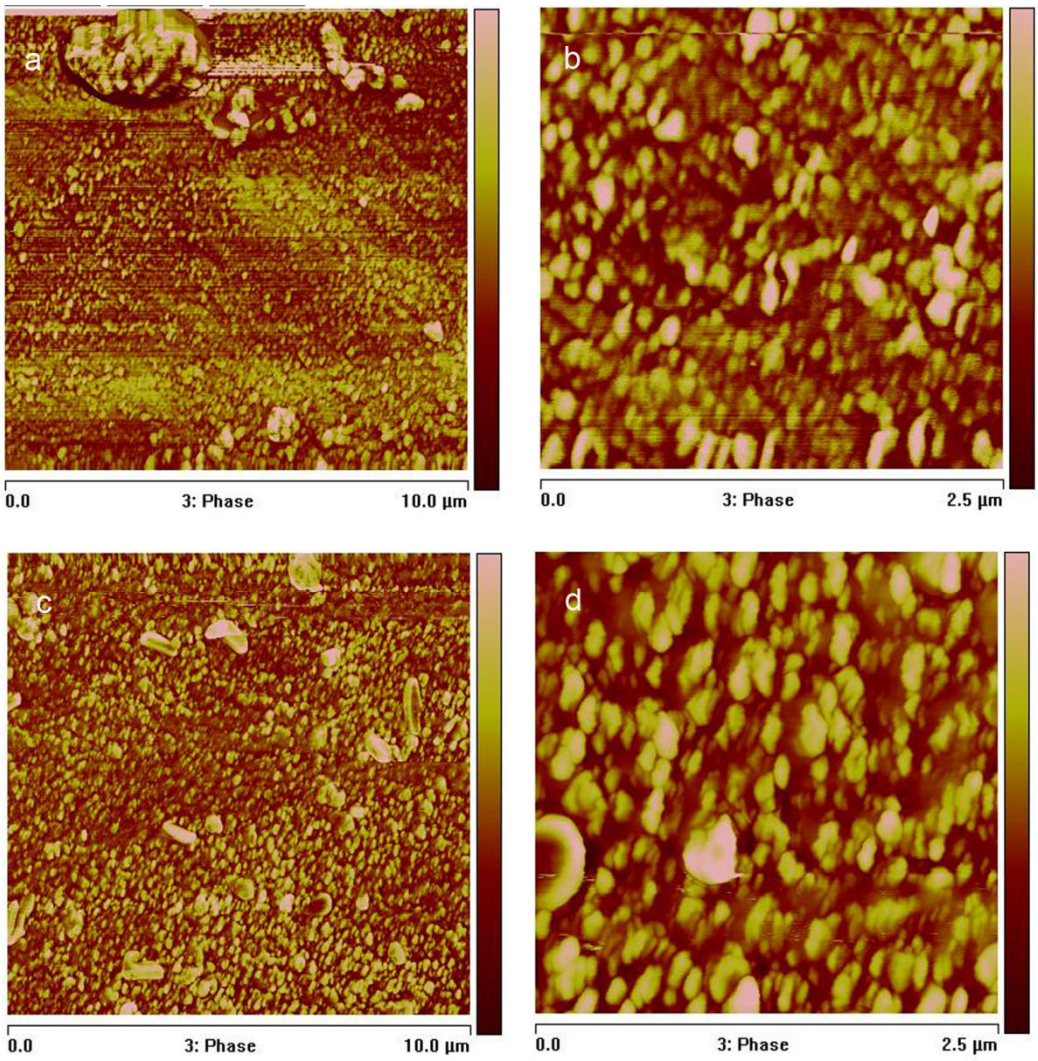

Figure 53. Cross sections of crosslinked nanocomposites with 25CNW; a) overview b) detailed view and 50CNW c) overview d) detailed view.

In the AFM micrographs, the oval-shaped structures are attributed to cellulose nanowhiskers or clusters of nanowhiskers embedded in the PMVEMA-PEG phase. A broad range of nanowhisker sizes can be observed in the nanocomposites images, which may be due to the fact that the nanowhiskers are cut at different angles during sample

preparation. This is expected, as the nanowhiskers are randomly oriented in solution-cast films, and the AFM image is obtained from the ultramicrotomed cross-section.

In addition, it was noted that the size of the nanowhiskers in the embedded phase showed a tendency to increase as the CNW content increased from 25% to 50 wt. %. This may suggest larger agglomerates of CNWs in solutions with higher CNW content.

7.3.3 Mechanical properties.

The stress-strain properties of the prepared hydrogels were studied as a function of CNW content and relative humidity (RH) conditions. The nanocomposite hydrogels with 25, 50, 75 and 100 wt.-% CNW content, all of which had been conditioned at 92% RH, were evaluated for physical properties. These results are shown in Table 21. It can be seen that the tensile strength increased when the nanowhisker content increased from 25 wt.-% to 50 wt.-%. The modulus (stiffness) of the hydrogels was very low for 25% and 50% CNW, but increased for the hydrogels with 75% and 100 wt.-% CNW content. All hydrogels exhibited a very high ability to withstand strain, between 120-306%, with the highest values for the gels with a lower nanowhisker content. Compared to the toughness values of cellulose nanofiber networks (nanopaper) as reported by Henriksson [365], the in-situ crosslinked materials had superior toughness but lower stiffness and strength. The effect that the relative humidity has on the mechanical properties is demonstrated in Figure 54. These values are based on the mechanical performance of 75 wt.-% CNW gels that had been conditioned at three different relative humidity conditions (2, 54 and 92%). The percent elongation at break increased as the relative humidity increased, while the maximum stress at break was achieved at the lowest relative humidity. From Table 21, it is possible to see the correlation between composition and

relative humidity where, as the relative humidity increased, elongation at break (%) also increased, while the tensile strength (MPa) decreased. It is known that water can act as a plasticizer due to the swelling mechanism and concomitant relaxation of the hydrogel hydrophilic polymer chains [261, 366]. Water will hydrogen bond to the hydrogel, preventing intermolecular entanglements via hydrogen bonding of the PMVEMA with PMVEMA and with PEG molecules due to shielding effect of the water; this results in a decrease in tensile strength and an embrittlement observed when the hydrogels were conditioned at 2% relative humidity. Singh reported similar behaviour with solution cast PMVEMA-PEG films [367]. These results show that these materials are capable of a wide range of properties depending on the moisture conditions.

Table 21. Mechanical properties of matrix and crosslinked nanocomposite hydrogels at different relative humidities.

Sample	Relative Humidity [%]	Tensile Strength [MPa]	Strain [%]	E-modulus [GPa]
25CNW	92	2.3 ± 0.8	309 ± 16	0.09 ± 0.06
50CNW	92	4.2 ± 0.2	227 ± 24	0.19 ± 0.06
75CNW	92	4.0 ± 0.1	120 ± 2	2.3 ± 0.1
100CNW	92	4.0 ± 1.6	105 ± 0	3.9 ± 0.8
75CNW	2	36.8 ± 5.3	106 ± 2	14.3 ± 3.3
75CNW	54	8.5 ± 2.7	116 ± 4	8.7 ± 0.9
75CNW	92	4.0 ± 0.05	120 ± 2	2.3 ± 0.1

The representative stress-strain curves of the crosslinked composites varied according to CNW content. The 92% RH conditioned samples are shown in Figure 54.

As the nanowhisker content increased, the stress and modulus increased, while the strain decreased. As Table 14 and Figure 54 demonstrate, the strain and the stress varied based on the composition of the materials. However, the relationship between CNW content and mechanical properties is non-linear. It appears as though the 50CNW gel at 92% RH (Figure 54c) is able to balance stress verse strain demands better than the 25CNW or 75CNW nanocomposite hydrogels.

In summary, each of the nanocomposite hydrogels behaved differently from the others. This furthers our belief that these materials have developed differing degrees of crosslinking between the matrix and the cellulose nanowhiskers. This allows for the possibility to potentially tailor these materials to a specific set of conditions, depending upon the desired application.

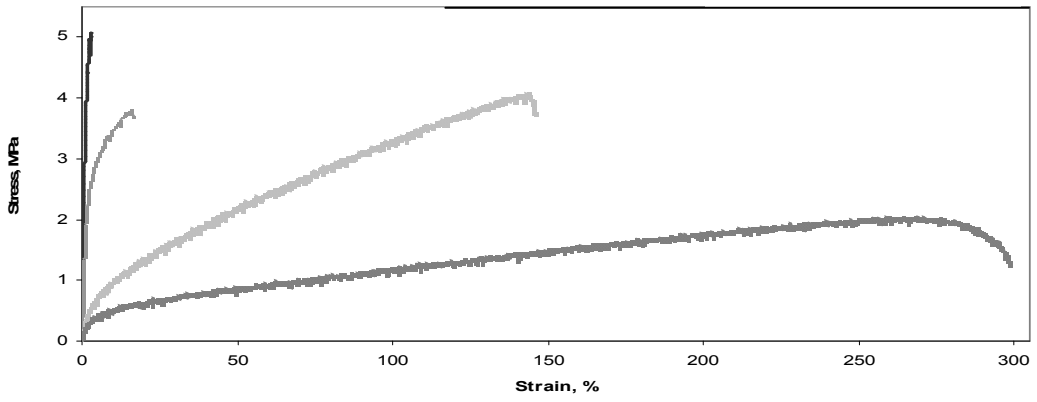

Figure 54. The stress-strain curves of prepared hydrogels a) 100CNW, b) 75CNW, c) 50CNW, d) 25CNW nanocomposite hydrogels at 92% relative humidity.

7.4 Conclusion.

In-situ co-crosslinked nanocomposite hydrogels were developed by dispersing and crosslinking cellulose nanowhiskers with a poly(methyl vinyl ether-co-maleic acid)–polyethylene glycol matrix using solution casting and a subsequent thermal crosslinking technique. Nuclear magnetic resonance studies supported the crosslinking between the matrix and the cellulose nanowhiskers via an esterification reaction. The T-2 relaxation profiles suggest that the proposed crosslinking is occurring, with the PMVEMA binding to the cellulose whiskers and the PEG binding solely to the PMVEMA. It also suggests that the crosslinking density is greater for the 50CNW than the 25CNW films. The water sorption experiments in Chapter 9 will further explore this. These NMR results also support the results and explanations for the overall water absorption trends demonstrated by the crosslinked pulp fibers in Chapters 4 and 5.

The atomic force microscopy images show that the nanowhiskers were dispersed homogenously in the matrix indicating that in-situ co-crosslinking of cellulose nanowhiskers with a matrix polymer is a promising way to prevent nanowhisker aggregation and obtain good dispersion at the nanolevel.

The mechanical behaviour of the crosslinked nanocomposite hydrogels differed significantly as the material percentages were varied. Typically, the mechanical property increased as nanowhisker content increased, and decreased as relative humidity increased. However, the 50 wt.-% CNW composite was able to achieve both high strain and high tensile values, relative to the other composites. In addition, the overall trend of increasing strain values as the relative humidity was increased is most likely due to the plasticization effect of the water content with the PMVEMA-PEG.

This new methodology of nanocomposite processing is expected to provide an efficient route to developing tailor-made nanocomposites controlled by the degree of co-crosslinking, the nanowhisker concentration, and the relative humidity conditions. A thermogravimetric analysis (TGA) of the film compositions was next performed in order to determine the effect that the cellulose whiskers had on the thermal stability of the PMVEMA-PEG matrix. This work is detailed in the following chapter.

CHAPTER EIGHT

THERMOGRAVIMETRIC ANALYSIS OF IN-SITU CROSSLINKED CELLULOSE WHISKER PMVEMA – PEG COMPOSITES AND STARTING MATERIALS[5]

8.1 Introduction.

Interest in developing biobased materials as an alternative to petroleum-derived materials has significantly increased in the past decade. One such source for these materials is cellulose, especially cellulose derived from woody biomass, since such biomass is a high volume bioresource that can be harvested in a sustainable manner. Within this broad field of study, cellulose whiskers are an example of cellulosic materials that show much promise.

Cellulose whiskers are crystalline cellulose rods that typically range in size from 100 nm to 1 μm in length and 5 – 50 nm in width [8, 53, 120, 335]. The size variations can be attributed, in part, to differences in the starting material and experimental conditions employed for their generation [8, 53, 120, 335]. Cellulose whiskers are commonly prepared via the acid hydrolysis of a variety of cellulose sources including

---

[5] This work was published in the TAPPI Journal as "Thermal gravimetric analysis of in-situ crosslinked nanocellulose whiskers-poly(methyl vinyl ether-co-maleic acid)-polyethylene glycol." TAPPI Journal, (2011), 10(4), 29-33. Other authors were Arthur J. Ragauskas from the Institute of Paper Science and Technology and School of Chemistry and Biochemistry at Georgia Institute of Technology and Aji Mathew and Kristiina Oksman from the Division of Manufacturing and Design of Wood and Bionanocomposites, Luleå Institute of Technology, Skellefteå, Sweden.

microcrystalline cellulose, wood pulps, and tunicates. The development of biomaterials utilizing cellulose whiskers has been focused frequently on composite formulations and the material characterization of whisker-based composite materials. Thermal stability studies are also necessary to evaluate the potential application of these new materials.

This thesis study has focused on in-situ crosslinking of cellulose whiskers with poly (methyl vinyl ether co maleic acid) (PMVEMA) and polyethylene glycol (PEG). The current study has shown that all three components are required for crosslinking, and when the necessary experimental conditions are accomplished, the resulting composite exhibits unique physical properties that are dependent upon the ratio of the constituents employed. The resulting crosslinked nanocomposites were found to have uniformly-distributed cellulosic whiskers, and to display hydrogel properties that facilitated an up to ~900% mass absorption of water, of special interest due to the potential applications of this characteristic. This study examines the thermal degradation properties of these cross-linked nanogels for the purposes of evaluating future applications.

8.2 Materials and methods.

8.2.1 Materials.

Poly(methyl vinyl ether –co–maleic acid), poly (ethylene glycol) (MW 3000), microcrystalline cellulose (VIVAPUR® 105), and all other reagents were used as received and described in Chapter 3. Cellulose whiskers were prepared via acid hydrolysis of microcrystalline cellulose using procedure in Chapter 3 (Section 3.3.1 Preparation of cellulose whiskers using microcrystalline cellulose.). These were then used to prepare the crosslinked nanocomposite films.

8.2.2 Crosslinked nanocomposite films.

Cellulose whisker-PMVEMA-PEG films were prepared as described in Chapter 3 (Section 3.3.3 Preparation of crosslinked cellulose whisker film hydrogels.). Five film compositions were prepared and classified based on the percent cellulose whisker content (by weight) in each film – 0%, 25%, 50% 75%, and 100%. These will be referred to as 0CNW, 25CNW, 50CNW, 75CNW, and 100CNW, respectively. The films were then stored in a desiccator at 54% relative humidity for one week prior to testing. The chemistry of cross-linking PMVEMA, PEG, and CNW is illustrated in Chapter 4 Figure 30.

8.2.3 Thermogravimetric Analysis.

A thermogravimetric analysis (TGA) of the starting materials and prepared films was performed on a TA TGA 500 (USA) as described in Chapter 3 (Section 3.4.10 Thermogravitmetric analysis.). T_{onset} was determined as the temperature at which the sample weight was 93% of the sample mass at 105 °C [56].

8.3 Results and Discussion.

8.3.1 Thermal gravimetric analysis of starting materials.

The thermal decomposition and degradation behavior of the nanocomposites is an important parameter by which to evaluate their potential applications and the manufacturing of these materials. Control studies demonstrated that PMVEMA TGA/DTG results aligned with the data reported by Chung, Wu and Malawar [368]. During the dehydration of PMVEMA, three distinct peaks appeared at 80 °C, 175 °C, and

325 °C. The decomposition of the combined matrix of PMVEMA-PEG (0CNW) is shown in Figure 55a. There was a slight loss of water starting at approximately 40 °C. The T_{onset} of degradation of PMVEMA-PEG (0CNW) was measured at 149 °C, lower than the T_{onset} of degradation of both PMVEMA (159 °C) and PEG (190 °C). The T_{max} of the first decomposition of PMVEMA-PEG (150 °C), which is associated with the dehydration of the diacid groups of the PMVEMA, was less than the T_{max} of the pure PMVEMA (154 °C). The second decomposition process of the PMVEMA-PEG also had a lower T_{max} (226 °C) than that of the PMVEMA (240 °C). The peak at 226 °C could be attributed to the combined decomposition of PMVEMA and PEG. Possible degradation reactions include decarboxylation. The next decomposition peaks, which occurred at 404 °C and 568 °C, were most likely due to polymer chain degradation.

The degradation behavior of cellulose nanowhiskers (100CNW) is shown in Figure 55b. The decomposition of the whisker film shows an initial period of weight loss. This is attributed to the loss of free water. A constant weight was then maintained from approximately 90 °C to ~150 °C, with an onset of thermal degradation occurring at 206 °C. This is typical for whiskers prepared using the sulfuric acid-based method. These results indicate that the cellulose nanowhisker film was the most thermally stable of all the starting materials, based on the T_{onset} values.

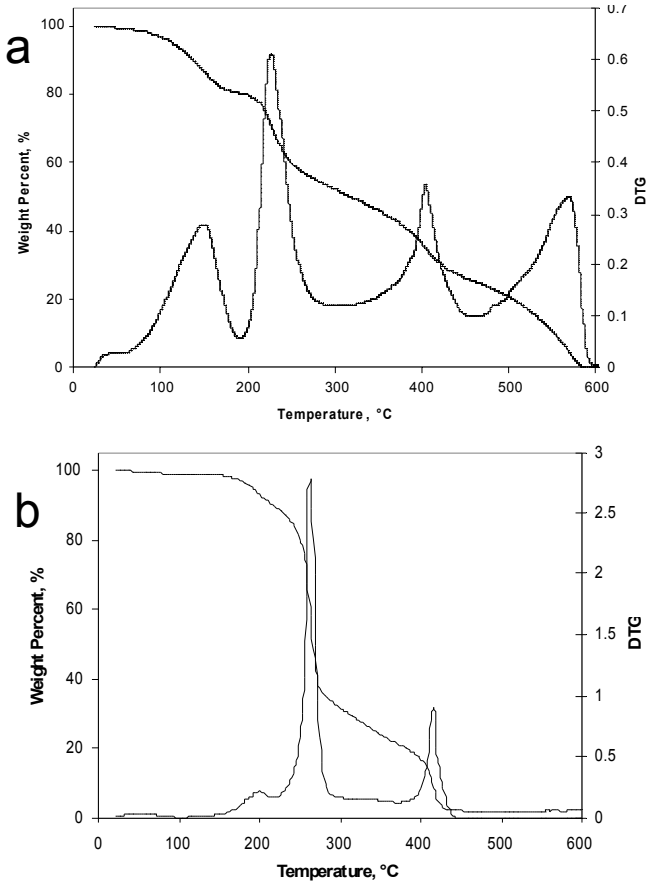

Figure 55. TGA and DTG of (a) 0CNW (PMVEMA-PEG matrix) and (b) 100CNW.

8.3.2 Thermal gravimetric analysis of the crosslinked nanocomposites.

Figure 56 shows the TGA and DTG curves of the 25CNW, 50CNW, and 75CNW films. The TGA and DTG curves of the prepared nanocomposite materials illustrate the way in which the films behave differently as the percent cellulose nanowhiskers is varied. Based on the temperature of the first stage of decomposition, T_{onset}, the most thermally stable of the three compositions is the 75CNW film. The 100CNW film (Figure 56b) was slightly less thermally stable than the 75CNW film (Figure 56a). The least thermally

stable of all the materials used was the 0CNW matrix film (Figure 56a), which demonstrated essentially no thermal stability throughout the test.

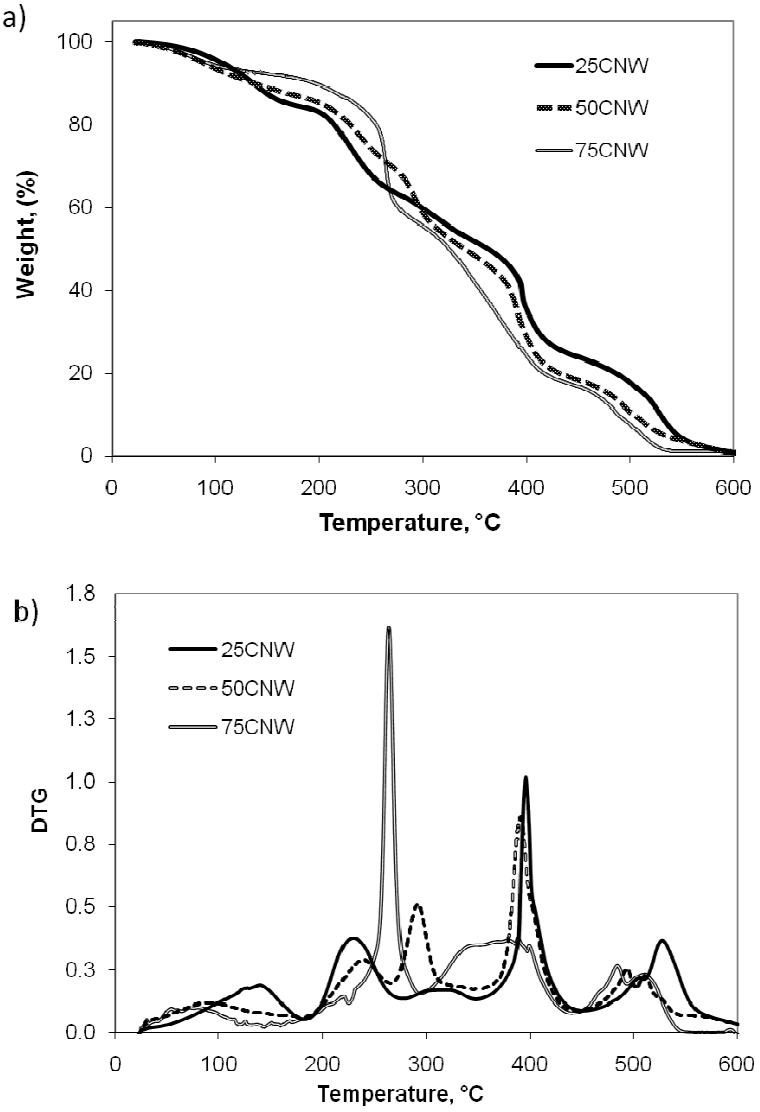

Figure 56. The (a) TGA and (b) DTG of the 25CNW, 50CNW, 75CNW crosslinked nanocomposites differ with the varying percentages of whiskers.

The thermal stability of the matrix was improved by the addition of the whiskers, as can be seen in the T_{onset} data in Table 22. T_{onset} was determined as the temperature at

which the sample weight was 93% of the sample mass at 105 °C. The T_{onset} of the matrix (0CNW) and whiskers (100 CNW) were 149 °C and 206 °C respectively, while in the crosslinked films the T_{onset} increased linearly ($R^2 = 0.99$) as the percent of whiskers in the nanocomposites increased. The T_{onset} of the 25CNW, 50CNW, and 75CNW crosslinked nanocomposites were 145 °C, 187 °C, and 219 °C, respectively. The differing TGA curves for each of the compositions confirm that these materials are unique, and do not act simply as blends of the starting components (i.e., PMVEMA, PEG, and cellulose whiskers).

The decomposition of the 75CNW film (Figure 56b) shows the loss of free water and other volatiles. A peak appears at approximately 80 °C. However, the next distinct peak does not occur until 264 °C, and is attributed to whisker degradation. The decomposition of the 50CNW film (Figure 56b) has a peak at approximately 95 °C, which is most likely due to free water loss. The first significant decomposition peak in the 50CNW film occurs at 242 °C.

The 25CNW film derivative weight curve (Figure 56b) is distinct from that of both the 50CNW and 75CNW films, and combines derivative weight information from both the matrix and the whiskers, with the greater influence emerging from the increased matrix concentration. There is not a distinctive free water loss peak in the 25CNW film as there are in the 50CNW and 75CNW films. However, there is a peak at 143 °C that is not seen in either the 50CNW or the 75CNW films. This may be due to the dehydration of the unreacted acid groups present in the PMVEMA portion of the matrix (Figure 55a). The derivative weight peaks at 233 °C and 317 °C are broad enough that they could possibly be a combination of two peaks, combining influences from the matrix and from

the whiskers, unlike the peak separation seen in the 50CNW film. The peak at 395 °C has been attributed to the decomposition of the matrix and the breakdown of the polymer chain, as was the peak at 531 °C, while the peak at 510 °C is due to further breakdown of the cellulose whiskers.

Overall, there is a shift in the derivative weight peaks due to both the decomposition of the whiskers in each film and the narrowing of the temperature range of decomposition as the percentage of whiskers increases (Figure 56). The increase in the decomposition temperature of the whiskers in the 25CNW and 50CNW films indicates good whisker-matrix interactions and can be attributed to more efficient crosslinking occurring between the whiskers and the matrix. The 75CNW film had the same peak decomposition temperature as the pure whiskers (100CNW), which could possibly indicate less efficient crosslinking.

Table 22. The onset of thermal degradation and the first derivative peaks of the starting materials and crosslinked nanocomposites show how the overall improvement of the thermal stability of the PMVEMA-PEG matrix by the addition cellulose whiskers.

	T_{onset} (°C)	T_{max} (°C)	Weight % at T_{max}
PEG	190.0	231	43.8
		305	4.3
PMVEMA	159.2	154	94.3
		240	76.9
		367	45.3
		504	14.9
0CNW (PMVEMA -PEG)	149.2	150	89.9
		227	73.5
		404	36.3
		568	5.0
25CNW	144.7	145	92.9
		229	78.7
		306	61.7
		395	40.8
		509	16.6
		527	11.0
50CNW	187.3	239	83.0
		292	67.0
		391	37.2
		494	12.6
		510	9.1
		529	5.7
75CNW	218.9	264	75.6
		350	44.6
		389	30.0
		399	29.1
		484	11.8
		511	5.6
100CNW	206.2	201	94.0
		264	58.9
		416	11.9

The residual weight and char at 350, 500, and 600 °C for the starting materials and crosslinked whisker materials are presented in Table 23. The char percentage at both 350 °C and 500 °C decreased as the whisker content increased in the films. However, at 600 °C this pattern reversed, with the char percentage increasing as the whisker content increased.

Table 23. Char content of the starting materials and the crosslinked whisker films were evaluated at 350 °C, 500 °C, and 600 °C.

	% Char, 350 °C	**% Char, 500 °C**	**% Char, 600 °C**
PMVEMA	48.8	16.3	0.312
PEG	1.7	0.121	0.083
0CNW	47.7	21.4	0.029
25CNW	54.5	18.6	0.218
50CNW	51.8	11.3	0.954
75CNW	44.6	8.17	1.02
100CNW	24.2	1.74	1.77

8.4 Conclusion.

In-situ crosslinking of cellulose whiskers is an attractive method for incorporating cellulose whiskers into a polymer matrix. TGA can be an effective tool to evaluate the thermal stability and degradation reactions in composites, especially for future manufacturing process evaluations. The thermal stability of the PMVEMA-PEG matrix was improved by the addition of 50 wt% or 75 wt.-% cellulose whiskers by 38.1 °C and 69.7 °C, respectively. The cellulose whiskers improved the thermal stability of the

PMVEMA-PEG matrix, and the T_{onset} values therefore increased as the whisker percentage in each formulation increased. This study demonstrates how cellulose whiskers can affect thermal stability and also highlights the challenges of utilizing such materials in manufacturing process due to their relative low thermal stability.

CHAPTER NINE

WATER UPTAKE AND ABSORPTION CHARACTERIZATION OF IN-SITU CROSSLINKED CELLULOSE WHISKERS – PMVEMA - PEG

9.1 Introduction.

Hydrogels are three dimensional materials consisting of macromolecules either physically entangled, covalently or ionically bonded to each other that are capable of absorbing water without dissolving. Interest in hydrogels has increased in recent years as new applications have been developed to include biomedical and drug delivery type devices, such as wound dressings, biosensors, and tissue engineering, as well as more traditional applications in contact lenses, adult incontinence, feminine hygiene, disposable diapers, and agriculture [369] [318, 369-379]. Another trend in development of hydrogels is interest in finding greener natural biomaterial alternatives such as lignocellusics to substitute for modern petroleum based reactants [175].

Grafting of various hydrophilic polymers, such as those containing polycarboxylic acids, on to lignocellulosics such as various chemical pulps and cotton cellulose, has been shown to increase the water absorbing properties of the base fibers, creating a cellulose-based hydrogel [175]. While a wide range of lignocellulosic based hydrogels have been prepared and their water uptake characteristics investigated, cellulose whisker based hydrogels are just beginning to be explored.

Cellulose whiskers are crystalline cellulose rods ranging in size from 100 nm up to 1 um in length and 3 – 10 nm in width [7, 10, 53, 335]. Cellulose whiskers are commonly

prepared by acid hydrolysis of a variety of cellulose sources such as microcrystalline cellulose, wood pulps, and tunicates. The development of biomaterials utilizing cellulose whiskers has mostly been focused on composite formulation and materials characterization of whiskers based composites. The study of the transport of liquids through these whisker composites is still also needed. This is important as practical applications for these materials are further explored.

Cellulose whiskers were in situ crosslinked with a poly(methyl vinyl ether – co – maleic acid) – polyethylene glycol (PMVEMA-PEG) matrix and initially characterized as described earlier. PMVEMA is a very hydrophilic polymer and will fully dissolve in water. The cellulose whiskers were mixed and crosslinked with the solubilized PMVEMA-PEG and the resulting product formed a gel-like material when immersed in water. Most recently, PMVEMA has been explored for uses in biomedical and drug delivery applications, including commercially in oral applications, due to its bioadhesive nature [302, 304, 357-359, 363, 380-393]. As future applications for these crosslinked films is most likely as a hydrogel, the further characterization of their behavior in water using the Fickian theory of diffusion, the Flory-Huggins theory, and the Flory-Rehner equation and the resulting conclusions is presented.

9.2. Experimental materials and methods.

9.2.1 Materials.

Poly(methyl vinyl ether – co – maleic acide) (PMVEMA), poly(ethylene glycol), MW 3000, microcrystalline cellulose (VIVAPUR® 105) and all other reagents were used as received. Cellulose whiskers were prepared through acid hydrolysis of

microcrystalline cellulose using method in Chapter 3 (Section 3.3.1 Preparation of cellulose whiskers. Microcrystalline cellulose.) [67].

9.2.2 Crosslinked nanocomposite films.

Cellulose whisker-PMVEMA-PEG films were prepared as described in Chapter 3 (Section 3.3.3 Preparation of crosslinked cellulose whisker film hydrogels.). Five film compositions were prepared and classified based on the percent cellulose whisker content (by weight) in each film – 0%, 25%, 50% 75%, and 100% and are referred to as 0CNW, 25CNW, 50CNW, 75CNW, and 100CNW, respectively.

9.2.3 Sorption experiments.

The experimental procedure to determine the timed water uptake of the prepared crosslinked cellulose whisker films is described in Chapter 3 (Section 3.4.5 Water sorption studies. Whisker films.).

9.2.4 Scanning electron microscopy.

SEM images of the whisker films were imaged using a JEOL JSM-5200 SEM as described in Chapter 3 (Section 3.4.8 Scanning electron microscopy. Solution cast cellulose whisker films.). Water swelled, freeze dried crosslinked cellulose whisker films were prepared and imaged using a Hitachi S800 SEM with the procedure in Chapter 3 (Section 3.4.9 Scanning electron microscopy. Water swollen cellulose whisker films.).

9.2.5 Soxhlet extraction.

Soxhlet extractions of the 0CNW, 25CNW, 50CNW, and 75CNW crosslinked films as well as an unreacted mixture of the 50CNW were conducted as per the procedure in

Chapter 3 (Section 3.4.7 Cellulose whisker films soxhlet extraction.) to determine the percent extractable content.

9.3 Results and discussion.

9.3.1 Water sorption analysis.

The proposed crosslinked structure, shown in Chapter 4 Figure 30, was confirmed in Chapter 7 with the PMVEMA and the cellulose nanowhiskers undergoing an esterification reaction between the primary hydroxyl group of the cellulose and the acid group of the PMVEMA. In addition, PEG was shown to be capable of crosslinks with the PMVEMA in a second esterification reaction. As reported in Chapter 6 Figure 47, the crosslinked whisker films swelled and absorbed water at different rates and volumes. These initial results indicated that the degree of crosslinking in each composition varies as the percent whiskers changes. To confirm this hypothesis, a dynamic equilibrium swelling study was utilized to describe the mechanism of water diffusion using the Fickian model and the degree of crosslinking of these crosslinked materials using Flory-Rehner and Flory-Huggins theories.

The results of the dynamic equilibrium study of the water absorption by the 25CNW, 50CNW and 75CNW films are shown in Figure 57, where the mole percent uptake, Q_t is plotted as a function of the square root of time. The mole percent uptake of water by the whisker films, Q_t, is calculated using the following equation.

$$Q_t = \frac{mass\ of\ solvent\ absorbed\ at\ time\ t}{\frac{molecular\ mass\ of\ solvent}{initial\ mass\ of\ film}} \times 100\%$$

Equation 1

When equilibrium absorption is reached, then $Q_t = Q_\infty$.

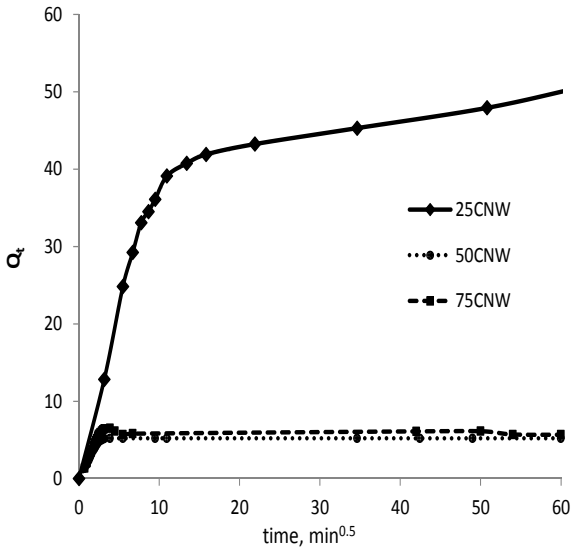

Figure 57. Sorption curve of the mol % water uptake by the crosslinked films at room temperature.

The 25CNW, 50CNW, and 75CNW film data are presented as both the 100CNW and the 0CNW films demonstrated little structural integrity when immersed in water. The 25CNW had the highest mole percent uptake of water, while the 50CNW film had the lowest mole percent uptake of water. However, the 75CNW film achieves

equilibrium first, followed by the 50CNW and the 25CNW films, respectively. These results were used to further study the kinetics of diffusion, sorption, and permeability of the crosslinked films.

Fick's law describes the process of diffusion of a solvent by relating the flow rate of the solvent to the area of the material, so that

$$\frac{f}{A} = -D\frac{dc}{dx}$$

Equation 2

where f is the flow rate in the x direction, A is the cross-sectional area of the sample, and D is the diffusion coefficient. The mechanism of diffusion was determined using the dynamic portion of the gravimetric curve in Figure 57 by applying the diffusion power law model [394, 395] [396] [397],

$$\frac{Q_t}{Q_\infty} = kt^n$$

Equation 3

Rearranged to become,

Equation 4

,

Where Q_∞ is the swelling capacity at equilibrium, Q_t is the swelling capacity at time interval t, and k is the first order rate constant. The slope of log *t* vs. log (Q_t/Q_∞) is used to calculate *n*, while *k* is calculated from the slope intercept; *k* is dependent on the structural features of the material and its interaction with the solvent, *n* is the swelling exponent used to determine the diffusion mechanism, and *t* is the time.

Diffusion mechanisms can be described as Class I: Fickian, Class II: non-Fickian, or anomalous transport and are classified with the calculated value of *n* from the previous equation [394, 398]. If $n = 0.5$, the diffusion is Fickian, where the rate of diffusion of the penetrating molecules is less than the relaxation rate of the polymers. If $n = 1$, non-Fickian diffusion is occurring where the rate of diffusion is much greater than the relaxation rate of the polymers. If *n* is between 0.5 and 1, then the diffusion is classified as anomalous where the diffusion of the solvent molecules and the relaxation rates of the polymer are similar.

Table 24 summarizes the *n* and *k* values for the three crosslinked films. While all three compositions can be classified as having anomalous diffusion, the *n* values decrease towards a more Fickian-type diffusion process as the percent of cellulose whiskers decreases, with the *n* value of the 25CNW film, 0.52, smaller than the *n* values of the 50CNW and 75CNW films, 0.56 and 0.57, respectively. The *k* values indicate that the 50CNW and 75CNW are similar structurally while the 25CNW film is significantly different structurally.

Table 24. Diffusion mechanism (n) and k values of crosslinked nanocomposite films.

	$n_{average}$ (±SD)	$k_{average}$ (±SD)
25CNW	0.52 (0.13)	1.11 (0.26)
50CNW	0.56 (0.059)	0.44 (0.030)
75CNW	0.56 (0.14)	0.39 (0.16)

The transport, or permeation, of a solvent through a material is dependent upon both the rate of diffusion and the absorption capability of the solvent. To determine the permeability the diffusion coefficient and sorption coefficient were calculated. The diffusion coefficient, D, describes the rate of diffusion through a specific thickness dimension. It can be calculated using the following equation when the sample is immersed in an infinite volume of solvent [394, 396, 399],

$$\frac{Q_t}{Q_\infty} = 1 - (8/\pi^2) \sum_{n=0}^{n=\infty} [1/(2n+1)^2 \exp[-D(2n+1)^2\pi^2\, t/h^2]]$$

Equation 5

Where Q_t and Q_∞ are mole percent uptake of the water by the material at time, *t,* and equilibrium, respectively, *h* is the initial thickness of the film, *D* is the diffusion coefficient, and *n* an integer. As a short time limit can be applied, the short-time limited expression results in

$$D = \pi\left(\frac{h\theta}{4Q_\infty}\right)^2$$

Equation 6

Where h is the initial thickness of the film and θ is the slope of the linear portion of the Q_t vs $t^{1/2}$ sorption curve [385, 387, 389]. Table 25 summarizes the average film thicknesses and diameters at time zero and equilibrium.

Overall, all three film compositions increased in diameter and thickness after immersion in water at their respective equilibrium uptake times (Table 25). The 25CNW had the most significant changes in thickness with an increase of 147%, while the 50CNW and 75CNW showed more moderate thickness dimensional increases of 84% and 62%, respectively. These values were then used to calculate the diffusion coefficient, D, for each film (Table 26).

Table 25. The films increased in both diameter and thickness between the initial pre-water dimensions and the time where the films reached Q_∞.

Time (min)	25CNW		50CNW		75CNW	
	Diameter (mm) (± SD)	**Thickness (mm) (±SD)**	**Diameter (mm) (± SD)**	**Thickness (mm) (±SD)**	**Diameter (mm) (± SD)**	**Thickness (mm) (±SD)**
0	19.94 (0.40)	0.36 (0.02)	20.67 (0.13)	0.35 (0.03)	19.82 (0.37)	0.31 (0.02)
Q_∞	37.35 (2.57)	0.89 (0.11)	23.62 (0.66)	0.63 (0.093)	22.72 (0.23)	0.50 (0.02)
Percent Change, %	87.31 (12.96)	146.66 (19.00)	14.32 (3.56)	84.00 (33.83)	13.85 (1.29)	62.45 (4.34)

The sorption coefficients were calculated using the equation,

$$S = \frac{M_\infty}{M_0}$$

Equation 7

Where M_s is the mass of the solvent at equilibrium swelling and M_p is the initial mass of the film [396]. The sorption coefficient for the 25CNW film was nearly 10 times the sorption coefficient of the 50CNW film. The 75CNW film had the lowest sorption coefficient of the crosslinked films as in Table 26.

The permeation of water through the films can also be characterized using the permeation coefficient, P, which is calculated using the equation,

$$P = DS$$

Equation 8

Where D is the diffusion coefficient and S is the sorption coefficient already calculated [396]. Diffusion coefficient is dependent on the relaxation of the polymer chains whereas sorption is a surface phenomenon dependent on the affinity of the penetrant towards the substrate. The permeation coefficient gives an indication of the steady state rate of transport of the penetrant (water) through the polymer films. Table 26 summarizes the permeation values for the three films.

Table 26. The diffusion coefficient ($D_{average}$), sorption coefficient ($S_{average}$) and permeation co-efficient ($P_{average}$) were calculated of the crosslinked films.

Sample	$D_{average}$ (Std dev) (mm^2/sec)	$S_{average}$ (Std dev)	$P_{average}$ (Std dev) (mm/sec)
25CNW	3.270×10^{-6} (5.593×10^{-7})	9.635 (3.845)	3.224×10^{-5} (1.725×10^{-5})
50CNW	4.897×10^{-5} (6.128×10^{-6})	0.9315 (0.03752)	4.577×10^{-5} (7.420×10^{-6})
75CNW	3.205×10^{-4} (1.328×10^{-4})	0.9864 (0.4082)	2.8476×10^{-4} (6.671×10^{-5})

The permeation coefficient values indicate that water is able to traverse the films at a greater rate as cellulose whisker content increases. This is shown by the data where the 75CNW film permeation occurs at a rate ~9 times faster than the 25CNW film and ~6 times faster than in the 50CNW film. Correspondingly, the diffusion coefficient values also increased as cellulose whisker content increased, where the diffusion coefficient value of the 75CNW is ~98 and ~6.5 times greater than that of the 25CNW or the 50CNW, respectively. Dufresne and Cavaille also observed a similar trend where the diffusion coefficient of starch-poly(styrene-co-butylacrylate) latex composites increased as the starch microcrystalline content was increased [399]. However, when a microfibrilcellulose-gelatinized starch-glycerol composite was evaluated for water diffusivity, Dufresne, Dupeyre, and Vignon found that the glycerol inhibited the diffusion of water through composite, resulting in lower diffusion coefficients when compared to similarly prepared cellulose-starch composites without glycerol; for example at the 30% cellulose content the diffusion coefficient decreased from 1.65×10^{-8} mm/sec to 5.25×10^{-9} mm^2/sec [400]. While the influence of the increase in concentration of the

hydrophilic PMVEMA-PEG polymer matrix could be attributed to both the comparative greater sorption coefficient and lower diffusion coefficient observed in the 25CNW film, a second factor appears at play in the comparison between the 50CNW and 75CNW. While both film compositions had similar sorption coefficient values, the diffusion coefficients were an order of magnitude different. This implies a difference in the degree of crosslinking between the 50CNW and the 75CNW materials. The Flory-Rehner equation was applied to the experimental data to determine the molar mass between crosslinks and the degree of crosslinking of the 25CNW, 50CNW, and 75CNW films.

The molar mass between crosslinks (M_c) was estimated using the Flory-Rehner equation,

$$M_c = \frac{-\rho_p V \phi^{1/3}}{\ln(1-\phi) + \phi + \chi\phi^2}$$

Equation 9

Where ρ_p is the density of the film, V is the molar volume of water, ϕ is the volume fraction of the film at equilibrium, and χ is the Flory-Huggins solvent interaction parameter [396] [312]. The density, ρ_p, was calculated using the theory of sums of the individual components where the densities of the whiskers, PMVEMA, and PEG were 1.60 g/cm^3, 0.977 g/cm^3, and 1.0926 g/cm^3, respectively [401] [402] [10, 335]. The solvent interaction parameter was calculated for each composition using Equation 10 [403] [258].

$$\chi = \frac{1}{2} + \frac{\phi_2}{3}$$

Equation 10

Table 27. Calculated theoretical density, solvent interaction parameter, molecular mass between crosslinks and crosslink density of the crosslinked films.

Film	Density, g/cm^3, ρ_p	χ	M_c	ν
25CNW	1.14	0.53	504182	3.41 x 10^{18}
50CNW	1.30	0.70	277	2.86 x 10^{21}
75CNW	1.45	0.64	971	4.35 x 10^{21}

The crosslink density of the films, υ, was determined based on the estimated M_c using the equation [404],

$$\nu = \frac{\rho_p N_A}{M_C}$$

Equation 11

The estimated M_c and ν for each film are shown in Table 27. The 25CNW film has the largest molar mass between crosslinks, implying a relatively light crosslinking density and which explains the difference in equilibrium water absorption between the films. The 75CNW film has the next greatest molar mass between crosslinks, while the 50CNW film has the lowest molar mass between crosslinks, 971 and 277, respectively. This follows the equilibrium swelling value order. The results are explained by the Flory-

Huggins theory which describes the equilibrium swelling thermodynamically as the sum of the effects that the free energy of mixing, elasticity of chains, and the ideal Donnan equilibrium. As crosslinking density increases, there is an increase in the number of junctions within the polymeric hydrogel. This decreases the elasticity ability of the polymer chains to move in response to water diffusion, resulting in a decrease in the amount of water the hydrogel is capable of interacting with and thus absorbing.

Xia, Patchan, Maranchi, Elisseeff, and Trexler determined the crosslinking density of all microcrystalline cellulose hydrogels at 2-5% dissolved cellulose concentrations and showed that that the crosslinking density increased as the cellulose content increased [405]. The crosslinking density increased by 200% from the 2% to the 5% concentration. A secondary explanation, in addition to the influence of the lower percent of PMVEMA-PEG, for the lower M_c values of the 75CNW and 50CNW relative to the 25CNW could be thus attributed to the cellulose whisker interactions.

9.3.2 Morphology.

The swollen films were imaged through SEM by freezing fully water swollen films and then freeze drying them to retain the open pore structure where the water had penetrated into the films. This procedure was successful and differences can be seen between the fractured edges of the crosslinked films are compared. Figure 58 shows the SEM images of the fractured edges of water swollen films contrasted with the edges of the original films. The open pore structure that results from the swelling of the films in water is evident. However differences do exist between the 25CNW and the

50CNW/75CNW films where it appears as though the pore size is larger in the 25CNW films when compared to the 50CNW/75CNW films. This lends further support to the theoretical calculations of the molar mass between crosslinks being the greatest for the 25CNW films and of similar value between the 50CNW and 75CNW films. These pores were not observed with the non-swollen tensile fractured films (Figure 58c). This could possibly be interpreted that sorption, diffusion and permeation of water into and through the films is able to occur on all sides of the films.

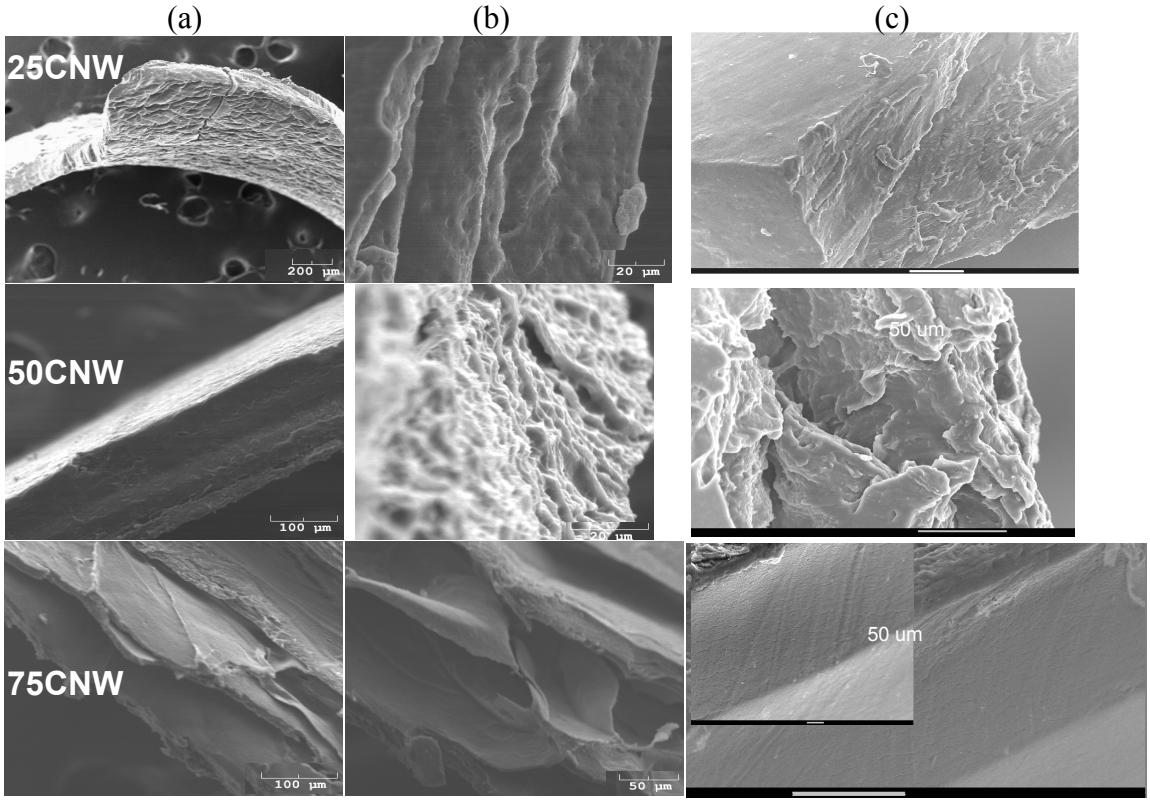

Figure 58. SEM of the morphology of fractured edges swollen freeze dried nanocomposites, (a) and (b), compared to the air dry nanocomposite morphology (c).

9.3.3 Soxhlet extraction.

Samples were soxhlet extracted with water for 24 h to determine the efficiency of the crosslinking of the PMVEMA, PEG, and whiskers. The lack of intermolecular bonding has been attributed to the large percent extractable fractions in films. The 25CNW/75PMVEMA-PEG and 50CNW/50PMVEMA-PEG prepared films retained similar percentages of the starting film mass as shown in Table 28. However, the 75CNW/25PMVEMA-PEG crosslinked film was shown to be not very efficiently crosslinked as just 32.3% of the starting mass of the film was retained after extraction for 24 h.

A 50% whisker-50% PMVEMA crosslinked film was prepared according to the same technique as the other films and soxhlet extracted with water for 24 h to compare the crosslinking efficiency with the 50CNW/50PMVEMA-PEG film. The 50CNW/50PMVEMA film retained 54% of the starting material. This value, less than that of the 50CNW/50PMVEMA-PEG, indicates the role that the PEG is involved the crosslinking between the PMVEMA and the whiskers.

Table 28. Soxhlet extraction with water of crosslinked whisker films.

Sample	% Retained	% Extracted
25CNW/75(PMVEMA-PEG)	77.4	22.6
50CNW/50(PMVEMA-PEG)	72.6	27.4
75CNW/25(PMVEMA-PEG)	32.3	67.7
50CNW-50PMVEMA	54.0	46.0
Non-crosslinked mixture control (50CNW, 50PMVEMA-PEG)	55.2	44.8

9.4 Conclusion.

The three formulations of PMVEMA-PEG-cellulose whisker nanocomposites show varying water uptake kinetics. However, all three composite formulations demonstrate anomalous diffusion characteristic, with values of 0.52 – 0.56 showing a slight Fickian influence. The permeation coefficient describing the movement of water through the films decreased as cellulose whisker content increased, from 3.224×10^{-5} mm/sec (25CNW) to 2.8476×10^{-4} mm/sec (75CNW). The Flory-Rehner equation for determine the mass between crosslinks was calculated using the experimental data and showed that the 25CNW had the largest M_c value, followed by the 75CNW and 50CNW compositions. These results confirm the T2 relaxation results presented in Chapter 7. These results help to understand the ultimate water absorption characteristics of these PMVEMA-PEG-cellulose whisker nanocomposite materials for future utilization of these materials.

CHAPTER TEN

CONCLUSIONS

The work presented in this thesis details the results of crosslinking lignocellulose based materials with poly(methylvinylether co maleic acid) (PMVEMA) and polyethylene glycol (PEG) to create water absorbing materials. The lignocellulosic materials chosen were ECF bleached softwood kraft pulp fibers, ECF bleached birch kraft pulp fibers, and cellulose nanowhiskers (CNW). In Chapter 4, ECF bleached softwood kraft pulp fibers were crosslinked with PMVEMA and PEG in situ using both microwave and thermal initiated methods. The microwave assisted crosslinking method demonstrated a decrease in reaction time from the thermal reaction time of 6.5 min to 1.75 min while producing crosslinked fibers capable of absorbing water. The resulting crosslinked pulp fibers were evaluated using equilibrium swelling for water absorption, water retention, and 0.1 M NaCl absorption and retention values. The microwave-prepared hydrogels absorbed similar or greater amounts of water than did the thermally prepared hydrogels, 40 - 125 g H_2O/g and 30 – 85 g H_2O/g respectively. In addition, the milled pulp-based hydrogels absorbed 30 – 292% more water than did the non-milled pulp hydrogels. This suggests that the absorption abilities of the hydrogels have a fiber-size dependence. Chapter 5 continued the investigation by utilizing ECF birch kraft pulp fibers as the cellulose source in both thermal and microwave initiated crosslink process. ECF birch kraft pulp fibers were chosen as a representative hardwood pulp fiber and to compare with the softwood fibers with regards to starting pulp fiber size as the birch fibers are smaller than the softwood fibers. The crosslinked birch fibers absorbed more

water than the comparative crosslinked fibers from Chapter 4, 40 – 200 g/g, demonstrating a possible size effect on the equilibrium swelling.

Chapter 6 described the initial method of in situ crosslinking cellulose nanowhiskers with PMVEMA and PEG to form a film-like material which when immersed in water acted as a hydrogel. Cellulose nanowhiskers were prepared via sulfuric acid hydrolysis of microcrystalline cellulose and characterized using AFM. The cellulose nanowhiskers used were confirmed to have birefringent properties characteristic of the presence of crystalline nanocellulose whiskers and size dimensions of 5 ± 2 nm width and a length of 210 ± 75 nm. The water solubilized PMVEMA and PEG were blended with the cellulose whiskers, solution cast, dried, and crosslinked thermally. The crosslinking chemistry was evaluated using FT-IR (Chapter 6) and NMR (Chapter 7), ultimately showing that the PMVEMA binds to the cellulose whiskers and the PEG binds exclusively to the PMVEMA. FT-IR was used to confirm an esterification reaction between the PMVEMA carboxylic acid and a cellulose alcohol group by the appearance of both the non-carboxylated ester peak at 1734 cm^{-1} and a carboxylated peak at 1587 cm^{-1}.

The mechanical behavior of these crosslinked cellulose whisker materials was evaluated for tensile strength, strain, and E-modulus in Chapter 7. As cellulose whisker content increased, tensile strength and E-modulus values increased. The hydrogels exhibited increasing ability to withstand strain as the percentage of cellulose whiskers decreased, with the 25CNW conditioned at 92% relative humidity having the greatest at 306%. The mechanical behaviour of the crosslinked films was also dependent upon the conditioned relative humidity due to the plasticization effect of water. This is important

to evaluate as future applications of these materials lend themselves to varying humidity-controlled environments.

Thermogravimetric analysis (TGA) was conducted of the crosslinked composites as well as the starting materials to evaluate the thermal stability and degradation reactions (Chapter 8). The cellulose whiskers improved the thermal stability of the PMVEMA-PEG matrix, and the T_{onset} values therefore increased as the whisker percentage in each formulation increased. The T_{onset} of the matrix (0CNW) and whiskers (100 CNW) were 149 °C and 206 °C respectively, while the T_{onset} of the 25CNW, 50CNW, and 75CNW crosslinked nanocomposites were 145 °C, 187 °C, and 219 °C, respectively.

The resulting materials were then further characterized for water uptake where the 25CNW absorbed the greatest volume of water, 9.449 g H_2O/g, while the 50CNW and 75CNW absorbed 0.942 g/g and 1.097 g/g, respectively. The swelling behavior was further evaluated in Chapter 9 where the Flory-Huggins thermodynamic model of swelling and the Flory-Rehner equation were used to determine the molecular weight between crosslinking points. The molecular weight between crosslinks was greatest for the 25CNW, followed by the 75CNW and 50CNW films. The movement of water through the films was evaluated using Peppas' Fickian power model and it was determined that the crosslinked polymers demonstrate anomalous diffusion where the movement of the water through the hydrogel occurs at approximately the same rate as the polymer chains elastically relax.

Overall, these results demonstrate that cellulose-based materials can be used to prepare novel water absorbing crosslinked materials with unique tailorable properties. The cellulose whisker characterization helps to expand the knowledge of the fundamental

chemistry and material behaviors of in situ crosslinked cellulose whiskers, while the microwave assisted crosslinking of ECF bleached kraft pulp fibers opens a new avenue of approach in preparing surface modified pulp fibers.

CHAPTER ELEVEN

RECCOMENDATIONS FOR FUTURE WORK

While this has been an in-depth study on the chemistry and materials behaviors of cellulose-PMVEMA-PEG, there are several recommendations for future work in both the cellulose whisker and the lignocellulosic pulp areas.

- Further study of in situ crosslinked whiskers is needed in the area of developing materials and films that are capable of regulating humidity, specifically investigating barrier and transmission properties of such crosslinked films. These should be tailored to possible future applications, including biomedical or environmental packaging.

- Further comparison of size effects on the performance of crosslinked cellulosics, to include both spherical nanocrystalline cellulose and nanofibrillated cellulose, to measure and compare water uptake properties and physical properties to cellulose whisker crosslinked CNWs. Other crosslinking methods should be attempted with whisker composites with a focus to compare both “grafting to” and “grafting from” methodologies via thermal and microwave technologies.

- Practical applied product development analysis of feasibility and capability studies of cellulose fiber and cellulose whisker composites is needed.

APPENDIX A

COPYRIGHT PERMISSIONS

Copyright permissions were obtained as noted throughout the text. Appendix A contains the formal approvals provided by the publishers.

A.1 Journal of Applied Polymer Science

This work was published in the Journal of Applied Polymer Science as "Preparation of microwave-assisted polymer-grafted softwood kraft pulp fibers. Enhanced water absorbency." Journal of Applied Polymer Science (2011), 119 (1), 387-395. Other authors were Jessica R. Sladky and Arthur J. Ragauskas from the Institute of Paper Science and Technology and School of Chemistry and Biochemistry at Georgia Institute of Technology.

Permission was granted to use this work by John Wiley and Sons.

JOHN WILEY AND SONS LICENSE
TERMS AND CONDITIONS

Aug 10, 2012

This is a License Agreement between Lee A Goetz ("You") and John Wiley and Sons ("John Wiley and Sons") provided by Copyright Clearance Center ("CCC"). The license consists of your order details, the terms and conditions provided by John Wiley and Sons, and the payment terms and conditions.

All payments must be made in full to CCC. For payment instructions, please see information listed at the bottom of this form.

License Number	2965150574917
License date	Aug 10, 2012
Licensed content publisher	John Wiley and Sons
Licensed content publication	Journal of Applied Polymer Science
Licensed content title	Preparation of microwave-assisted polymer-grafted softwood kraft pulp fibers. Enhanced water absorbency
Licensed content author	Lee A. Goetz,Jessica R. Sladky,Arthur J. Ragauskas
Licensed content date	Jul 27, 2010
Start page	387
End page	395
Type of use	Dissertation/Thesis
Requestor type	Author of this Wiley article
Format	Print and electronic
Portion	Full article
Will you be translating?	No
Order reference number	
Total	0.00 USD
Terms and Conditions	

TERMS AND CONDITIONS

This copyrighted material is owned by or exclusively licensed to John Wiley & Sons, Inc. or one of its group companies (each a "Wiley Company") or a society for whom a Wiley Company has exclusive publishing rights in relation to a particular journal (collectively WILEY"). By clicking "accept" in connection with completing this licensing transaction, you agree that the following terms and conditions apply to this transaction (along with the billing and payment terms and conditions established by the Copyright Clearance Center Inc., ("CCC's Billing and Payment terms and conditions"), at the time that you opened your Rightslink account (these are available at any time at http://myaccount.copyright.com)

The waiver by or consent of a party to a breach of any provision of this Agreement shall not operate or be construed as a waiver of or consent to any other or subsequent breach by such other party.

11. This Agreement may not be assigned (including by operation of law or otherwise) by you without WILEY's prior written consent.

12. Any fee required for this permission shall be non-refundable after thirty (30) days from receipt.

13. These terms and conditions together with CCC's Billing and Payment terms and conditions (which are incorporated herein) form the entire agreement between you and WILEY concerning this licensing transaction and (in the absence of fraud) supersedes all prior agreements and representations of the parties, oral or written. This Agreement may not be amended except in writing signed by both parties. This Agreement shall be binding upon and inure to the benefit of the parties' successors, legal representatives, and authorized assigns.

14. In the event of any conflict between your obligations established by these terms and conditions and those established by CCC's Billing and Payment terms and conditions, these terms and conditions shall prevail.

15. WILEY expressly reserves all rights not specifically granted in the combination of (i) the license details provided by you and accepted in the course of this licensing transaction, (ii) these terms and conditions and (iii) CCC's Billing and Payment terms and conditions.

16. This Agreement will be void if the Type of Use, Format, Circulation, or Requestor Type was misrepresented during the licensing process.

17. This Agreement shall be governed by and construed in accordance with the laws of the State of New York, USA, without regards to such state's conflict of law rules. Any legal action, suit or proceeding arising out of or relating to these Terms and Conditions or the breach thereof shall be instituted in a court of competent jurisdiction in New York County in the State of New York in the United States of America and each party hereby consents and submits to the personal jurisdiction of such court, waives any objection to venue in such court and consents to service of process by registered or certified mail, return receipt requested, at the last known address of such party.

Wiley Open Access Terms and Conditions

All research articles published in Wiley Open Access journals are fully open access: immediately freely available to read, download and share. Articles are published under the terms of the Creative Commons Attribution Non Commercial License. which permits use, distribution and reproduction in any medium, provided the original work is properly cited and is not used for commercial purposes. The license is subject to the Wiley Open Access terms and conditions: Wiley Open Access articles are protected by copyright and are posted to repositories and websites in accordance with the terms of the Creative Commons Attribution Non Commercial License. At the time of deposit, Wiley Open Access articles include all changes made during peer review, copyediting, and publishing. Repositories and websites that host the article are responsible for incorporating any publisher-supplied amendments or retractions issued subsequently.
Wiley Open Access articles are also available without charge on Wiley's publishing platform, **Wiley Online Library** or any successor sites.

Use by non-commercial users

A.2 Holzforschung

This work was published in Holzforschung as "**Analysis of microwave vs. thermally assisted grafting of poly(methyl-vinyl ether co-maleic acid)-polyethylene glycol to birch kraft pulp**." Holzforschung (2009), 63(4), 414-417. Other authors were Jessica R. Sladky and Arthur J. Ragauskas from the Institute of Paper Science and Technology and School of Chemistry and Biochemistry at Georgia Institute of Technology. It is available for purchase through www.degruyter.com .

Permission was granted from Degruyter.

> Dear Lee Goetz,
>
> Thanks for your e-mail and your request.
> We are glad to grant you permission for the mentioned material for your Phd provided full credit is given to the original publication and De Gruyter as the publisher. Ideally, the credit also includes a hint to the availability for the article for purchase on our website.
> Please notice that permission is given for the muse described below only.
>
> All the best and best regards
> Tiziana Ziesing
>
> Tiziana Ziesing
> Director Rights & Licences
> DE GRUYTER
> Mies-van-der-Rohe-Straße 1
> **80807 München, Germany**
> T +49 (0)89.76902-318
> F +49 (0)89.76902-350
> M +49 (0)160 72 59 461
> **tiziana.ziesing@degruyter.com**
> **www.degruyter.com**
>
> Verlag Walter de Gruyter GmbH & Co. KG. Genthiner Str. 13. 10785 Berlin.
> Sitz Berlin. Amtsgericht Charlottenburg HR A 2065. Rechtsform: Kommanditgesellschaft.
> Komplementär: de Gruyter Verlagsbeteiligungs GmbH, Sitz Berlin, Amtsgericht Charlottenburg, HR B 46487.
> Geschäftsführer: Dr. Sven Fund
> Beiratsvorsitzender: Rüdiger Gebauer

A.3 Carbohydrate Polymers

This work was published in the journal Carbohydrate Polymers as "A novel nanocomposite film prepared from crosslinked cellulosic whiskers." Carbohydrate Polymers (2009), 75 (1), 85-89. Other authors were Arthur J. Ragauskas from the Institute of Paper Science and Technology and School of Chemistry and Biochemistry at Georgia Institute of Technology, Aji Mathew and Kristiina Oksman from the Division of Manufacturing and Design of Wood and Bionanocomposites, Luleå Institute of Technology, Skellefteå, Sweden, and Paul Gatenholm of the Department of Chemical and Biological Engineering Biopolymer Technology, Chalmers University, Göteborg, Sweden.

Permission was granted for use of this work in this thesis by Elsevier.

Copyright Clearance Center

Home | Account Info | Help

Title:	A novel nanocomposite film prepared from crosslinked cellulosic whiskers
Author:	Lee Goetz,Aji Mathew,Kristiina Oksman,Paul Gatenholm,Arthur J. Ragauskas
Publication:	Carbohydrate Polymers
Publisher:	Elsevier
Date:	5 January 2009

Logged in as:
Lee Goetz
Account #:
3000394475

LOGOUT

Order Completed

Thank you very much for your order.

This is a License Agreement between Lee A Goetz ("You") and Elsevier ("Elsevier"). The license consists of your order details, the terms and conditions provided by Elsevier, and the payment terms and conditions.

Get the printable license.

License Number	2965150146633
License date	Aug 10, 2012
Licensed content publisher	Elsevier
Licensed content publication	Carbohydrate Polymers
Licensed content title	A novel nanocomposite film prepared from crosslinked cellulosic whiskers
Licensed content author	Lee Goetz,Aji Mathew,Kristiina Oksman,Paul Gatenholm,Arthur J. Ragauskas
Licensed content date	5 January 2009
Licensed content volume number	75
Licensed content issue number	1
Number of pages	5
Type of Use	reuse in a thesis/dissertation
Portion	full article
Format	both print and electronic
Are you the author of this Elsevier article?	Yes
Will you be translating?	No
Order reference number	
Title of your thesis/dissertation	PREPARATION AND ANALYSIS OF CROSSLINKED LIGNOCELLUSOIC FIBERS AND CELLULOSE NANOWHISKERS WITH POLY(METHYL-VINYL ETHER CO MALEIC ACID) – POLYETHYLENE GLYCOL TO CREATE NOVEL WATER ABSORBING MATERIALS
Expected completion date	Dec 2012
Estimated size (number of pages)	265
Elsevier VAT number	GB 494 6272 12
Permissions price	0.00 USD
VAT/Local Sales Tax	0.0 USD / 0.0 GBP
Total	0.00 USD

ORDER MORE... | CLOSE WINDOW

ELSEVIER LICENSE
TERMS AND CONDITIONS

Aug 10, 2012

This is a License Agreement between Lee A Goetz ("You") and Elsevier ("Elsevier") provided by Copyright Clearance Center ("CCC"). The license consists of your order details, the terms and conditions provided by Elsevier, and the payment terms and conditions.

All payments must be made in full to CCC. For payment instructions, please see information listed at the bottom of this form.

Supplier	Elsevier Limited The Boulevard,Langford Lane Kidlington,Oxford,OX5 1GB,UK
Registered Company Number	1982084
Customer name	Lee A Goetz
Customer address	500 10th street NW Atlanta, GA 30332
License number	2965150146633
License date	Aug 10, 2012
Licensed content publisher	Elsevier
Licensed content publication	Carbohydrate Polymers
Licensed content title	A novel nanocomposite film prepared from crosslinked cellulosic whiskers
Licensed content author	Lee Goetz,Aji Mathew,Kristiina Oksman,Paul Gatenholm,Arthur J. Ragauskas
Licensed content date	5 January 2009
Licensed content volume number	75
Licensed content issue number	1
Number of pages	5
Start Page	85
End Page	89
Type of Use	reuse in a thesis/dissertation
Portion	full article
Format	both print and electronic
Are you the author of this Elsevier article?	Yes
Will you be translating?	No
Order reference number	None
Title of your thesis/dissertation	PREPARATION AND ANALYSIS OF CROSSLINKED LIGNOCELLUSOIC FIBERS AND CELLULOSE NANOWHISKERS WITH POLY(METHYL-VINYL ETHER CO MALEIC ACID) – POLYETHYLENE GLYCOL TO CREATE NOVEL WATER ABSORBING MATERIALS
Expected completion date	Dec 2012

VAT/Local Sales Tax	0.0 USD / 0.0 GBP
Total	**0.00 USD**

Terms and Conditions

INTRODUCTION

1. The publisher for this copyrighted material is Elsevier. By clicking "accept" in connection with completing this licensing transaction, you agree that the following terms and conditions apply to this transaction (along with the Billing and Payment terms and conditions established by Copyright Clearance Center, Inc. ("CCC"), at the time that you opened your Rightslink account and that are available at any time at http://myaccount.copyright.com).

GENERAL TERMS

2. Elsevier hereby grants you permission to reproduce the aforementioned material subject to the terms and conditions indicated.
3. Acknowledgement: If any part of the material to be used (for example, figures) has appeared in our publication with credit or acknowledgement to another source, permission must also be sought from that source. If such permission is not obtained then that material may not be included in your publication/copies. Suitable acknowledgement to the source must be made, either as a footnote or in a reference list at the end of your publication, as follows:
"Reprinted from Publication title, Vol /edition number, Author(s), Title of article / title of chapter, Pages No., Copyright (Year), with permission from Elsevier [OR APPLICABLE SOCIETY COPYRIGHT OWNER]." Also Lancet special credit - "Reprinted from The Lancet, Vol. number, Author(s), Title of article, Pages No., Copyright (Year), with permission from Elsevier."
4. Reproduction of this material is confined to the purpose and/or media for which permission is hereby given.
5. Altering/Modifying Material: Not Permitted. However figures and illustrations may be altered/adapted minimally to serve your work. Any other abbreviations, additions, deletions and/or any other alterations shall be made only with prior written authorization of Elsevier Ltd. (Please contact Elsevier at permissions@elsevier.com)
6. If the permission fee for the requested use of our material is waived in this instance, please be advised that your future requests for Elsevier materials may attract a fee.
7. Reservation of Rights: Publisher reserves all rights not specifically granted in the combination of (i) the license details provided by you and accepted in the course of this licensing transaction, (ii) these terms and conditions and (iii) CCC's Billing and Payment terms and conditions.
8. License Contingent Upon Payment: While you may exercise the rights licensed immediately upon issuance of the license at the end of the licensing process for the transaction, provided that you have disclosed complete and accurate details of your proposed use, no license is finally effective unless and until full payment is received from you (either by publisher or by CCC) as provided in CCC's Billing and Payment terms and conditions. If full payment is not received on a timely basis, then any license preliminarily granted shall be deemed automatically revoked and shall be void as if never granted. Further, in the event that you breach any of these terms and conditions or any of CCC's Billing and Payment terms and conditions, the license is automatically revoked and shall be void as if never granted. Use of materials as described in a revoked license, as well as any use of the materials beyond the scope of an unrevoked license, may constitute copyright infringement and publisher reserves the right to take any and all action to protect its copyright in the materials.
9. Warranties: Publisher makes no representations or warranties with respect to the licensed material.
10. Indemnity: You hereby indemnify and agree to hold harmless publisher and CCC, and their respective officers, directors, employees and agents, from and against any and all claims arising out of your use of the licensed material other than as specifically authorized pursuant to this license.
11. No Transfer of License: This license is personal to you and may not be sublicensed, assigned, or transferred by you to any other person without publisher's written permission.
12. No Amendment Except in Writing: This license may not be amended except in a writing signed by both parties (or, in the case of publisher, by CCC on publisher's behalf).
13. Objection to Contrary Terms: Publisher hereby objects to any terms contained in any purchase order, acknowledgment, check endorsement or other writing prepared by you, which terms are inconsistent with these terms and conditions or CCC's Billing and Payment terms and conditions. These terms and conditions, together with CCC's Billing and Payment terms and conditions (which are incorporated herein), comprise the entire agreement between you and publisher (and CCC) concerning this licensing transaction. In the event of any conflict between your obligations established by these terms and conditions and those established by CCC's Billing and Payment terms and conditions, these terms and conditions shall control.
14. Revocation: Elsevier or Copyright Clearance Center may deny the permissions described in this License at their sole discretion, for any reason or no reason, with a full refund payable to you. Notice of such denial will be made using the contact information provided by you. Failure to receive such notice will not alter or invalidate the denial. In no event will Elsevier or Copyright Clearance Center be responsible or liable for any costs, expenses or damage incurred by you as a result of a denial of

translation rights. If you licensed translation rights you may only translate this content into the languages you requested. A professional translator must perform all translations and reproduce the content word for word preserving the integrity of the article.
If this license is to re-use 1 or 2 figures then permission is granted for non-exclusive world rights in all languages.
16. **Website**: The following terms and conditions apply to electronic reserve and author websites:
Electronic reserve: If licensed material is to be posted to website, the web site is to be password-protected and made available only to bona fide students registered on a relevant course if:
This license was made in connection with a course,
This permission is granted for 1 year only. You may obtain a license for future website posting,
All content posted to the web site must maintain the copyright information line on the bottom of each image,
A hyper-text must be included to the Homepage of the journal from which you are licensing at http://www.sciencedirect.com /science/journal/xxxxx or the Elsevier homepage for books at http://www.elsevier.com , and
Central Storage: This license does not include permission for a scanned version of the material to be stored in a central repository such as that provided by Heron/XanEdu.
17. **Author website** for journals with the following additional clauses:
All content posted to the web site must maintain the copyright information line on the bottom of each image, and the permission granted is limited to the personal version of your paper. You are not allowed to download and post the published electronic version of your article (whether PDF or HTML, proof or final version), nor may you scan the printed edition to create an electronic version. A hyper-text must be included to the Homepage of the journal from which you are licensing at http://www.sciencedirect.com/science/journal/xxxxx . As part of our normal production process, you will receive an e-mail notice when your article appears on Elsevier's online service ScienceDirect (www.sciencedirect.com). That e-mail will include the article's Digital Object Identifier (DOI). This number provides the electronic link to the published article and should be included in the posting of your personal version. We ask that you wait until you receive this e-mail and have the DOI to do any posting.
Central Storage: This license does not include permission for a scanned version of the material to be stored in a central repository such as that provided by Heron/XanEdu.
18. **Author website** for books with the following additional clauses:
Authors are permitted to place a brief summary of their work online only.
A hyper-text must be included to the Elsevier homepage at http://www.elsevier.com . All content posted to the web site must maintain the copyright information line on the bottom of each image. You are not allowed to download and post the published electronic version of your chapter, nor may you scan the printed edition to create an electronic version.
Central Storage: This license does not include permission for a scanned version of the material to be stored in a central repository such as that provided by Heron/XanEdu.
19. **Website** (regular and for author): A hyper-text must be included to the Homepage of the journal from which you are licensing at http://www.sciencedirect.com/science/journal/xxxxx. or for books to the Elsevier homepage at http://www.elsevier.com
20. **Thesis/Dissertation**: If your license is for use in a thesis/dissertation your thesis may be submitted to your institution in either print or electronic form. Should your thesis be published commercially, please reapply for permission. These requirements include permission for the Library and Archives of Canada to supply single copies, on demand, of the complete thesis and include permission for UMI to supply single copies, on demand, of the complete thesis. Should your thesis be published commercially, please reapply for permission.
21. **Other Conditions**:

v1.6

If you would like to pay for this license now, please remit this license along with your payment made payable to "COPYRIGHT CLEARANCE CENTER" otherwise you will be invoiced within 48 hours of the license date. Payment should be in the form of a check or money order referencing your account number and this invoice number RLNK500836033. Once you receive your invoice for this order, you may pay your invoice by credit card. Please follow instructions provided at that time.

Make Payment To:
Copyright Clearance Center
Dept 001
P.O. Box 843006
Boston, MA 02284-3006

For suggestions or comments regarding this order, contact RightsLink Customer Support: customercare@copyright.com

A.4 Biomacromolecules

This work was published in the journal Biomacromolecules as "Poly(methyl vinyl ether-co-maleic acid)-polyethylene glycol nanocomposites cross-linked in situ with cellulose nanowhiskers." Biomacromolecules, (2010), 11(10), 2660-2666. Other authors were Marcus Foston and Arthur J. Ragauskas from the Institute of Paper Science and Technology and School of Chemistry and Biochemistry at Georgia Institute of Technology and Aji Mathew and Kristiina Oksman from the Division of Manufacturing and Design of Wood and Bionanocomposites, Luleå Institute of Technology, Skellefteå, Sweden.

Permission to use this was granted by ACS Publications.

PERMISSION/LICENSE IS GRANTED FOR YOUR ORDER AT NO CHARGE

This type of permission/license, instead of the standard Terms & Conditions, is sent to you because no fee is being charged for your order. Please note the following:

- Permission is granted for your request in both print and electronic formats, and translations.
- If figures and/or tables were requested, they may be adapted or used in part.
- Please print this page for your records and send a copy of it to your publisher/graduate school.
- Appropriate credit for the requested material should be given as follows: "Reprinted (adapted) with permission from (COMPLETE REFERENCE CITATION). Copyright (YEAR) American Chemical Society." Insert appropriate information in place of the capitalized words.
- One-time permission is granted only for the use specified in your request. No additional uses are granted (such as derivative works or other editions). For any other uses, please submit a new request.

BACK | CLOSE WINDOW

A.5 TAPPI Journal

This work was published in the TAPPI Journal as "Thermal gravimetric analysis of in-situ crosslinked nanocellulose whiskers-poly(methyl vinyl ether-co-maleic acid)-polyethylene glycol." TAPPI Journal, (2011), 10(4), 29-33. Other authors were Arthur J. Ragauskas from the Institute of Paper Science and Technology and School of Chemistry and Biochemistry at Georgia Institute of Technology and Aji Mathew and Kristiina Oksman from the Division of Manufacturing and Design of Wood and Bionanocomposites, Luleå Institute of Technology, Skellefteå, Sweden.

Permission was granted to use this work by TAPPI.

Subject: RE: Copyright permission request for thesis/dissertation use

From: Lisa Stephens (lstephens@tappi.org)

To: leeanngoetz@yahoo.com;

Date: Thursday, August 9, 2012 12:34 PM

Dear Lee Goetz:

TAPPI is pleased to grant you permission to use the article, Thermal gravimetric analysis of in-situ crosslinked nanocellulose whiskers • poly(methyl vinyl ether-co-maleic acid), authored by Lee A. Goetz, Ajip P. Mathew, Kristiina Oksman, and Arthur Ragauskas, and published in the April 2011 issue of *TAPPI Journal* with your thesis/dissertation. We do ask that you please refer to TAPPI as the source.

Thank you for giving TAPPI the opportunity to review your paper for publication. If you have any questions, please let me know.

Sincerely,

Lisa Stephens

PRESS Operations Manager

lstephens@tappi.org

REFERENCES

1. Smock, D., *Heinz will use sugar-based plastics in ketchup bottles*, in *Engineering Materials*. 2011, Design News.

2. Smock, D., *Toyota accelerates use of bioplastics*, in *Design News*. 2010, UBM Electronics: Lexington, MA.

3. Moore, L., *Celluforce plant opening "a significant milestone"*, in *The Gazette*. 2012, Postmedia Network: Montreal, Quebec, Canada.

4. Morales, A. and L. Downing (2011) *Fat replaces oil for f-16s as biofuels head to war: Commodities*.

5. Hon, D.N.S. and N. Shiraishi, *Wood and cellulosic chemistry*. 2nd ed. 2001, New York: Marcel Dekker. viii, 914 p.

6. Monserrate, E., S.B. Leschine, and E. Canale-Parola, *Clostridium hungatei sp. Nov., a mesophilic, n2-fixing cellulolytic bacterium isolated from soil.* International Journal of Systematic and Evolutionary Microbiology, 2001. **51**(1): p. 123-32.

7. Samir, M.A.S.A., F. Alloin, and A. Dufresne, *Review of recent research into cellulosic whiskers, their properties and their application in nanocomposite field.* Biomacromolecules, 2005. **6**(2): p. 612-626.

8. Dufresne, A., *Polysaccharide nano crystal reinforced nanocomposites.* Canadian Journal of Chemistry, 2008. **86**(6): p. 484-494.

9. Habibi, Y. and A. Dufresne. *Nanocrystals from natural polysaccharides*. 2011: CRC Press.

10. Moon, R.J., A. Martini, J. Nairn, J. Simonsen, and J. Youngblood, *Cellulose nanomaterials review: Structure, properties and nanocomposites.* Chemical Society Reviews, 2011. **40**(7): p. 3941-3994.

11. Üner, B., İ. Karaman, H. Tanrıverdi, and D. Özdemir, *Determination of lignin and extractive content of turkish pine (pinus brutia) trees using near infrared spectroscopy and multivariate calibration.* Wood Science and Technology, 2010: p. 1-14.

12. Ona, T., T. Sonoda, J. Ohshima, S. Yokota, and N. Yoshizawa, *A rapid quantitative method to assess eucalyptus wood properties for kraft pulp*

production by ft-raman spectroscopy. Journal of Pulp and Paper Science, 2003. **29**(1): p. 6-10.

13. Rana, R., R. Langenfeld-Heyser, R. Finkeldey, and A. Polle, *Ftir spectroscopy, chemical and histochemical characterisation of wood and lignin of five tropical timber wood species of the family of dipterocarpaceae.* Wood Science and Technology, 2010. **44**(2): p. 225-242.

14. Timmel, T.E., *Recent progress in the chemistry of wood hemicelluloses.* Wood Sci. Technol, 1967. **1**: p. 45-70.

15. Bertaud, F. and B. Holmbom, *Chemical composition of earlywood and latewood in norway spruce heartwood, sapwood and transition zone wood.* Wood Science and Technology, 2004. **38**(4): p. 245-256.

16. Jones, P.D., L.R. Schimleck, G.F. Peter, R.F. Daniels, and A. Clark, *Nondestructive estimation of wood chemical composition of sections of radial wood strips by diffuse reflectance near infrared spectroscopy.* Wood Science and Technology, 2006. **40**(8): p. 709-720.

17. Ragauskas, A.J., C.K. Williams, B.H. Davison, G. Britovsek, J. Cairney, C.A. Eckert, W.J. Frederick, Jr., J.P. Hallett, D.J. Leak, C.L. Liotta, J.R. Mielenz, R. Murphy, R. Templer, and T. Tschaplinski, *The path forward for biofuels and biomaterials.* Science, 2006. **311**(5760): p. 484-489.

18. van Heiningen, A., M.S. Tunc, Y. Gao, and D. da Silva Perez, *Relationship between alkaline pulp yield and the mass fraction and degree of polymerization of cellulose in the pulp.* Journal of Pulp and Paper Science, 2004. **30**(8): p. 211-217.

19. Holt, C., W. Mackie, and D.B. Sellen, *Degree of polymerization and polydispersity of native cellulose.* Journal of Polymer Science: Polymer Symposia, 1973. **42**(3): p. 1505-1512.

20. Kumar, R., G. Mago, V. Balan, and C.E. Wyman, *Physical and chemical characterizations of corn stover and poplar solids resulting from leading pretreatment technologies.* Bioresource Technology, 2009. **100**(17): p. 3948-3962.

21. Pala, H., M. Mota, and F.M. Gama, *Enzymatic depolymerisation of cellulose.* Carbohydrate Polymers, 2007. **68**(1): p. 101-108.

22. Klimentov, A.S., G.A. Petropavlovskii, N.E. Kotel'nikova, S.V. Skvortsov, and L.A. Volkova, *Radiation-induced degradation of wood cellulose.* Cellul. Chem. Technol., 1985. **19**(3): p. 251-5.

23. Puri, V.P., *Effect of crystallinity and degree of polymerization of cellulose on enzymatic saccharification.* Biotechnology and Bioengineering, 1984. **26**(10): p. 1219-1222.

24. Lennholm, H., T. Larsson, and T. Iversen, *Determination of cellulose ialpha and ibeta in lignocellulosic materials.* Carbohydrate Research, 1994. **261**(1): p. 119-31.

25. Hult, E.-L., T. Liitiä, S.L. Maunu, B. Hortling, and T. Iversen, *A cp/mas 13c-nmr study of cellulose structure on the surface of refined kraft pulp fibers.* Carbohydrate Polymers, 2002. **49**(2): p. 231-234.

26. Sannigrahi, P., A.J. Ragauskas, and S.J. Miller, *Effects of two-stage dilute acid pretreatment on the structure and composition of lignin and cellulose in loblolly pine.* Bioenergy Research, 2008. **1**(3-4): p. 205-214.

27. Parikh, D.V., D.P. Thibodeaux, and B. Condon, *X-ray crystallinity of bleached and crosslinked cottons.* Textile Research Journal, 2007. **77**(8): p. 612-616.

28. O'Sullivan, A., *Cellulose: The structure slowly unravels.* Cellulose, 1997. **4**(3): p. 173-207.

29. Atalla, R.H. and D.L. VanderHart, *Native cellulose: A composite of two distinct crystalline forms.* Science 1984. **223**(4633): p. 283-5.

30. Onsager, L., *The effects of shapes on the interaction of colloidal particles.* Ann. N. Y. Acad. Sci., 1949. **51**: p. 627-59.

31. Heiner, A.P., J. Sugiyama, and O. Teleman, *Crystalline cellulose iα and iβ studied by molecular dynamics simulation.* Carbohydrate Research, 1995. **273**(2): p. 207-223.

32. Atalla, R.H. and D.L. VanderHart, *The role of solid state 13c nmr spectroscopy in studies of the nature of native celluloses.* Solid State Nuclear Magnetic Resonance, 1999. **15**(1): p. 1-19.

33. Wada, M., T. Okano, and J. Sugiyama, *Synchrotron-radiated x-ray and neutron diffraction study of native cellulose.* Cellulose, 1997. **4**(3): p. 221-232.

34. Wada, M., T. Okano, J. Sugiyama, and F. Horii, *Characterization of tension and normally lignified wood cellulose in<i>populus maximowiczii</i&gt.* Cellulose, 1995. **2**(4): p. 223-233.

35. Sugiyama, J., J. Persson, and H. Chanzy, *Combined infrared and electron diffraction study of the polymorphism of native celluloses.* Macromolecules, 1991. **24**: p. 2461-6.

36. Sugiyama, J., R. Vuong, and H. Chanzy, *Electron diffraction study on the two crystalline phases occurring in native cellulose from an algal cell wall.* Macromolecules, 1991. **24**: p. 4168-75.

37. Larsson, P.T., U. Westermark, and T. Iversen, *Determination of the cellulose ialpha allomorph content in a tunicate cellulose by cp/mas 13c-nmr spectroscopy.* Carbohydrate Research, 1995. **278**(2): p. 339-43.

38. Larsson, P.T., K. Wickholm, and T. Iversen, *A cp/mas carbon-13 nmr investigation of molecular ordering in celluloses.* Carbohydrate Research, 1997. **302**(1-2): p. 19-25.

39. Pu, Y., C. Ziemer, and A.J. Ragauskas, *Cp/mas 13c nmr analysis of cellulase treated bleached softwood kraft pulp.* Carbohydrate Research, 2006. **341**(5): p. 591-597.

40. Wickholm, K., P.T. Larsson, and T. Iversen, *Assignment of non-crystalline forms in cellulose i by cp/mas carbon-13 nmr spectroscopy.* Carbohydrate Research, 1998. **312**(3): p. 123-129.

41. Ishii, T. and K. Shimizu, *Chemistry of cell wall polysaccharides*, in *Wood and cellulosic chemistry*, D.N.-S. Hon, Editor. 2001, Marcel Dekker, Inc: New York City. p. 175-212.

42. Gullichsen, J. and H. Paulapuro, in *Forest products chemistry*, P. Stenius, Editor. 2000, Fapet:Oy: Helsinki. p. 350.

43. Sjostrom, E., *Wood chemistry: Fundamentals and application*. 1993, Orlando: Academic Press.

44. Sakakibara, A. and Y. Sano, *Chemistry of lignin*, in *Wood and cellulosic chemistry*, D.N.S. Hon and N. Shiraishi, Editors. 2001, Marcel Dekker: New York City. p. 109-173.

45. Fengel and Wegner, 1984.

46. Freudenberg, K. and A.C. Neish, eds. *Constitution and biosynthesis of lignin*. ed. G.F. Springer and A. Kleinzeller. 1968, Springer-Verlag: New York. 129.

47. Chakar, F.S. and A.J. Ragauskas, *Review of current and future softwood kraft lignin process chemistry.* Industrial Crops and Products, 2004. **20**(2): p. 131-141.

48. Adler, E., *Lignin chemistry - past, present and future.* Wood Sci. Technol, 1977. **11**: p. 69-218.

49. Sarkanen, K.V. and C.H. Ludwig, eds. *Lignin: Occurrence, formation, structure and reactions*. 1971, Wiley Interscience: New York City. 916.

50. Karhunen, P., P. Rummakko, J. Sipilä, G. Brunow, and I. Kilpeläinen, *Dibenzodioxocins; a novel type of linkage in softwood lignins.* Tetrahedron Letters, 1995. **36**(1): p. 169-170.

51. Karhunen, P., P. Rummakko, J. Sipilä, G. Brunow, and I. Kilpeläinen, *The formation of dibenzodioxocin structures by oxidative coupling. A model reaction for lignin biosynthesis.* Tetrahedron Letters, 1995. **36**(25): p. 4501-4504.

52. Klemm, D., F. Kramer, S. Moritz, T. Lindström, M. Ankerfors, D. Gray, and A. Dorris, *Nanocelluloses: A new family of nature-based materials.* Angewandte Chemie International Edition, 2011. **50**(24): p. 5438-5466.

53. Habibi, Y., L.A. Lucia, and O.J. Rojas, *Cellulose nanocrystals: Chemistry, self-assembly, and applications.* Chemical Reviews, 2010. **110**(6): p. 3479-3500.

54. Araki, J. and S. Kuga, *Effect of trace electrolyte on liquid crystal type of cellulose microcrystals.* Langmuir, 2001. **17**: p. 4493-4496.

55. Grunert, M. and W.T. Winter, *Nanocomposites of cellulose acetate butyrate reinforced with cellulose nanocrystals.* Journal of Polymers and the Environment, 2002. **10**(1/2): p. 27-30.

56. Roman, M. and W.T. Winter, *Effect of sulfate groups from sulfuric acid hydrolysis on the thermal degradation behavior of bacterial cellulose.* Biomacromolecules, 2004. **5**: p. 1671-1677.

57. Araki, J., M. Wada, and S. Kuga, *Steric stabilization of a cellulose microcrystal suspension by poly(ethylene glycol) grafting.* Langmuir, 2001. **17**: p. 21-27.

58. Dong, X.M., T. Kimura, J.-F. Revol, and D.G. Gray, *Effects of ionic strength on the isotropic-chiral nematic phase transition of suspensions of cellulose crystallites.* Langmuir, 1996. **12**: p. 2076-82.

59. Heux, L., G. Chauve, and C. Bonini, *Nonflocculating and chiral-nematic self-ordering of cellulose microcrystals suspensions in nonpolar solvents.* Langmuir, 2000. **16**: p. 8210-8212.

60. de Souza Lima, M.M., J.T. Wong, M. Paillet, R. Borsali, and R. Pecora, *Translational and rotational dynamics of rodlike cellulose whiskers.* Langmuir, 2003. **19**(1): p. 24-29.

61. Miller, A.F. and A.M. Donald, *Imaging of anisotropic cellulose suspensions using environmental scanning electron microscopy.* Biomacromolecules, 2003. **4**(3): p. 510-517.

62. Roohani, M., Y. Habibi, N.M. Belgacem, G. Ebrahim, A.N. Karimi, and A. Dufresne, *Cellulose whiskers reinforced polyvinyl alcohol copolymers nanocomposites.* European Polymer Journal, 2008. **44**(8): p. 2489-2498.

63. Elazzouzi-Hafraoui, S., Y. Nishiyama, J.-L. Putaux, L. Heux, F. Dubreuil, and C. Rochas, *The shape and size distribution of crystalline nanoparticles prepared by acid hydrolysis of native cellulose.* Biomacromolecules, 2007. **9**(1): p. 57-65.

64. Li, Q., J. Zhou, and L. Zhang, *Structure and properties of the nanocomposite films of chitosan reinforced with cellulose whiskers.* Journal of Polymer Science Part B: Polymer Physics, 2009. **47**(11): p. 1069-1077.

65. Capadona, J.R., K. Shanmuganathan, S. Trittschuh, S. Seidel, S.J. Rowan, and C. Weder, *Polymer nanocomposites with nanowhiskers isolated from microcrystalline cellulose.* Biomacromolecules, 2009. **10**(4): p. 712-716.

66. Pranger, L. and R. Tannenbaum, *Biobased nanocomposites prepared by in situ polymerization of furfuryl alcohol with cellulose whiskers or montmorillonite clay.* Macromolecules, 2008. **41**(22): p. 8682-8687.

67. Bondeson, D., A. Mathew, and K. Oksman, *Optimization of the isolation of nanocrystals from microcrystalline cellulose by acid hydrolysis.* Cellulose, 2006. **13**(2): p. 171-180.

68. Kvien, I., B.S. Tanem, and K. Oksman, *Characterization of cellulose whiskers and their nanocomposites by atomic force and electron microscopy.* Biomacromolecules, 2005. **6**(6): p. 3160-3165.

69. Habibi, Y., A.-L. Goffin, N. Schiltz, E. Duquesne, P. Dubois, and A. Dufresne, *Bionanocomposites based on poly(ε-caprolactone)-grafted cellulose nanocrystals by ring-opening polymerization.* Journal of Materials Chemistry, 2008. **18**(41): p. 5002-5010.

70. Junior de Menezes, A., G. Siqueira, A.A.S. Curvelo, and A. Dufresne, *Extrusion and characterization of functionalized cellulose whiskers reinforced polyethylene nanocomposites.* Polymer, 2009. **50**(19): p. 4552-4563.

71. Garcia de Rodriguez, N.L., W. Thielemans, and A. Dufresne, *Sisal cellulose whiskers reinforced polyvinyl acetate nanocomposites.* Cellulose, 2006. **13**(3): p. 261-270.

72. Siqueira, G., J. Bras, and A. Dufresne, *Cellulose whiskers versus microfibrils: Influence of the nature of the nanoparticle and its surface functionalization on the thermal and mechanical properties of nanocomposites.* Biomacromolecules, 2008. **10**(2): p. 425-432.

73. Terech, P., L. Chazeau, and J.Y. Cavaille, *A small-angle scattering study of cellulose whiskers in aqueous suspensions.* Macromolecules, 1999. **32**: p. 1872-1875.

74. Angles, M.N. and A. Dufresne, *Plasticized starch/tunicin whiskers nanocomposites. 1. Structural analysis.* Macromolecules, 2000. **33**(22): p. 8344-8353.

75. Kimura, F., T. Kimura, M. Tamura, A. Hirai, M. Ikuno, and F. Horii, *Magnetic alignment of the chiral nematic phase of a cellulose microfibril suspension.* Langmuir, 2005. **21**(5): p. 2034-2037.

76. Elazzouzi-Hafraoui, S., Y. Nishiyama, J.-L. Putaux, L. Heux, F. Dubreuil, and C. Rochas, *The shape and size distribution of crystalline nanoparticles prepared by acid hydrolysis of native cellulose.* Biomacromolecules, 2008. **9**: p. 57-65.

77. Revol, J.F., *On the cross-sectional shape of cellulose crystallites in valonia ventricosa.* Carbohydr. Polym., 1982. **2**: p. 123-34.

78. Araki, J., M. Wada, S. Kuga, and T. Okano, *Influence of surface charge on viscosity behavior of cellulose microcrystal suspension.* J. Wood Sci., 1999. **45**: p. 258-261.

79. Araki, J., M. Wada, S. Kuga, and T. Okano, *Flow properties of microcrystalline cellulose suspension prepared by acid treatment of native cellulose.* Colloids Surf., A, 1998. **142**: p. 75-82.

80. Beck-Candanedo, S., M. Roman, and D.G. Gray, *Effect of reaction conditions on the properties and behavior of wood cellulose nanocrystal suspensions.* Biomacromolecules, 2005. **6**: p. 1048-1054.

81. Samir, M.A.S.A., F. Alloin, M. Paillet, and A. Dufresne, *Tangling effect in fibrillated cellulose reinforced nanocomposites.* Macromolecules, 2004. **37**: p. 4313-4316.

82. Nickerson, R.F. and J.A. Habrle, *Cellulose intercrystalline structure.* Industrial & Engineering Chemistry, 1947. **39**(11): p. 1507-1512.

83. Staudinger, H. and M. Sorkin, Chemische Berichte, 1937. **70**: p. 1565.

84. Ranby, B.G., *Aqueous colloidal solutions of cellulose micelles.* Acta Chem. Scand., 1949. **3**: p. 649-50.

85. Ranby, B.G. and E. Ribi, *The fine structure of cellulose.* Experientia, 1950. **6**: p. 12-14.

86. Mukherjee, S.M. and H.J. Woods, *X-ray and electron-microscope studies of the degradation of cellulose by sulfuric acid.* Biochim. Biophys. Acta, 1953. **10**: p. 499-511.

87. Mukherjee, S.M., J. Sikorski, and H.J. Woods, *Electron-microscopy of degraded cellulose fibres.* Journal of the Textile Institute Transactions, 1952. **43**(4): p. T196-T201.

88. Marchessault, R.H., F.F. Morehead, and N.M. Walter, *Liquid crystal systems from fibrillar polysaccharides.* Nature, 1959. **184**: p. 632-3.

89. Marchessault, R.H., F.F. Morehead, and M.J. Koch, *Hydrodynamic properties of neutral suspensions of cellulose crystallites as related to size and shape.* J. Colloid Sci., 1961. **16**: p. 327-44.

90. Battista, O.A., S. Coppick, J.A. Howsmon, F.F. Morehead, and W.A. Sisson, *Level-off degree of polymerization. Relation to polyphase structure of cellulose fibers.* J. Ind. Eng. Chem., 1956. **48**: p. 333-5.

91. Revol, J.F., H. Bradford, J. Giasson, R.H. Marchessault, and D.G. Gray, *Helicoidal self-ordering of cellulose microfibrils in aqueous suspension.* Int. J. Biol. Macromol., 1992. **14**: p. 170-2.

92. Revol, J.F., L. Godbout, X.M. Dong, D.G. Gray, H. Chanzy, and G. Maret, *Chiral nematic suspensions of cellulose crystallites; phase separation and magnetic field orientation.* Liq. Cryst., 1994. **16**: p. 127-34.

93. Kamel, S., *Nanotechnology and its applications in lignocellulosic composites, a mini review.* eXPRESS Polymer Letters, 2007. **1**(9): p. 546-575.

94. Koshizawa, T., *Degradation of wood cellulose and cotton linters in phosphoric acid.* Kami Pa Gikyoshi, 1960. **14**: p. 455-8.

95. Usuda, M., O. Suzuki, J. Nakano, and N. Migita, *Acid hydrolysis of cellulose in concentrated phosphoric acid; effects of modified groups of cellulose on the rate of hydrolysis.* Kogyo Kagaku Zasshi, 1967. **70**: p. 349-52.

96. Rinaldi, R. and F. Schüth, *Acid hydrolysis of cellulose as the entry point into biorefinery schemes.* ChemSusChem, 2009. **2**(12): p. 1096-1107.

97. Gray, D.G., *Chiral nematic ordering of polysaccharides.* Carbohydrate Polymers, 1994. **25**(4): p. 277-284.

98. Revol, J.-F., J.D.L. Godbout, and D.G. Gray, *Solidified liquid crystals of cellulose with optically variable properties*. 1995, Pulp and Paper Research Institute of Canada, Can. . p. 33 pp.

99. Gray, D.G., *Chirality in cellulose and cellulose-based materials.* Polym. Prepr., 1996. **37**: p. 485-486.

100. Dong, X.M., J.-F. Revol, and D.G. Gray, *Effect of microcrystallite preparation conditions on the formation of colloid crystals of cellulose.* Cellulose, 1998. **5**: p. 19-32.

101. Orts, W.J., L. Godbout, R.H. Marchessault, and J.F. Revol, *Enhanced ordering of liquid crystalline suspensions of cellulose microfibrils: A small-angle neutron scattering study.* Macromolecules, 1998. **31**: p. 5717-5725.

102. Bhatt, N., P.K. Gupta, and S. Naithani, *Preparation of cellulose sulfate from α-cellulose isolated from lantana camara by the direct esterification method.* Journal of Applied Polymer Science, 2008. **108**(5): p. 2895-2901.

103. Beck-Candanedo, S., M. Roman, and G. Gray Derek, *Effect of reaction conditions on the properties and behavior of wood cellulose nanocrystal suspensions.* Biomacromolecules, 2005. **6**(2): p. 1048-54.

104. Favier, V., H. Chanzy, and J.Y. Cavaille, *Polymer nanocomposites reinforced by cellulose whiskers.* Macromolecules, 1995. **28**: p. 6365-7.

105. Habibi, Y., H. Chanzy, and M.R. Vignon, *Tempo-mediated surface oxidation of cellulose whiskers.* Cellulose, 2006. **13**: p. 679-687.

106. Helbert, W., J.Y. Cavaille, and A. Dufresne, *Thermoplastic nanocomposites filled with wheat straw cellulose whiskers. Part i: Processing and mechanical behavior.* Polym. Compos., 1996. **17**: p. 604-611.

107. Cao, X., Y. Habibi, and L.A. Lucia, *One-pot polymerization, surface grafting, and processing of waterborne polyurethane-cellulose nanocrystal nanocomposites.* J. Mater. Chem., 2009. **19**: p. 7137-7145.

108. Dong, X.M., J.-F. Revol, and D.G. Gray, *Effect of microcrystallite preparation conditions on the formation of colloid crystals of cellulose.* Cellulose, 1998. **5**(1): p. 19-32.

109. Habibi, Y., L. Foulon, V. Aguie-Beghin, M. Molinari, and R. Douillard, *Langmuir-blodgett films of cellulose nanocrystals: Preparation and characterization.* Journal of Colloid and Interface Science, 2007. **316**: p. 388-397.

110. Eichhorn, S.J. and R.J. Young, *The young's modulus of a microcrystalline cellulose.* Cellulose, 2001. **8**: p. 197-207.

111. Rusli, R. and S.J. Eichhorn, *Determination of the stiffness of cellulose nanowhiskers and the fiber-matrix interface in a nanocomposite using raman spectroscopy.* Appl. Phys. Lett., 2008. **93**: p. 033111/1-033111/3.

112. Sturcova, A., G.R. Davies, and S.J. Eichhorn, *Elastic modulus and stress-transfer properties of tunicate cellulose whiskers.* Biomacromolecules, 2005. **6**: p. 1055-1061.

113. Tashiro, K. and M. Kobayashi, *Theoretical evaluation of three-dimensional elastic constants of native and regenerated celluloses: Role of hydrogen bonds.* Polymer, 1991. **32**(8): p. 1516-26.

114. Habibi, Y., I. Hoeger, S.S. Kelley, and O.J. Rojas, *Development of langmuir-schaeffer cellulose nanocrystal monolayers and their interfacial behaviors.* Langmuir, 2010. **26**: p. 990-1001.

115. Martins, M., E. Teixeira, A. Corrêa, M. Ferreira, and L. Mattoso, *Extraction and characterization of cellulose whiskers from commercial cotton fibers.* Journal of Materials Science, 2011. **46**(24): p. 7858-7864.

116. Sugiyama, J., R. Vuong, and H. Chanzy, *Electron diffraction study on the two crystalline phases occurring in native cellulose from an algal cell wall.* Macromolecules, 1991. **24**(14): p. 4168-75.

117. Nishiyama, Y., P. Langan, and H. Chanzy, *Crystal structure and hydrogen-bonding system in cellulose iβ from synchrotron x-ray and neutron fiber diffraction.* Journal of the American Chemical Society, 2002. **124**(31): p. 9074-9082.

118. Dufresne, A., M.B. Kellerhals, and B. Witholt, *Transcrystallization in mcl-phas/cellulose whiskers composites.* Macromolecules, 1999. **32**(22): p. 7396-7401.

119. Angles, M.N. and A. Dufresne, *Plasticized starch/tunicin whiskers nanocomposites. 1. Structural analysis.* Macromolecules, 2000. **33**(Copyright (C) 2011 American Chemical Society (ACS). All Rights Reserved.): p. 8344-8353.

120. Azizi Samir My Ahmed, S., F. Alloin, and A. Dufresne, *Review of recent research into cellulosic whiskers, their properties and their application in nanocomposite field.* Biomacromolecules, 2005. **6**(2): p. 612-26.

121. Alloin, F., A. D'Aprea, A. Dufresne, K.N. El, and F. Bossard, *Poly(oxyethylene) and ramie whiskers based nanocomposites: Influence of processing: Extrusion and casting/evaporation.* Cellulose, 2011. **18**: p. 957-973.

122. de, M.A.J., G. Siqueira, A.A.S. Curvelo, and A. Dufresne, *Extrusion and characterization of functionalized cellulose whiskers reinforced polyethylene nanocomposites.* Polymer, 2009. **50**: p. 4552-4563.

123. Jiang, L., E. Morelius, J. Zhang, M. Wolcott, and J. Holbery, *Study of the poly(3-hydroxybutyrate-co-3-hydroxyvalerate)/cellulose nanowhisker composites prepared by solution casting and melt processing.* J. Compos. Mater., 2008. **42**: p. 2629-2645.

124. Mahmoud, K.A., J.A. Mena, K.B. Male, S. Hrapovic, A. Kamen, and J.H.T. Luong, *Effect of surface charge on the cellular uptake and cytotoxicity of fluorescent labeled cellulose nanocrystals.* ACS Applied Materials & Interfaces, 2010. **2**(10): p. 2924-2932.

125. Oksman, K., A.P. Mathew, D. Bondeson, and I. Kvien, *Manufacturing process of cellulose whiskers/polylactic acid nanocomposites.* Composites Science and Technology, 2006. **66**: p. 2776-2784.

126. Alloin, F., A. D'Aprea, A. Dufresne, K.N. El, and F. Bossard, *Poly(oxyethylene) and ramie whiskers based nanocomposites: Influence of processing: Extrusion and casting/evaporation.* Cellulose (Dordrecht, Neth.), 2011. **18**(Copyright (C) 2011 American Chemical Society (ACS). All Rights Reserved.): p. 957-973.

127. Bondeson, D. and K. Oksman, *Dispersion and characteristics of surfactant modified cellulose whiskers nanocomposites.* Compos. Interfaces, 2007. **14**: p. 617-630.

128. Bondeson, D. and K. Oksman, *Polylactic acid/cellulose whisker nanocomposites modified by polyvinyl alcohol.* Composites, Part A, 2007. **38A**: p. 2486-2492.

129. Hajji, P., J.Y. Cavaille, V. Favier, C. Gauthier, and G. Vigier, *Tensile behavior of nanocomposites from latex and cellulose whiskers.* Polymer Composites, 1996. **17**: p. 612-619.

130. Lemahieu, L., J. Bras, P. Tiquet, S. Augier, and A. Dufresne, *Extrusion of nanocellulose-reinforced nanocomposites using the dispersed nano-objects protective encapsulation (dope) process.* Macromol. Mater. Eng., 2011. **296**: p. 984-991.

131. Mathew, A.P., A. Chakraborty, K. Oksman, and M. Sain, *The structure and mechanical properties of cellulose nanocomposites prepared by twin screw extrusion.* ACS Symp. Ser., 2006. **938**: p. 114-131.

132. Mathew, A.P., G. Gong, N. Bjorngrim, D. Wixe, and K. Oksman, *Moisture absorption behavior and its impact on the mechanical properties of cellulose whiskers-based polyvinylacetate nanocomposites.* Polym. Eng. Sci., 2011. **51**: p. 2136-2142.

133. Abitbol, T., J.T. Wilson, and D.G. Gray, *Electrospinning of fluorescent fibers from cdse/zns quantum dots in cellulose triacetate.* J. Appl. Polym. Sci., 2011. **119**: p. 803-810.

134. Gardner, D.J., G.S. Oporto, R. Mills, and M.A.S.A. Samir, *Adhesion and surface issues in cellulose and nanocellulose.* Journal of Adhesion Science and Technology, 2008. **22**(5-6): p. 545-567.

135. Park, W.-I., M. Kang, H.-S. Kim, and H.-J. Jin, *Electrospinning of poly(ethylene oxide) with bacterial cellulose whiskers.* Macromolecular Symposia, 2007. **249/250**: p. 289-294.

136. Peresin, M.S., Y. Habibi, J.O. Zoppe, J.J. Pawlak, and O.J. Rojas, *Nanofiber composites of polyvinyl alcohol and cellulose nanocrystals: Manufacture and characterization.* Biomacromolecules, 2010. **11**: p. 674-681.

137. Rojas, O.J., G.A. Montero, and Y. Habibi, *Electrospun nanocomposites from polystyrene loaded with cellulose nanowhiskers.* J. Appl. Polym. Sci., 2009. **113**: p. 927-935.

138. Xiang, C., Y.L. Joo, and M.W. Frey, *Nanocomposite fibers electrospun from poly(lactic acid)/cellulose nanocrystals.* J. Biobased Mater. Bioenergy, 2009. **3**: p. 147-155.

139. Zoppe, J.O., M.S. Peresin, Y. Habibi, R.A. Venditti, and O.J. Rojas, *Reinforcing poly(caprolactone) nanofibers with cellulose nanocrystals.* ACS Appl. Mater. Interfaces, 2009. **1**: p. 1996-2004.

140. Aguie-Beghin, V., M. Molinari, A. Hambardzumyan, L. Foulon, Y. Habibi, T. Heim, R. Blossey, and R. Douillard, *Preparation of ordered films of cellulose nanocrystals.* ACS Symp. Ser., 2009. **1019**: p. 115-136.

141. Habibi, Y., L. Foulon, V. Aguie-Beghin, M. Molinari, and R. Douillard, *Langmuir-blodgett films of cellulose nanocrystals: Preparation and characterization.* J. Colloid Interface Sci., 2007. **316**(Copyright (C) 2011 American Chemical Society (ACS). All Rights Reserved.): p. 388-397.

142. Favier, V., G.R. Canova, J.Y. Cavaille, H. Chanzy, A. Dufreshne, and C. Gauthier, *Nanocomposite materials from latex and cellulose whiskers.* Polymers for Advanced Technologies, 1995. **6**: p. 351-5.

143. Helbert, W., J.Y. Cavaille, and A. Dufresne, *Thermoplastic nanocomposites filled with wheat straw cellulose whiskers. Part i: Processing and mechanical behavior.* Polymer Composites, 1996. **17**(Copyright (C) 2011 American Chemical Society (ACS). All Rights Reserved.): p. 604-611.

144. Dufresne, A., J.-Y. Cavaille, and W. Helbert, *Thermoplastic nanocomposites filled with wheat straw cellulose whiskers. Part ii: Effect of processing and modeling.* Polymer Composites, 1997. **18**: p. 198-210.

145. Favier, V., G.R. Canova, S.C. Shrivastava, and J.Y. Cavaille, *Mechanical percolation in cellulose whisker nanocomposites.* Polym. Eng. Sci., 1997. **37**: p. 1732-1739.

146. Favier, V., R. Dendievel, G. Canova, J.Y. Cavaille, and P. Gilormini, *Simulation and modeling of three-dimensional percolating structures: Case of a latex matrix reinforced by a network of cellulose fibers.* Acta Mater., 1997. **45**: p. 1557-1565.

147. Chazeau, L., J.Y. Cavaille, G. Canova, R. Dendievel, and B. Boutherin, *Viscoelastic properties of plasticized pvc reinforced with cellulose whiskers.* J. Appl. Polym. Sci., 1999. **71**: p. 1797-1808.

148. Chazeau, L., J.Y. Cavaille, and P. Terech, *Mechanical behaviour above tg of a plasticized pvc reinforced with cellulose whiskers; a sans structural study.* Polymer, 1999. **40**: p. 5333-5344.

149. Chazeau, L., M. Paillet, and J.Y. Cavaille, *Plasticized pvc reinforced with cellulose whiskers. I. Linear viscoelastic behavior analyzed through the quasi-point defect theory.* J. Polym. Sci., Part B: Polym. Phys., 1999. **37**: p. 2151-2164.

150. Chazeau, L., J.Y. Cavaille, and J. Perez, *Plasticized pvc reinforced with cellulose whiskers. Ii. Plastic behavior.* J. Polym. Sci., Part B: Polym. Phys., 2000. **38**: p. 383-392.

151. Oksman, K., A.P. Mathew, D. Bondeson, and I. Kvien, *Manufacturing process of cellulose whiskers/polylactic acid nanocomposites.* Compos. Sci. Technol., 2006. **66**(Copyright (C) 2011 American Chemical Society (ACS). All Rights Reserved.): p. 2776-2784.

152. Azizi, S.M.A.S., A.M. Mateos, F. Alloin, J.-Y. Sanchez, and A. Dufresne, *Plasticized nanocomposite polymer electrolytes based on poly(oxyethylene) and cellulose whiskers.* Electrochim. Acta, 2004. **49**: p. 4667-4677.

153. Angles, M.N., M.R. Vignon, and A. Dufresne, *Plasticized starch and cellulose whiskers composites.* Mater. Tech., 2000. **88**: p. 59-61.

154. Angles, M.N. and A. Dufresne, *Plasticized starch/tunicin whiskers nanocomposite materials. 2. Mechanical behavior.* Macromolecules, 2001. **34**: p. 2921-2931.

155. Mathew, A.P. and A. Dufresne, *Morphological investigation of nanocomposites from sorbitol plasticized starch and tunicin whiskers.* Biomacromolecules, 2002. **3**: p. 609-617.

156. Mathew, A.P., W. Thielemans, and A. Dufresne, *Mechanical properties of nanocomposites from sorbitol plasticized starch and tunicin whiskers.* J. Appl. Polym. Sci., 2008. **109**: p. 4065-4074.

157. Wang, Y., X. Cao, and L. Zhang, *Effects of cellulose whiskers on properties of soy protein thermoplastics.* Macromol. Biosci., 2006. **6**: p. 524-531.

158. Sassi, J.-F. and H. Chanzy, *Ultrastructural aspects of the acetylation of cellulose.* Cellulose, 1995. **2**(2): p. 111-127.

159. Gousse, C., H. Chanzy, G. Excoffier, L. Soubeyrand, and E. Fleury, *Stable suspensions of partially silylated cellulose whiskers dispersed in organic solvents.* Polymer, 2002. **43**: p. 2645-2651.

160. Heux, L., G. Chauve, and C. Bonini, *Nonflocculating and chiral-nematic self-ordering of cellulose microcrystals suspensions in nonpolar solvents.* Langmuir, 2000. **16**(21): p. 8210-8212.

161. Bonini, C., L. Heux, J.-Y. Cavaille, P. Lindner, C. Dewhurst, and P. Terech, *Rodlike cellulose whiskers coated with surfactant: A small-angle neutron scattering characterization.* Langmuir, 2002. **18**: p. 3311-3314.

162. Montanari, S., M. Roumani, L. Heux, and M.R. Vignon, *Topochemistry of carboxylated cellulose nanocrystals resulting from tempo-mediated oxidation.* Macromolecules, 2005. **38**: p. 1665-1671.

163. Habibi, Y., H. Chanzy, and M.R. Vignon, *Tempo-mediated surface oxidation of cellulose whiskers.* Cellulose (Dordrecht, Neth.), 2006. **13**(Copyright (C) 2011 American Chemical Society (ACS). All Rights Reserved.): p. 679-687.

164. Zhang, J., N. Jiang, Z. Dang, T.J. Elder, and A.J. Ragauskas, *Oxidation and sulfonation of cellulosics.* Cellulose 2008. **15**: p. 489-496.

165. Ljungberg, N., C. Bonini, F. Bortolussi, C. Boisson, L. Heux, and J.Y. Cavaille, *New nanocomposite materials reinforced with cellulose whiskers in atactic polypropylene: Effect of surface and dispersion characteristics.* Biomacromolecules, 2005. **6**: p. 2732-2739.

166. Yuan, H., Y. Nishiyama, M. Wada, and S. Kuga, *Surface acylation of cellulose whiskers by drying aqueous emulsion.* Biomacromolecules, 2006. **7**: p. 696-700.

167. Wang, N., E. Ding, and R. Cheng, *Surface modification of cellulose nanocrystals.* Front. Chem. Eng. China, 2007. **1**: p. 228-232.

168. Braun, B. and J.R. Dorgan, *Single-step method for the isolation and surface functionalization of cellulosic nanowhiskers.* Biomacromolecules, 2008. **10**(2): p. 334-341.

169. Berlioz, S., S. Molina-Boisseau, Y. Nishiyama, and L. Heux, *Gas-phase surface esterification of cellulose microfibrils and whiskers.* Biomacromolecules, 2009. **10**: p. 2144-2151.

170. Samir, M.A.S.A., F. Alloin, J.-Y. Sanchez, and A. Dufresne, *Cross-linked nanocomposite polymer electrolytes reinforced with cellulose whiskers.* Macromolecules, 2004. **37**(13): p. 4839-4844.

171. Roy, D., M. Semsarilar, J.T. Guthrie, S. Perrier, x00e, and bastien, *Cellulose modification by polymer grafting: A review.* Chemical Society Reviews, 2009. **38**(7).

172. Ondruschka, B., W. Bonrath, and D. Stuerga, *Development and design of laboratory and pilot scale reactors for microwave-assisted chemistry*, in *Microwaves in organic synthesis*. 2008, Wiley-VCH Verlag GmbH. p. 62-107.

173. Rezai, E. and R.R. Warner, *Polymer-grafted cellulose fibers. I. Enhanced water absorbency and tensile strength.* J. Appl. Polym. Sci., 1997. **65**: p. 1463-1469.

174. Dahou, W., D. Ghemati, A. Oudia, and D. Aliouche, *Preparation and biological characterization of cellulose graft copolymers.* Biochemical Engineering Journal, 2010. **48**(2): p. 187-194.

175. Chang, C. and L. Zhang, *Cellulose-based hydrogels: Present status and application prospects.* Carbohydrate Polymers, 2011. **84**(1): p. 40-53.

176. Akers, P.J., *Absorbent nonwoven fabrics and their preparation*. 1994, Courtaulds Fibres Holdings Ltd., UK . p. 14 pp.

177. Anupama, M., R. Kumar, and B.S. Parmar, *Novel super absorbent hydrogels and the method of obtaining the same*. 2008, Indian Council of Agricultural Research, India . p. 22pp.

178. Barcus, R.L. and D.W. Bjorkquist, *Fibers and pulps for papermaking based on chemical combination of acrylate-itaconate copolymer, polyol, and cellulosic fiber*. 1991, Procter and Gamble Co., USA . p. 56 pp.

179. Chen, L., Z. Zhang, Y. Bai, H. Shan, X. Chen, and X. Zhuang, *Poly(l-glutamic acid-g-hydroxyethyl methacrylate)-hydroxypropylcellulose-g-acrylic acid copolymer hydrogel and its preparation method*. 2010, Northeast Normal University, Peop. Rep. China . p. 8pp.

180. Engelhardt, F., U. Riegel, H.J. Kleiner, R. Funk, and G. Ebert, *Hydrophilic hydrogels with a high swelling capacity, their preparation and use*. 1993, Cassella AG, Germany . p. 17 pp.

181. Herron, C.M. and W.L. Dean, *Acrylic polymer-crosslinked cellulosic fiber webs with high absorbent capacity and wet compressibility*. 1995, Procter and Gamble Co., USA . p. 45 pp.

182. Stoyanov, A. and C.E. Miller, *Cellulose fibers crosslinked with low molecular weight phosphorous-containing polyacrylic acid and method*. 2011, Weyerhaeuser NR Company, USA . p. 8 pp.

183. Westland, J.A., R.A. Jewell, and A.N. Neogi, *Polymeric polycarboxylic acid crosslinked cellulosic fibers*. 1999, Weyerhaeuser Company, USA . p. 13 pp., Cont.-in-part of U.S. 5,840,787.

184. Westlund, J.A., R.A. Jewel, and A.N. Neogi, *Polymeric polycarboxylic acid crosslinked cellulosic fibers, their formation and use as absorbents*. 1999, Weyerhaeuser Company, USA . p. 44 pp.

185. Wong, A., *Absorbents for disposable absorbent products*. 1987, Procter and Gamble Co., USA . p. 30 pp.

186. Lepoutre, P., *Modified cellulose materials*. 1976, Pulp and Paper Research Institute of Canada, Can. . p. 22 pp.

187. Warner, R.R. and E. Rezai, *Polymer-grafted cellulose fibers. Iii. Interactions of grafted and ungrafted fibers in handsheets.* J. Appl. Polym. Sci., 1997. **65**: p. 1487-1492.

188. Warner, R.R. and E. Rezai, *Polymer-grafted cellulose fibers. Ii. Polymer localization and induced alterations in fiber morphology.* J. Appl. Polym. Sci., 1997. **65**: p. 1471-1485.

189. Lepoutre, P., S.H. Hui, and A.A. Robertson, *Water absorbency of hydrolyzed polyacrylonitrile-grafted cellulose fibers.* J. Appl. Polym. Sci., 1973. **17**: p. 3141-54.

190. Lepoutre, P. and S.H. Hui, *Grafting acrylonitrile onto wood pulp. Influence of process variables.* J. Appl. Polym. Sci., 1975. **19**: p. 1257-68.

191. Jain, V., H. Xiao, and Y. Ni, *Grafting of poly(methyl acrylate) onto sulfite pulp fibers and its effect on water absorbance.* J. Appl. Polym. Sci., 2007. **105**: p. 3195-3203.

192. Vitta, S.B., E.P. Stahel, and V.T. Stannett, *The preparation and properties of acrylic and methacrylic-acid grafted cellulose prepared by ceric ion initiation. 2. Water retention properties* Journal of Applied Polymer Science, 1986. **32**(7): p. 5799-5810.

193. Kim, B.-S. and S.-P. Mun, *Effect of ce4+ pretreatment on swelling properties of cellulosic superabsorbents.* Polymers for Advanced Technologies, 2009. **20**(12): p. 899-906.

194. Ali, F., C.N. Saikia, and S.R. Sen, *Grafting of acrylonitrile onto high α-cellulose extracted from hibiscus sabdariffa.* Industrial Crops and Products, 1997. **6**(2): p. 121-129.

195. Deo, H.T. and V.D. Gotmare, *Acrylonitrile monomer grafting on gray cotton to impart high water absorbency.* J. Appl. Polym. Sci., 1999. **72**: p. 887-894.

196. Aliouche, D., B. Sid, and H. Ait-Amar, *Graft-copolymerization of acrylic monomers onto cellulose. Influence on fibre swelling and absorbency.* Annales De Chimie-Science Des Materiaux, 2006. **31**(5): p. 527-540.

197. Jain, V., H. Xiao, and Y. Ni. *Effect of fiber concentration during grafting of poly(methyl acrylate) onto wood cellulose fibers to prepared superabsorbent hydrogels*. 2006: Pulp and Paper Technical Association of Canada.

198. Xu, G.G., C.Q. Yang, and Y. Den, *Mechanism of paper wet strength development by polycarboxylic acids with different molecular weight and glutaraldehyde/poly(vinyl alcohol).* J. Appl. Polym. Sci., 2006. **101**: p. 277-284.

199. Suo, A., J. Qian, Y. Yao, and W. Zhang, *Synthesis and properties of carboxymethyl cellulose-graft-poly(acrylic acid-co-acrylamide) as a novel cellulose-based superabsorbent.* Journal of Applied Polymer Science, 2007. **103**(3): p. 1382-1388.

200. Mondal, M.I.H., Y. Uraki, M. Ubukata, and K. Itoyama, *Graft polymerization of vinyl monomers onto cotton fibres pretreated with amines.* Cellulose, 2008. **15**(4): p. 581-592.

201. Pourjavadi, A., F. Seidi, H. Salimi, and R. Soleyman, *Grafted cmc/silica gel superabsorbent composite: Synthesis and investigation of swelling behavior in various media.* J. Appl. Polym. Sci., 2008. **108**: p. 3281-3290.

202. Singha, A.S. and R.K. Rana, *Microwave induced graft copolymerization of methyl methacrylate onto lignocellulosic fibers.* International Journal of Polymer Analysis and Characterization, 2010. **15**(6): p. 370-386.

203. Ekebafe, L.O., M.O. Ekebafe, F.A.O. Akpa, G. Erhuanga, and B.W. Etiobhio, *Graft copolymerization of acrylonitrile onto delignified native bamboo (bambusa vulgaris) cellulosic and its utilization potential for heavy metal uptake from aqueous medium.* Chem. Ind. Chem. Eng. Q., 2011. **17**: p. 133-140.

204. Coskun, M. and M.M. Temüz, *Grafting studies onto cellulose by atom-transfer radical polymerization.* Polymer International, 2005. **54**(2): p. 342-347.

205. Temuez, M.M., M. Coskun, and A. Oelcuecue, *Synthesis of graft copolymers of cellulose with 4-acryloylmorpholine, 2-methacrylamidopyridine and n-phenylmethacrylamide, and determination of some sorption properties.* J. Macromol. Sci., Part A: Pure Appl. Chem., 2007. **44**: p. 947-952.

206. Karlsson, J.O. and P. Gatenholm, *Preparation and characterization of cellulose-supported hema hydrogels.* Polymer, 1997. **38**: p. 4727-4731.

207. Ostenson, M. and P. Gatenholm, *Improvement of the wetting and absorption properties of lignocellulosic fibers by means of gas phase ozonation.* Langmuir, 2005. **21**(1): p. 160-165.

208. Kang, I.-S., C.Q. Yang, W. Wei, and G.C. Lickfield, *Mechanical strength of durable press finished cotton fabrics. Part i: Effects of acid degradation and*

crosslinking of cellulose by polycarboxylic acids. Text. Res. J., 1998. **68**: p. 865-870.

209. Wei, W. and C.Q. Yang, *Polymeric carboxylic acid and citric acid as a nonformaldehyde dp finish.* Text. Chem. Color. Am. Dyest. Rep., 2000. **32**: p. 53-57.

210. Yang, C.Q., *Characterizing ester crosslinkages in cotton cellulose with ftir photoacoustic spectroscopy.* Text. Res. J., 1991. **61**: p. 298-305.

211. Yang, C.Q., *Effect of ph on nonformaldehyde durable press finishing of cotton fabric: Ft-ir spectroscopy study. Part ii: Formation of the anhydride intermediate.* Text. Res. J., 1993. **63**: p. 706-11.

212. Yang, C.Q. and G.D. Bakshi, *Quantitative analysis of the nonformaldehyde durable press finish on cotton fabric: Acid-base titration and infrared spectroscopy.* Text. Res. J., 1996. **66**: p. 377-384.

213. Yang, C.Q., D. Chen, J. Guan, and Q. He, *Cross-linking cotton cellulose by the combination of maleic acid and sodium hypophosphite. 1. Fabric wrinkle resistance.* Ind. Eng. Chem. Res., 2010. **49**: p. 8325-8332.

214. Yang, C.Q., X. Wang, and I.-S. Kang, *Ester crosslinking of cotton fabric by polymeric carboxylic acids and citric acid.* Text. Res. J., 1997. **67**: p. 334-342.

215. Yang, C.Q. and W. Wei, *Mechanical strength of durable press finished cotton fabric, part iii: Change in cellulose molecular weight.* Text. Res. J., 2000. **70**: p. 910-915.

216. Wu, X., C.Q. Yang, and Q. He, *Flame retardant finishing of cotton fleece: Part vii. Polycarboxylic acids with different numbers of functional group.* Cellulose, 2010. **17**: p. 859-870.

217. Yang, C.Q., Q. He, and B. Voncina, *Cross-linking cotton cellulose by the combination of maleic acid and sodium hypophosphite. 2. Fabric fire performance.* Ind. Eng. Chem. Res., 2011. **50**: p. 5889-5897.

218. Xu, G.G. and C.Q. Yang, *Studies of polymeric carboxylic acids of different molecular size for improving paper strength.* Polym. Mater. Sci. Eng., 1999. **80**: p. 343-344.

219. Xu, G.G. and C.Q.-X. Yang, *Comparison of the kraft paper crosslinked by polymeric carboxylic acids of large and small molecular sizes: Dry and wet performance.* J. Appl. Polym. Sci., 1999. **74**: p. 907-912.

220. Yang, C.Q. and Y. Xu, *Paper wet performance and ester crosslinking of wood pulp cellulose by poly(carboxylic acid)s.* J. Appl. Polym. Sci., 1998. **67**: p. 649-658.

221. Yang, C.Q., Y. Xu, and D. Wang, *Ft-ir spectroscopy study of the polycarboxylic acids used for paper wet strength improvement.* Ind. Eng. Chem. Res., 1996. **35**: p. 4037-4042.

222. Herron, C.M. and D.J. Cooper, *Absorbent structure containing individualized, polycarboxylic acid crosslinked fibers*. 1991, Procter and Gamble Cellulose Co., USA . p. 21 pp.

223. Herron, C.M., T.R. Hanser, D.J. Cooper, and B.S. Hersko, *Process for preparing individualized, polycarboxylic acid-crosslinked cellulose fibers*. 1991, Procter and Gamble Cellulose Co., USA . p. 17 pp.

224. Kokko, B.J., *Manufacture and uses of high-bulking, resilient, and absorbent fibers by crosslinking wood pulp with polycarboxylic acids*. 1991, James River Corp., USA . p. 19 pp.

225. Komura, A. and R. Akaishi, *Biodegradable water-absorbing materials and their manufacture*. 1998, Fuji Xerox Co., Ltd., Japan . p. 4 pp.

226. Sears, K.D., W.J. Cooper, and T.R. Murguia, *Crosslinked cellulose fibers, compositions, and fibrous sheet manufacture*. 2005, Rayonier Products & Financial Services Company, USA . p. 11 pp.

227. Westland, J.A., R.A. Jewell, and A.N. Neogi, *Absorbent composite containing polymaleic acid crosslinked cellulosic fibers*. 2001, Weyerhaeuser Company, USA . p. 13 pp., Cont.-in-part of U.S. 5,998,511.

228. Pantze, A., O. Karlsson, and U. Westermark, *Esterification of carboxylic acids on cellulosic material: Solid state reactions.* Holzforschung, 2008. **62**(2): p. 136-141.

229. Barcus, R.L. and D.W. Bjorkquist, *Absorbent cellulosic fibers modified with maleate-methyl vinyl ether copolymer and polyol*. 1991, Procter and Gamble Co., USA . p. 48 pp.

230. Nüchter, M., B. Ondruschka, W. Bonrath, and A. Grum, *Microwave assisted synthesis - a critical technology overview.* Green Chemistry, 2004. **6**: p. 128-141.

231. Stuerga, D., *Microwave-material interactions and dielectric properties, key ingredients for mastery of chemical microwave processes*, in *Microwaves in organic synthesis*. 2008, Wiley-VCH Verlag GmbH. p. 1-61.

232. Gedye, R., F. Smith, K. Westaway, H. Ali, L. Baldisera, L. Laberge, and J. Rousell, *The use of microwave ovens for rapid organic synthesis.* Tetrahedron Letters, 1986. **27**(3): p. 279-282.

233. Giguere, R.J., T.L. Bray, S.M. Duncan, and G. Majetich, *Application of commercial microwave ovens to organic synthesis.* Tetrahedron Letters, 1986. **27**(41): p. 4945-4948.

234. Grelier, S., A. Castellan, S. Desrousseaux, A. Nourmamode, and L. Podgorski, *Attempt to protect wood colour against uv/visible light by using antioxidants bearing isocyanate groups and grafted to the material with microwave.* Holzforschung, 1997. **51**(6): p. 511-518.

235. Kamdem, D.P. and S. Grelier, *Surface roughness and color change of copper-amine treated red maple (acer rubrum) exposed to artificial ultraviolet light.* Holzforschung, 2002. **56**(5): p. 473-478.

236. Bischof Vukusic, S., D. Katovic, C. Schramm, J. Trajkovic, and B. Sefc, *Polycarboxylic acids as non-formaldehyde anti-swelling agents for wood.* Holzforschung, 2006. **60**(4): p. 439-444.

237. Hooda, U. and S. Banerjee, *Microwave-enhanced transport of chemicals into green wood under low-headspace conditions.* Holzforschung, 2000. **54**(3): p. 331-333.

238. Timar, M.C., K. Maher, M. Irle, and M.D. Mihai, *Preparation of wood with thermoplastic properties, part 2. Simplified technologies.* Holzforschung, 2000. **54**(1): p. 77-82.

239. Fishman, M.L., H.K. Chau, D.R. Coffin, P.H. Cooke, P. Qi, M.P. Yadav, and A.T. Hotchkiss, Jr., *Physico-chemical characterization of a cellulosic fraction from sugar beet pulp.* Cellulose 2011. **18**: p. 787-801.

240. Ooi, B.G., A.L. Rambo, and M.A. Hurtado, *Overcoming the recalcitrance for the conversion of kenaf pulp to glucose via microwave-assisted pre-treatment processes.* Int J Mol Sci, 2011. **12**: p. 1451-63.

241. Sasaki, C., R. Takada, T. Watanabe, Y. Honda, S. Karita, Y. Nakamura, and T. Watanabe, *Surface carbohydrate analysis and bioethanol production of sugarcane bagasse pretreated with the white rot fungus, ceriporiopsis subvermispora and microwave hydrothermolysis.* Bioresour. Technol., 2011. **102**: p. 9942-9946.

242. Orozco, A.M., A.a.H. Al-Muhtaseb, A.B. Albadarin, D. Rooney, G.M. Walker, and M.N.M. Ahmad, *Acid-catalyzed hydrolysis of cellulose and cellulosic waste using a microwave reactor system.* RSC Adv., 2011. **1**: p. 839-846.

243. Shi, J., Y. Pu, B. Yang, A. Ragauskas, and C.E. Wyman, *Comparison of microwaves to fluidized sand baths for heating tubular reactors for hydrothermal and dilute acid batch pretreatment of corn stover.* Bioresour Technol, 2011. **102**: p. 5952-61.

244. Xu, J., H. Chen, Z. Kadar, A.B. Thomsen, J.E. Schmidt, and H. Peng, *Optimization of microwave pretreatment on wheat straw for ethanol production.* Biomass Bioenergy, 2011. **35**: p. 3859-3864.

245. Wan, J., M. Radoiu, I. Kalatchev, and M. Depew, *Microwave enhanced non-alkaline bleaching of mechanical pulps: A new solution to an old problem.* Research on Chemical Intermediates, 2000. **26**(9): p. 931-939.

246. Wu, C., C. Zhao, J. Li, and K. Chen, *The effect of microwave treatment on the hydrogen peroxide bleaching of soda-aq wheat straw pulp.* Adv. Mater. Res. , 2011. **236-238**: p. 1307-1312.

247. Chadlia, A. and M.H.M. Farouk, *Rapid homogeneous esterification of cellulose extracted from posidonia induced by microwave irradiation.* J. Appl. Polym. Sci., 2011. **119**: p. 3372-3381.

248. Satge, C., R. Granet, B. Verneuil, P. Branland, and P. Krausz, *Synthesis and properties of biodegradable plastic films obtained by microwave-assisted cellulose acylation in homogeneous phase.* Comptes Rendus Chimie, 2004. **7**(2): p. 135-142.

249. Takano, T., J. Ishikawa, H. Kamitakahara, and F. Nakatsubo, *The application of microwave heating to the synthesis of 6-amino-6-deoxycellulose.* Carbohydrate Research, 2007. **342**(16): p. 2456-2460.

250. Zhu, S., Y. Wu, Q. Chen, Z. Yu, C. Wang, S. Jin, Y. Ding, and G. Wu, *Dissolution of cellulose with ionic liquids and its application: A mini-review.* Green Chem., 2006. **8**: p. 325-327.

251. Lin, C.-X., H.-Y. Zhan, M.-H. Liu, S.-Y. Fu, and L.-H. Huang, *Rapid homogeneous preparation of cellulose graft copolymer in bmimcl under microwave irradiation.* Journal of Applied Polymer Science, 2010. **118**(1): p. 399-404.

252. Li, J., L.-P. Zhang, F. Peng, J. Bian, T.-Q. Yuan, F. Xu, and R.-C. Sun, *Microwave-assisted solvent-free acetylation of cellulose with acetic anhydride in the presence of iodine as a catalyst.* Molecules, 2009. **14**: p. 3551-66.

253. Lin, N., G. Chen, J. Huang, A. Dufresne, and P.R. Chang, *Effects of polymer-grafted natural nanocrystals on the structure and mechanical properties of poly(lactic acid): A case of cellulose whisker-graft-polycaprolactone.* J. Appl. Polym. Sci., 2009. **113**: p. 3417-3425.

254. Feng, H., J. Li, and L. Wang, *Preparation of biodegradable flax shive cellulose-based superabsorbent polymer under microwave irradiation.* BioResources, 2010. **5**: p. 1484-1495.

255. Yang, H., H. Mao, Q. Lu, M. Ran, J. Gu, and Y. Liu, *Esterification of luffa with acetic anhydride under microwave radiation determined by ftir.* J. Macromol. Sci., Part B: Phys., 2011. **50**: p. 319-328.

256. Wan, Z., Z. Xiong, H. Ren, Y. Huang, H. Liu, H. Xiong, Y. Wu, and J. Han, *Graft copolymerization of methyl methacrylate onto bamboo cellulose under microwave irradiation.* Carbohydr. Polym., 2011. **83**: p. 264-269.

257. Antova, G., P. Vasvasova, and M. Zlatanov, *Studies upon the synthesis of cellulose stearate under microwave heating.* Carbohydr. Polym., 2004. **57**: p. 131-134.

258. Zhao, B.-X., P. Wang, T. Zheng, C.-y. Chen, and J. Shu, *Preparation and adsorption performance of a cellulosic-adsorbent resin for copper(ii).* J. Appl. Polym. Sci., 2006. **99**: p. 2951-2956.

259. Matahwa, H., V. Ramiah, W.L. Jarrett, J.B. McLeary, and R.D. Sanderson, *Microwave assisted graft copolymerization of n-isopropyl acrylamide and methyl acrylate on cellulose: Solid state nmr analysis and caco3 crystallization.* Macromol. Symp., 2007. **255**: p. 50-56.

260. Guo, Y., J. Zhou, Y. Song, and L. Zhang, *An efficient and environmentally friendly method for the synthesis of cellulose carbamate by microwave heating.* Macromol. Rapid Commun., 2009. **30**: p. 1504-1508.

261. Kaith, B.S., R. Jindal, A.K. Jana, and M. Maiti, *Rapid synthesis of graft copolymer of mma onto saccharum spontaneum l. Under microwave irradiation for enhanced thermal modifications.* Int. J. Polym. Anal. Charact., 2009. **14**: p. 364-387.

262. Hua, F. and M. Qian, *Synthesis of self-crosslinking sodium polyacrylate hydrogel and water-absorbing mechanism.* Journal of Materials Science, 2001. **36**(3): p. 731-738.

263. Yang, C.Q., *Ft-ir spectroscopy study of the ester crosslinking mechanism of cotton cellulose.* Textile Research Journal, 1991. **61**(8): p. 433-40.

264. Petersson, L., *Biopolymer-based nanocomposites: A comparison between renewable cellulose reinforcements and layered silicates*, in *Faculty of Engineering Science and Technology*. 2007, Norwegian University of Science and Technology: Trondheim

265. Mathew, A.P., S. Packirisamy, R. Stephen, and S. Thomas, *Transport of aromatic solvents through natural rubber/polystyrene (nr/ps) interpenetrating polymer network membranes.* J. Membr. Sci., 2002. **201**: p. 213-227.

266. International, A., *Astm d2756 standard test methods for determination of gel content and swell ratio of crosslinked ethylene plastics*. 2006, ASTM International: West Conshohocken, PA.

267. FitzPatrick, M., P. Champagne, M.F. Cunningham, and R.A. Whitney, *A biorefinery processing perspective: Treatment of lignocellulosic materials for the*

production of value-added products. Bioresource Technology, 2010. **101**(23): p. 8915-8922.

268. Petersen, N. and P. Gatenholm, *Bacterial cellulose-based materials and medical devices: Current state and perspectives.* Appl. Microbiol. Biotechnol., 2011. **91**: p. 1277-1286.

269. Sczostak, A., *Cotton linters: An alternative cellulosic raw material.* Macromolecular Symposia, 2009. **280**: p. 45-53.

270. Berglund, L.A. and T. Peijs, *Cellulose biocomposites - from bulk moldings to nanostructured systems.* MRS Bull., 2010. **35**: p. 201-207.

271. John, R.P., G.S. Anisha, K.M. Nampoothiri, and A. Pandey, *Micro and macroalgal biomass: A renewable source for bioethanol.* Bioresour. Technol., 2010. **102**: p. 186-193.

272. Petrus, L. and M.A. Noordermeer, *Biomass to biofuels, a chemical perspective.* Green Chem., 2006. **8**: p. 861-867.

273. Liu, S. and T.E. Amidon, *Essential components of a wood-based biorefinery.* Papel, 2007. **68**: p. 84-105.

274. Kukhar, V.P., *Biomass - renewable feedstock for organic chemicals ("white chemistry").* Kem. Ind., 2009. **58**: p. 57-71.

275. Hunter, N., *'Fuel plus' from the forest: A short review and introduction to the 'biorefinery' concept.* Appita J., 2007. **60**: p. 10-12.

276. Gandini, A., *Polymers from renewable resources: A challenge for the future of macromolecular materials.* Macromolecules, 2008. **41**: p. 9491-9504.

277. Fernandes, S.C.M., C.S.R. Freire, A.J.D. Silvestre, N.C. Pascoal, and A. Gandini, *Novel materials based on chitosan and cellulose.* Polym. Int., 2011. **60**: p. 875-882.

278. Carroll, A. and C. Somerville, *Cellulosic biofuels.* Annu. Rev. Plant Biol., 2009. **60**: p. 165-182.

279. Ragauskas, A.J., M. Nagy, D.H. Kim, C.A. Eckert, J.P. Hallett, and C.L. Liotta, *From wood to fuels: Integrating biofuels and pulp production.* Industrial Biotechnology, 2006. **2**(1): p. 55-65.

280. Pu, Y., D. Zhang, P.M. Singh, and A.J. Ragauskas, *The new forestry biofuels sector.* Biofuels, Bioproducts & Biorefining, 2008. **2**(1): p. 58-73.

281. Yang, C.Q., X. Wang, and I.-S. Kang, *Ester crosslinking of cotton fabric by polymeric carboxylic acids and citric acid.* Textile Research Journal, 1997. **67**(5): p. 334-342.

282. Xu, Y., C.-M. Chen, and C.Q. Yang, *Application of polymeric multifunctional carboxylic acids to improve wet strength.* Tappi Journal, 1998. **81**(11): p. 159-164.

283. Yang, C.Q. and Y. Xu, *Paper wet performance and ester crosslinking of wood pulp cellulose by poly(carboxylic acid)s.* Journal of Applied Polymer Science, 1998. **67**(4): p. 649-658.

284. Xu, G.G. and C.Q.-X. Yang, *Comparison of the kraft paper crosslinked by polymeric carboxylic acids of large and small molecular sizes: Dry and wet performance.* Journal of Applied Polymer Science, 1999. **74**(4): p. 907-912.

285. Xu, Y., C.Q. Yang, and C.-M. Chen, *Wet reinforcement of paper with high-molecular-weight multifunctional carboxylic acid.* Tappi Journal, 1999. **82**(8): p. 150-156.

286. Byoung-Suhk, K. and M. Sung-Phil, *Effect of ce4+ pretreatment on swelling properties of cellulosic superabsorbents.* Polymers for Advanced Technologies, 2009. **20**(12): p. 899-906.

287. Dahou, W., D. Ghemati, A. Oudia, and D. Aliouche, *Preparation and biological characterization of cellulose graft copolymers.* Biochem. Eng. J., 2010. **48**: p. 187-194.

288. Jain, V., H. Xiao, and Y. Ni, *Grafting of poly(methyl acrylate) onto sulfite pulp fibers and its effect on water absorbance.* Journal of Applied Polymer Science, 2007. **105**: p. 3195-3203.

289. Maha, M.I. and K.E.-Z. Waleed, *Preparation, characterization, and properties of fast-responding bulk hydrogel and treated bleached banana pulp.* Polymers for Advanced Technologies, 2004. **15**(5): p. 275-283.

290. Coskun, M. and M.M. Temuez, *Grafting studies onto cellulose by atom-transfer radical polymerization.* Polym. Int., 2005. **54**: p. 342-347.

291. Barcus, R.L. and D.W. Bjorkquist, *Absorbent cellulosic fibers modified with maleate-methyl vinyl ether copolymer and polyol*. 1991, (Procter and Gamble Co., USA). Application: WO
WO. p. 48 pp.

292. Reynolds, E.C., *Oral care formulation comprising calcium phosphopeptide complex*. 2006, The University of Melbourne, Australia . p. 34pp.

293. Prosise, W.E. and J. Hilsenbeck, *Oral care compositions comprising a non-cationic antibacterial agent and a surface active vegetable gum*. 2008, Isp Investments Inc., USA . p. 10pp.

294. Patel, D., A.W. Smith, N. Grist, P. Barnett, and J.D. Smart, *An in vitro mucosal model predictive of bioadhesive agents in the oral cavity.* Journal of Controlled Release, 1999. **61**: p. 175-183.

295. Nabi, N. and A. Gaffar, *Antibacterial antiplaque oral compositions containing anionic polycarboxylates and halogenated diphenyl ethers*. 1990, Colgate-Palmolive Co., USA . p. 9 pp. Cont.-in-part of U.S. Ser. No. 8,901.

296. Kim, J.Y., J.H. Kim, S.Y. Chang, and S.Y. Yun, *Peroxide-based patches for teeth whitening*. 2001, LG Chemical Co., Ltd., S. Korea . p. 36 pp.

297. Hassan, M., K.N. Brogden, G. Durga, N.S. Dixit, and R.L. Mitchell, *Color stable anticalculus composition*. 1999, Colgate Palmolive Company, USA . p. 4 pp.

298. Gaffar, A., J.J. Afflitto, and M.T. Joziak, *Anticalculus oral compositions comprising a maleic copolymer*. 1992, Colgate-Palmolive Co., USA . p. 10 pp.

299. Eldridge, G.R. and M. Goering, *Composition comprising pentacyclic acid triterpene for controlling biofilm and bacterial infection*. 2007, Sequoia Sciences, Inc., USA . p. 33 pp.

300. Chang, S.-Y., J.-Y. Kim, J.-H. Kim, and S.-Y. Yun, *Patches for teeth whitening*. 2003, LG Houshold & Healthcare Ltd., S. Korea . p. 10 pp., Cont.-in-part of U.S. Ser. No. 49,817.

301. McConnell, M.D., Y. Liu, A.P. Nowak, S. Pilch, J.G. Masters, and R.J. Composto, *Bacterial plaque retention on oral hard materials: Effect of surface roughness, surface composition, and physisorbed polycarboxylate.* Journal of Biomedical Materials Research, Part A, 2010. **92A**: p. 1518-1527.

302. Salman, H.H., C. Gamazo, M. Agueeros, and J.M. Irache, *Bioadhesive capacity and immunoadjuvant properties of thiamine-coated nanoparticles.* Vaccine, 2007. **25**(48): p. 8123-8132.

303. Gomez, S., C. Gamazo, B. San Roman, M. Ferrer, M.L. Sanz, and J.M. Irache, *Gantrez an nanoparticles as an adjuvant for oral immunotherapy with allergens.* Vaccine, 2007. **25**(29): p. 5263-5271.

304. Gomez, S., C. Gamazo, B. San Roman, C. Vauthier, M. Ferrer, and J.M. Irache, *Development of a novel vaccine delivery system based on gantrez nanoparticles.* Journal of Nanoscience and Nanotechnology, 2006. **6**(9/10): p. 3283-3289.

305. Bogdal, D., P. Penczek, J. Pielichowski, and A. Prociak, *Microwave assisted synthesis, crosslinking, and processing of polymeric materials.* Advances in Polymer Science, 2003. **163**: p. 193-263.

306. Ratanakamnuan, U., D. Atong, and D. Aht-Ong, *Microwave assisted esterification of waste cotton fabrics for biodegradation films preparation.* Advanced Materials Research, 2007. **26-28**(Advanced Materials and Processing): p. 457-460.

307. Tomanova, V., K. Pielichowski, I. Srokova, A. Zoldakova, V. Sasinkova, and A. Ebringerova, *Microwave-assisted synthesis of carboxymethylcellulose - based polymeric surfactants.* Polymer Bulletin 2008. **60**(1): p. 15-25.

308. Matahwa, H., V. Ramiah, W.L. Jarrett, J.B. McLeary, and R.D. Sanderson, *Microwave assisted graft copolymerization of n-isopropyl acrylamide and methyl acrylate on cellulose: Solid state nmr analysis and caco3 crystallization.* Macromolecular Symposia, 2007. **255**: p. 50-56.

309. Wan, J.K.S., M. Radoiu, I. Kalatchev, and M.C. Depew, *Microwave enhanced non-alkaline bleaching of mechanical pulps: A new solution to an old problem.* Research on Chemical Intermediates, 2000. **26**(9): p. 931-939.

310. McMurry, J., *Organic chemistry*. 5th ed. 2000, Pacific Grove, CA: Brooks/Cole.

311. Flory, P.J. and 1953., *Principles of polymer chemistry*. 1953, Ithaca, New York, USA: Cornell University Press.

312. Flory, P.J. and J.J. Rehner, *Statistical mechanics of cross-linked polymer networks ii. Swelling.* The Journal of Chemical Physics, 1943. **11**(11): p. 521-526.

313. Flory, P.J. and J.J. Rehner, *Statistical mechanics of cross-linked polymer networks i. Rubberlike elasticity.* The Journal of Chemical Physics, 1943. **11**(11): p. 512-517.

314. Omidian, H. and K. Park, *Introduction to hydrogels*, in *Biomedical applications of hydrogels handbook*, R.M. Ottenbrite, K. Park, and T. Okano, Editors. 2010, Springer New York. p. 1-16.

315. Jhon, M.S. and J.D. Andrade, *Water and hydrogels.* Journal of Biomedical Materials Research, 1973. **7**(6): p. 509-522.

316. Wang, W. and A. Wang, *Preparation, swelling and water-retention properties of superabsorbent hydrogels based on guar gum.* Advanced Materials Research, 2010. **96**: p. 177-182.

317. Rocco, A.M., R.P. Pereira, and M.I. Felisberti, *Miscibility, crystallinity and morphological behavior of binary blends of poly(ethylene oxide) and poly(methyl vinyl ether-maleic acid).* Polymer, 2001. **42**(12): p. 5199 - 5205.

318. Bodin, A., H. Backdahl, B. Risberg, and P. Gatenholm, *Nanocellulose as scaffolds for tissue engineering and organ regeneration.* Abstracts of Papers, 233rd ACS National Meeting, Chicago, IL, United States, March 25-29, 2007, 2007: p. CELL-107.

319. Teeri, T.T., H. Brumer, G. Daniel, and P. Gatenholm, *Biomimetic engineering of cellulose-based materials.* Trends in Biotechnology, 2007. **25**(7): p. 299-306.

320. Chanzy, H. *Aspects of cellulose structure*. 1990: Horwood.

321. Sugiyama, J., H. Chanzy, and J.F. Revol, *On the polarity of cellulose in the cell wall of valonia.* Planta, 1994. **193**: p. 260-5.

322. Nishino, T., K. Takano, and K. Nakamae, *Elastic modulus of the crystalline regions of cellulose polymorphs.* Journal of Polymer Science, Part B: Polymer Physics, 1995. **33**(11): p. 1647-51.

323. Tashiro, K. and M. Kobayashi, *Calculation of crystallite modulus of native cellulose.* Polym. Bull., 1985. **14**: p. 213-18.

324. Sturcova, A., I. His, D.C. Apperley, J. Sugiyama, and M.C. Jarvis, *Structural details of crystalline cellulose from higher plants.* Biomacromolecules, 2004. **5**: p. 1333-1339.

325. Petersson, L., A.P. Mathew, and K. Oksman, *Dispersion and properties of cellulose nanowhiskers and layered silicates in cellulose acetate butyrate nanocomposites.* J. Appl. Polym. Sci., 2009. **112**: p. 2001-2009.

326. Yang, C.Q., Y. Xu, and D. Wang, *Ft-ir spectroscopy study of the polycarboxylic acids used for paper wet strength improvement.* Industrial & Engineering Chemistry Research, 1996. **35**(11): p. 4037-4042.

327. Yang, C.Q., *Infrared spectroscopy studies of the cyclic anhydride as the intermediate for the ester crosslinking of cotton cellulose by polycarboxylic acids. I. Identification of the cyclic anhydride intermediate.* Journal of Polymer Science, Part A: Polymer Chemistry, 1993. **31**(5): p. 1187-93.

328. Yang, C.Q., *Infrared spectroscopy studies of the effects of the catalyst on the ester crosslinking of cellulose by poly(carboxylic acids).* J. Appl. Polym. Sci., 1993. **50**: p. 2047-53.

329. Carter, L.W., J.G. Hendricks, and D.S. Bolley, *Elastomer reinforced with modified clay*. 1950, (National Lead Co.). US.

330. Kojima, Y., A. Usuki, M. Kawasumi, A. Okada, Y. Fukushima, T. Kurauchi, and O. Kamigaito, *Mechanical properties of nylon 6-clay hybrid.* Journal of Materials Research, 1993. **8**(5): p. 1185-9.

331. Tjong, S.C., *Novel nanoparticle-reinforced metal matrix composites with enhanced mechanical properties.* Advanced Engineering Materials, 2007. **9**(8): p. 639-652.

332. Alexandre, M. and P. Dubois, *Polymer-layered silicate nanocomposites: Preparation, properties and uses of a new class of materials.* Materials Science and Engineering: R: Reports, 2000. **28**(1-2): p. 1-63.

333. Chanzy, H., ed. *Cellulose sources and exploitation*. ed. J.F. Kennedy, G.O. Phillips, and P.A. Williams. 1990, Ellis Horwood Ltd.: New York

334. Samir, M.A.S.A., F. Alloin, J.-Y. Sanchez, and A. Dufresne, *Nanocomposite polymer electrolytes based on poly(oxyethylene) and cellulose whiskers.* Polim. Cienc. Tecnol., 2005. **15**: p. 109-113.

335. Eichhorn, S.J., *Cellulose nanowhiskers: Promising materials for advanced applications.* Soft Matter, 2011. **7**(2): p. 303-315.

336. Sturcova, A., R. Davies Geoffrey, and J. Eichhorn Stephen, *Elastic modulus and stress-transfer properties of tunicate cellulose whiskers.* Biomacromolecules, 2005. **6**(2): p. 1055-61.

337. Hajji, P., J.Y. Cavaille, V. Favier, C. Gauthier, and G. Vigier, *Tensile behavior of nanocomposites from latex and cellulose whiskers.* Polymer Composites, 1996. **17**(4): p. 612-619.

338. Pu, Y., J. Zhang, T. Elder, Y. Deng, P. Gatenholm, and A.J. Ragauskas, *Investigation into nanocellulosics versus acacia reinforced acrylic films.* Composites, Part B: Engineering, 2007. **38B**(3): p. 360-366.

339. Kvien, I., J. Sugiyama, M. Votrubec, and K. Oksman, *Characterization of starch based nanocomposites.* Journal of Materials Science, 2007. **42**(19): p. 8163-8171.

340. Mathew, A.P. and A. Dufresne, *Plasticized waxy maize starch: Effect of polyols and relative humidity on material properties.* Biomacromolecules, 2002. **3**: p. 1101-1108.

341. Mathew, A.P., W. Thielemans, and A. Dufresne, *Mechanical properties of nanocomposites from sorbitol plasticized starch and tunicin whiskers.* Journal of Applied Polymer Science, 2008. **109**(6): p. 4065-4074.

342. Grunert, M. and W.T. Winter, *Cellulose nanocrystal reinforced cellulose acetate butyrate nanocomposites.* PMSE Prepr., 2002. **86**: p. 367-368.

343. Bondeson, D. and K. Oksman, *Polylactic acid/cellulose whisker nanocomposites modified by polyvinyl alcohol.* Composites, Part A: Applied Science and Manufacturing, 2007. **38A**(12): p. 2486-2492.

344. Lin, N., G. Chen, J. Huang, A. Dufresne, and P.R. Chang, *Effects of polymer-grafted natural nanocrystals on the structure and mechanical properties of poly(lactic acid): A case of cellulose whisker-graft-polycaprolactone.* Journal of Applied Polymer Science, 2009. **113**(5): p. 3417-3425.

345. Petersson, L., I. Kvien, and K. Oksman, *Structure and thermal properties of poly(lactic acid)/cellulose whiskers nanocomposite materials.* Composites Science and Technology, 2007. **67**(11-12): p. 2535-2544.

346. Yu, J., F. Ai, A. Dufresne, S. Gao, J. Huang, and P.R. Chang, *Structure and mechanical properties of poly(lactic acid) filled with (starch nanocrystal)-graft-poly(ε-caprolactone).* Macromol. Mater. Eng., 2008. **293**: p. 763-770.

347. Bondeson, D. and K. Oksman, *Dispersion and characteristics of surfactant modified cellulose whiskers nanocomposites.* Composite Interfaces, 2007. **14**(7-9): p. 617-630.

348. Bonini, C., L. Heux, J.-Y. Cavaille, P. Lindner, C. Dewhurst, and P. Terech, *Rodlike cellulose whiskers coated with surfactant: A small-angle neutron scattering characterization.* Langmuir, 2002. **18**(8): p. 3311-3314.

349. Kim, J., G. Montero, Y. Habibi, J.P. Hinestroza, J. Genzer, D.S. Argyropoulos, and O.J. Rojas, *Dispersion of cellulose crystallites by nonionic surfactants in a hydrophobic polymer matrix.* Polym. Eng. Sci., 2009. **49**: p. 2054-2061.

350. Angles, M.N. and A. Dufresne, *Plasticized starch/tunicin whiskers nanocomposite materials. 2. Mechanical behavior.* Macromolecules, 2001. **34**(9): p. 2921-2931.

351. Samir, M.A.S.A., A.M. Mateos, F. Alloin, J.-Y. Sanchez, and A. Dufresne, *Plasticized nanocomposite polymer electrolytes based on poly(oxyethylene) and cellulose whiskers.* Electrochimica Acta, 2004. **49**(26): p. 4667-4677.

352. Mathew, A.P. and A. Dufresne, *Morphological investigation of nanocomposites from sorbitol plasticized starch and tunicin whiskers.* Biomacromolecules, 2002. **3**(3): p. 609-17.

353. Viguie, J., S. Molina-Boisseau, and A. Dufresne, *Processing and characterization of waxy maize starch films plasticized by sorbitol and reinforced with starch nanocrystals.* Macromol. Biosci., 2007. **7**: p. 1206-1216.

354. Chazeau, L., J.Y. Cavaille, and J. Perez, *Plasticized pvc reinforced with cellulose whiskers. Ii. Plastic behavior.* Journal of Polymer Science, Part B: Polymer Physics, 2000. **38**(3): p. 383-392.

355. Chazeau, L., M. Paillet, and J.Y. Cavaille, *Plasticized pvc reinforced with cellulose whiskers. I. Linear viscoelastic behavior analyzed through the quasi-*

point defect theory. Journal of Polymer Science, Part B: Polymer Physics, 1999. **37**(16): p. 2151-2164.

356. Goetz, L., A. Mathew, K. Oksman, P. Gatenholm, and A.J. Ragauskas, *A novel nanocomposite film prepared from crosslinked cellulosic whiskers.* Carbohydrate Polymers, 2009. **75**(1): p. 85-89.

357. Dhiman, M., P. Yedurkar, and K.K. Sawant, *Formulation, characterization, and in vitro evaluation of bioadhesive gels containing 5-fluorouracil.* Pharmaceutical Development and Technology, 2008. **13**(1): p. 15-25.

358. Gomez, S., C. Gamazo, S. Roman Beatriz, M. Ferrer, L. Sanz Maria, and M. Irache Juan, *Gantrez an nanoparticles as an adjuvant for oral immunotherapy with allergens.* Vaccine, 2007. **25**(29): p. 5263-71.

359. Gomez, S., C. Gamazo, R.B. San, C. Vauthier, M. Ferrer, and J.M. Irache, *Development of a novel vaccine delivery system based on gantrez nanoparticles.* Journal of Nanoscience and Nanotechnology, 2006. **6**: p. 3283-3289.

360. Salas, S., B. Talero, A.M. Rabasco, and M.L. Gonzalez-Rodriguez, *Development and validation of a reverse-phase liquid chromatographic method for the assay of lidocaine hydrochloride in alginate-gantrez microspheres.* Journal of Pharmaceutical and Biomedical Analysis, 2008. **47**(3): p. 501-507.

361. Salman Hesham, H., C. Gamazo, M. Agueros, and M. Irache Juan, *Bioadhesive capacity and immunoadjuvant properties of thiamine-coated nanoparticles.* Vaccine, 2007. **25**(48): p. 8123-32.

362. Yoncheva, K., N. Centelles Miguel, and M. Irache Juan, *Development of bioadhesive amino-pegylated poly(anhydride) nanoparticles designed for oral DNA delivery.* Journal of Microencapsulation, 2008. **25**(2): p. 82-9.

363. Yoncheva, K., E. Lizarraga, and J.M. Irache, *Pegylated nanoparticles based on poly(methyl vinyl ether-co-maleic anhydride): Preparation and evaluation of their bioadhesive properties.* European Journal of Pharmaceutical Sciences, 2005. **24**(5): p. 411-419.

364. Khutoryanskaya, O.V., V.V. Khutoryanskiy, and R.A. Pethrick, *Characterisation of blends based on hydroxyethylcellulose and maleic acid-alt-methyl vinyl ether.* Macromolecular Chemistry and Physics, 2005. **206**(15): p. 1497-1510.

365. Henriksson, M., L.A. Berglund, P. Isaksson, T. Lindström, and T. Nishino, *Cellulose nanopaper structures of high toughness.* Biomacromolecules, 2008. **9**(6): p. 1579-1585.

366. Doolittle, A.K., *Plasticizer technology*, in *Plasticizer technology*, P.F. Brunis, Editor. 1965, Reinhold: New York p. 1.

367. Singh, T.R.R., P.A. McCarron, A.D. Woolfson, and R.F. Donnelly, *Physicochemical characterization of poly(ethylene glycol) plasticized poly(methyl vinyl ether-co-maleic acid) films.* Journal of Applied Polymer Science, 2009. **112**(5): p. 2792-2799.

368. Chung, K.H., C.S. Wu, and E.G. Malawer, *Glass transition temperatures of poly(methyl vinyl ether-co-maleic anhydride) (pmvema) and poly(methyl vinyl ether-co-maleic acid) (pmvemac) and the kinetics of dehydration of pmvemac by thermal analysis.* Journal of Applied Polymer Science, 1990. **41**(3-4): p. 793-803.

369. Kashyap, N., N. Kumar, and M.N.V.R. Kumar, *Smart gels for drug delivery applications.* Drug Delivery Technology, 2004. **4**(7): p. 32, 34, 36, 38-39.

370. Li, J., *Polymeric hydrogels.* Biomaterials Engineering and Processing Series, 2004. **1**(Engineering Materials for Biomedical Applications): p. 7/1-7/18.

371. Sannino, A., G. Mensitieri, and L. Nicolais, *Water and synthetic urine sorption capacity of cellulose-based hydrogels under a compressive stress field.* Journal of Applied Polymer Science, 2004. **91**(6): p. 3791-3796.

372. Bajpai, S.K. and S. Johnson, *Superabsorbent hydrogels for removal of divalent toxic ions. Part i: Synthesis and swelling characterization.* Reactive & Functional Polymers, 2005. **62**(3): p. 271-283.

373. Burdick, J.A. and M.M. Stevens, *Biomedical hydrogels.* Biomaterials, Artificial Organs and Tissue Engineering, 2005: p. 107-115.

374. Elvira, C., G.A. Abraham, A. Gallardo, and J. San Roman, *Smart biodegradable hydrogels with applications in drug delivery and tissue engineering.* Biodegradable Systems in Tissue Engineering and Regenerative Medicine, 2005: p. 493-508.

375. Lin, C.-C. and A.T. Metters, *Hydrogels in controlled release formulations: Network design and mathematical modeling.* Advanced Drug Delivery Reviews, 2006. **58**(12-13): p. 1379-1408.

376. Bodin, A., L. Ahrenstedt, H. Fink, H. Brumer, B. Risberg, and P. Gatenholm, *Modification of nanocellulose with a xyloglucan-rgd conjugate enhances adhesion and proliferation of endothelial cells: Implications for tissue engineering.* Biomacromolecules, 2007. **8**(12): p. 3697-3704.

377. Omidian, H., K. Park, and J.G. Rocca, *Recent developments in superporous hydrogels.* Journal of Pharmacy and Pharmacology, 2007. **59**(3): p. 317-327.

378. Hoare, T.R. and D.S. Kohane, *Hydrogels in drug delivery: Progress and challenges.* Polymer, 2008. **49**(8): p. 1993-2007.

379. Oh, J.K., R. Drumright, D.J. Siegwart, and K. Matyjaszewski, *The development of microgels/nanogels for drug delivery applications.* Progress in Polymer Science, 2008. **33**(4): p. 448-477.

380. Khodairy, K.A.E., *Drug release from compressed hydrophilic matrix: Influence of matrix swelling and solubility on the in-vitro release characteristics of ketoprofen.* Alexandria J. Pharm. Sci., 2000. **14**: p. 69-74.

381. Arbos, P., M.A. Campanero, M.A. Arangoa, M.J. Renedo, and J.M. Irache, *Influence of the surface characteristics of pvm/ma nanoparticles on their bioadhesive properties.* Journal of Controlled Release, 2003. **89**: p. 19-30.

382. Luppi, B., T. Cerchiara, F. Bigucci, P.A.M. Di, I. Orienti, and V. Zecchi, *Crosslinked poly(methyl vinyl ether-co-maleic anhydride) as topical vehicles for hydrophilic and lipophilic drugs.* Drug Delivery, 2003. **10**: p. 239-244.

383. McCarron, P.A., A.D. Woolfson, R.F. Donnelly, G.P. Andrews, A. Zawislak, and J.H. Price, *Influence of plasticizer type and storage conditions on properties of poly(methyl vinyl ether-co-maleic anhydride) bioadhesive films.* Journal of Applied Polymer Science, 2004. **91**(3): p. 1576-1589.

384. McCarron, P.A., R.F. Donnelly, G.P. Andrews, and A.D. Woolfson, *Stability of 5-aminolevulinic acid in novel non-aqueous gel and patch-type systems intended for topical application.* Journal of Pharmaceutical Sciences, 2005. **94**(8): p. 1756-1771.

385. Andrews, G.P., L. Donnelly, D.S. Jones, R.M. Curran, R.J. Morrow, A.D. Woolfson, and R.K. Malcolm, *Characterization of the rheological, mucoadhesive, and drug release properties of highly structured gel platforms for intravaginal drug delivery.* Biomacromolecules, 2009. **10**: p. 2427-2435.

386. Ojer, P., H. Salman, C.M.R. da, J. Calvo, C.A.L. de, C. Gamazo, J.L. Lavandera, and J.M. Irache, *Spray-drying of poly(anhydride) nanoparticles for drug/antigen delivery.* J. Drug Delivery Sci. Technol., 2010. **20**: p. 353-359.

387. Vandamme, K., V. Melkebeek, E. Cox, P. Adriaensens, V.S. Van, P. Dubruel, C. Vervaet, and J.P. Remon, *Influence of polymer hydrolysis on adjuvant effect of gantrezan nanoparticles: Implications for oral vaccination.* European Journal of Pharmaceutics and Biopharmaceutics, 2011. **79**: p. 392-398.

388. McConnell, M.D., Y. Liu, A.P. Nowak, S. Pilch, J.G. Masters, and R.J. Composto, *Bacterial plaque retention on oral hard materials: Effect of surface roughness, surface composition, and physisorbed polycarboxylate.* Journal of Biomedical Materials Research, Part A, 2010. **92A**: p. 1518-1527.

389. Patel, D., A.W. Smith, N. Grist, P. Barnett, and J.D. Smart, *An in vitro mucosal model predictive of bioadhesive agents in the oral cavity.* Journal of Controlled Release, 1999. **61**: p. 175-183.

390. Chang, S.-Y., J.-Y. Kim, J.-H. Kim, and S.-Y. Yun, *Patches for teeth whitening*. 2003, LG Houshold & Healthcare Ltd., S. Korea . p. 10 pp., Cont.-in-part of U.S. Ser. No. 49,817.

391. Gaffar, A., J.J. Afflitto, and M.T. Joziak, *Anticalculus oral compositions comprising a maleic copolymer*. 1992, Colgate-Palmolive Co., USA . p. 10 pp.

392. Kim, J.Y., J.H. Kim, S.Y. Chang, and S.Y. Yun, *Peroxide-based patches for teeth whitening*. 2001, LG Chemical Co., Ltd., S. Korea . p. 36 pp.

393. Zimmer, J. and J.H. Fechner, *Use of an antimicrobial alkali-silicate glass-ceramic for dental care and oral hygiene*. 2003, Schott Glas, Germany; Carl-Zeiss-Stiftung . p. 72 pp.

394. Li, H., *Introduction smart hydrogel modelling*. 2009, Springer Berlin Heidelberg. p. 1-55.

395. Astarita, G., *Heat and mass transfer in solid polymer system*, in *Transport phenomena in polymeric systems*, R.A. Mashelkar, A.S. Mujumdar, and R. Kamal, Editors. 1989, Wiley: New York. p. 339–351.

396. Mathew, A.P., S. Packirisamy, R. Stephen, and S. Thomas, *Transport of aromatic solvents through natural rubber/polystyrene (nr/ps) interpenetrating polymer network membranes.* Journal of Membrane Science, 2002. **201**(1–2): p. 213-227.

397. Korsmeyer, R.W., R. Gurny, E.M. Doelker, P.L. Buri, and N.A. Peppas, *Mechanism of solute release from porous hydrophilic polymers.* International Journal of Pharmaceutics, 1983. **15**: p. 25-35.

398. Masaro, L. and X.X. Zhu, *Physical models of diffusion for polymer solutions, gels and solids.* Progress in Polymer Science, 1999. **24**: p. 731-775.

399. Dufresne, A. and J.-Y. Cavaillé, *Clustering and percolation effects in microcrystalline starch-reinforced thermoplastic.* Journal of Polymer Science Part B: Polymer Physics, 1998. **36**(12): p. 2211-2224.

400. Dufresne, A., D. Dupeyre, and M.R. Vignon, *Cellulose microfibrils from potato tuber cells: Processing and characterization of starch-cellulose microfibril composites.* Journal of Applied Polymer Science, 2000. **76**: p. 2080-2092.

401. Ashland. *Gantrez s-97 bf product description*. [cited 2012 August 7]; Available from: http://online1.ispcorp.com/en-US/Pages/ProductDetail.aspx?BU=Personal%20Care&l1=Oral%20Care&l2=Bioadhesive%20Polymers&prodName=Gantrez%C2%AE%20S-97%20BF&prdId=74101.

402. ScienceLab. *Polyethylene glycol*. [cited 2012 August 7]; Available from: http://www.sciencelab.com/msds.php?msdsId=9926625.

403. Xue, W., S. Champ, and M.B. Huglin, *Network and swelling parameters of chemically crosslinked thermoreversible hydrogels.* Polymer, 2001. **42**: p. 3665-3669.

404. Sunil, K.B. and S. Surinderpal, *Analysis of swelling behaviour of poly(methacrylamide-co-methacrylic acid) hydrogels and effect of synthesis conditions on water uptake.* React. Funct. Polym, 2006. **66**: p. 431-440.

405. Xia, Z., M. Patchan, J. Maranchi, J. Elisseeff, and M. Trexler, *Determination of crosslinking density of hydrogels prepared from microcrystalline cellulose.* Journal of Applied Polymer Science, 2012: p. n/a-n/a.